Determining the role of *Aedes aegypti* host SUMOylation in suppressing arbovirus replication

Samuel Stokes

A thesis presented for the degree of Doctor of Philosophy in the College of Medical, Veterinary, and Life Sciences

Biotechnology and Biological Sciences Research Council Doctoral Training Partnership programme - University of Glasgow Centre for Virus Research (CVR)

Abstract

Approximately half the world's human population is at risk of infection from mosquito-borne arboviruses. Currently, interactions between the mosquito antiviral response and infecting arboviruses remains poorly understood; deciphering these will be crucial to the development of novel methods to limit replication and transmission that could help control future outbreaks. Previous mammalian studies have shown that the *Homo sapiens* Small Ubiquitin-related Modifier (SUMO) pathway plays a fundamental role in multiple aspects of cell biology, including the regulation of host cell immunity. However, this pathway and its impact on arbovirus replication remain uncharacterised in mosquito hosts such as *Aedes aegypti* (*Ae. aegypti*; *Aa*).

Comparison between the *Ae. aegypti* and *H. sapiens* (*Hs*) SUMOylation pathways demonstrated a high degree of amino acid sequence and structural similarity. The most notable predicted difference is the lack of ability of *Aa*SUMO to form poly-SUMO chains, which have important functions in *H. sapiens*. Biochemical analysis of the *Aa*SUMOylation pathway identified a conserved function, and confirmed that *Aa*SUMO could not efficiently form poly-SUMO chains, unlike *Hs*SUMO3 (its closest *H. sapiens* homologue) due to the absence of an internal SUMO conjugation motif. Catalytically inactive mutants revealed the necessity of *Aa*PIAS (Protein inhibitor of activated STAT) to induce the formation of poly-SUMO chains. Confocal microscopy confirmed that *Aa*SUMO protein is expressed in haemocytes, the salivary glands, ovaries, and midgut, all of which are sites of arboviral replication. Q-PCR investigations have also revealed the *Aa*SUMOylation pathway to be ubiquitously expressed. *In vitro* depletion of the *Aa*SUMOylation pathway led to significantly enhanced levels of Zika, Semliki Forest, and Bunyamwera virus replication, identifying a vital role for *Aa*SUMOylation in the suppression of these arboviruses. Subsequent studies in *H. sapiens* cells have also identified a significant role for *Hs*PIAS1 in suppressing the replication of Zika, Semliki Forest, and Bunyamwera viruses. Furthermore, depletion of *Hs*SUMO1 significantly enhanced the replication of Bunyamwera virus, indicating that SUMOylation suppresses arbovirus in a virus dependent manner. Collectively, these data have identified a novel role for the SUMOylation pathway in

suppressing arbovirus replication in both the vertebrate and invertebrate species in which arboviruses replicate.

Contents

Abstract 2
Contents 4
List of Figures 9
List of Tables 11
Acknowledgements 12
Authors Declaration 15
List of Abbreviations 16
1. Introduction 24
1.1. Overview 25
1.2. Importance of studying vector-borne diseases 26
1.2.1. Aedes aegypti 26
1.2.1.1. Mosquito-arbovirus interactions 29
1.3. Arboviruses 32
1.3.1. Alphaviruses 34
1.3.1.1. Alphavirus epidemiology 35
1.3.1.2. Alphavirus disease 36
1.3.1.3. Alphavirus replication 37
1.3.2. Flaviviruses 40
1.3.2.1. Flavivirus epidemiology 41
1.3.2.2. Flavivirus disease 41
1.3.2.3. Flavivirus replication 43
1.3.3. Orthobunyaviruses 45
1.3.3.1. Orthobunyavirus epidemiology 47
1.3.3.2. Orthobunyavirus disease 47
1.3.3.3. Orthobunyavirus replication 48
1.4. Post-translational modification 51
1.4.1. Ubiquitin 51
1.4.2. Overview of the Small Ubiquitin-like MOdifer (SUMO) protein 53
1.4.2.1. SUMO proteins 54
1.4.2.2. SUMO interaction motifs (SIMs) 57
1.4.2.3. SUMO pathway 57
1.4.2.3.1. Activating enzyme 59
1.4.2.3.2. Conjugating enzyme 59
1.4.2.3.3. Ligating enzyme 60
1.4.2.3.4. Sentrin specific proteases (SENPs) 62
1.5. Interactions between the viruses and the immune responses regulated by SUMO 63

1.5.1. Vertebrate innate immune response 63
1.5.1.1. Alphaviruses and innate immune evasion 67
1.5.1.2. Flaviviruses and innate immune evasion 70
1.5.1.3. Orthobunyaviruses and innate immune evasion 74
1.5.2. Invertebrate innate immune response 76
1.5.2.1. Alphaviruses and *Ae. aegypti* immune response 80
1.5.2.2. Flaviviruses and *Ae. aegypti* immune response 81
1.5.2.3. Orthobunyaviruses and *Ae. aegypti* immune response 82
1.5.3. SUMOylation pathway interactions with viruses 83
1.5.4. SUMO and arboviruses 84
1.6. Premise and primary objectives of the project 85
2. Materials & Methods 86
2.1. Materials 87
2.1.1. Cells and cell culture reagents 87
2.1.1.1. Cell lines utilised 87
2.1.1.2. Cell culture reagents utilised 89
2.1.1.3. Viruses 90
2.1.2. Antibodies 92
2.1.3. Plasmids 94
2.1.4. Primer sequences 98
2.1.5. Reagents, chemicals, buffers, and kits 101
2.1.5.1. Commercial kits 101
2.1.5.2. Buffers made in house 102
2.1.5.3. Reagents used 103
2.1.6. Enzymes 105
2.1.7. Reagents used for prokaryotic work 106
2.1.7.1. Bacterial strains and culture media 106
2.1.6.2. Buffers for protein purification from bacterial extracts 106
2.2. Methods 108
2.2.1. Cloning and DNA manipulation 108
2.2.1.1. DNA quantitation 108
2.2.1.2. Polymerase Chain Reaction (PCR) amplification 108
2.2.1.3. Restriction endonuclease digestion 110
2.2.1.4. Agarose gel electrophoresis 110
2.2.1.5. DNA Ligation 110
2.2.1.6. Transforming competent bacteria 111
2.2.1.7. Growing bacterial cultures of *E. coli* DH5α 111
2.2.1.8. Isolation and amplification of DNA using kits 112
2.2.1.9. Sequencing by commercial companies 112
2.2.1.10. Site directed mutagenesis of plasmid DNA by PCR 113

2.2.1.11. dsRNA synthesis for cell culture 115
2.2.1.12. dsRNA synthesis for adult *Ae. aegypti* 115
2.2.2. Purification of recombinant proteins 119
2.2.2.1. Expression in recombinant BL21 (DE3) 119
2.2.2.2. Purification of 6xHis tagged proteins 119
2.2.2.3. Purification of Strep.II tagged proteins 120
2.2.2.4. Quantification of proteins by BSA titration 120
2.2.3. *In vitro* assays of recombinant proteins 121
2.2.3.1. SUMOylation assays 121
2.2.4. Cell culture methods 122
2.2.4.1. Maintenance, growth, and passaging of cells 122
2.2.4.2. Seeding of cells 122
2.2.4.3. Transfection of mammalian cells 123
2.2.4.4. Lentivirus transduction of cells 124
2.2.4.5. dsRNA transfection of mosquito cells 124
2.2.5. Virology 125
2.2.5.1. Propagation of SFV 125
2.2.5.2. Propagation of BUNV 125
2.2.5.3. Propagation of ZIKV 125
2.2.5.4. Determining viral titre 126
2.2.5.5. Infection of cultured cells 127
2.2.6. Analytical techniques 128
2.2.6.1. Sodium dodecyl sulfate – Polyacrylamide gel electrophoresis 128
2.2.6.2. Coomassie staining of SDS-PAGE gels 128
2.2.6.3. Western blotting 128
2.2.6.4. RNA extraction 129
2.2.6.5. Complementary DNA (cDNA) synthesis 129
2.2.6.6. Quantitative polymerase chain reaction (q-PCR) 130
2.2.6.7. ICC-staining plaque assay 131
2.2.6.8. In Cell Western Blot (ICWB) 131
2.2.7. Reporter assays 133
2.2.7.1. Firefly-luciferase reporter assay 133
2.2.7.2. NanoLuciferase reporter assay 133
2.2.7.3. Protein quantification assay 134
2.2.8. Bioinformatics 135
2.2.8.1. Joined Advanced SUMOylation site and SIM Analyser (JASSA) 135
2.2.8.2. Modelling software 135
2.2.8.3. Amino acid alignment 136
2.2.8.4. Statistical analysis 136
2.2.9. Cloning strategies used in this study 137

2.2.9.1. Cloning of pACYC-*Aa*SAE1/2 137
2.2.9.2. Cloning of pET28a-SUMO chimaera and pET28a-SUMO chimaera K11R 139
2.2.9.3. Cloning of pET45b-*Aa*Ubc9 and pET45b-*Aa*Ubc9 C93S 140
2.2.9.4. Cloning of pET45b-*Aa*PIAS and pET45-*Aa*PIAS C371A 141
2.2.9.5. Cloning of pET28a-*Aa*SUMO 141
3. Conservation of the SUMOylation pathway between *Ae. aegypti* and *H. sapiens* 142
3.1. Overview 143
3.2. Conservation of the SUMOylation pathway 145
3.2.1. Conservation of SUMO 145
3.2.2. Conservation of Ubc9 148
3.2.3. Conservation of SAE1/2 151
3.2.4. Conservation of PIAS 154
3.2.5. Confirmation of pathway expression 158
3.2.6. Summary 164
3.3. Viral proteins contain SUMO conjugation motifs 165
3.2.1. SCM sites on BUNV proteins 165
3.2.2. SCM sites on SFV proteins 167
3.3.5. SCM sites on CHIKV proteins 169
3.3.6. SCM sites on ZIKV proteins 171
3.3.7. SCM sites on DENV proteins 173
3.3.8. Summary 175
3.4. Discussion 177
4. Biochemical analysis of the *Ae. aegypti* and *H. sapiens* SUMOylation pathways 181
4.1. Overview 182
4.2. Purification of the *Aa*SUMOylation pathway 184
4.3. Comparison of the biochemical properties of the *Ae. aegypti* and *H. sapiens* SUMOylation pathways 187
4.3.1. Recombinant *Aa*Ubc9 forms a thioester bond with SUMO at a similar rate to recombinant *Hs*Ubc9 187
4.3.2. Recombinant *Aa*SUMO is more biochemically comparable to *Hs*SUMO1 than *Hs*SUMO3 in an *in vitro* biochemical assay 190
4.3.3. A chimaeric SUMO protein efficiently forms HMW SUMO conjugates 195
4.3.4. *Aa*PIAS enhances rate of HMW SUMO conjugate formation 198
4.4. Biochemical activity of the pathways is conserved between species 202
4.4.1. *Aa*SUMO can be utilised by the *Hs*SUMOylation pathway 202
4.4.2. *Aa*Ubc9 can be utilised in the *Hs*SUMOylation pathway with *Hs*SUMO2 204
4.4.3. *Aa*SAE1/2 utilise in *Hs*SUMOylation pathway 206
4.4.4. *Aa*PIAS can enhance rate of *Hs*SUMO3 chain formation 208
4.5. Discussion 210
5. *Aa*SUMOylation pathway suppresses arbovirus replication 214
5.1. Overview 215

5.2. Expression of the *Aa*SUMOylation pathway 217

5.2.1. Q-PCR analysis shows the *Aa*SUMOylation pathway is differentially expressed in *Ae. aegypti* tissues 217

5.2.2. *Aa*SUMO is expressed in all *Ae. aegypti* tissues studied 219

5.2.2.1. *Aa*SUMO is expressed in the haemocytes 219

5.2.2.2. *Aa*SUMO is expressed in the salivary glands 221

5.2.2.3. *Aa*SUMO is expressed in the gut 222

5.2.2.4. *Aa*SUMO is expressed in the ovaries 223

5.3. Depletion of *Aa*SUMO *in vivo* does not significantly enhance ZIKV replication 225

5.4. dsRNA can deplete expression of the *Aa*SUMOylation pathway in AF5 cells 230

5.5. Interaction of the *Aa*SUMOylation pathway and arboviruses *in vitro* 233

5.5.1. Depletion of the *Aa*SUMOylation pathway enhances replication of BUNV 233

5.5.2. Depletion of the *Aa*SUMOylation pathway enhances replication of SFV 235

5.5.3. Depletion of the *Aa*SUMOylation pathway enhances replication of ZIKV 237

5.6. Discussion 239

6. *Hs*SUMOylation pathway suppresses arbovirus expression 245

6.1. Overview 246

6.2. Lentiviral transduction with shRNAs depletes expression of components of the SUMOylation pathway in HFt cells 247

6.3. Depletion of components of the *Hs*SUMOylation pathway enhances arbovirus expression *in vitro* 250

6.4. Discussion 255

7. Discussion 258

7.1. Overview 259

7.2. Conservation of the sequence, structure, biochemical function, and expression of the *Aa*- and *Hs*-SUMOylation pathways 259

7.3. Biochemical properties of the *Aa*SUMOylation pathway 261

7.4. The SUMOylation pathway is broadly antiviral to arboviruses 263

7.5. Concluding remarks 268

8. References 269

Appendix A: Amino acid sequence comparison between *Hs* and *Aa*SAE1/2, and *Hs* and *Aa*PIAS 297

Appendix B: Purification of *Aa*SAE1/2 302

Appendix C: Purified *Aa*Ubc9 C93S, the SUMO chimaera, and the SUMO chimaera K11R 307

Appendix D: No primary antibody controls of SUMO expression in *Ae. aegypti* tissues 310

Appendix E: Melt curve analysis of q-PCR primers 312

List of Figures

Figure 1.1 Predicted distribution of *Ae. aegypti*. 27
Figure 1.2 Mechanisms used to suppress arbovirus infection 28
Figure 1.3 Mosquito anatomy 31
Figure 1.4 A basic arbovirus transmission cycle 33
Figure 1.5 The alphavirus genome 35
Figure 1.6 Alphavirus life cycle 39
Figure 1.7 The flavivirus genome 40
Figure 1.8 Flavivirus life cycle 44
Figure 1.9 The orthobunyaviridae genome 46
Figure 1.10 Orthobunyavirus life cycle 50
Figure 1.11 *H. sapiens* SUMOylation pathway. 58
Figure 1.12 Schematic of PIAS1 domains 61
Figure 1.13 Overview of the antiviral interferon response 66
Figure 1.14 Innate immune evasion strategies employed by alphaviruses 69
Figure 1.15 Innate immune evasion strategies employed by flaviviruses 73
Figure 1.16 Innate immune strategies utilised by orthobunyaviruses 75
Figure 1.17 Mosquito immune response 79

Figure 2.1 Schematic of site directed mutagenesis protocol for *Aa*Ubc9 114
Figure 2.2 pACYCDuet-1 expression plasmid map 138
Figure 2.3 *Aa*SAE2 primer binding sites 138
Figure 2.4 pET28a vector map 139
Figure 2.5 pET45b vector map 140

Figure 3.1 Conservation of SUMO between *Ae. aegypti* and *H. sapiens*. 147
Figure 3.2 Conservation of Ubc9 between *Ae. aegypti* and *H. sapiens*. 150
Figure 3.3 Conservation of SAE1/2 between *Ae. aegypti* and *H. sapiens*. 153
Figure 3.4 Conservation of PIAS between *Ae. aegypti* and *H. sapiens*. 157
Figure 3.5 A heatmap of amino acid identity between the *Aa* and *Hs* SUMOylation pathways 164
Figure 3.6 Predicted SUMO conjugation motifs on BUNV proteins 166
Figure 3.7 Predicted SUMO conjugation motifs on SFV polyproteins 168
Figure 3.8 Predicted SUMO conjugation motifs on CHIKV polyproteins 170
Figure 3.9 Predicted SUMO conjugation motifs on the ZIKV polyprotein 172
Figure 3.10 Predicted SUMO conjugation motifs on the DENV-2 virus polyprotein 174

Figure 4.1 Recombinant *H. sapiens* SUMOylation proteins 185
Figure 4.2 Recombinant *Ae. aegypti* SUMOylation enzymes 186
Figure 4.3 Comparison of *Hs*Ubc9 and *Aa*Ubc9 rate of thioester formation 189
Figure 4.4 Comparison of *Aa* and *Hs* SUMOylation pathways activity at 28 ˚C 192

Figure 4.5 Comparison of *Aa* and *Hs* SUMOylation pathways activity at 37 ˚C 194
Figure 4.6 Comparison of SUMO chimaera with a K11R chimaera mutant 197
Figure 4.7 Comparison of PIAS activity with a catalytically inactive PIAS mutant 199
Figure 4.8 Mass spectrometry analysis reveals which lysine's SUMO is binding to 201
Figure 4.9 *Aa*SUMO is biochemically active with *Hs*SUMOylation machinery 203
Figure 4.10 *Aa*Ubc9 is biochemically active with *Hs*SUMOylation machinery 205
Figure 4.11 *Aa*SAE1/2 is biochemically active with *Hs*SUMOylation machinery 207
Figure 4.12 *Aa*PIAS is biochemically active with *Hs*SUMOylation machinery 209

Figure 5.1 Q-PCR of SUMOylation pathway transcript expression in *Ae. aegypti* tissues 218
Figure 5.2 Confocal microscopy of SUMO expression in *Ae. aegypti* haemocytes 220
Figure 5.3 Confocal microscopy of SUMO expression in *Ae. aegypti* salivary glands 221
Figure 5.4 SUMO expression in the *Ae. aegypti* gut by confocal microscopy 222
Figure 5.5 Expression of SUMO in *Ae. aegypti* ovaries 224
Figure 5.6 SUMO transcript expression levels achieved by q-PCR after dsRNA knockdown 227
Figure 5.7 Effect of knocking down SUMO expression on ZIKV replication in *Ae. aegypti* mosquitoes 229
Figure 5.8 Depletion of the *Aa*SUMOylation pathway by q-PCR and Western blot 232
Figure 5.9 Effect of depletion of the *Aa*SUMOylation pathway on BUNV replication 234
Figure 5.10 Effect of depletion of the *Aa*SUMOylation pathway on SFV replication 236
Figure 5.11 Effect of depletion of the *Aa*SUMOylation pathway on ZIKV replication 238

Figure 6.1 Depletion of SUMOylation pathway from HFt cells 249
Figure 6.2 Effect of depletion of the *Hs*SUMOylation pathway on arbovirus expression 254

List of Tables

Table 2-1 Summary table of cell lines used in this study 87
Table 2-2 List of cell culture reagents used in this study 89
Table 2-3 Viruses used in this study 90
Table 2-4 Antibodies used in this study 92
Table 2-5 Plasmids used in this study 94
Table 2-6 Oligonucleotide sequences used in this study 98
Table 2-7 Commercial kits used in this study 101
Table 2-8 List of buffers made in house and used throughout the study 102
Table 2-9 Reagents used in the study 103
Table 2-10 Standard PCR cycle 109
Table 2-11 T7 PCR cycle 109
Table 2-12 Components in a nuclease digestion for mosquito depletion 117
Table 2-13 dsRNA synthesis reaction for mosquito depletion 117
Table 2-14 dsRNA binding solution for mosquito depletion 118

Table 3-1 The SUMOylation pathway specific peptide sequences identified from *Ae. aegypti* cells by mass spectrometry. 159
Table 3-2 Summary of the SCM sequences found on the relevant proteins of different arboviruses 176

Acknowledgements

This PhD was funded by the Biotechnology and Biological Sciences Research Council Doctoral Training Partnership programme, without which I would have been unable to undertake this work. I have also had a great deal of support (and funding) from The Pirbright Institute and the Medical Research Council funded Centre for Virus Research at the University of Glasgow.

I am sincerely grateful to the support from my only remaining full time supervisor, Dr Chris Boutell. Professor Peter Mertens has also been a valuable source of insight and calm in an often troubled journey. Dr Mike Tatham and Professor Ron Hay, our collaborators at the University of Dundee have been incredibly helpful in allowing the work to progress (and asking some obvious questions we hadn't thought of). Finally, I am hugely grateful for the talent and help of Floriane Almire, and Dr Emilie Pondeville based at the CVR. Without your willingness to painstakingly dissect and inject hundreds of mosquitoes this project wouldn't have been nearly as interesting as it turned out to be! Many thanks also to my examiners – Professor Steven Sinkins and Dr David Hughes, for making my viva as pain free as possible, to the point that it was verging on enjoyable (I wouldn't choose to go through it again though).

The BBSRC also provided me with the opportunity to go on a three month placement in the sunny South East during the hottest June day in 41 years (as of June 2017). To the amazing people I met while on placement, thank you for showing me a life outside of academia! The memory of ignoring work as soon as I step foot out of the door will long be cherished. In particular I would like to thank my supervisor while on placement – Sarah Barnett. Your enthusiasm for your work was really inspiring; hopefully we'll continue to stay in touch in future.

To the friends I made while at Pirbright, you've genuinely been amazing. I have no doubt I'd have quit early in my first year without your support and laughter. Especially thanks to Gennaro and Rich, for keeping in touch with constant updates on any drama as it unfolds, and Dr Hu, for being ~~one of~~ the best housemate I've had (so far, let's not get ahead of ourselves). Between the walls

of tea boxes and GÜ glasses, champagne, £35 lamb roasts, constant quiz shows, all the Parks, and blood from broken “safety glass” windows I had a pretty fun year, all things considered.

To friends at Glasgow, thanks for often being the first port of call when I needed help; it’s good to know people are there to support me when I get stubborn. Specifically, Meredith, thank you for helping with all things science and learning to snowboard with me. Watching that video of you falling over will always make me chuckle. Liz, thanks for help with SUMO related questions when I was after a quick answer, and thanks Betty for checking my writing when I was too tired to grammar check myself. Claire and Margus, thank you for constantly being on hand to answer my many, many questions about the viruses and cells I use and Jamie, thank you for making the ZIKV-nl construct, and for constantly seeing the clouds behind the silver lining (just like me). Jack and Pippa, you also wanted a mention.

Many thanks to all the members of the Boutell lab. Steven, there aren’t enough words to describe how helpful/generally amazing you are. James, Matt, and Thamir, working with you all was brilliant. I’ll fondly remember all of you complaining about writing your respective theses (it wasn’t so fun going through it myself). Victor, follow my example and you’ll be an amazing PhD. My former student Matt - thanks for being a pleasure to supervise (and giving me a 100% distinction rate from my students). Kristen, you were great fun, if I’m ever in Canada, I’ll track you down ‘eh.

Friends from the ‘Shire: First off, to be honest I’m surprised you’ve read this far, don’t worry about reading beyond this section, only Lloyd and Rob will understand bits of it (the nerds). Secondly, and more importantly, thank you for being there, thank you for still going on holidays together like we always have, thank you for reminding me that there’s a life outside of science and the PhD, and thank you for constantly getting married blowing a hole into my savings. My bank balance is all the poorer for it.

Finally, I am incredibly grateful to my grandparents for staying interested when I talk about my work, and constantly offering to send food parcels up to Glasgow

(although we do have meat in Scotland too). My sister, Jess, thank you for constantly pushing me to be better, and for constantly offering to go through my work / thesis / presentations / CV / anything else, hopefully one day I can return the favour. To my parents, thank you for your constant support, love, and snarky comments. Your retirement and subsequent holidays have made me very jealous. I hope you're proud.

"Life's not fair. And then you die."

– Denise (Mum) Stokes

"The only stupid mistake is the one you make twice"

https://photos.app.goo.gl/UH1Bns3CQpsEEmis9

- Cheese rolling, Coopers Hill, Gloucestershire

Authors Declaration

All the results presented in this thesis were obtained by the authors own efforts, unless stated otherwise.

List of Abbreviations

(-) ssRNA	negative sense single strand RNA
(+) ssRNA	positive sense single strand RNA
µg	microgram
µl	microliter
µM	micromolar
A; Ala	Alanine
A20	*Aedes aegypti* cell line
A549	Human alveolar carcinoma cells
Aa	*Aedes aegypti*
Aag2	*Aedes aegypti* cell line
AF5	Clonal population of Aag2 cells
Ago2	Argonaute 2
AMP	Adenosine monophosphate
ATG8	Autophagy-related protein 8
ATP	Adenosine triphosphate
BATV	Batai virus
BFV	Barmah forest virus
BHK	Baby hamster kidney cells
bp	base pairs
BUNV	Bunyamwera virus
C	Capsid
C; Cys	Cysteine
CCLR	Cell culture lysis reagent
CEV	Californian encephalitis virus
cGAS-STING	GMP-AMP synthesase-stimulator of interferon genes

CHIKV	Chikungunya virus
CPE	Cytopathic effect
cRNA	Complementary RNA
CVV	Cache valley virus
D; Asp	Aspartic acid
DENV	Dengue virus
DL	Distal lateral lobe
DMEM	Dulbecco's modified Eagle medium
DMSO	Dimethyl sulphoxide
DNA	Deoxyribonucleic acid
dNTP	deoxynucleotide triphosphates
dsRNA	Double stranded RNA
E	Envelope protein
E; Glu	Glutamic acid
E1	Activating enzyme
E2	Conjugating enzyme
E3	Ligating enzyme
EBV	Epstein Barr virus
EEEV	Eastern equine encephalitis virus
eIF2α	eukaryotic translation initiation factor 2α
EILV	Eilat virus
ER	Endoplasmic reticulum
FAT10	Fau-ubiquitin like protein
FBS	Foetal bovine serum
Ffluc	Firefly-luciferase
G; Gly	Glycine

G3BP	Ras-GAP SH3-domain-binding-protein
Gc	Glycoprotein at the C-terminal of the Medium segment
GFP	Green fluorescent protein
GMEM	Glasgow's minimum essential medium
Gn	Glycoprotein at the N-terminal of the Medium segment
H; His	Histidine
HEK-293T	Human embryonic kidney cells immortalised by insertion of hTERT
HFt	Human fibroblasts immortalised by insertion of hTERT
Hs	*Homo sapiens*
HSV-1	Herpes simplex virus type-1
I; Ile	Isoleucine
ICWB	In cell Western Blot
IFN	Interferon
IMD	Immune Deficiency
IRF	Interferon regulatory factor
ISG	Interferon stimulated genes
ISG15	Interferon stimulated gene 15
JAK	Janus-associated kinase
JASSA	Joined advanced SUMOylation site and SIM analyser
JCV	Jamestown canyon virus
JNK	c-Jun N-terminal kinase
K; Lys	Lysine
kb	kilobase
kDa	kilo-Daltons
L; Leu	Leucine
LACV	La Crosse virus

LacZ	ß-galactosidase
LB	Luria-Bertani broth
LPS	Lipopolysaccharide
MAYV	Mayaro virus
MED8	Mediator of polymerase II transcription subunit 8
mg	milligram
$MgCl_2$	Magnesium Chloride
MIDV	Middleburg virus
Min	minutes
miRNA	micro RNA
ML	Median lobe
ml	millilitres
mm	millimeter
MOI	Multiplicity of Infection
mRNA	messenger RNA
MyD88	Myeloid differentiation primary response 88
N	Nucelocapsid protein
NaCl	Sodium Chloride
NDUV	Ndumu virus
NEDD8	Neural-precursor-cell-expressed developmentally down-regulated 8
NEMO	NF-κB essential modulator
NF-κB	Nuclear factor kappa-light-chain-enhancer of activated B cells
ng	Nanogram
nl	Nano-luciferase
nm	Nanometres
nM	nanomolar

NOD	Nucleotide-binding oligomerization domain
NRIV	Ngari virus
ns	Not significant
NS1-5	Non-structural protein 1-5
NSm	Non-structural protein encoded by the Medium segment
nsP1-4	Non-structural protein 1-4
NSs	Non-structural protein encoded by the Small segment
o/n	Over night
ONNV	O'nyong-nyong virus
P	Phosphate
P; Pro	Proline
PAMPS	Pathogen associated molecular patterns
PBS	Phosphate buffered saline
PCR	Polymerase Chain Reaction
pfu	Plaque forming units
PGRP	Peptidoglycan recognition proteins
PIAS	Protein inhibitor of activated STAT
piRNA	Piwi-interacting RNA
PKR	Protein kinase R
PL	Proximal lateral lobe
PML	Promyelocytic leukemia protein
PML-NB	PML-nuclear body
PRRs	Pattern recognition receptors
PTM	Post-translational modification
Pup	prokaryotic ubiquitin-like protein
Q; Gln	Glutamine

QPCR	Quantitative Polymerase Chain Reaction
R; Arg	Arginine
RDRP	RNA-dependent RNA polymerase
RIDL	Release of insects carrying a dominant lethal genetic system
RIG-I	Retinoic acid inducible gene I
RISC	RNA induced silencing complex
RNA	Ribonucleic acid
RNAi	RNA interference
RNC	Ribonucleocapsid
RPB1	RNA polymerase binding protein 1
rpm	Revolutions per minute
RT	Room temperature
s	Seconds
S; Ser	Serine
SAE1/2	SUMO activating enzyme 1 / SUMO activating enzyme 2
SAP	Scaffold associating region/Acinus/PIAS
SARS	Severe acute respiratory syndrome
SCM	SUMO conjugation motif
SDS-PAGE	Sodium dodecyl sulfate-polyacrylamide gel electrophoresis
SENP	Sentrin specific protease
SESV	Southern elephant seal virus
sfRNA	subgenomic flavivirus RNA
SFV	Semliki forest Virus
SIM	SUMO interaction motif
siRNA	small interfering RNA
SLEV	St Louis encephalitis virus

SOCS	Suppressors of cytokine signalling
SPDV	Salmon pancreas disease virus
SP-RING	SP- Really Interesting New Gene
STAT	Signal transducer and activator of transcription
STUbLs	SUMO targeted Ubiquitin Ligase
SUMO	Small ubiquitin-like modifier
T; Thr	Threonine
TAM	Tyro3/Axl/Mer
TCV	Trocara virus
TLR	Toll-like receptor
TPB	Tryptose phosphate broth
TRAF	TNF receptor-associated factor
TRIM	Tripartite Motif family
TYK2	Tyrosine Kinase 2
Ubc9	Ubiquitin conjugating enzyme 9
UFM1	ubiquitin-fold modifier 1
Upd	Unpaired
UV	Ultraviolet
V; Val	Valine
VEEV	Venezuelan equine encephalitis virus
Vero	African green monkey kidney epithelial cells
vRNA	Viral RNA
WEEV	Western equine encephalitis virus
WNV	West Nile virus
XRN1	Exoribonuclease 1
YFV	Yellow Fever virus

ZIKV	Zika virus

1. Introduction

1.1. Overview

This chapter aims to inform the reader about the importance of studying mosquito vector species and the arboviruses they transmit. The clinical importance of vector-borne diseases will be covered, before describing the distribution of *Aedes aegypti* (*Ae. aegypti*), the vector responsible for the transmission of many clinically and economically important arboviruses. Further details about *alphaviruses*, *flaviviruses*, and *orthobunyaviruses* will be provided, including their clinical significance, epidemiology of disease, genome structure, and replication. The introduction will then cover post-translational modification by ubiquitin-related modifiers, specifically the Small Ubiquitin-like Modifier (SUMO) pathway. What is known about arbovirus interactions with the cellular immune response will be described, followed by what is known about SUMO-virus interactions and SUMO-arbovirus interactions.

1.2. Importance of studying vector-borne diseases

Vector-borne diseases cause of one-sixth of the human illness and disabilities suffered worldwide (WHO 2014). Diseases transmitted by vectors are also widely reported to threaten global food security. They can be a significant threat to plant health, including commercially important crops, and can lead to outbreaks of diseases amongst livestock, which result in illness, loss of productivity, and the death of large numbers of animals (Kilpatrick and Randolph 2012, Whitfield, Falk et al. 2015).

Vector-borne diseases are ubiquitous around the world, including areas inhabited by *Homo sapiens,* where ticks, midges, flies, sandflies, and mosquitoes are highly prevalent. The only areas where vector-borne diseases are not found is the Polar Regions. Each individual species of arthropod vector possess its own unique geographical distribution (Borkent 2014, WHO 2014).

Mosquitoes act as vector species to a wide range of pathogens. This includes malaria, caused by the parasite *Plasmodium falciparum*, and tularemia, caused by the bacteria *Francisella tularensis* (Ulu-Kilic and Doganay 2014). Mosquitoes are also known to be prominent vectors of viral diseases, including dengue virus (DENV), chikungunya virus (CHIKV), and Japanese Encephalitis virus (JEV). Viral diseases transmitted by the mosquito species *Aedes aegypti* will be the focus of the study.

1.2.1. Aedes aegypti

Aedes aegypti (*Ae. aegypti*) is amongst the most clinically important vector-species, it is known to be the primary vector for DENV, yellow fever virus (YFV), Zika virus (ZIKV), Semliki Forest virus (SFV), CHIKV, and Bunyamwera virus (BUNV). Together these clinically important arboviruses are responsible for endemic disease burdens in developing areas, and can cause large epidemic outbreaks of disease. Consequently, when *Ae. aegypti* comes into contact with humans there can be a massive health and economic burden (**Figure 1.1**, and

described further in **Sections 1.3.1; Section 1.3.2; Section 1.3.3**). The range of *Ae. aegypti* incorporates countries with very large populations including Brazil, India, Indonesia, and throughout South East Asia. Together, they threaten approximately half of the world's population (Bhatt, Gething et al. 2013). *Ae. aegypti* is predominantly an urban vector which utilises the abundance of artificial containers that contain stagnant water as larval sites, and feeds almost entirely on humans (Kraemer, Sinka et al. 2015).

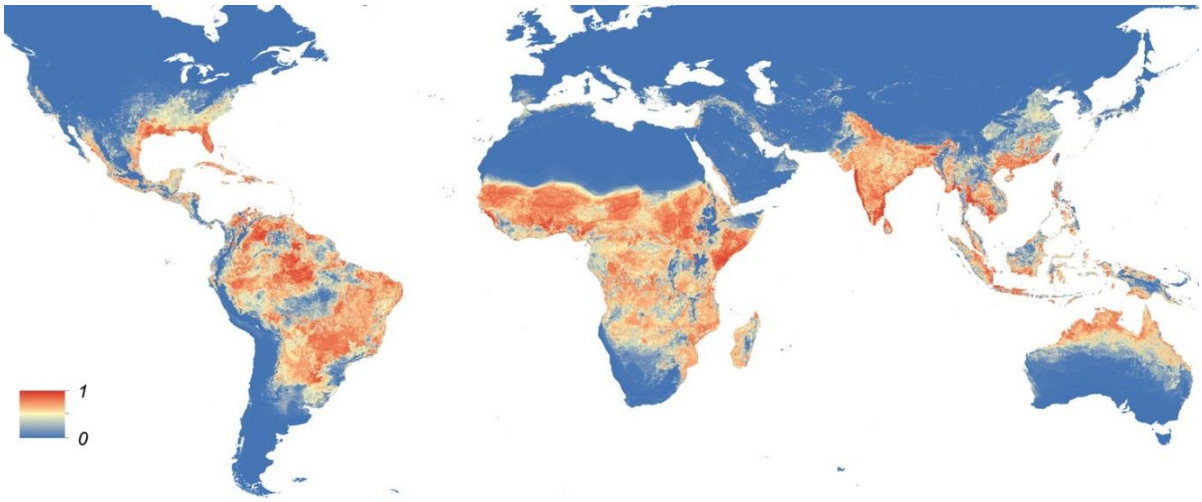

Figure 1.1 Predicted distribution of *Ae. aegypti*.

A depiction of the predicted probability that *Ae. aegypti* is located in an area (from blue 0, to red 1) from (Kraemer, Sinka et al. 2015)

As a vector species, *Ae. aegypti* is involved in a complex interplay between the human host and vector associated arboviruses. Consequently, multiple methods are currently being employed in an attempt to reduce the impact of arboviruses transmitted by *Ae. aegypti* to humans. These include the use of pesticides and habitat destruction to restrict *Ae. aegypti* population levels. The development of vaccines, such as the vaccine for yellow fever virus, 17D, and supportive treatments to alleviate symptoms are used to limit the disease burden in specific cases (Smith, Penna et al. 1938). Recently there has also been work to suppress arbovirus replication in the vector species. This can be achieved through the release of *Wolbachia* infected mosquitoes, or genetically engineering mosquitoes

to be resistant to arboviruses (Flores and O'Neill 2018). Alternative methods include the release of insects carrying a dominant lethal genetic system (RIDL) (Alphey 2014) (**Figure 1.2**). In order to develop novel strategies to further restrict arbovirus infection, interactions between *Ae. aegypti* and the arboviruses they transmit need to be better studied.

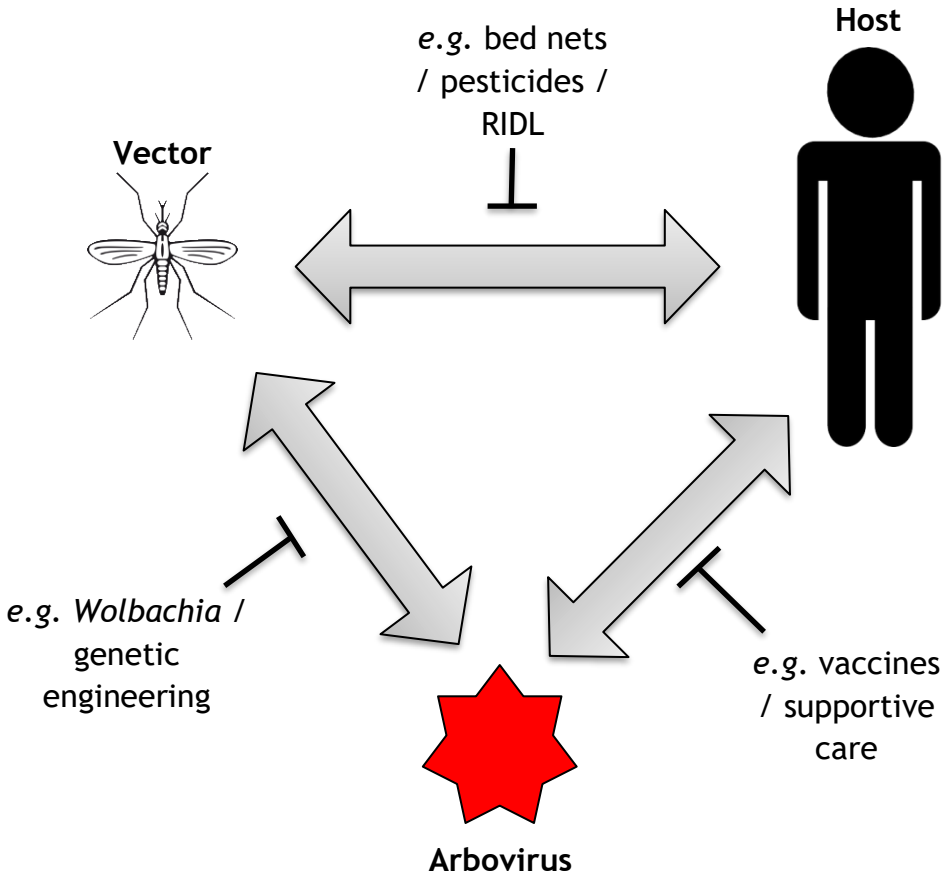

Figure 1.2 Mechanisms used to suppress arbovirus infection

Multiple mechanisms are utilised to prevent arboviral illness in humans (or other host species). Where vaccines are available, the arboviruses can be prevented from establishing an infection in the human host. For other arboviruses where no vaccines are available, supportive care may be used to alleviate symptoms. Various pesticides are used to suppress the population of mosquitoes in urban areas, and bed nets can also be used as a physical barrier preventing mosquitoes from biting and infecting people who live in areas where mosquitoes and arboviruses are endemic. Genetic engineering of mosquitoes, or infecting mosquitoes with strains of *Wolbachia* are recent techniques being utilised to suppress arbovirus replication in the mosquito, or to suppress the population of mosquitoes.

Abbreviations: RIDL, release of insects carrying a dominant lethal genetic system.

1.2.1.1. Mosquito-arbovirus interactions

Within the *Ae. aegypti* vector, arboviruses are well reported to be capable of establishing an infection in a range of cells and organs. Initially, arboviruses are taken up by *Ae. aegypti* in a blood meal from an infected vertebrate host. Consequently, the first site of infection is the midgut and the first barrier to arboviral infection is the midgut epithelium. Longitudinal and circular tracheal and muscle cells wrap around the midgut. Digestion products are absorbed and transported through the midgut into the haemolymph, which acts as the mosquito plasma (Okuda, de Souza Caroci et al. 2002). Arboviruses need to enter and successfully replicate in mosquito midgut epithelial cells, which has been shown to be a barrier to arboviral replication (Whitfield, Murphy et al. 1973, Scholle, Girard et al. 2004, Smith, Adams et al. 2008). After escaping the midgut into the haemocoel, the arbovirus needs to amplify, disseminating throughout the mosquito and infecting the salivary glands, before being transmitted horizontally to a new vertebrate host (**Figure 1.3A**). Many arboviruses can replicate in a range of insect tissues including the fat body, tracheal system, haemocytes, and nerve tissue. Very few arboviruses have been shown to be capable of replicating in muscle cells (Girard, Klingler et al. 2004, Salazar, Richardson et al. 2007, Dong, Kantor et al. 2016). Haemocytes are believed to form an important site of arboviral replication, as studies have shown over 90% of mosquito haemocytes can become infected within four days of infection (Parikh, Oliver et al. 2009, Carissimo, Pondeville et al. 2015). Arboviruses are also known to be capable of infecting mosquito ovaries. Infection of the ovaries can result in vertical transmission of the arbovirus, which can be an important mechanism for arboviral survival during unfavourable conditions (Lequime and Lambrechts 2014). Mosquito ovaries are comprised of multiple synchronous ovarioles. Ovarioles contain a germarium where follicles, or egg chambers, are initially formed. An egg chamber is capable of producing one egg, and is made up of one future oocyte and seven larger interconnected nurse cells. The egg chamber is surrounded by an epithelium of follicle cells covered by an ovarian sheath which contains muscle cells that function to slowly propel the egg chamber towards the oviduct (Snodgrass 1935, Hudson, Petrella et al. 2008) (**Figure 1.3B**). Primary follicles will develop after emergence to the previtellogenic stage, where follicle development is stopped until a blood meal.

After blood feeding, the follicle undergoes vitellogenesis. Eggs are laid two to three days after a blood meal, allowing the secondary follicles to develop into egg chambers (Nicholson 1921, Clements 1992).

Once the arboviruses have been amplified and disseminated throughout the mosquito, salivary glands need to be infected to enable the arbovirus to be injected into a new host with the saliva. The salivary glands are a pair of organs which comprise of two lateral lobes, and one shorter median lobe connected to the salivary duct (**Figure 1.3C**). Different sections of the salivary glands secrete different proteins. For instance, proteins involved in interfering with the host immune response or host haemeostasis are produced in the distal lateral lobes (Phattanawiboon, Jariyapan et al. 2014, Pingen, Bryden et al. 2016, Jin, Guo et al. 2018). Arboviruses tend to establish an infection in the mosquito salivary glands at the distal or proximal lateral lobes (Salazar, Richardson et al. 2007, Raquin, Wannagat et al. 2012, Tchankouo-Nguetcheu, Bourguet et al. 2012).

A

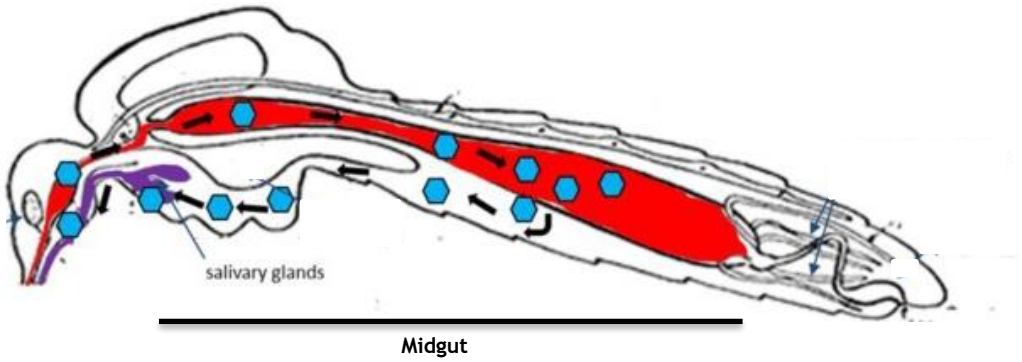

B

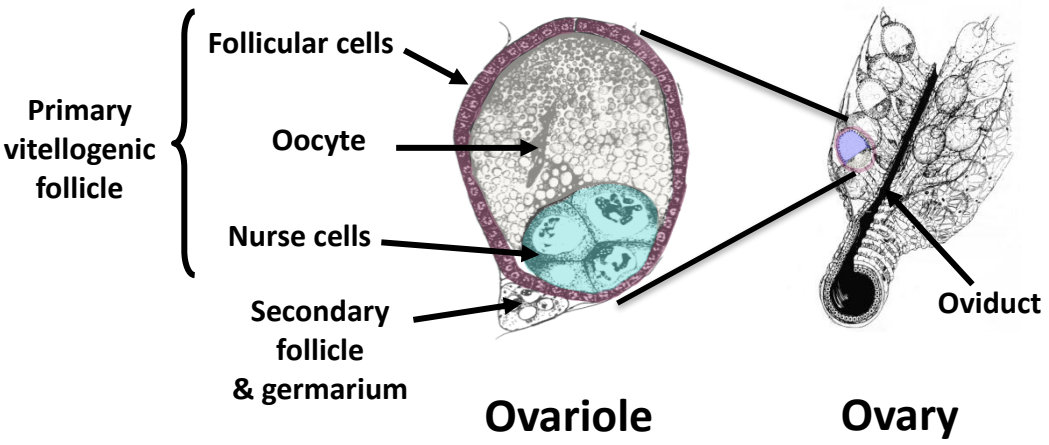

C

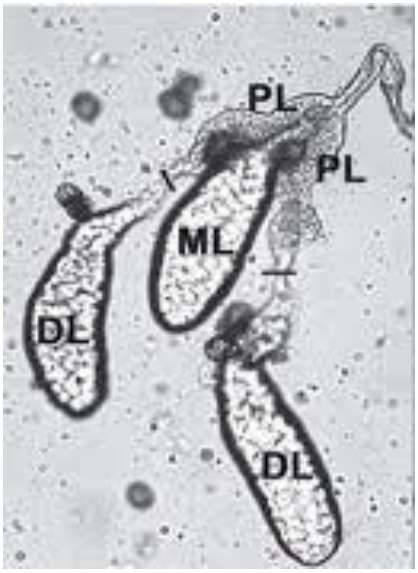

Figure 1.3 Mosquito anatomy

(**A**) A schematic of the mosquito showing the pathway arboviruses must follow to continue their life cycle. Arboviruses enter the mosquito midgut in a blood meal, replicate to escape, and disseminate throughout the mosquito until the salivary glands are infected. Arboviruses can then infect a new host. Adapted from Franz, Kantor et al. (2015). (**B**) The mosquito ovary and an individual ovariol. The ovariol is made up of the secondary follicle, germarium, and the primary vitellogenic follicle, containing nurse cells (sea green), the oocyte (grey) and follicular cells (red). Adapted from (Clements 1992) (**C**) A single adult female salivary glands comprising of two lateral lobes, separated into the proximal region (PL), and distal region (DL) and a median lobe (ML). Adapted from Jariyapan, Choochote et al. (2007)

1.3. Arboviruses

Arboviruses generally have four distinct types of genome: a single strand positive sense RNA genome (within the families *Flaviviridae* and *Togaviridae*), a genome composed of 9 to 12 segments of double stranded RNA (within the family *Reoviridae*), a genome composed of 1, 2, or 3 segments of negative sense RNA (within the families *Peribunyaviridae*, *Orthomyxoviridae, Feraviridae, Fimoviridae, Jonviridae, Nairoviridae, Tospoviridae, Phasmaviridae,* and *Phenuiviridae*), or a DNA genome (the only known DNA arbovirus is in the family *Asfarviridae*) (Hubalek, Rudolf et al. 2014, Adams, Lefkowitz et al. 2017).

There are many clinically important arboviruses that infect humans, including West Nile virus (WNV), DENV, CHIKV, and JEV. Other economically important arboviruses of livestock include Venezuelan equine encephalomyelitis virus (VEEV), bluetongue virus, and Schmallenberg virus (Mellor 2000). These viruses are emerging into new areas due to climate change resulting in an extended transmission season and increased migration of vectors. The impact of increased globalisation through travel and trade is another cause of arbovirus introduction into new areas (Semenza and Menne 2009). This results in some arboviruses, such as DENV, increasing in incidence by 30 fold since the 1960s (World Health Organization. 2012). Other arboviruses, such as ZIKV, or Keystone virus, have been known for a long time but have only recently been associated with outbreaks and disease in humans (Duffy, Chen et al. 2009, Lednicky, White et al. 2018). The life cycle of the arboviruses involves cycling between the invertebrate vector and vertebrate host (Lundstrom 1999, Mellor 2000, Hubalek, Rudolf et al. 2014). Arboviruses are transmitted from the reservoir host to a new uninfected host through a haematophagous arthropod such as a mosquito, tick, sand fly, or midge vector. These vectors may sometimes infect incidental hosts, which are animals that aren't the usual feeding source for the vector, and are usually associated with more severe clinical consequences (**Figure 1.4**). All viruses, arboviruses included, need to manipulate the host cellular system in order to survive and replicate efficiently.

Due to differences in the vertebrate host and arthropod vector, arboviruses have evolved very different replicative mechanisms for each. It has long been known

that arboviruses often establish a persistent infection in the arthropod vector, which may come with a 'fitness cost' to the vector. However, infection of mammalian cells usually results in a lytic infection, resulting in cell death (Peleg 1968, Riedel and Brown 1979, Newton, Short et al. 1981, Sirisena, Kumar et al. 2018).

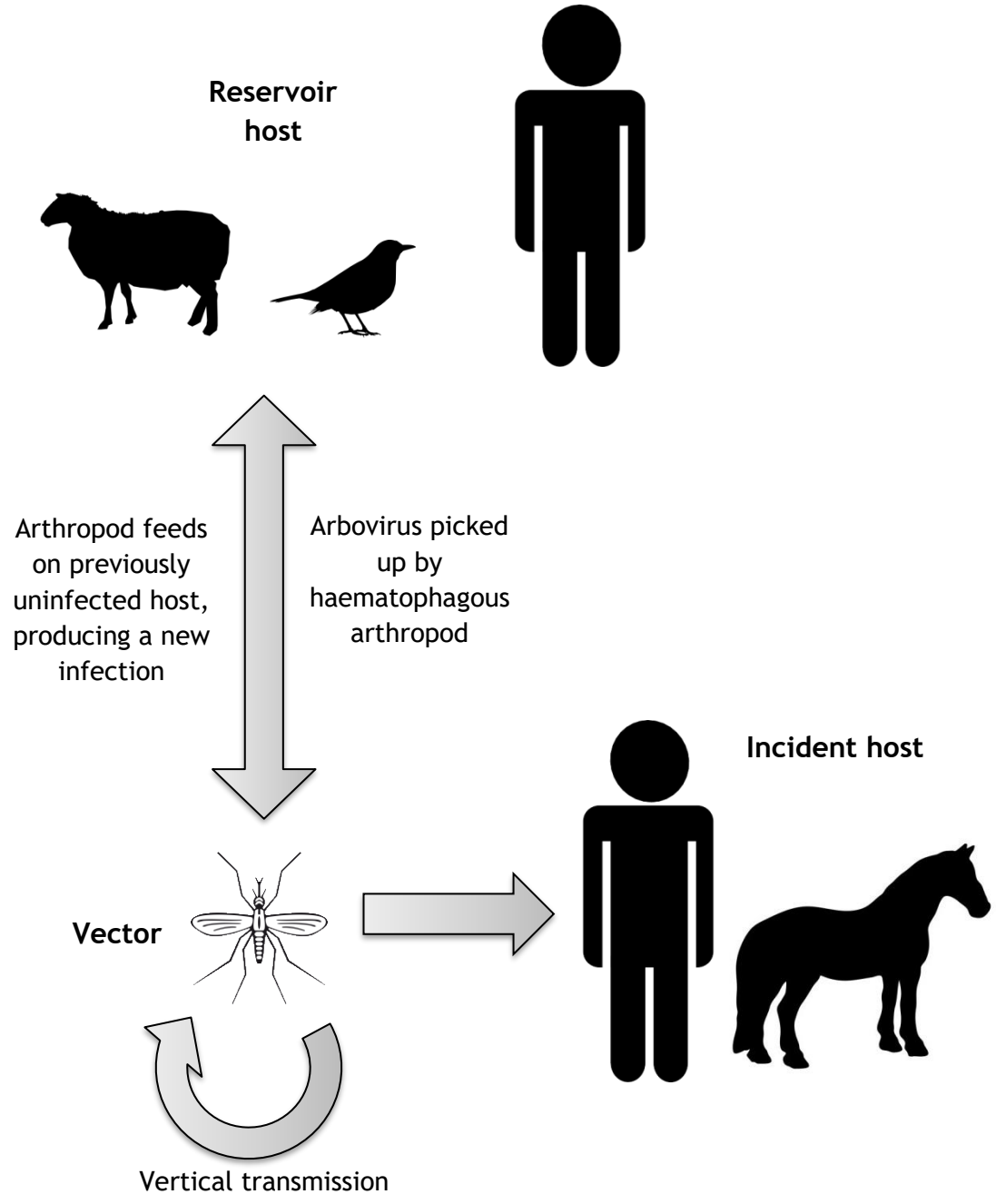

Figure 1.4 A basic arbovirus transmission cycle

The virus normally transmits between the reservoir host and the arthropod vector. Occasionally the vector infects an incident host, or the virus may be transmitted vertically to vector offspring.

There are two primary mechanisms of vertical transmission. Transovarial transmission, where the virus infects germinal cells, is generally more efficient that results in the majority of future eggs being infected (Rosen 1988). Trans-egg infection is the second mechanism, where the virus infects the eggs during egg laying. Trans-egg infection process is generally regarded as less efficient (Rosen 1988, Lequime and Lambrechts 2014). It is estimated that less than 0.1% of mosquito-based infections are due to vertical transmission and that it is only believed to be important for arboviral survival during unfavourable conditions (Lequime and Lambrechts 2014).

1.3.1. Alphaviruses

Alphaviruses are a genus within the *Togaviridae* family. The other genus in the *Togaviridae* family is Rubiviridae, whose only species is the Rubella virus (Dominguez, Wang et al. 1990). Alphaviruses are 50-70 nm in diameter and have a single strand of positive sense RNA ((+)ssRNA) approximately 10 – 11 kb in length (Fuscaldo, Aaslestad et al. 1971, Arif and Faulkner 1972, Westaway, Brinton et al. 1985, Leung, Ng et al. 2011). The genome is initially transcribed into a polyprotein of non-structural proteins 1-4 (nsP1-4), which are subsequently cleaved into the constituent proteins. A second polyprotein of structural proteins is then transcribed, translated, and cleaved (**Figure 1.5**). Alphaviruses are spherical, possess T4 icosahedral symmetry, and a total of 240 capsid protein monomers make up the capsid (Soderlund, Kaariainen et al. 1975). The envelope contains approximately 80 spikes formed of trimers of E1/E2 heterodimers (Vogel, Provencher et al. 1986). Alphaviruses are split antigenically into eleven complexes. These are the Western equine encephalitis virus (WEEV), VEEV, Eastern equine encephalitis virus (EEEV), SFV, Middelburg virus (MIDV), Ndumu virus (NDUV), Barmah Forest virus (BFV), Trocara virus (TCV), salmon pancreas disease virus (SPDV), Southern elephant seal virus (SESV), and Eilat virus (EILV) (Kaslow, Stanberry et al. 2014). MIDV, NDUV, BFV, and SESV have no recognised clinical symptoms and EILV is incapable of infecting vertebrates (Kaslow, Stanberry et al. 2014). This section will detail diseases

commonly associated with alphaviruses, their epidemiology, and their replication.

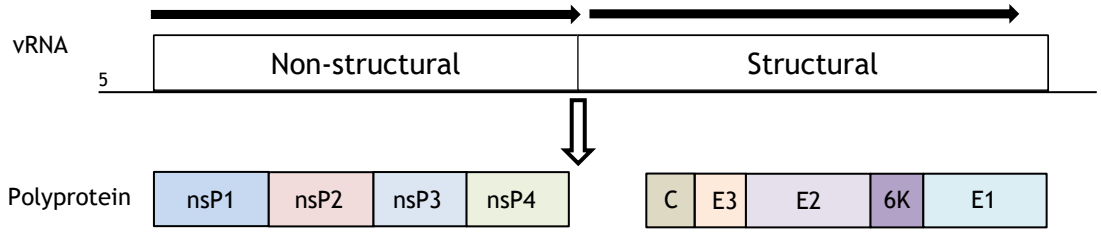

Figure 1.5 The alphavirus genome

The alphavirus genome (vRNA) is transcribed and translated into two polyproteins, the 5' region of the genome encodes the non-structural polyprotein, which is subsequently cleaved into the constituent parts (nsP1-4), while the 3' terminal of the genome encodes the structural polyprotein which is cleaved into the capsid (C), the assembly protein (E3), spike glycoprotein E1 (E1), 6K protein (6K), and spike glycoprotein E2 (E2). The individual proteins are annotated within the polyproteins.

1.3.1.1. Alphavirus epidemiology

Alphaviruses can be broadly split into two categories based on their geographical separation; Old World and New World. The Old World alphaviruses include CHIKV (primarily found in Africa, India, and South East Asia), SFV (Africa), and o'nyong-nyong (ONNV) (Africa). New World alphaviruses include VEEV (Americas) and Mayaro virus (MAYV) (South America) (Schmaljohn and McClain 1996, Paredes, Weaver et al. 2005). The distribution of alphaviruses was believed to be due to at least 2 transoceanic migratory events (Powers, Brault et al. 2001). Although, more recent data suggests that the alphavirus genus originated in the southern oceans and spread equally into the Old World and New World (Forrester, Palacios et al. 2012).

1.3.1.2. Alphavirus disease

There are two broad disease phenotypes. Old World alphaviruses, such as CHIKV, are rarely fatal. Symptoms presented are generally fever, rash, and myalgia. CHIKV infection can also result in polyarthralgia in peripheral small joints, which can last weeks to months and is generally debilitating (Deller and Russell 1968, Adebajo 1996). The arthralgia can become chronic, likely due to the virus persisting in macrophages in the joints and results in an inflammatory immune response (Toivanen 2008). During the previous 60 years there have been sporadic epidemic outbreaks of CHIKV every 2-20 years, although due to the disease similarities with DENV, other small outbreaks may have been missed (Powers and Logue 2007). A large epidemic which lasted from 2004 – 2011 and was reported in over 40 countries resulted in 1.4 – 6.5 million cases (Suhrbier, Jaffar-Bandjee et al. 2012). These were predominantly located around the Indian Ocean, with La Reunion island being severely affected in 2005-2006, resulting in a total estimated economic burden of €43.9 million (at 2006 values) (Soumahoro, Boelle et al. 2011). This outbreak was later found to be driven by a single point mutation (A266V) in the E protein (Tsetsarkin, Vanlandingham et al. 2007). There were also localised outbreaks found in some European countries (Moro, Gagliotti et al. 2010, Frank, Schoneberg et al. 2011).

New World alphaviruses, such as VEEV or EEEV, are generally associated with more severe disease phenotypes. This ranges from headaches and vomiting to encephalitis, respiratory symptoms, hematuria, seizures, and coma. Humans infected with EEEV can have a case fatality rate of between 50-70% (Zacks and Paessler 2010). VEEV results in encephalitis less frequently than EEEV, and infection generally results in flu-like symptoms. Case fatality rates in humans is low (<1%), although there are still neurological symptoms associated with infection including disorientation, mental depression, and convulsions in up to 14% of infected people (Johnson and Martin 1974). The most recent major VEEV outbreak was in 1995 in Venezuela and Colombia, where estimated 75,000 - 100,000 cases occurred (Rivas, Diaz et al. 1997).

1.3.1.3. Alphavirus replication

Alphaviruses gain entry to the cell via the viral E glycoprotein. In mosquito salivary glands, the heparin sulfate proteoglycan is believed to mediate entry, although in human tissues the cellular receptor(s) remain unknown (Ciano, Saredy et al. 2014, Vancini, Hernandez et al. 2015). This binding is believed to mediate clathrin-dependent entry into the cell (Sourisseau, Schilte et al. 2007). Low pH triggers fusion of the endosomal membrane with the viral membrane, which then allows for viral RNA (vRNA) to be released into the cytoplasm (White and Helenius 1980, Vancini, Hernandez et al. 2015).

The alphavirus genome is split into two main sections, the non-structural and structural sections (**Figure 1.5**). There is a opal 'UGA' termination codon between nsP3 and nsP4, which approximately 10% of the time is read-through. This read-through is due to the presence of the following cytosine nucleotide (as part of a 'CUA' codon). In mutational studies, the read through efficiency decreased from approximately 10% to less than 1% when the cytosine was mutated into a uracil, adenosine, or guanine (Li and Rice 1993). Isolates of SFV which have previously been found encoding an arginine amino acid instead of a stop codon expressed an increased proportion of the nsP1-4 polyprotein and were linked to increased neurovirulence (Tuittila, Santagati et al. 2000).

After being translated, the non-structural polyprotein is cleaved into the constituent proteins through the protease action of nsP2. The nsP1-4 polyprotein is initially cleaved to produce nsP1-3 and nsP4. These form an unstable replication complex which can synthesise a negative strand of vRNA (de Groot, Hardy et al. 1990). nsP1 is then cleaved off the nsP1-3 polyprotein in *trans*, resulting in nsP1, and nsP2-3. These three proteins form another replication complex which is active on the negative strand to mediate genomic vRNA synthesis (De, Sawicki et al. 1996, Kujala, Ikaheimonen et al. 2001). Negative vRNA synthesis is prevented once the cleavage of nsP1-4 is complete, and the replication complex induces replication of the positive sense vRNA (Shirako and Strauss 1994). The structural polyprotein is translated under the control of the 26S subgenomic promoter, the capsid auto-cleaves from the remainder of the polyprotein as it is being translated (Melancon and Garoff 1987). The capsid

protein is then available to associate with the region coding for nsP1 in the vRNA, ensuring full-length vRNA strands are packaged into nucleocapsid-like particles (**Figure 1.6**) (Weiss, Nitschko et al. 1989).

The envelope glycoprotein E3 signals for the remainder of the polyprotein to be transferred to the endoplasmic reticulum, where host peptidases cleave it into the constituent proteins (Lobigs, Zhao et al. 1990). Another envelope glycoprotein, 6K, acts as a signalling mechanism for the processing of the downstream E1 glycoprotein (Sanz, Madan et al. 2003). The E1 and E2 precursor glycoproteins interact to form a heterodimer (Andersson, Barth et al. 1997). This heterodimer is transported to the Golgi complex from the endoplasmic reticulum and subsequently onto the cell surface where budding occurs (Fields and Kielian 2013). During transport to the cell surface, host Furin proteases cleave the E2 precursor glycoprotein into E2 and E3 (Zhang, Fugere et al. 2003, Fields and Kielian 2013). Upon release from the cells, an envelope is acquired from the host cell plasma membrane. This process has been shown to occur quickly, with SFV replication in chick embryo cells occuring at a rate of 200 plaque forming units/cell/hour (Acheson and Tamm 1967).

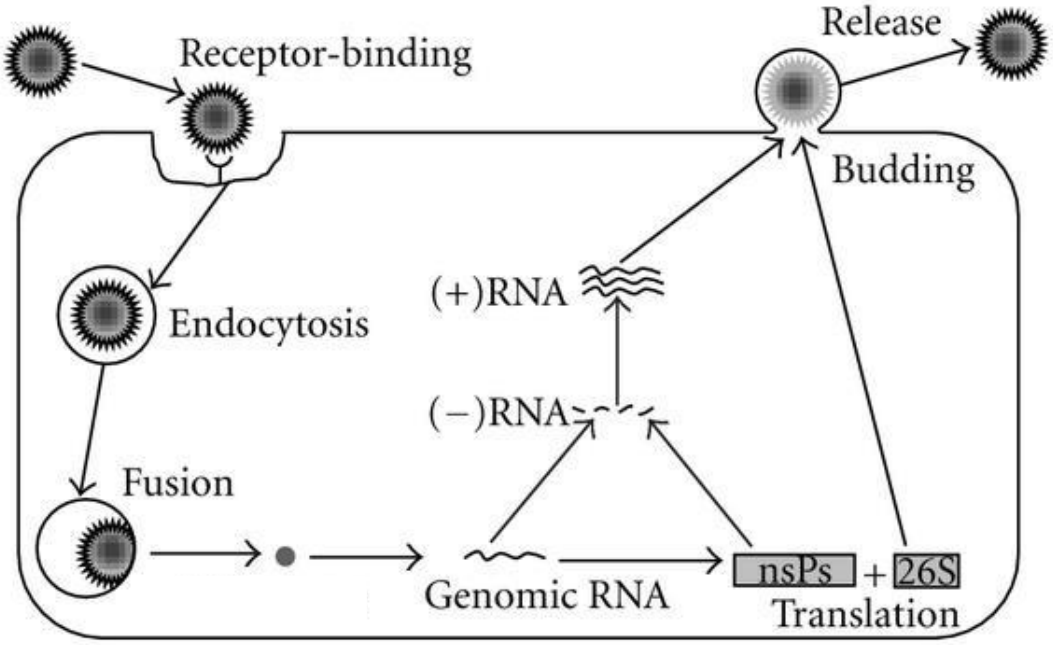

Figure 1.6 Alphavirus life cycle

Alphaviruses are initially endocytosed into the cell through the viral E glycoprotein. The drop in pH results in fusion of the endosomal and viral membranes. Genomic RNA is released into the cytoplasm initially translating the non-structural polyprotein (nsPs). An unstable complex of nsP1-3 and nsP4 can synthesise a negative sense RNA ((-)RNA) genome which functions as a template for future positive strands of viral RNA ((+)RNA) to be produced. The structural proteins are translated under the control of an internal 26S subgenomic promoter. The (+)RNA and structural proteins migrate to the Golgi complex, followed by budding at the cell surface and release into a new envelope of host cell membrane. Adapted from Leung, Ng et al. (2011)

1.3.2. Flaviviruses

Flaviviruses are a genus in the *Flaviviridae* family. Other members of the *flaviviridae* family include the genus pegivirus, pestivirus, and hepacivirus, which contain hepatitis C virus (HCV). This genus contains some of the most clinically important arboviruses, including DENV, JEV, WNV, and ZIKV. Most of the viruses in the flavivirus genus are transmitted by arthropods, and are approximately 40-65 nm in diameter (Smith, Brandt et al. 1970, Yang, Kim et al. 2004). The genome of a flavivirus is a single strand of positive sense RNA which is approximately 11 kb in length (Yaegashi, Vakharia et al. 1986). The genome consists of one open reading frame which produces a poly-protein that is cleaved into a total of 11 proteins during and after translation and maturation (**Figure 1.7**) (Cleaves 1985). DENV, one of the most well studied flaviviruses, comprises a capsid protein which forms a complex with the RNA genome. Approximately 180 envelope (E) and 180 membrane proteins are found in the outer lipid envelope in a T=3 icosahedral symmetry (Zhang, Chipman et al. 2003, Strauss and Strauss 2008, Byk and Gamarnik 2016). Flaviviruses are distributed over a large geographical range and rapidly spread into new ecological niches (Mutebi, Rijnbrand et al. 2004). Most flaviviruses use birds and small mammals as natural hosts. Humans can also be hosts, capable of amplifying the virus to titres high enough to establish a new infection in a naïve mosquito. Only a relatively small proportion of infections result in deadly diseases (Solomon and Mallewa 2001).

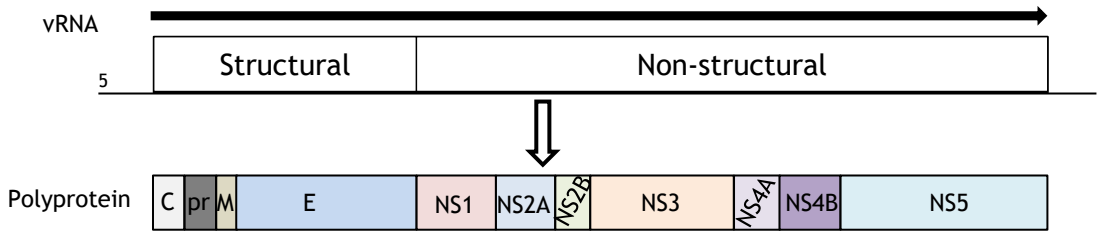

Figure 1.7 The flavivirus genome

The flavivirus genome (vRNA) is transcribed and translated into one polyprotein. The 5' region of the genome and polyprotein encodes the structural proteins (the capsid protein (C), peptide pr (pr), small envelope protein M (M), and envelope protein (E)). The 3' region of the genome and polyprotein encodes the non-structural proteins (non-structural proteins 1-5 (NS1-5). The final cleaved proteins are indicated within the polyprotein.

1.3.2.1. Flavivirus epidemiology

Flaviviruses which infect humans can be broadly split into three categories, those with no known vectors, those which use ticks as vectors, and those which use mosquitoes as vectors (Kuno, Chang et al. 1998, Gaunt, Sall et al. 2001). The mosquito borne flaviviruses can be further categorised into those which cause neurotropic diseases, such as JEV, and those which cause haemorrhagic diseases, such as DENV (Gaunt, Sall et al. 2001). Generally, flaviviruses which cause neurotropic diseases are transmitted by *Culex* species of mosquito, while flaviviruses associated with haemorrhagic diseases are more commonly transmitted by *Aedes* species of mosquito (Waddell and Taylor 1948, Haddow, Williams et al. 1964, Chamberlain, Gogel et al. 1966, Mattingly 1967, Nir, Goldwasser et al. 1968, Sucharit, Surathin et al. 1989). Flaviviruses are distributed throughout the world, with specific geographic spreads dependent on the vector. Generally, flaviviruses transmitted by mosquitoes are located around the tropics, such as India and South East Asia, and flaviviruses transmitted by ticks are more commonly located in the cooler climates, such as Russia or Northern Europe (Solomon and Mallewa 2001).

Flaviviruses are believed to have originated from a common ancestor approximately 10,000 years ago in Africa (Billoir, de Chesse et al. 2000, Solomon and Mallewa 2001). It is believed that the tick-borne lineage diverged, prior to the mosquito-borne lineage (Gaunt, Sall et al. 2001, Mackenzie, Gubler et al. 2004).

1.3.2.2. Flavivirus disease

There are three main disease phenotypes associated with flavivirus infection. These are neurological, viral haemorrhagic fever, and fever–arthralgia–rash symptoms (Solomon and Mallewa 2001). Neurological symptoms, such as encephalitis, can be caused by TBEV, JEV, and St Louis encephalitis virus (SLEV). An example of a haemorrhagic virus is DENV, or YFV.

The neurotropic flavivirus, JEV, is regarded as the most important cause of mosquito-borne encephalitis in Asia and the Western Pacific (WHO 2015, Simon and Kruse 2018). Approximately 1 in 250 infections develop symptoms, which may include headache, fever, tremors, coma, and encephalitis. Up to 33% of symptomatic cases are fatal (NHS 2016). Each year there are between 60,000-70,000 cases of JEV, which predominantly affects children, as infection results in lifelong immunity (WHO 2015).

Haemorrhagic flaviviruses, which include DENV and YFV, are regarded as the most important arbovirus. This is due to their global distribution and significant clinical burden. It is estimated that half the world's population is at risk of DENV infection, with approximately 390 million people being infected each year (Bhatt, Gething et al. 2013, WHO 2018). Of these, it is predicted that 96 million develop symptoms that include headache, muscle and joint pains, high fever (~105 ˚F / 40 ˚C), rash, vomiting, and swollen glands (Harris and Duval 1924, WHO 2018). Symptoms generally develop 3-15 days following the bite from an infected mosquito and may last between 2-7 days (WHO 2009). Haemorrhagic fever may develop as a consequence of plasma leaking from blood vessels which can result in severe bleeding, fluid accumulation, respiratory distress, or organ failure. There are five distinct DENV serotypes (DENV-1, DENV-2, DENV-3, DENV-4, and DENV-5, although there is currently debate about whether DENV-5 exists) (Mustafa, Rasotgi et al. 2015). All serotypes appear to be able to circulate within the same population, although one serotype tends to dominate (Singh, Maitra et al. 1999, Dash, Parida et al. 2006, Shrivastava, Tiraki et al. 2018).

ZIKV is another flavivirus closely related to DENV. ZIKV was identified in Zika forest in 1947, initially associated with only mild clinical symptoms in approximately 20% of cases until the 2015 outbreak in South and Central America (Dick, Kitchen et al. 1952). During this outbreak, ZIKV infection was found to correlate with an increase in the number of cases of Guillain-Barré Syndrome and foetal microcephaly (Oehler, Watrin et al. 2014, Rasmussen, Jamieson et al. 2016, Styczynski, Malta et al. 2017, Wen, Song et al. 2017). This could be due to the effect of ZIKV NS4A and NS4B proteins, which disrupts the Akt-mTOR signalling pathway. The Akt-mTOR signalling pathway is known to have roles in cell development, proliferation, and inhibition of autophagy. Consequently, a

dysregulated Akt-mTOR pathway during neuronal development can lead to microcephaly (Liang, Luo et al. 2016).

1.3.2.3. Flavivirus replication

As arboviruses, the flaviviruses studied here replicate in both mammalian and insect cells. The replication strategy has been shown to be similar in the host and vector species. Generally, entry of flaviviruses into cells follows a similar mechanism to alphaviruses (Strauss and Strauss 2008). Flaviviruses bind the external viral E protein to a cellular receptor that trigger internalisation through specific cell-type dependent mechanisms (Ang, Wong et al. 2010, Piccini, Castilla et al. 2015). The cellular receptor varies depending on the flavivirus; DENV has been reported to bind to heparin sulfate, while ZIKV has been reported to bind to DC-SIGN, AXL, Tyro3, and TIM-1 in human skin cells (Chen, Maguire et al. 1997, Hamel, Dejarnac et al. 2015). Once the virus has been imported into endosomes, the fall in pH resulted in E-homodimers forming E-homotrimers (Zhang, Zhang et al. 2004, Huang, Butrapet et al. 2010). The E-homotrimers then reorientate so the fusion peptide is able to fuse the viral membrane with the host membrane. This results in the release of the viral genome into the cytoplasm. As flaviviruses possess a genome consisting of a single strand of positive sense RNA ((+)ssRNA), the genome is directly translated into a polyprotein which is cleaved into the individual constituent proteins by the auto-catalytic NS3/NS2B enzymes and host cell proteases, including furin and signal peptidase (Bazan and Fletterick 1989, Falgout, Chanock et al. 1989, Markoff 1989, Chambers, Grakoui et al. 1991, Stadler, Allison et al. 1997). NS5, the viral polymerase molecule is capable of synthesising a double strand RNA (dsRNA) viral genome (Chu and Westaway 1987, Guyatt, Westaway et al. 2001). The dsRNA genome is then transcribed into more viral (+)ssRNA, and translated into the polyprotein. This process occurs in cytoplasmic replication factories, prior to viral assembly occurring on the rough endoplasmic reticulum (Welsch, Miller et al. 2009, Cortese, Goellner et al. 2017). Progeny viruses are then transported to the Golgi apparatus and exocytosed at the cell surface (Hase, Summers et al. 1987) (**Figure 1.8**). Interestingly, in mosquito cells, some flaviviruses, such as

DENV-2, appear to mature in nucleocapsid-like structures in the cytoplasm. Virions then bud at the plasma membrane or into cytoplasmic vacuoles (Hase, Summers et al. 1987).

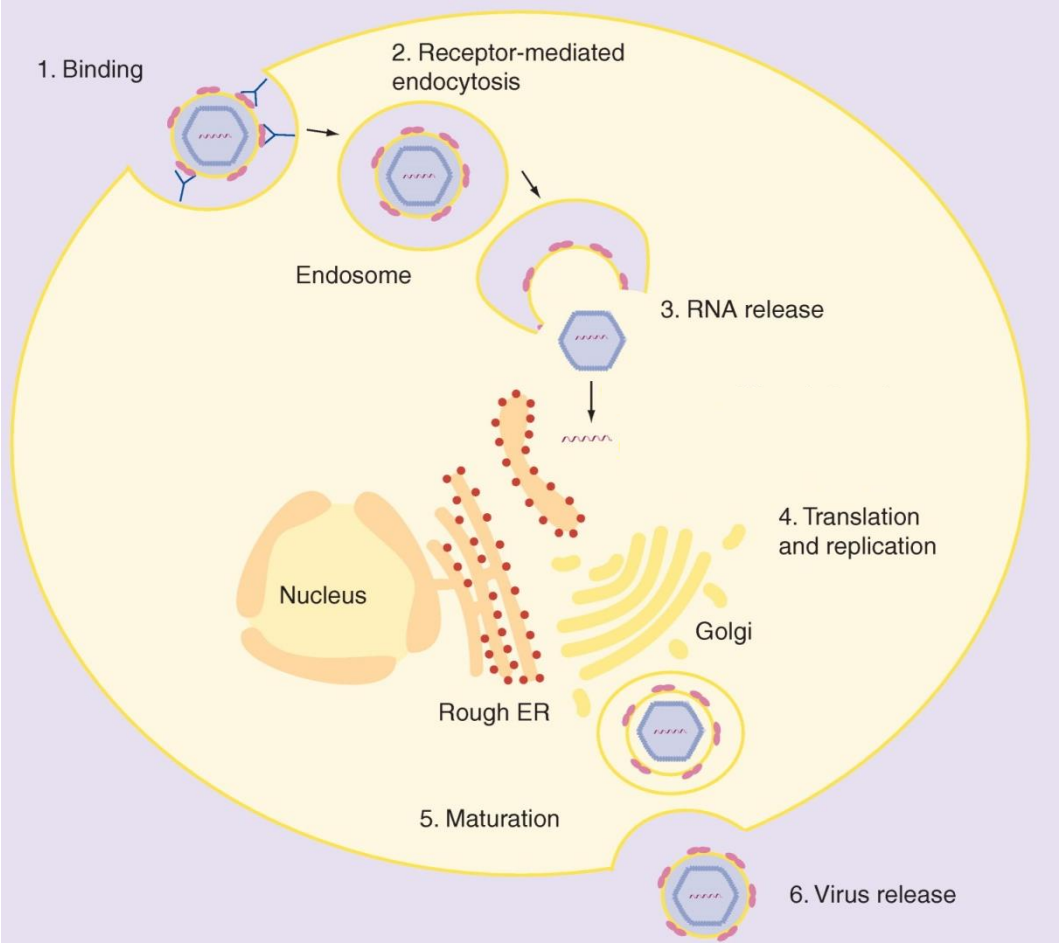

Figure 1.8 Flavivirus life cycle

(1) A flavivirus E protein binds to a virus specific cellular receptor. (2) The virus enters the cell through receptor-mediated endocytosis. (3) Fall in pH causes a conformational change resulting in the viral RNA genome being released into the cytoplasm. (4) Genome is translated into a polyprotein which auto-cleaves. NS5 functions as a polymerase which is responsible for replication of viral genome. Viral assembly occurs on the rough endoplasmic reticulum (Rough ER). (5) Progeny viruses are transported to the Golgi for maturation and transport to the cell surface. (6) Virus is released from the cell surface. Adapted from Bartenschlager and Miller (2008).

1.3.3. Orthobunyaviruses

Orthobunyaviruses are a genus of the *Peribunyaviridae* family, within the *Bunyavirales* order. There are over 170 viruses in the *orthobunyavirus* genus (Calisher 1996). The prototype species is BUNV. Most viruses in this genus are arboviruses, with a virion diameter of approximately 80-120 nm (Obijeski, Bishop et al. 1976, Talmon, Prasad et al. 1987). Heterodimers of envelope glycoproteins form on the surface of the virion. Orthobunyaviruses possess a genome made of three single strands of negative sense RNA ((-)ssRNA); termed the Small (S), Medium (M), and Large (L) segments (**Figure 1.9**). BUNV is reported to be pleomorphic in shape with locally-ordered lattices of glycoprotein spikes (Bowden, Bitto et al. 2013). Due to segmented structure of the genome, it has the potential to naturally re-assort genome segments between strains co-infecting the same host cell.

The viral genome comprises three single strands of negative sense RNA of approximately 1 kb, 4.5 kb, and 6.5 kb. The S segment transcribes two genes, the nucleocapsid protein (N), and a non-structural (NSs) protein (Elliott 1989). The M genome translates a polyprotein which is cleaved into a non-structural protein (NSm), and two glycoproteins (Gn, and Gc, corresponding to the location on the N- or C- terminal) (Lees, Pringle et al. 1986). The L genome translates a large protein which serves as the RNA-dependent RNA polymerase (RDRP) (**Figure 1.9**) (Elliott 1989).

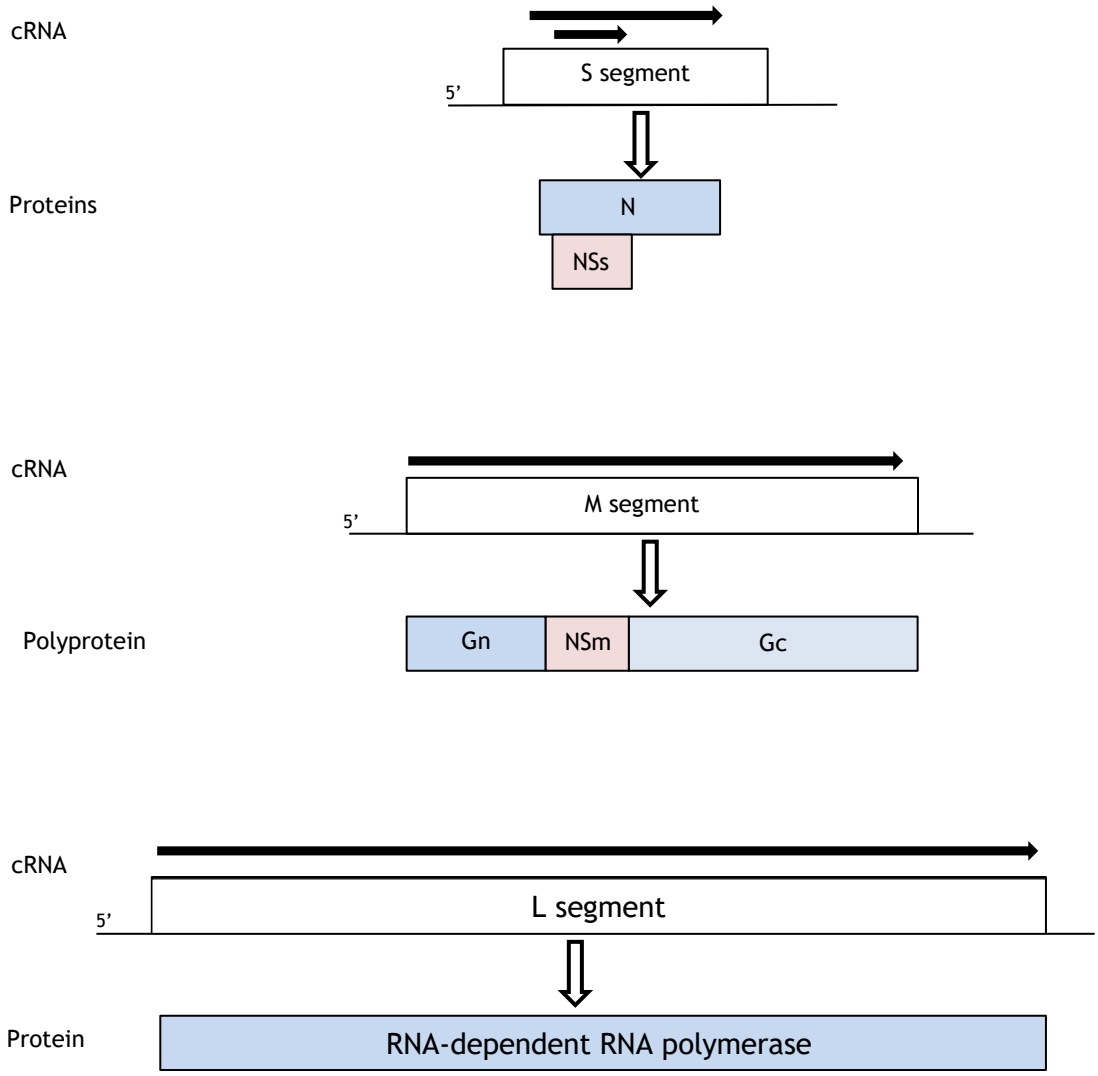

Figure 1.9 The *orthobunyaviridae* genome

Orthobunyaviridae have a genome comprising three single strands of negative sense RNA which is used to produce complementary RNA (cRNA) that is then transcribed and translated. The S segment encodes both the nucleocapsid protein (N) and an overlapping genomic region encodes the non-structural protein (NSs). The M segment encodes a polyprotein that is cleaved to produce Glycoproteins Gn and Gc, and a non-structural protein (NSm). Finally, the L segment encodes the RNA-dependent RNA polymerase.

1.3.3.1. Orthobunyavirus epidemiology

Within the *orthobunyavirus* genus, there is the clinically important Bunyamwera serogroup that contains the prototype virus, BUNV. Other notable members of the Bunyamwera serogroup include Ngari virus (NRIV), Batai virus (BATV), and Cache Valley virus (CVV). BATV has been identified throughout Europe and Asia, while BUNV is predominantly distributed throughout Africa (Smithburn, Haddow et al. 1946, Kokernot, Smithburn et al. 1958, Bardos and Cupkova 1962, Liu, Shao et al. 2014). NRIV is a naturally occurring recombinant virus comprising of BATV M segment, and BUNV S and L segments (**Section 1.3.3.3**) (Yanase, Kato et al. 2006). As NRIV is a recombinant of BATV and BUNV. NIRV can be vectored by a wide range of mosquito species, including *Aedes*, *Culex*, and *Anopheles*. Consequently, it has a broad geographical spread throughout Europe, Central, and Eastern Asia (Bardos and Cupkova 1962, Singh and Pavri 1966, Yadav, Sudeep et al. 2012, Liu, Shao et al. 2014). To date, BATV has only been isolated in Africa once (Briese, Bird et al. 2006). However, due to the presence of vector species and the existence of NRIV, BATV distribution is believed to be severely underreported. Other viral members of this serogroup, such as CVV, are found distributed throughout North America, and can be spread by *Ae. aegypti*, although the evolutionary history of these viruses remains unknown (Holden and Hess 1959, Edwards, Higgs et al. 1998, Dutuze, Nzayirambaho et al. 2018).

1.3.3.2. Orthobunyavirus disease

There are a range of disease phenotypes experienced by people infected with *orthobunyaviruses*. Those infected with members of the California serogroup of *orthobunyaviruses,* such as La Crosse Virus (LACV), Californian encephalitis virus (CEV), or Jamestown Canyon virus (JCV), ranges from mild febrile disease to fatal encephalitis (CDC 2018). Most symptomatic cases experience sudden fever, followed by headache, fatigue, and vomiting, although symptoms usually end within 7 days. Up to half of cases may experience seizures, but fatalities are rare (<1%) (CDC 2018).

Within the *bunyamwera* serogroup, BUNV, BATV, and NRIV are known to cause disease in both humans and animals. BUNV infection generally results in mild symptoms, if any, which include fever, headache, joint pain, rash and occasional CNS symptoms (Southam and Moore 1951, Kokernot, Smithburn et al. 1958). BATV infection may result in flu-like symptoms in humans, although it has a more severe disease phenotype in ruminants, which includes abortions and premature births (Hubalek 2008). NRIV can result in more severe clinical symptoms, including haemorrhagic fever (Bowen, Trappier et al. 2001). NRIV has also been associated with a large outbreak in Sudan in 1988, although reported symptoms were less clinically severe (Nashed, Olson et al. 1993, Groseth, Weisend et al. 2012).

1.3.3.3. Orthobunyavirus replication

Generally, the viral Gn-Gc heterodimer binds to the cell receptor, enabling the virus to undergo endocytosis into the cell (Schmaljohn, Connie et al. 2007). The viral membrane fuses with the vesicle membrane after acidification of the vesicle, due to a conformational change in Gc, allowing the viral genome to be released (Gonzalez-Scarano, Janssen et al. 1985). Initially, viral cDNA of the S and L gene is transcribed through the action of virion-associated RDRP, the viral mRNA is then translated into the N, NSs, and RDRP proteins by free ribosomes. The M gene is translated by ribosomes bound to the endoplasmic reticulum, to produce Gc, Gn, and NSm. Gn and Gc are transported to the Golgi through Golgi targeting signals in Gn for viral assembly (Lappin, Nakitare et al. 1994, Shi, Lappin et al. 2004).

A switch occurs from protein synthesis to viral replication, through a currently unknown mechanism. RDRP transcribes more viral genome in the cytoplasm. vRNA and complementary RNA (cRNA) are both encapsidated by the N protein, although with a higher affinity for vRNA (Severson, Partin et al. 1999, Kaukinen, Koistinen et al. 2001). This produces the ribonucleocapsid, which serves as an anti-termination signal enabling the entire genome to be synthesised (Eifan and Elliott 2009). Orthobunyaviruses usually mature by budding at smooth

membranes of the Golgi. A build-up of Gn and Gc proteins in the Golgi triggers viral assembly. The ribonucleocapsid carrying S, M, and L genes localizes to the Golgi, for some viruses in the *bunyavirales* order, including Seoul virus and Hantaan virus, this has been shown to be through interactions with the Human Small Ubiquitin-like Modifier-1 (SUMO1), the SUMO conjugating enzyme (Ubc9), and the Protein Inhibitor of Activated STAT (PIAS) 1, and PIAS2β (Lee, Yoshimatsu et al. 2003, Maeda, Lee et al. 2003). After budding at the Golgi, the virion is released from the cell by exocytosis due to signalling by the Gn cytoplasmic tail (**Figure 1.10**) (Överby, Pettersson et al. 2007).

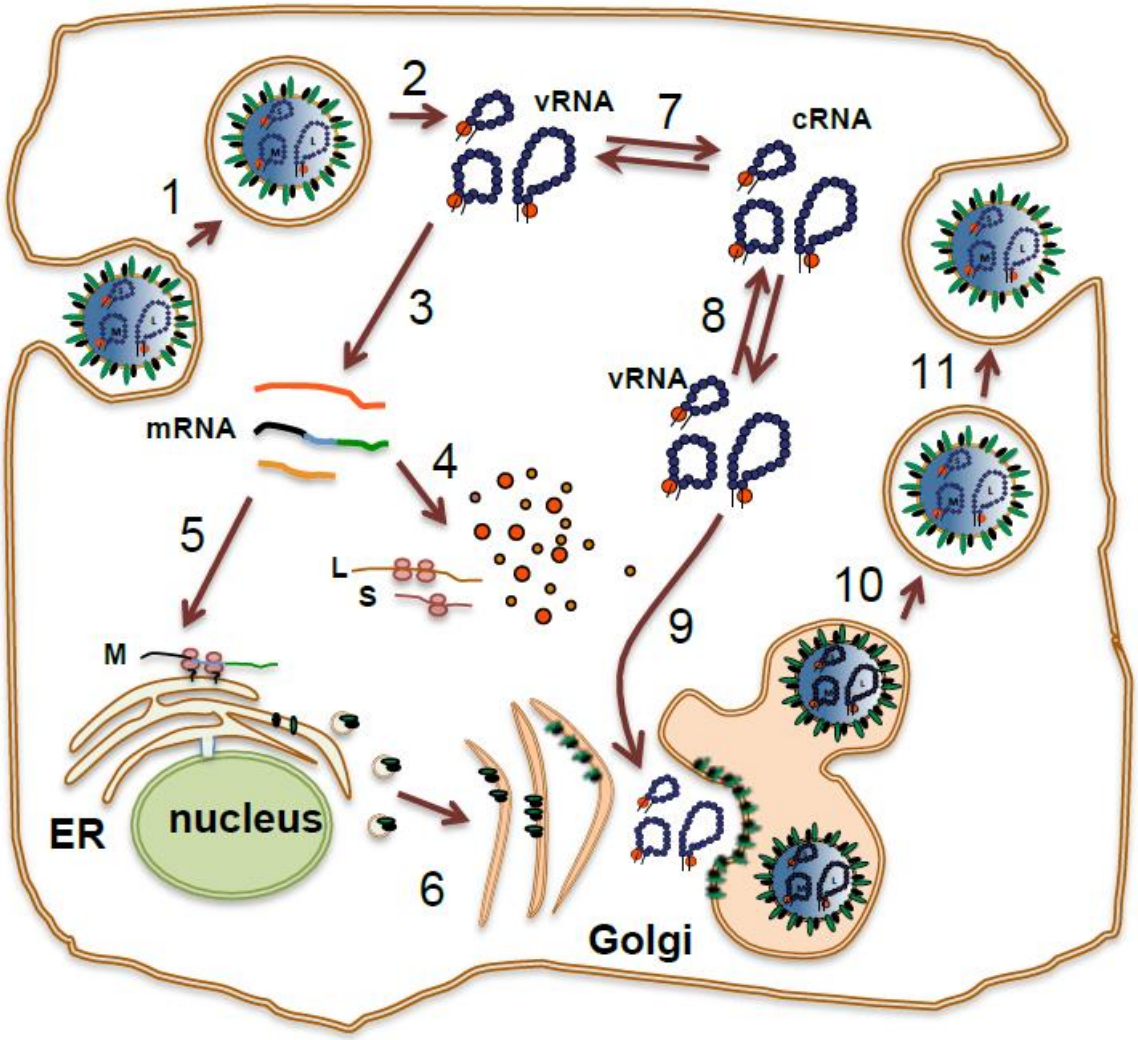

Figure 1.10 Orthobunyavirus life cycle

(1) The orthobunyavirus enters through pH mediated endocytosis. (2) pH induced conformational change allows the release of viral RNA (vRNA) into the cytoplasm. (3) vRNA is transcribed into viral mRNA by virion associated RNA-dependent RNA polymerase (L). (4) The viral mRNA is translated into the L, nucleocapsid and non-structural proteins (S) by cytoplasmic ribosomes. (5) The viral mRNA from the M genome is translated into a polyprotein by ribosomes attached to the endoplasmic reticulum, the polyprotein is then cleaved into the glycoproteins Gn, and Gc, and the non-structural NSm protein. (6) Gn-Gc heterodimers localize to the Golgi for virus assembly. (7, 8) Replication of vRNA is required to build-up sufficient quantities of genomic vRNA to be packaged into virions. (9) Ribonucleocapsids of S, M, and L segments are transported to the Golgi to be packaged with the Gn-Gc glycoproteins. (10, 11) The virus undergoes exocytosis into the extracellular space. From Szemiel (2011).

1.4. Post-translational modification

The post-translational modification (PTM) of proteins plays an important role in the regulation of protein function within cells. PTMs can do this by providing a new charge or surface that influences protein-protein interactions, conformational structural changes, and catalytic or substrate binding properties of target proteins. Some well-characterised examples of PTMs include glycosylation, methylation, phosphorylation or acetylation. Along with these, the addition of small proteins or chains of proteins can be added onto acceptor sites of target proteins undergoing modification. Ubiquitin and related family members, including Small Ubiquitin-like MOdifier (SUMO) are key examples of such protein PTMs that influence target protein function or sub-cellular location.

This section will focus on the ubiquitin family of PTMs, which is a group of nine members including ubiquitin, SUMO, Neural-precursor-cell-expressed developmentally down-regulated 8 (Nedd8), Interferon-Stimulated Gene 15 (ISG15), Fau-ubiquitin like protein (FAT10), Autophagy-related protein 8 (ATG8), and Ubiquitin-fold modifier 1 (UFM1) (Pickart and Eddins 2004, Hochstrasser 2009). These members all display similar structural homology but very divergent amino acid identity. For instance, there is only ~20% amino acid sequence identity between human ubiquitin and human SUMO1 (Bayer, Arndt et al. 1998). Another shared characteristic of all members of the ubiquitin-like family is the C-terminal diglycine motif, which is only exposed after proteolysis of the terminal region (Pickart and Eddins 2004). This terminal diglycine is responsible for enabling the mature ubiquitin family of proteins to modify the target protein through the formation of an isopeptide bond to lysine residues found within target substrate proteins.

1.4.1. Ubiquitin

Ubiquitin, the founding member of the family, was initially identified in 1975 as an inducer of differentiation of T-cells and B-cells. Ubiquitin was identified in animal cells, yeast, and higher plants using radioisotope studies (Goldstein, Scheid et al. 1975). Using this method ubiquitin was also identified in bacteria.

It was therefore believed to be found universally throughout life and given the name ubiquitin (Goldstein, Scheid et al. 1975). Later work showed that ubiquitin was only found in eukaryotic organisms (Rechsteiner 1988, Gottesman 1989). Bacteria have been shown to possess a ubiquitin-like pathway, called prokaryotic ubiquitin-like protein (Pup), which performs a similar biological function to ubiquitin (Pearce, Mintseris et al. 2008).

The ubiquitination pathway involves a three step enzymatic cascade comprised of an activating enzyme (E1), conjugating enzyme (E2), and ligating enzymes (E3) (Scheffner, Nuber et al. 1995). The enzymes exist in a hierarchical structure. There are two known activating enzymes in humans (Pickart 2001), and 35 E2 enzymes. The larger number of E2 enzymes is due to their selective interactions with the E3 ligating enzymes. There are hundreds of E3 ligating enzymes, which provide specialised substrate protein interactions and functions (Pickart 2001, van Wijk and Timmers 2010). One of the best-understood biological roles for ubiquitin is ATP dependent protein degradation through the 26S proteasome. Poly-ubiquitin chains are covalently bound to the target protein, which then activate subunits of the proteasome that subsequently degrade the modified protein (Elsasser, Gali et al. 2002, Kerscher, Felberbaum et al. 2006).

Various forms of PTM have been shown to influence arboviral replication. For instance, the E2 ubiquitin conjugating enzyme, UbcH10, is usually downregulated in cells following CHIKV infection. Studies which over expressed UbcH10 resulted in reduced cellular susceptibility to CHIKV infection indicating a role for ubiquitin conjugation in suppressing CHIKV replication, although no precise mechanism was identified (Treffers, Tas et al. 2015). Furthermore, nsP2 from CHIKV and SFV have been shown to avoid the cellular transcriptional shut off by targeting RNA polymerase binding protein 1 (RPB1), a catalytic subunit of RNA Polymerase II, for ubiquitin mediated degradation (Akhrymuk, Kulemzin et al. 2012). Demonstrating that arboviruses hijack the ubiquitin pathway to benefit arboviral replication. Furthermore, a recently identified mosquito ubiquitin, named Ub3881, has been identified in mosquitoes to possess antiviral activity against DENV infection. DENV infection was found to downregulate expression of Ub3881, and overexpression studies indicate Ub3881 was required

to target DENV envelope protein for degradation, decreasing the number of infectious virions produced. Further depletion studies in mosquito cell culture and mosquitoes correlated with an increase in DENV replication, although it was not statistically significant (Troupin, Londono-Renteria et al. 2016).

1.4.2. Overview of the Small Ubiquitin-like MOdifer (SUMO) protein

This section aims to provide an overview of the SUMO modification pathway. PTM by SUMO can result in a range of altered biological roles, including protein localisation, protein-protein interactions, and regulation of gene expression through the modification of transcription factors (Geiss-Friedlander and Melchior 2007, Cubenas-Potts and Matunis 2013). SUMO can also modify proteins through multiple mechanisms, including both covalent and non-covalent interactions. Various types of SUMO interactions include: covalent mono-SUMOylation bonds to SUMO conjugation sites on a target protein, covalent poly-SUMO chains on a target protein, or non-covalent interactions mediated by SUMO Interaction Motifs (SIMs) within target proteins. SUMO can also interact with the ubiquitin pathway through competitively binding to the same lysine residue on the substrate proteins thereby preventing protein degradation, or by acting as a signal for poly-ubiquitin chain formation mediated by SUMO targeted Ubiquitin ligases (STUbLs), such as RING finger protein 4 (RNF4), thereby promoting protein degradation (Pickart and Eddins 2004, Miteva, Keusekotten et al. 2010). SUMO modification has been shown to be involved in cellular immunity helping the cell overcome viral infection. This can occur through the actions of SUMO modification of RIG-I, enhancing its interaction with the downstream acceptor molecule Cardif, which increases the expression of IFN (Mi, Fu et al. 2010). Melanoma differentiation associated gene 5 (MDA5) has also been reported to be SUMOylated, resulting in an increase in IFN expression (Fu, Xiong et al. 2011). One member of the Tripartite Motif family (TRIM) of proteins, TRIM19, or promyelocytic leukaemia (PML) protein, contains three SIM sites, and four SUMO conjugation motif (SCM) sites, and has been shown to possess antiviral activity against a range of viruses including herpesviruses, papillomaviruses and

retroviruses (Maul, Ishov et al. 1996, Mossman, Saffran et al. 2000, Everett 2001, Shen, Lin et al. 2006).

SUMO is known to have roles in cell cycle progression, and dysregulation of the SUMOylation pathway has well documented roles in cancer (Seeler and Dejean 2017). SUMO also plays a role in the development of both mammals and *Drosophila*. Many signalling pathways with roles linked to embryonic development are known to be regulated by SUMO. For instance, SUMO negatively regulates JNK signalling that is responsible for dorsal closure in embryos, thorax closure in pupae, and stress induced apoptosis (Igaki 2009, Huang, Du et al. 2011). Furthermore, *Drosophila's* SUMO conjugating enzyme, Ubc9 (initially identified as *Lesswright*) has roles in anterior patterning, and is believed to be required for the nuclear localisation of Bicoid, a transcription factor (Epps and Tanda 1998). Currently, the only studies investigating the *Ae. aegypti* SUMOylation pathway have been based on bioinformatics, detailing the conservation of the pathway between *Ae. aegypti* and *H. sapiens,* demonstrating that the pathway is broadly conserved except the SUMO protein is lacking an internal SCM in insects (Choy, Severo et al. 2013, Urena, Pirone et al. 2016).

1.4.2.1. SUMO proteins

SUMO was initially identified in 1996 in mammalian cells (Matunis, Coutavas et al. 1996). There are 5 SUMO paralogues in humans; SUMO1, SUMO2, SUMO3, SUMO4, and SUMO5. mRNA for SUMO4 has been shown to be predominantly detected in the kidneys, while SUMO5 is more abundantly expressed in the testes and peripheral blood leukocytes (Bohren, Nadkarni et al. 2004, Liang, Lee et al. 2016). All 5 paralogues are between 10.5-12 kDa in size (GenBank FJ042790.1 , Uniprot P55854 2014, Uniprot P61956 2014, Uniprot P63165 2014, Uniprot Q6EEV6 2014). Once SUMO mRNA has been transcribed, it is translated into an immature SUMO protein. The C-terminal of SUMO is cleaved by sentrin specific proteases (SENPs). This reveals the diglycine (GG) motif and produces a mature SUMO protein (Kamitani, Nguyen et al. 1997, Suzuki, Ichiyama et al. 1999). The structure of SUMO has previously been resolved and shown to be similar to the

tertiary structure of ubiquitin (Bayer, Arndt et al. 1998). Like ubiquitin, SUMO is known to covalently bind to the ε-amino group on an acceptor lysine residue located in the substrate protein. Studies have previously shown that SUMO and ubiquitin can compete for binding at the same lysine residue (Desterro, Rodriguez et al. 1998). The target lysine residue is commonly found in a SUMO Conjugation Motif (SCM; Ψ-Lys-X-[Asp/Glu]), where Ψ represents a branched amino acid and X represents any amino acid (Rodriguez, Dargemont et al. 2001). Analysis of various studies reveals that glutamic acid is preferentially bound over aspartic acid within the SCM (Wang and Dasso 2009, Wasik and Filipek 2014). SUMO has also been reported to be capable of binding inverted SCMs (Matic, Schimmel et al. 2010). Moreover, there are reports of SUMO modification that is dependent on phosphorylation, extended SUMO conjugation motifs, and SUMO that binds to negatively charged amino acids (Hietakangas, Anckar et al. 2006, Yang, Galanis et al. 2006). Approximately 25% of SUMO conjugation sites with target substrates occur at non-canonical SCMs (Matic, Schimmel et al. 2010).

For an efficient transfer of SUMO from Ubc9 to the target acceptor lysine, the interaction needs to be stabilised. The SCM acts as a site with affinity for the amino acid residues in the Ubc9 near the active site. The four residues in the SCM interact with Ubc9. The first residue is hydrophobic which allows the side chains to form Van der Waals forces with four different Ubc9 residues (Pro^{128}, Ala^{129}, Gln^{130}, and Ala^{131}). The second residue is the conserved lysine that is the target for SUMO modification. Due to the interactions between the interfaces of Ubc9 and the target protein, the acceptor lysine can be observed to fit in a hydrophobic shallow groove. The orientation of the amino acid side chain of the third residue directs away from Ubc9. However, the amino acid space is required to saddle the consensus peptide through Van der Waals forces. The fourth residue, commonly Asp/Glu are believed to be preferred due to the longer side chain which enables hydrophobic Van der Waals forces to form (Bernier-Villamor, Sampson et al. 2002). For SUMO modification of a target protein to occur more efficiently, an E3 ligase may help to stabilize the interaction between the target protein and Ubc9. Alternatively, extended versions of SCMs, or phosphorylation sites at the C-terminal have also been identified which enhance affinity for Ubc9 (Hietakangas, Anckar et al. 2006, Yang, Galanis et al. 2006, Mohideen, Capili et al. 2009, Matic, Schimmel et al. 2010).

SUMO2 and SUMO3 proteins share 87% nucleotide sequence identity and 97% amino acid sequence identity (Saitoh and Hinchey 2000). Due to the high degree of homology at the amino acid level, these two proteins can't be distinguished using antibodies, and therefore are often referred to as SUMO2/3. SUMO1 can be distinguished by antibodies as there is less amino acid identity, approximately 47% (Saitoh and Hinchey 2000). SUMO2/3 also contains an internal SCM, which allows chains of SUMO2/3 to efficiently form (Muller, Hoege et al. 2001, Tatham, Jaffray et al. 2001). SUMO1, does not contain an SCM and consequently doesn't efficiently form chains *in vivo*, but can be incorporated into the SUMO2/3 chains as a chain terminator (Tatham, Jaffray et al. 2001).

In some eukaryotes including the fruit fly *D. melanogaster,* baker's yeast *Saccromyces cerevisiae* and the nematode *Caenorhabditis elegans*, only one SUMO protein has been identified (Matunis, Coutavas et al. 1996, Lehembre, Badenhorst et al. 2000). This SUMO protein shares a high degree of sequence identity with human SUMO2/3 (Matunis, Coutavas et al. 1996, Saitoh and Hinchey 2000). The *D. melanogasters* homologue is believed to function more like human SUMO1, due to the lack of internal SCM, and studies have suggested that uncontrolled SUMO chain formation can be lethal (Urena, Pirone et al. 2016). However, the SUMO homologue in *S. cerevisiae* has been found to be capable of forming poly-SUMO chains, due to the presence of three SCMs in its N-terminus (Bylebyl, Belichenko et al. 2003). The gene sequences of two SUMO proteins have been identified in the cockroach *Blattella germanica*, and in *Ae. aegypti* (Choy, Severo et al. 2013, Urena, Pirone et al. 2016). No biochemical studies have been performed thus far on an *Ae. aegypti* SUMO.

Once SUMO is covalently bound to the substrate, non-covalent interactions can form that are mediated by SIMs in other proteins. This non-covalent interaction allows temporary protein-protein interactions to form. Multiple SIM motifs have been identified, the best characterized being the hydrophobic [Val/Ile]-X-[Val/Ile]-[Val/Ile] (Minty, Dumont et al. 2000, Wang and Dasso 2009).

1.4.2.2. SUMO interaction motifs (SIMs)

SIM sites are known to be important in regulating SUMO interactions. SIM sites function by binding onto the surface patch of the SUMO substrate between the α-helix and a ß-sheet, extending the ß-sheet by one strand. This interaction extends the ß-strand in either a parallel or antiparallel orientation (Namanja, Li et al. 2012, Jardin, Horn et al. 2015). In *S. cerevisiae*, it has been found that in all SIM sites studied, antiparallel binding interactions are more stable when compared to parallel binding interactions (Jardin, Horn et al. 2015). SIM sites are frequently flanked by acidic residues or phosphorylated serine residues (Stehmeier and Muller 2009). In the mammalian system these can help determine SUMO2/3 specificity (Hecker, Rabiller et al. 2006).

1.4.2.3. SUMO pathway

The SUMOylation system is comprised of an analogous set of enzymes to the ubiquitin pathway as both contain E1, E2, and E3 enzymes. The ubiquitin pathway contains several E2 conjugation enzymes and many E3s (Rotin and Kumar 2009, Wasik and Filipek 2014). The SUMO pathway, however, only contains one E2 (Ubc9), and a limited number of E3s. Examples of E3 enzymes include the RING-finger-domain families, such as 'SAP and Miz-finger domain-containing protein 1 / Protein Inhibitor of Activated STAT' (SIZ/PIAS), or RanBP2. E3 enzymes help increase the rate and specificity of SUMO ligation *in vivo,* although aren't necessary *in vitro* if target proteins contain an SCM (Verger, Perdomo et al. 2003). The ubiquitin pathway also contains an E4 enzyme specifically responsible for efficient formation of poly-ubiquitin chains (Huang, Minaker et al. 2014). A potential SUMO E4-like enzyme, ZNF451, has also been identified as part of the vertebrate SUMOylation pathway (Eisenhardt, Chaugule et al. 2015).

The mature SUMO protein binds E1 through the generated C-terminal glycine residue. E1 exists as a heterodimer comprising of the SUMO activating enzymes SAE1 and SAE2 (Desterro, Rodriguez et al. 1999). Using ATP and a magnesium ion, the E1 heterodimer activates SUMO, allowing it to form a thioester bond

with E1. Subsequently, SUMO forms a thioester bond with the E2 conjugating enzyme, Ubc9 (Schwarz, Matuschewski et al. 1998, Desterro, Rodriguez et al. 1999). E3 enzymes are known to play important regulatory roles in SUMOylation, as they increase SUMOylation efficiency (Johnson and Gupta 2001). SENPs, initially utilised to mature SUMO, are also required to deSUMOylate target proteins, releasing SUMO into a pool of unconjugated SUMO. The SUMOylation pathway can be seen depicted in **Figure 1.11**.

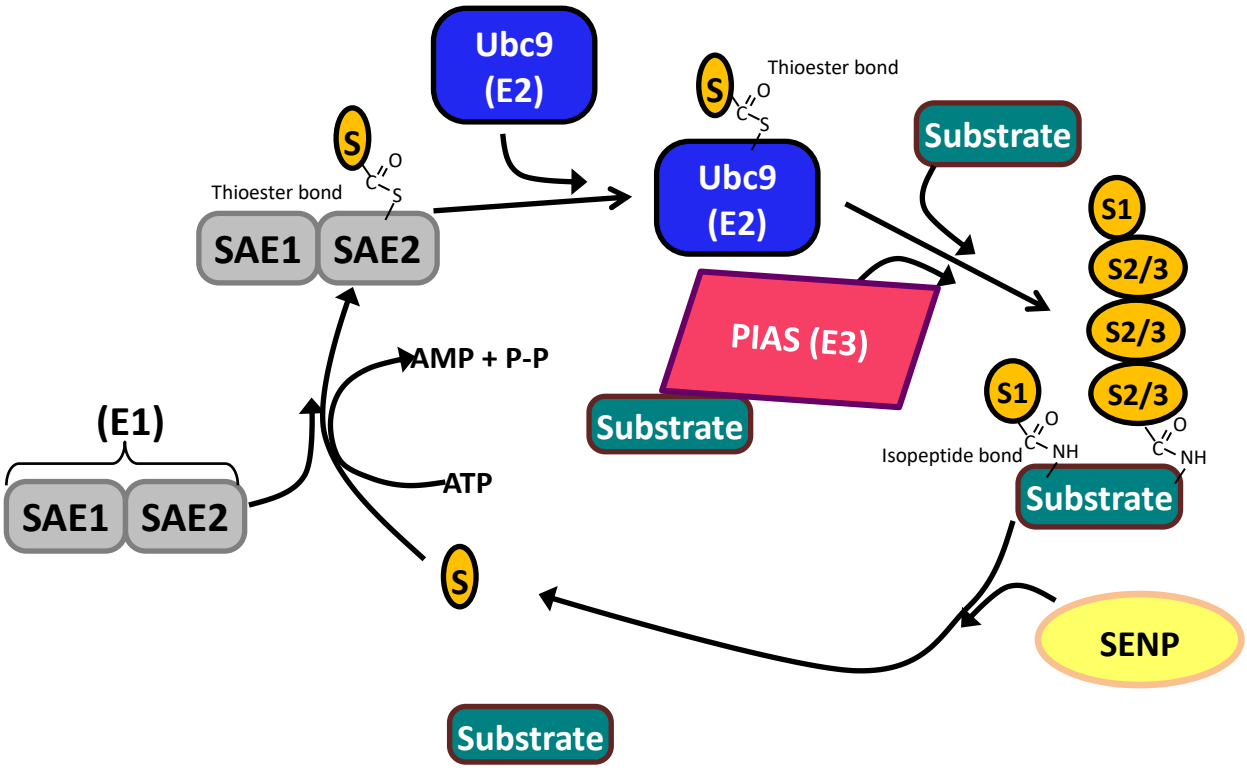

Figure 1.11 *H. sapiens* SUMOylation pathway.

SUMO is activated by the SAE1/SAE2 activating heterodimer in an ATP dependent manner. SAE1/2 (grey) forms a thioester bond with the terminal glycine of SUMO (yellow) and then passes SUMO to Ubc9 (blue), forming a second thioester bond. Ubc9 can directly SUMOylate a substrate protein at a SCM, but *in vivo* this process is often assisted by the presence on an E3 ligase (PIAS; pink). Modification of substrate proteins occurs via an isopeptide linkage at a target lysine residue. SENPs can deSUMOylate proteins contributing to a pool of unconjugated SUMO.

1.4.2.3.1. Activating enzyme

The mature SUMO protein is activated by the SUMO activating enzyme (SAE) 1 - SAE2 heterodimer. There is only one SUMO E1 activating heterodimer which activates SUMO in two steps. ATP and magnesium are utilised to prime the terminal glycine of SUMO, and a conserved catalytic cysteine residue located within SAE1/2. The subsequent binding of the terminal glycine of SUMO to the cysteine residue of SAE1/2 results in a thioester bond forming (Desterro, Rodriguez et al. 1999). Some viruses, such as adenovirus has been shown to target the SAE1 protein of the heterodimer for degradation. This occurs through the action of the Gam1 protein, which forms a complex with ubiquitin in order to degrade the protein. As there is no longer an activating enzyme, cellular SUMOylation is prevented (Boggio, Passafaro et al. 2007). A combination of the activating enzyme and the C-terminal of the ubiquitin-like modifier which interacts with the E1 have been shown to be responsible for E1-ubiquitin-like modifier specificity. For instance, the E1 for NEDD8 would not activate ubiquitin without specific mutations (Walden, Podgorski et al. 2003, Souphron, Waddell et al. 2008, Ronau, Beckmann et al. 2016). Furthermore, SAE1/2 has been shown to be a substrate for SUMO modification, altering its cellular localisation, and decreasing the interaction between SAE1/2 and Ubc9 (Truong, Lee et al. 2012, Truong, Lee et al. 2012). SAE1/2 has also previously been reported to be able to autoSUMOylate during *in vitro* studies (Truong, Lee et al. 2012).

1.4.2.3.2. Conjugating enzyme

The E2 conjugating enzyme is responsible for covalently binding SUMO onto the substrate protein. The SUMO system only has one known E2 enzyme, Ubc9 (Gong, Kamitani et al. 1997, Schwarz, Matuschewski et al. 1998). The surface of Ubc9 is known to possess a positive charge, while the corresponding surface in SUMO-1 possesses a negative charge resulting in an attraction between the proteins (Tong, Hateboer et al. 1997, Liu, Jin et al. 1999). Ubc9 initially forms a thioester bond with SUMO through the terminal glycine with the Cys^{93} in the Ubc9 catalytic triad (Schwarz, Matuschewski et al. 1998, Tatham, Kim et al. 2003).

The cysteine residue orientates itself in order to form a new thioester bond requiring another ATP (Gong, Kamitani et al. 1997, Olsen, Capili et al. 2010). The surface of Ubc9 opposing the catalytic site is known to possess a distinct charge, which may assist with conjugating SUMO instead of ubiquitin or other ubiquitin-like modifiers (Giraud, Desterro et al. 1998). Mammalian SUMO1, SUMO2, and SUMO3 can all also bind the N-terminal of Ubc9 with similar affinity, SUMOylating Ubc9 (Tatham, Kim et al. 2003). Interestingly, the formation of a thioester bond has been shown to be initially slowed by the presence of the amino acids Asp^{100} and Lys^{101}, the subsequent rate of transfer to the target protein is then enhanced by the presence of these amino acids (Tatham, Chen et al. 2003).

1.4.2.3.3. Ligating enzyme

The E3 ligating enzymes are responsible for increasing the rate of SUMO conjugation to substrate proteins. This is usually accomplished through two mechanisms. The E3 can enhance the rate of transfer by 'priming' the Ubc9~SUMO thioester and can also form a complex of the substrate protein with Ubc9~SUMO thioester. Consequently, the E3 enzymes are believed to be responsible for substrate specificity. However, relatively few E3 enzymes have been identified for the SUMO pathway (Cubenas-Potts and Matunis 2013, Jiang, Saavedra et al. 2014, Cappadocia and Lima 2018). Examples include RanBP2, Pc2 polycomb protein, ZNF451, and the PIAS family (Takahashi, Toh-e et al. 2001, Pichler, Gast et al. 2002, Merrill, Melhuish et al. 2010, Eisenhardt, Chaugule et al. 2015). The PIAS family have been studied in more detail and consequently, will be the focus of this section.

The PIAS proteins were initially identified due to their role in suppressing STAT and therefore suppressing the innate immune response, this was later found to be through PIAS activity as an E3 SUMO ligase (Chung, Liao et al. 1997, Liu, Liao et al. 1998, Takahashi, Toh-e et al. 2001, Kotaja, Karvonen et al. 2002, Rogers, Horvath et al. 2003). PIAS proteins are split into multiple functional domains including the SAP, PINIT, SP-RING, SIM, and S/T domains (**Figure 1.12**). The N-

terminal Scaffold Associating region/Acinus/PIAS (SAP) domain is responsible for binding to different biological factors, including DNA, transcription factors, and nuclear receptors (Liu, Gross et al. 2001, Tan, Hall et al. 2002). The PINIT domain is responsible for regulating the localisation of PIAS within the cell (Duval, Duval et al. 2003). The SP-RING domain functions in protein-protein interactions, and is the catalytically active site of the proteins SUMO ligase activity (Hochstrasser 2001). The C-terminal S/T domain has been shown to be highly variable, with several roles including binding to nuclear coactivators (Jiménez-Lara, Heine et al. 2002). Finally, between the S/T domain and the SP-RING domain there is one, or more, SIM site(s) which are believed to help facilitate SUMO interactions (Minty, Dumont et al. 2000, Kaur, Park et al. 2017). PIAS proteins have been found to be substrates of SUMO modification, recent studies have found that SUMO modification of PIAS1 inhibits its function as an inhibitor of activated STAT (Alagu, Itahana et al. 2018).

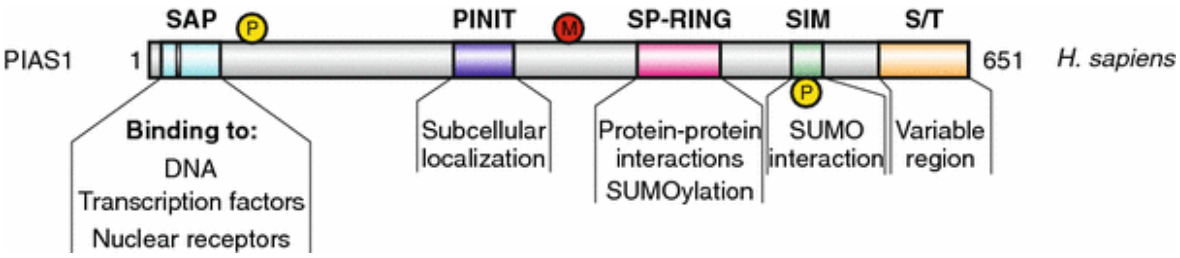

Figure 1.12 Schematic of PIAS1 domains

Domain structures, function, and PTM of *Hs*PIAS1 is indicated. P is phosphorylation site, M is methylation site, numbers indicate the number of amino acids. Adapted from (Rytinki, Kaikkonen et al. 2009).

Abbreviations: Scaffold Associating region/Acinus/PIAS (SAP), Siz PIAS-Really Interesting New Gene (SP-RING), SUMO Interaction Motif (SIM), Serine/threonine-rich C-terminal (S/T).

1.4.2.3.4. Sentrin specific proteases (SENPs)

SENPs are deSUMOylating enzymes which have two roles in the cell. They mature the SUMO protein by cleaving off the C-terminal, revealing a diglycine motif, and they deSUMOylate modified proteins (Li and Hochstrasser 1999, Gong, Millas et al. 2000, Mossessova and Lima 2000). This results in a constant cellular supply of unconjugated SUMO which can subsequently be used in other modifications. This is a tightly regulated process, as uncontrolled deSUMOylation is highly toxic to mammalian cells (Johnson 2004). Humans possess 6 reported SENPs (1-3, 5-7) which fall into two branches based on their genetic similarity. SENP6 and SENP7 are closely related to each other and share homology with the yeast homologue Ulp2, but more distant from SENP1-3, SENP5, and the yeast homologue Ulp1 (Li and Hochstrasser 2000, Nayak and Muller 2014). In humans, SENP-3, -5, -6, and -7 have all been shown to preferentially target poly-SUMO2/3 chains, likely by trimming the external SUMO proteins off one at a time (Di Bacco, Ouyang et al. 2006, Eckhoff and Dohmen 2015).

1.5. Interactions between the viruses and the immune responses regulated by SUMO

1.5.1. Vertebrate innate immune response

Vertebrates possess a complex immune system ranging from an initial intrinsic immune response within cells at the site of infection, to a complex extracellular immune system. As the focus of this study is on the cellular mechanisms that influence arbovirus replication, only the mechanisms associated with cell based immunity will be presented. Cellular innate immunity is provided by biological factors which are upregulated in response to infection. Cellular intrinsic immunity is provided by biological factors that are constitutively expressed in the cell. Both the intrinsic and innate cellular immune response is tightly regulated in order to efficiently respond to infection, but not be constantly active. SUMO modification is well reported to regulate a plethora of components in the host innate immune response ensuring the immune response is only active in response to infection (Adorisio, Fierabracci et al. 2017). As a consequence of host cell intrinsic and innate immune factors, viruses have evolved a range of mechanisms to interfere with regulators of the immune response in order to replicate more efficiently.

When a cell becomes infected, pattern recognition receptors (PRR), such as the family of Toll-like receptors (TLR), or the cytoplasmic Retinoic acid inducible gene I (RIG-I) receptor, detects the pathogen associated molecular patterns (PAMPS) and initiate expression of antimicrobial genes to prime neighbouring cells. The most effective immune strategy to prime neighbouring cells that all mammalian cells possess is the interferon (IFN) system. There are three types of IFN, named type I, type II, and type III, which are released from an infected cell to signal neighbouring cells to enter an antiviral state. Cells possess IFN receptors which can recognise the different types of IFN. Type I IFN, comprising IFNα, IFNß, IFNε, IFNκ, and IFNω are recognised by IFN alpha receptors 1 and 2 (IFNAR1/2), type II IFN, comprising IFNγ, is recognised by IFN gamma receptors (IFNGR), and type III IFN comprises IFNλ1, IFNλ2, and IFNλ3, and is recognised by IL-28 receptor α, and IL-10 receptor ß (Kotenko, Gallagher et al. 2003). The focus of this section will be on IFN types I and II.

Upon activation, IFN receptors activate the Janus kinase – signal transducer and activator of transcription (JAK-STAT) pathway. Briefly, activation of the IFN receptors by IFN results in the activation of members of the Janus kinase family. Janus Kinase 1 (JAK1) and tyrosine kinase 2 (TYK2) are activated in response to type I IFN, while JAK1 and JAK2 are activated in response to type II IFN. Following activation of JAK1/TYK2 STAT proteins form homo- or hetero-dimers of STAT1/STAT2, or STAT2/STAT2. When IFNγ activates the JAK1/JAK2 proteins, STAT1 form homodimers. These STAT dimers translocate to the nucleus and function as a transcription factor, activating antiviral genes, including the MxA protein, protein kinase R (PKR), and TLRs (**Figure 1.13**) (Shuai, Stark et al. 1993, Silvennoinen, Ihle et al. 1993, Watling, Guschin et al. 1993).

SUMO is reported to regulate the signalling pathways that result in translation of types I and II IFN, and components of the JAK-STAT pathway. For instance, ssRNA is a PAMP detected by TLR7 and TLR8, which activate the myeloid differentiation primary response 88 (MyD88) signalling pathway. The MyD88 signalling cascade activates many important cellular proteins, including the transcription factors interferon regulatory factor 7 (IRF7) and IRF8. IRF7 and IRF8 then translocate to the nucleus to trigger the transcription of IFN (Kawai, Sato et al. 2004). SUMO modification of IRF7 and IRF8 has been shown to prevent the activation of these proteins, thereby suppressing the IFN response. Furthermore, removal of SUMO by SENP1 allows IRF8 to be activated (Kubota, Matsuoka et al. 2008, Chang, Xu et al. 2012). Other IRF family members, including IRF1 and IRF3 have also been reported to be targets of PIAS mediated SUMO modification, which suppresses this transcriptional activity (Nakagawa and Yokosawa 2002, Han, Jiang et al. 2008). Within the JAK-STAT pathway of neighbouring cells, SUMO has a well reported role of modifying STAT1 in a PIAS dependent manner. This effectively inhibits the type II IFN response, although the type I response can still occur through the formation of STAT2 homo-dimers (Rogers, Horvath et al. 2003).

Another important PRR is the RIG-I protein. This cytoplasmic protein detects viral RNA triggering a signalling cascade which activates IRF3 and NF-κB. IRF3 triggers the transcription of IFN, while the NF-κB pathway triggers the production of a myriad of gene products, including antiviral proteins such as pro-inflammatory cytokines, interleukins, or Mx1 (Liu, McEachin et al. 2003,

Gérardin, Baise et al. 2004, Gao, Hannan et al. 2006). RIG-I is known to be a target for SUMO modification which enhances modification of RIG-I by ubiquitin, and therefore promotes interactions with downstream proteins, and upregulates the antiviral response (Mi, Fu et al. 2010). There are also components of the NF-kB pathway which are also targets for modification by SUMO. NF-κB essential modulator (NEMO), a subunit of the IκB kinase complex which activates NF-κB, is SUMO modified in a PIAS dependent manner. SUMO modification results in the nuclear localisation of NEMO, and allows the ubiquitylation of NEMO to activate downstream signalling proteins in the cytoplasm (Huang, Wuerzberger-Davis et al. 2003, Mabb, Wuerzberger-Davis et al. 2006). SENP2, a SUMO protease is upregulated by NF-κB activation and functions to deSUMOylate modified NEMO, resulting in a negative feedback loop, which restricts the activation of the NF-κB pathway (Lee, Mabb et al. 2011). SUMO modification is also capable of negatively regulating the NF-κB pathway. IκBα is an inhibitor of the NF-κB pathway which is usually degraded through the proteasome. However, SUMO modification of IκBα protects the inhibitor from degradation, resulting in SUMOylation maintaining the repression of the NF-κB pathway (Desterro, Rodriguez et al. 1998).

One important antiviral cellular mechanism is the phosphorylation of eukaryotic translation initiation factor 2α (eIF2α) by the dsRNA dependent protein kinase R (PKR). PKR is an ISG, induced by type I IFN, which is required to be SUMOylated in order to phosphorylate and activate eIF2α. The phosphorylation of eIF2α serves to prevent the initiation of translation of both cellular and viral proteins, and can result in cellular apoptosis indicating another antiviral role for SUMO modification (Harding, Novoa et al. 2000, Wek, Jiang et al. 2006, Muaddi, Majumder et al. 2010, de la Cruz-Herrera, Campagna et al. 2014).

When under stress, cells can also form nuclear stress granules formed of multiple strands of mRNA stalled in translation. They form through interactions between mRNA binding proteins through conventional protein-protein interactions, and intrinsically disordered regions. One mechanism by which stress granule formation is initiated is through the inhibition of eIF4A (Dang, Kedersha et al. 2006). eIF4A has been shown to be modified by SUMO1 and SUMO2 *in vivo*, where SUMO modification is required for the formation of eIF4A

induced stress granules (Jongjitwimol, Baldock et al. 2016). Stress granules recruit antiviral proteins including RIG-I and PKR that stimulates their activation (Onomoto, Jogi et al. 2012, Reineke, Kedersha et al. 2015, Reineke and Lloyd 2015).

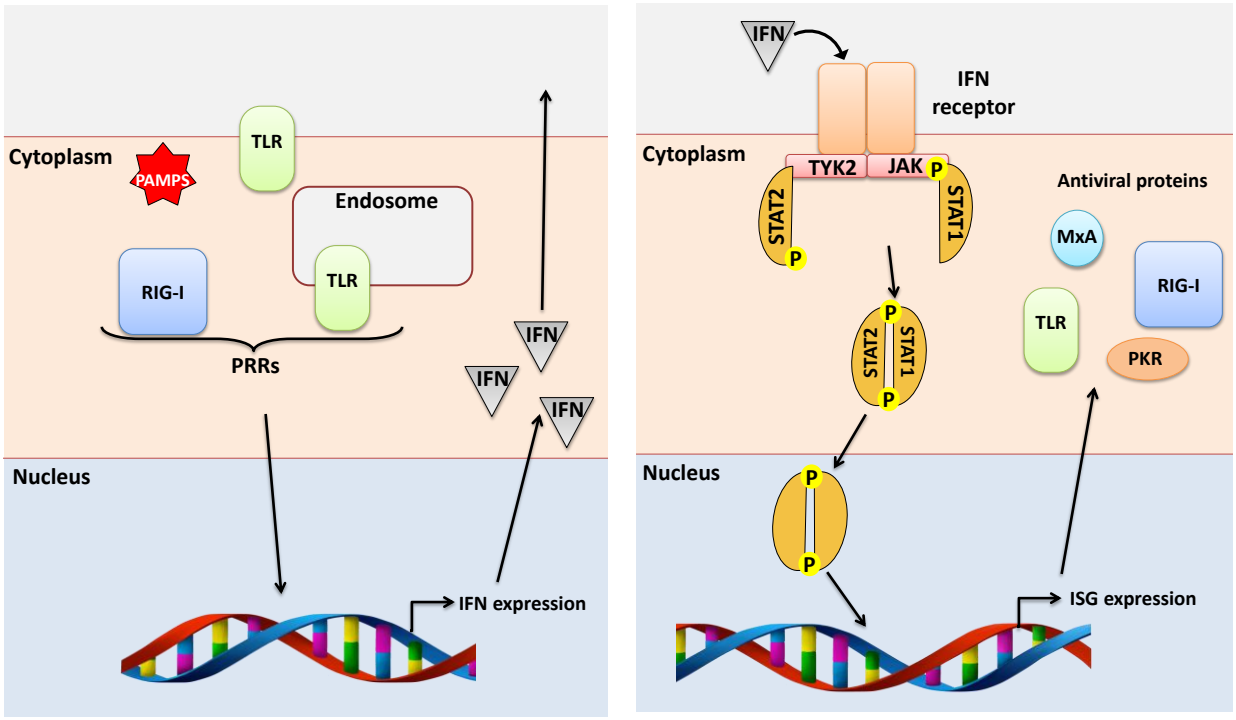

Figure 1.13 Overview of the antiviral interferon response

Left hand side: In an infected cell, viral pathogen associated molecular patterns (PAMPS) are detected by pattern recognition receptors (PRRs), such as the family of Toll-like receptors (TLR) or Retinoic acid inducible gene-I (RIG-I). Activation of these proteins triggers signalling pathways which induces expression of antiviral compounds, including interferon (IFN). Right hand side: extracellular IFN activates IFN receptors, which activates the Janus kinase – signal transducer and activator of transcription (JAK-STAT) signalling pathway. JAK phosphorylates STAT, STAT forms a hetero- or homo-dimer, and translocates to the nucleus to trigger expression of IFN stimulated genes (ISG), putting the cell into an antiviral state.

Abbreviations: phosphate (P); protein kinase R (PKR); tyrosine kinase (TYK2)

SUMO has been shown to regulate multiple aspects of the cellular innate immune response, yet currently very few studies have been published investigating interactions between arboviruses and host SUMOylation (**Section 1.5.4**). **Section**

1.5.1.1, **Section 1.5.1.2**, **Section 1.5.1.3** describe mechanisms that arboviruses from three distinct families employ to evade the mammalian innate immune response. Multiple components of these immune pathways described have been shown to be targets of SUMO mediated regulation. However, the role of host SUMOylation in response to arbovirus infection with respect to these immune pathways has yet to be investigated.

1.5.1.1. Alphaviruses and innate immune evasion

Members of the alphavirus family have been shown to suppress the host cell immune response by multiple mechanisms. Alphaviruses are capable of both, host-cell transcription and translation shut-off. Transcriptional shut-off is conducted through the activity of the viral nsP2 protein of Old World alphaviruses. nsP2 translocates to the nucleus where it targets the catalytic subunit of RNA polymerase II, RPB1, for ubiquitin mediated degradation (Peranen, Rikkonen et al. 1990, Akhrymuk, Kulemzin et al. 2012). New World alphaviruses use the capsid protein to mediate host-cell transcriptional shut-off, by forming a complex with nuclear import and export factors, thereby blocking nuclear import mediated by different karyopherins (Garmashova, Gorchakov et al. 2007, Atasheva, Fish et al. 2010).

During alphavirus infection, PKR becomes highly activated to the point where the cell experiences nearly complete eIF2α phosphorylation, resulting in translational shut-off (Ventoso, Sanz et al. 2006). Old World alphaviruses avoid this shut-off due to the presence of a highly stable hairpin loop in the RNA which provides resistance to eIF2α phosphorylation, by stalling the ribosome at the correct AUG, enabling viral RNA to be translated (Ventoso, Sanz et al. 2006, Toribio, Diaz-Lopez et al. 2016). Interestingly, New World alphaviruses enhance the shut-off of host cell translation by promoting phosphorylation of eIF2α then utilising the stable hairpin loop to continue translation of viral proteins, restricting the amount of host cell antiviral proteins that are translated (Aguilar, Weaver et al. 2007).

Alphaviruses have also developed mechanisms to interfere with the IFN pathway. CHIKV nsP2 has been identified as the protein responsible for inhibiting the nuclear localisation of STAT dimers, thereby reducing ISG expression. This appears to be independent of the function of nsP2 in host-cell shut-off, but the function is ablated if the nuclear localisation signals on nsP2 are mutated. This indicates that the nuclear localisation of nsP2 is required for it to inhibit STAT nuclear localisation (Fros, Liu et al. 2010, Fros, van der Maten et al. 2013). Together, these strategies ensure that alphaviruses are able to suppress the cellular immune response and are consequently able to replicate efficiently (**Figure 1.14**).

Like many other viruses, SFV is capable of disrupting the formation of cellular stress granules, preventing their antiviral activity. The c-terminal domain of nsP3 from SFV has been shown to sequester Ras-GAP SH3-domain-binding-protein (G3BP), a protein consistently found in all types of stress granule, and therefore inhibit stress granule formation (McInerney, Kedersha et al. 2005, Beckham and Parker 2008, Lloyd 2012, Panas, Varjak et al. 2012).

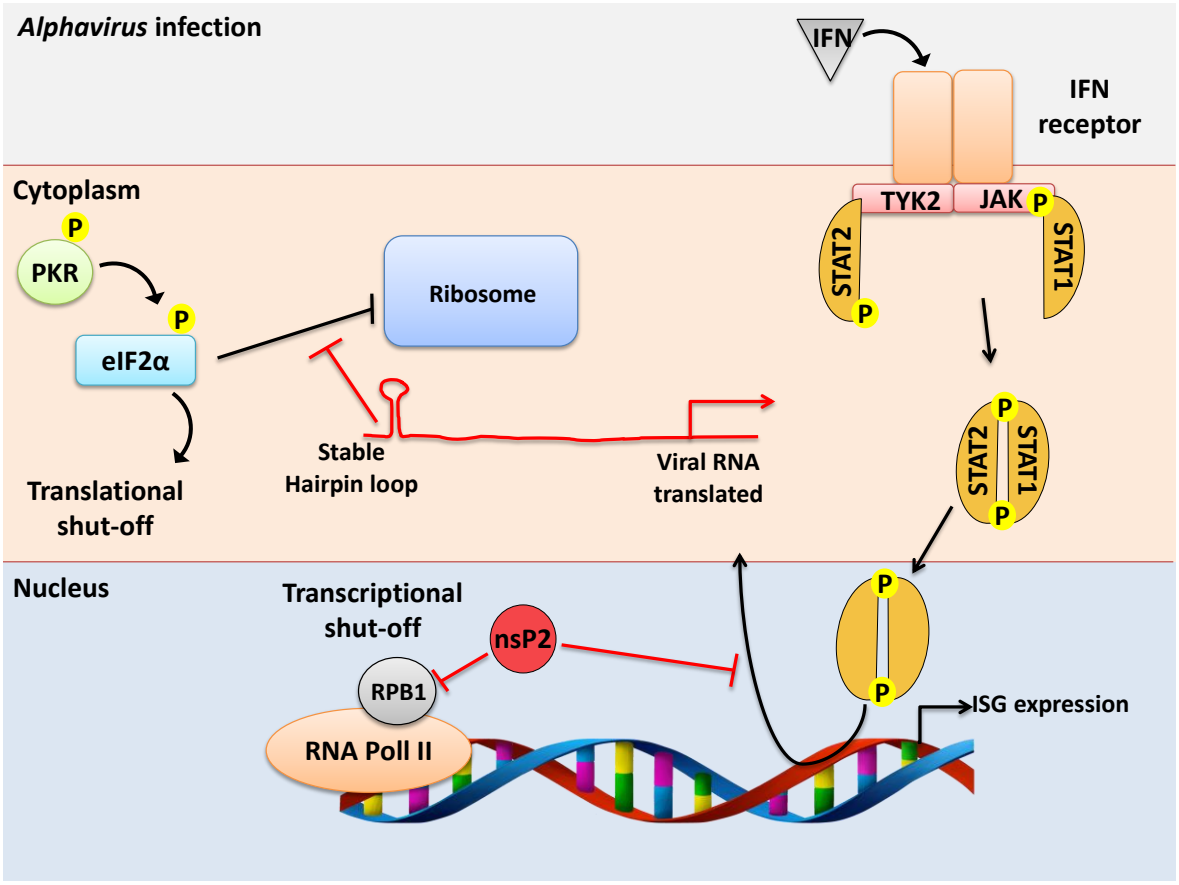

Figure 1.14 Innate immune evasion strategies employed by alphaviruses

Alphaviruses utilise different strategies to avoid the mammalian immune response. The viral RNA possesses a stable hairpin loop at the 5' end, resulting in successful translation initiation. This occurs following protein kinase R (PKR) phosphorylation of eukaryotic translation initiation factor 2α (eIF2α) which results in shut-off of host cell translation. The viral nonstructural protein 2 (nsP2) also translocates to the nucleus to degrade the RNA Polymerase II (RNA Pol II) subunit, RPB1, preventing host cell transcription. nsP2 is also capable of preventing the nuclear localisation of signal transducers and activators of transcription (STAT) dimers, both mechanisms reduce expression of interferon (IFN) stimulated genes (ISGs).

Abbreviations: tyrosine kinase (TYK2), Janus kinase (JAK), phosphate (P).

1.5.1.2. Flaviviruses and innate immune evasion

At least four PRRs are utilised by the cell to detect flaviviruses, these are the Retinoic acid-inducible gene I (RIG-I)-like receptors, TLR3, 7, and 8, nucleotide-binding oligomerization domain (NOD)-like receptors, and the cyclic GMP-AMP synthesase–stimulator of interferon genes (cGAS-STING) - dependent pathway (reviewed by Takeuchi and Akira (2010)). Consequently, many flaviviruses have developed mechanism to evade this host cell response. For instance, WNV, DENV, JEV, and TBEV have all been shown to delay the onset of IFN signalling by forming intracellular membranes to hide the viral dsRNA. dsRNA is a key PAMP that initiates an interferon response through the activation of a variety of PRRs including TLR3 and RIG-I (Fredericksen and Gale 2006, Welsch, Miller et al. 2009, Överby, Popov et al. 2010, Espada-Murao and Morita 2011, Junjhon, Pennington et al. 2014).

Many flaviviruses have also been shown to block the IFN response. For instance, NS2A of Kunjin virus (a strain of WNV; WNV_{KUN}) has been identified as an inhibitor to IFN-β transcription (Liu, Chen et al. 2004). DENV NS2A, NS4A and NS4B can prevent JAK-STAT signalling by reducing the phosphorylation and transport of STAT1 into the nucleus (Muñoz-Jordán, Sánchez-Burgos et al. 2003). Upon activation by interferon, the STAT family of proteins usually form homodimers or heterodimers which induce expression of ISGs, reviewed in Harrison (2012). DENV and ZIKV NS5 proteins have been shown to block STAT2 signalling. DENV blocks STAT2 through promoting proteasome mediated degradation of STAT2, following targeting by the E3 ubiquitin ligase UBR4 (Mazzon, Jones et al. 2009, Morrison, Laurent-Rolle et al. 2013). ZIKV blocks STAT2 signalling through the same pathway, but independent of the E3 ubiquitin ligase (Grant, Ponia et al. 2016). Both mechanisms prevent the cellular interferon-dependent innate immune response from restricting viral replication. Recent studies with ZIKV have also found that the NS5 protein blocks IFN induction and signalling, this was achieved by reducing levels of STAT2, and blocking phosphorylation of STAT1 (Hertzog, Dias Junior et al. 2018).

Other anti-antiviral mechanisms employed by flaviviruses include the NS3 protein of DENV, which has been reported to bind to a protein called 14-3-3ε, which functions to translocate RIG-I within the cell. NS3 binding to 14-3-3ε prevented translocation of RIG-I, and thereby blocked the RIG-I mediated antiviral response (Chan and Gack 2016).

DENV has also been shown to form a stable complex of NS2B-NS3 which is capable of inhibiting IFN signalling by proteolytically cleaving the STING protein, a component of the cGAS pathway. This has also been shown to be species specific, as the mouse STING was not cleaved by DENV NS2B-NS3 (Falgout, Pethel et al. 1991, Aguirre, Maestre et al. 2012). NS2B-NS3 has also been shown to block the induction of RIG-I through masking the kinase domain of IκB kinase ε, thereby preventing the phosphorylation and nuclear translocation of IFN regulatory factor 3 (IRF3) (Anglero-Rodriguez, Pantoja et al. 2014). NS4B from DENV has been implicated in suppressing the RNA interference (RNAi) response in the human liver Huh7 cell line (Kakumani, Ponia et al. 2013). Although as the RNAi response is not the most potent antiviral mechanism in mammals, this may have a more prominent role in the vector species.

Subgenomic flavivirus RNA (sfRNA), a non-coding RNA derived from the 3' untranslated region (reviewed by Clarke, Roby et al. (2015)), has also been implicated in being an antagonist of IFN production. This has been found to occur through multiple mechanisms, including inhibiting the activation of RIG-I, through blocking nuclear translocation of IRF3, and sfRNAs from ZIKV may also antagonise MDA5 activation (Schuessler, Funk et al. 2012, Chang, Hsu et al. 2013, Manokaran, Finol et al. 2015, Donald, Brennan et al. 2016). Furthermore, sfRNAs are resistant to Dicer or exoribonuclease 1 (XRN1) mediated degradation of the viral genome, due to the presence of pseudoknots and stem loops restricting the RNA interference response (Schnettler, Sterken et al. 2012).

Flaviviruses are capable of targeting individual ISGs in order to prevent antiviral mechanisms utilised by the cell. For instance, one family of ISGs, MxA, has been shown to have antiviral activity against various RNA viruses (Landis, Simon-Jodicke et al. 1998, Chieux, Chehadeh et al. 2001). WNV_{KUN} is believed to hide

from MxA through the induction of membranous structures (Hoenen, Liu et al. 2007).

Finally, it's also reported that various flaviviruses are capable of promoting suppressors of cytokine signalling (SOCS)-1 and SOCS3 expression through binding to the Tyro3/Axl/Mer (TAM) receptor on certain cell types, such as dendritic cells. This has the function of suppressing JAK-STAT signalling (Mansfield, Johnson et al. 2010, Bhattacharyya, Zagorska et al. 2013). Together, these demonstrate a wide range of strategies flaviviruses employ to evade antiviral responses in the cell (**Figure 1.15**).

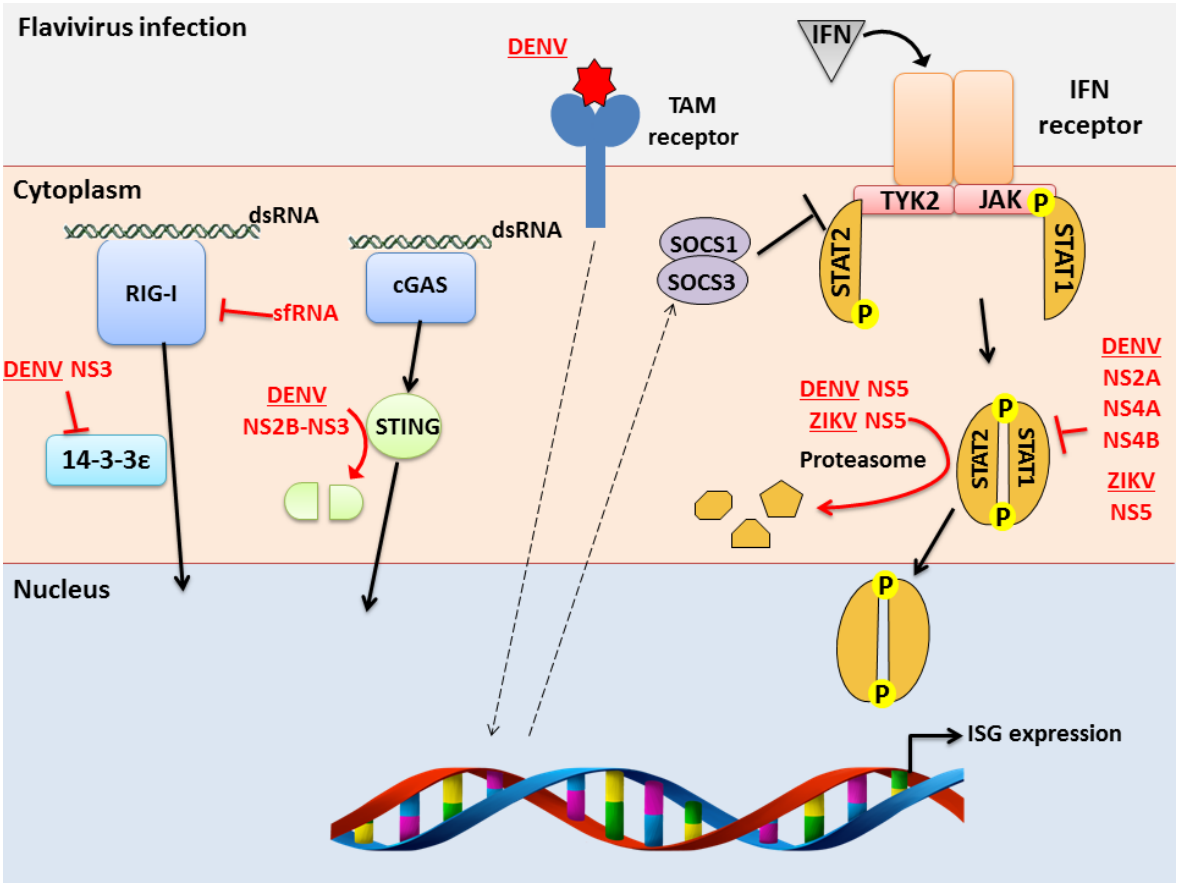

Figure 1.15 Innate immune evasion strategies employed by flaviviruses

Flaviviruses utilise various strategies to avoid the mammalian innate immune response. DENV and ZIKV non-structural protein 5 (NS5) have both been shown to degrade the signal transducer and activator of transcription 2 (STAT2). DENV non-structural protein 2A (NS2A), 2B (NS2B), 4B (NS4B), and ZIKV NS5 have also been shown to inhibit the phosphorylation of STAT1, which results in fewer STAT1/2 heterodimers forming. DENV NS3 also has roles in binding to 14-3-3ε, preventing 14-3-3ε from shuttling retinoic acid-inducible gene I (RIG-I) into the nucleus. Furthermore, subgenomic flaviviral RNA (sfRNA) can inhibit activation of RIG-I. DENV NS2B-NS3 also serves to proteolytically cleave stimulator of interferon genes (STING), a component of the cyclic GMP-AMP synthesase (cGAS) signalling pathway. DENV can also bind to Tyro3/Axl/Mer (TAM) receptors on specific cell types, which induces expression of suppressors of cytokine signalling (SOCS)-1 and -3, which suppress the janus kinase - signal transducers and activators of transcription (JAK-STAT) pathway.

Abbreviations: interferon (IFN), interferon stimulated genes (ISG), double stranded RNA (dsRNA), tyrosine kinase (TYK2), phosphate (P).

1.5.1.3. Orthobunyaviruses and innate immune evasion

Orthobunyaviruses have not been studied to the same extent as alphaviruses and flaviviruses. The majority the immune evasion mechanisms that are adopted by orthobunyaviruses utilise the non-structural NSs protein (**Section 1.3.3.3**). The NSs protein has been shown to act as an IFN antagonist. BUNV NSs inhibits the phosphorylation of the RNA polymerase II, which decreases the amount of host mRNA synthesis (Thomas, Blakqori et al. 2004). The C-terminal of BUNV NSs interacts with the protein Mediator of RNA polymerase II transcription subunit 8 (MED8), part of the mediator complex which regulates RNA polymerase II transcription, preventing transcription initiation (Léonard , Kohl et al. 2006). LACV NSs also targets the RNA polymerase II to block the IFN response, but this is achieved through degradation of the RNA pol II protein (Verbruggen, Ruf et al. 2011). Both of these mechanisms have the effect of restricting the cells antiviral response, while not restricting the viruses' transcription, due to the function of the viral RDRP. Finally, NSs has also been reported to delay cellular apoptosis through suppressing the interferon regulatory factor-3 signalling pathway (Kohl, Clayton et al. 2003). This extends the length of time which orthobunyaviruses are able to replicate for within the cell (**Figure 1.16**).

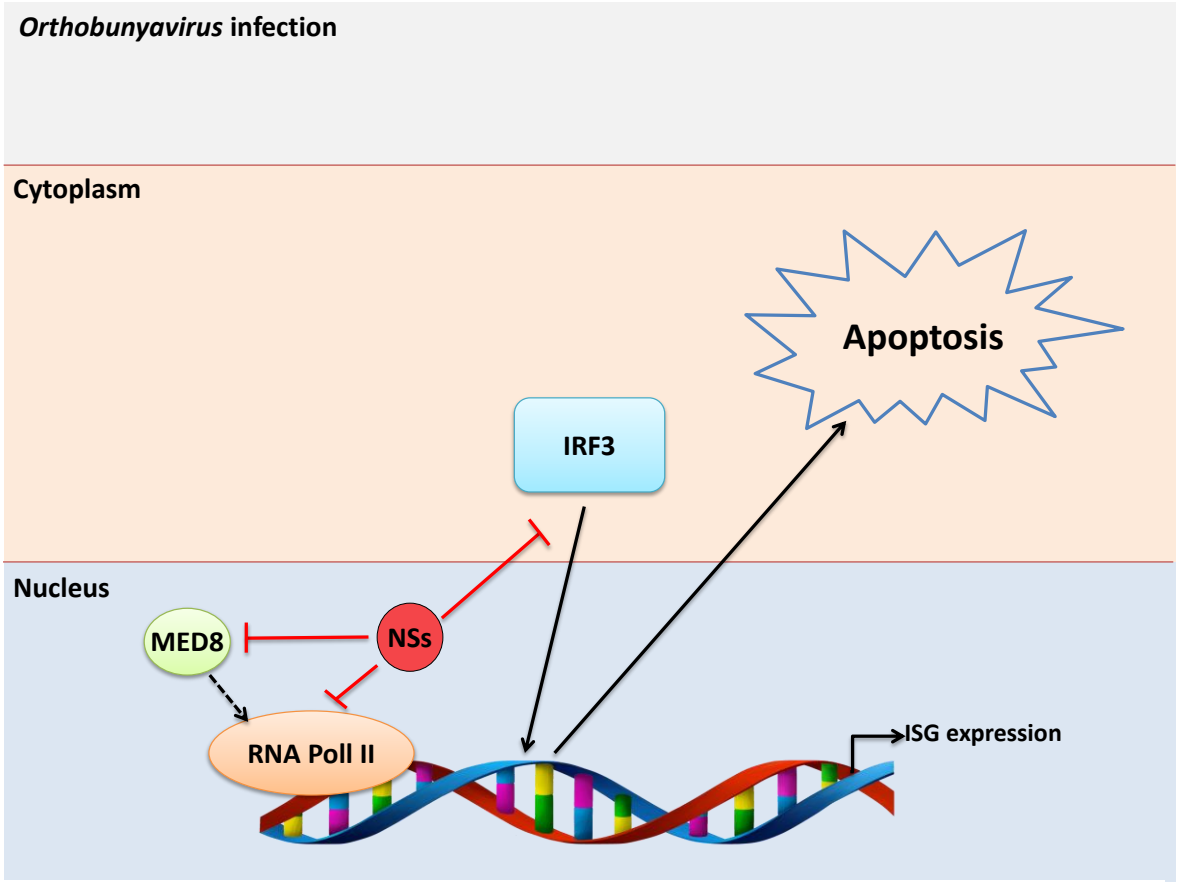

Figure 1.16 Innate immune strategies utilised by orthobunyaviruses

Innate immune evasion strategies employed by Orthobunyaviruses have only been reported to utilise the non-structural protein produced by the S gene (NSs). BUNV NSs serves to inhibit phosphorylation of RNA polymerase II (RNA Pol II), while LACV NSs degrades RNA Pol II. BUNV NSs can also interact with Mediator of RNA Pol II transcription subunit 8 (MED8), preventing MED8 from interacting with RNA Pol II, thereby reducing host cell gene expression. NSs can also suppress the interferon response factor 3 signalling pathway (IRF3), reducing the induction of interferon stimulated genes (ISG) and delaying apoptosis.

1.5.2. Invertebrate innate immune response

As the SUMOylation pathway in mosquitoes has yet to be fully deciphered, this section will broadly describe the vector innate immune response.

Mosquito cell culture is well known to develop a persistent infections which rarely result in cell death (Peleg 1968). This is believed to be due to the antiviral mechanisms of the vector cell restricting arboviral replication. Invertebrates do not have an adaptive immune response, or a directly equivalent IFN based antiviral response. Consequently, invertebrates predominantly rely on cellular based innate immune response, although they do possess haemocytes which act as circulating immune cells. Classically, most work on invertebrate immune responses was conducted on *Drosophila melanogaster* (*D. melanogaster*), although much of this work has now also been studied in more relevant species such as *Ae. aegypti*. Consequently, much of what is described here will focus on *D. melanogaster*. Important invertebrate innate antiviral pathways include the Toll, immune deficiency (IMD), JAK-STAT, and RNAi pathways as summarised in **Figure 1.17**, all of the following pathways have been shown to be antiviral in mosquitoes (for review see Sim, Jupatanakul et al. (2014)).

The Toll and IMD pathways are functionally similar to the mammalian nuclear factor kappa-light-chain-enhancer of activated B cells (NF-κB) pathway. The Toll pathway was initially identified as an antiviral pathway in *D. melanogaster* (Zambon, Nandakumar et al. 2005). Briefly, extracellular PAMPs are detected by PRRs which stimulates the secretion of a cytokine, Spätzle (DeLotto and DeLotto 1998). Spätzle activates the transmembrane Toll receptor, which signals through associated adaptor proteins to phosphorylate Cactus, a homologue of the IκB protein in humans (Nicolas, Reichhart et al. 1998). Cactus phosphorylation leads to proteasomal degradation, which allows Dorsal (named Rel1 in mosquitoes), to translocate to the nucleus and transcribe Toll-regulated antimicrobial genes (Lemaitre, Nicolas et al. 1996, Sim, Jupatanakul et al. 2014).

The IMD pathway is also activated through the detection of extracellular PAMPs by PRRs, resulting in the activation of the IMD protein. In *D. melanogaster* the Peptidoglycan Recognition Proteins (PGRP) are the PRRs which activate the IMD

pathway (Choe, Lee et al. 2005). The IMD pathway then splits into two branches; one activates the transcription factor AP-1 through the JNK signalling, the other branch results in the activation and translocation of the NF-κB like transcription factor, Relish (Rel2 in mosquitoes) (Davis 1994, Sluss, Han et al. 1996, Stöven, Ando et al. 2000, Sanders, Foy et al. 2005, Fragkoudis, Chi et al. 2008, Costa, Jan et al. 2009) (**Figure 1.17**).

The JAK-STAT pathway is widely known in mammals for its role in the IFN response. In *D. melanogaster*, the pathway is activated either by initial binding of the ligand Unpaired (Upd) to the extracellular region of the Domeless (Dome) receptor or through the action of the cytokine Vago, independent of Dome (Harrison, McCoon et al. 1998, Brown, Hu et al. 2001, Hombría, Brown et al. 2005, Paradkar, Trinidad et al. 2012). *D. melanogaster* is only reported to possess one Janus kinase (Hopscotch, or Hop in mosquitoes), and one STAT transcription factor (Binari and Perrimon 1994, Hou, Melnick et al. 1996, Yan, Small et al. 1996). Similar to mammals, receptor activation results in a conformational change and dimerization of Dome. This leads to self-phosphorylation of the receptor associated Hop, which recruit the STAT proteins to be phosphorylated by the Dome/Hop complex. STAT proteins are dimerized and translocate to the nucleus to induce gene expression (Arbouzova and Zeidler 2006) (**Figure 1.17**).

The most potent mechanism invertebrates have for restricting arbovirus replication is from the RNA interference (RNAi) pathway. There are three RNAi pathways, the small interfering RNA (siRNA) pathway, the micro RNA (miRNA) and Piwi-interacting RNA (piRNA) pathways (for review, see Blair and Olson (2015), Olson and Blair (2015)). miRNA genes are commonly utilised by the cell as a form of post-transcriptional gene regulation, affecting approximately 15% of the *Drosophila* genome (Grün, Wang et al. 2005). The function of the piRNA pathway is still largely unresolved. Generally they are thought to regulate transposons in germline cells. The piRNA pathway is distinct from miRNA and siRNA as the biogenesis is independent of Dicer (Vagin, Sigova et al. 2006). The siRNA pathway is the best studied of the RNAi pathways and has a widely known role in cellular antiviral defence. Upon arboviral replication in the host cell, the siRNA pathway is initiated by long strands of dsRNA located in the cytoplasm.

The dsRNA is cleaved by Dicer 2 into siRNA stretches of 21 nucleotides. The siRNA-Dicer 2 complex, in association with the dsRNA binding protein R2D2, enables the 21 nucleotide stretch of dsRNA to bind and load onto the RNA-induced silencing complex (RISC), which assembles differently in humans and invertebrates (Yoda, Kawamata et al. 2010). Argonaute 2 (Ago2) is the effector protein of the RISC complex, which unwinds the double stranded siRNA into a single guide strand of siRNA. If the guide siRNA forms a base paired duplex with the complementary viral RNA strand, Ago2 then cleaves the complementary RNA strand at the centre of the base paired duplex (Bernstein, Denli et al. 2001, Martinez, Patkaniowska et al. 2002, Pham, Pellino et al. 2004, Matranga, Tomari et al. 2005, Rand, Petersen et al. 2005).

There is also a degree of crosstalk between the immune pathways which likely evolved to ensure a comprehensive immune response. For instance, Dicer 2, along with its function in the RNAi pathway, also activates TNF receptor-associated factor (TRAF). TRAF cleaves and activates Rel2, the NF-κB like transcription factor utilised in the IMD pathway. This allows Rel2 to promote the transcription of Vago, which is secreted and activates the JAK-STAT pathway, in a similar manner to the IFN response in mammals (Deddouche, Matt et al. 2008, Paradkar, Trinidad et al. 2012, Paradkar, Duchemin et al. 2014) (**Figure 1.17**).

Many arboviruses have co-evolved with their vector species with the aim to minimise adverse effects on vector survival. Consequently the majority of the evidence of viruses possessing strategies to suppress the vector immune responses is recent and not fully uncovered. **Section 1.5.2.1, Section 1.5.2.2, Section 1.5.2.3** will describe what is currently known about mechanisms the arboviruses employ to evade the vector immune response.

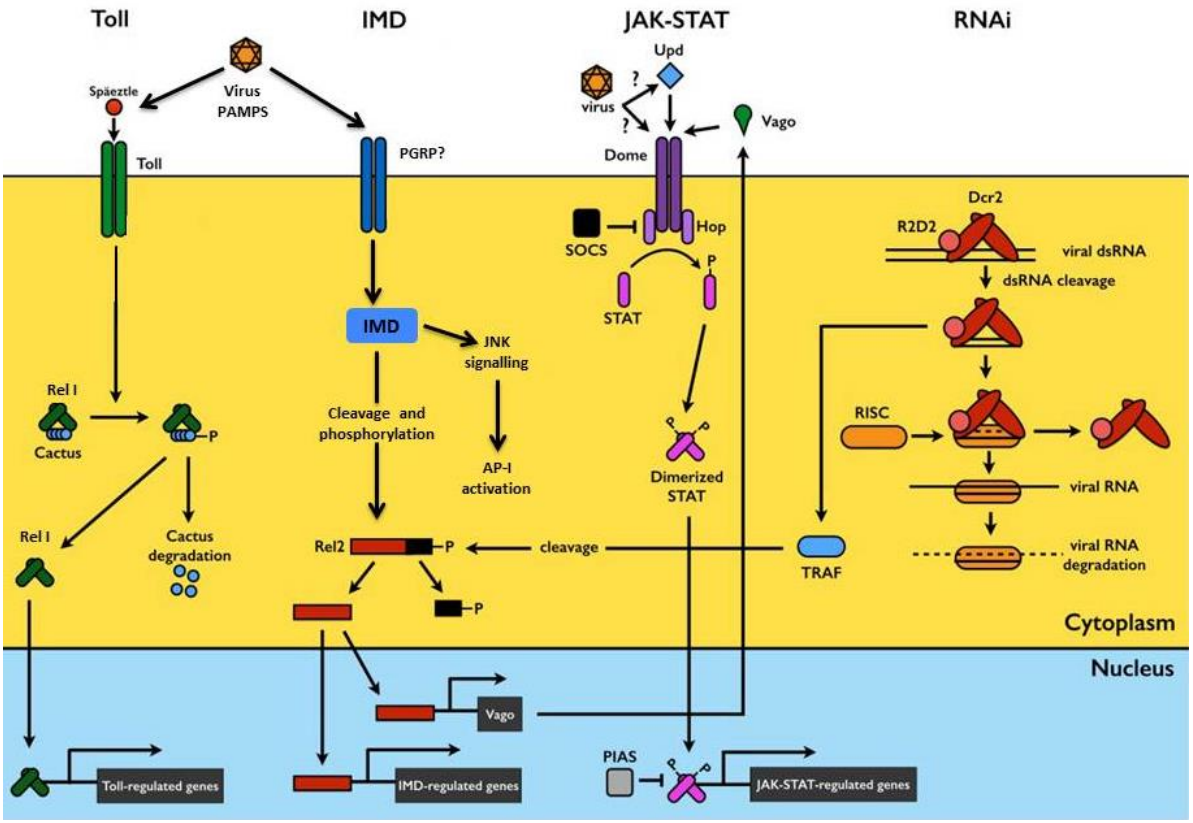

Figure 1.17 Mosquito immune response

In Toll pathway signalling, extracellular viral pathogen associated molecular patterns (PAMPS) are detected by pattern recognition receptors (PRR) which then cleave Spätzle. Spätzle binds and activates the Toll receptor which triggers the phosphorylation (P) and degradation of Cactus. Cactus degradation enables the transcription factor RelI to localise to the nucleus and induce expression of toll-regulated genes. The IMD pathway is also activated by viral PAMPS triggering PRR (probably the peptidoglycan recognition protein (PGRP)), resulting in IMD activation and a functional split in the pathway. One branch triggers the c-Jun N-terminal kinase (JNK) signalling pathway which activates the transcription factor activator protein I (AP-I). The other branch phosphorylates and cleaves the transcription factor Rel2, which activates it allowing Rel2 to translocate to the nucleus and induce IMD regulated gene expression. The JAK-STAT pathway is activated by unpaired (Upd) binding to the receptor, Dome. Binding activates the receptor associated Hop janus kinase, which then recruits and phosphorylates the transcription factor, STAT.

Continued on next page

STAT dimerises and translocates to the nucleus triggering JAK-STAT regulated genes. The JAK-STAT pathway can be inhibited by the suppressors of cytokine signalling (SOCS), preventing Hop from phosphorylating STAT, or protein inhibitor of activated STAT (PIAS) preventing dimerised STAT from inducing gene expression. The RNA interference (RNAi) pathway is activated by activation of Dicer 2 (Dcr2) by viral double stranded RNA (viral dsRNA). Dcr2 cleaves the viral dsRNA into 21 bp lengths called siRNA which are then loaded onto RNA induced silencing complex (RISC), which degrades one strand of siRNA and utilises the other for targeted degradation of viral RNA. Dcr2 activation also activates TRAF which results in Rel2 cleavage, transcription of Vago, and further activation of the JAK-STAT pathway. Adapted from Sim, Jupatanakul et al. (2014)

1.5.2.1. Alphaviruses and *Ae. aegypti* immune response

The primary mechanism of suppressing alphavirus replication in *Ae. aegypti* is through the action of the RNAi pathway. Old World alphaviruses have previously been reported to suppress the Toll, IMD, and JAK-STAT pathway immune responses in *Ae. aegypti* cell lines. Prior stimulation of the antiviral pathways has been shown to reduce SFV and CHIKV replication in invertebrate cell culture, this was achieved through non-specific and incomplete host cell transcriptional shut-off (Fragkoudis, Chi et al. 2008, McFarlane, Arias-Goeta et al. 2014). Although the specific viral protein was not identified, it is likely to be the function of nsP2 in the Old World alphaviruses, as this is the protein identified as being responsible for host cell shut-off in vertebrate cells, as described (**Section 1.5.1.1**) (Garmashova, Gorchakov et al. 2006, Breakwell, Dosenovic et al. 2007). CHIKV has also been shown to influence the RNAi pathway through altering miRNA expression within *Ae. albopictus* cells (a mosquito vector closely related to *Ae. aegypti*). For instance, CHIKV infection upregulated the miRNA named miR-2944b-5p, which is predicted to target four cellular pathways including

protein processing in the ER, citrate cycle, ribosome, and ubiquitin mediated proteolysis (Shrinet, Jain et al. 2014). SFV, however, contains viral siRNA 'hot spots' in its genome, which produce more abundant siRNAs with poor antiviral activity that act to suppress this arm of invertebrate immunity (Siu, Fragkoudis et al. 2011).

Interestingly, when mosquitoes are infected with SINV, the viral siRNA produced is crucial for vector survival. If the accumulation of this viral siRNA is suppressed, the virus replicates to higher titres but at the cost of vector survival, indicating an evolutionary trade-off for the virus (Myles, Wiley et al. 2008).

1.5.2.2. Flaviviruses and *Ae. aegypti* immune response

DENV infection of adult *Ae. aegypti* has been reported to down regulate several antimicrobial peptides that are promoted by the Toll signalling pathway (Ramirez and Dimopoulos 2010). The transcriptome of DENV infected mosquitoes and mosquitoes with an over-activated Toll pathway had overlapped intensity of up- and down-regulated transcripts. This indicates that the Toll pathway is a regulator of DENV infection in mosquitoes (Xi, Ramirez et al. 2008). Furthermore, similar studies in *Ae. aegypti* cell culture has also been shown to down-regulate the transcription of many antimicrobial compounds stimulated from both the IMD and Toll pathways (Sim and Dimopoulos 2010). JEV has also been reported to block the phosphorylation of the STAT protein of the JAK-STAT pathway in RNAi deficient *Ae. albopictus* cells (Lin, Chou et al. 2004). Together, this indicates that flaviviruses utilise a wide range of mechanisms to suppress the *Ae. aegypti* Toll, JAK-STAT, and IMD immune pathways.

As the RNAi pathway is the primary method of antiviral action in invertebrates, flaviviruses have reportedly evolved multiple mechanisms to suppress the RNAi response. DENV NS4B has been reported to suppress the RNAi response in both mammals and in the invertebrate fall armyworm *Spodopetra frugiperda*, possibly through interfering with Dicer 2 activity (Kakumani, Ponia et al. 2013), although

this has not yet been studied in *Ae. aegypti* vector. YFV capsid protein has also been implicated as a viral suppressor of RNA silencing, through interfering with Dicer 2, and with a conserved function in other flaviviruses (Samuel, Wiley et al. 2016). sfRNA also possesses a functional role in the *Ae. aegypti* vector, along with the *H. sapiens* host. sfRNAs have been shown to inhibit the processing of dsRNA by Dcr2 and Ago2 *in vitro* and vector mosquitos (Schnettler, Sterken et al. 2012, Moon, Dodd et al. 2015). Other studies investigating the role of sfRNAs in mosquitoes have suggested a tissue specific role for sfRNAs, as relatively larger quantities of sfRNA, and corresponding higher viral titres were produced in the salivary glands compared to the midgut or carcass (Pompon, Manuel et al. 2017). DENV infection can also lead to altered expression of cellular miRNA. The miRNAs altered included those involved in protein transport, transcriptional regulation, mitochondria, chromatin modification, and signal transduction processes in order to promote viral replication (Campbell, Harrison et al. 2014). WNV_{KUN} has also been shown to encode its own miRNA strand which targeted and increased accumulation of *Ae. aegypti GATA4* transcripts. When *GATA4* mRNA was silenced, WNV_{KUN} replication was significantly reduced, indicating that the arbovirus is able to manipulate expression of cellular proteins to benefit the virus in *Ae. aegypti* (Hussain, Torres et al. 2012).

1.5.2.3. Orthobunyaviruses and *Ae. aegypti* immune response

The NSs proteins from BUNV and LACV have been reported as viral suppressors of RNAi. Studies that deleted sections of NSs and assessed the replication in Dcr2 deficient mosquito cell lines found BUNVΔNSs to be less infectious in *Ae. aegypti* mosquitoes. This indicates that NSs has a role in suppressing the function of Dcr2 in the vector, although a mechanism has not been identified (Soldan, Plassmeyer et al. 2005, Szemiel, Failloux et al. 2012).

1.5.3. SUMOylation pathway interactions with viruses

PTM by SUMO is known to be an essential form of cellular modification. SUMOylation has previously been shown to either positively or negatively influence viral replication for a range of DNA and RNA viruses in mammalian cells (Wilson 2012, Wimmer and Schreiner 2015, Wilson 2017). SUMOylation is also known to help host cells enter an antiviral state, due to alterations of host cell signalling pathways (Hannoun, Maarifi et al. 2016). As a consequence, many viruses may need to alter cellular SUMOylation in order to propagate efficiently. This section will focus on interactions between the SUMOylation machinery and viral proteins.

Many aspects of viral replication are known to be regulated by SUMOylation of viral proteins. For instance, the N protein from severe acute respiratory syndrome (SARS) coronavirus is SUMO modified, promoting oligomerization (Li, Xiao et al. 2005). Furthermore, SUMO modification of the M1 matrix protein of influenza A virus promotes viral assembly and maturation (Wu, Jeng et al. 2011). Other studies have found components of the SUMOylation pathway to be targeted by viruses in order to promote viral replication. Human Papillomavirus has been found to decrease the cellular concentration of Ubc9 through the action of the E6 oncoprotein, decreasing overall cellular SUMOylation in order to promote viral propagation (Heaton, Deyrieux et al. 2011). Furthermore, the latent membrane protein 1 from Epstein Barr virus (EBV) has been found to possess a C-terminal activating region, which interacts with Ubc9 in order to increase cellular SUMOylation (Bentz, Whitehurst et al. 2011). RNAi studies have implicated SAE1/2 and Ubc9 in restricting adeno-associated virus replication by targeting entry of the capsids (Hölscher, Sonntag et al. 2015). Members of the PIAS family of proteins, which are classically regarded as suppressors of innate immunity, have also been reported to localise to nuclear domains during Herpes Simplex Virus-1 (HSV-1) infection to suppress replication as part of an intrinsic immune response (Brown, Conn et al. 2016, Conn, Wasson et al. 2016). In contrast, HCV infected cells upregulated the expression of SUMO1, with depletion of SUMO1 resulting in reduced viral replication, indicating that SUMO1 has a pro-viral effect on HCV replication (Akil, Wedeh et al. 2016).

1.5.4. SUMO and arboviruses

To date, there are three studies looking at the interaction between arboviruses and the SUMO pathway with contradictory outcomes (Chiu, Shih et al. 2007, Su, Tseng et al. 2016, Feng, Deng et al. 2018). Chiu, Shih et al. (2007) demonstrated that Ubc9 in human cells could interact with DENV E protein, possibly through SUMO modification of Lysines 51 and 241. Ubc9 could also restrict DENV replication following ectopic expression. This is supported by recent studies by Feng, Deng et al. (2018) who utilised siRNA to deplete expression of Ubc9 and found an increase in DENV RNA, although they did not investigate a phenotype. In contrast to this, Su, Tseng et al. (2016) demonstrated that the NS5 protein is a target for SUMO modification which prevents ubiquitin-mediated degradation and consequently helps to stabilize the viral protein, furthermore shRNA transduction to deplete expression of Ubc9 was found to suppress DENV replication (Su, Tseng et al. 2016). Together, these demonstrate that there is a role for the SUMOylation pathway in the regulation of arboviruses. However, currently the role of SUMOylation on arbovirus replication in *H. sapiens* is contradictory, and no work has yet been conducted in the mosquito vector species.

Studies have been conducted in *D. melanogaster* investigating changes in the SUMO proteome in response to bacterial lipopolysaccharide (LPS) activation of host immune responses. A total of 710 proteins were confidently identified as being SUMO modified, of which 4.8% were known to be in a functional group involved in an immune response. Proteins which were found to be SUMO modified include: STAT92E (transcription factor in JAK-STAT pathway), Basket (JNK signalling), 14-3-3ε (signalling and protein transport), Casp (negative regulator of IMD/NF-κB pathway), or Imd (signal transducer in IMD/NF-κB pathway) (Gronholm, Ungureanu et al. 2010, Handu, Kaduskar et al. 2015). This indicates a prominent role for SUMO modification during the regulation of invertebrate immunity.

1.6. Premise and primary objectives of the project

Arboviruses are a major pathogen of both humans and livestock. Understanding the molecular basis for how they replicate in both the host and vector species may be key to identifying novel strategies for controlling arbovirus replication.

The SUMO pathway is well known to both positively and negatively influence the replication of a wide range of RNA and DNA viruses in a virus dependent manner. However, to date, there are only two studies which focus on the influence of the SUMO pathway on arboviruses. Both focus on DENV, and both studies are conducted in *H. sapiens* cells. Consequently, there is a lack of understanding about the influence of this pathway on arboviruses in the vector species, and with a range of arboviruses from different viral families.

The primary objectives of the work presented here aims to:

- Investigate the homology between the *H. sapiens* and uninvestigated *Ae. aegypti* SUMOylation pathways

- Characterise the biochemical properties of the *Ae. aegypti* SUMOylation pathway with respect to the *H. sapiens* SUMOylation pathway

- Investigate the physiological effect of the *Ae. aegypti* SUMOylation pathway on arbovirus replication (SFV, BUNV, and ZIKV).

- Investigate the physiological effect of components of the *H. sapiens* SUMOylation pathway on SFV, BUNV, and ZIKV replication.

In doing so, the aim is to improve our understanding of the influence of invertebrate and vertebrate SUMOylation on arbovirus replication.

2. Materials & Methods

2.1. Materials

2.1.1. Cells and cell culture reagents

2.1.1.1. Cell lines utilised

Table 2-1 Summary table of cell lines used in this study

Name	Type	Growth and maintenance media	Growth and maintenance conditions
A20	Larval *Ae. aegypti* cell line originally cultured by Varma and Pudney (1969).	L15 supplemented with 10% FBS	28˚C
Aag2	Larval *Ae. aegypti* cell line originally cultured by Peleg (1968). Have been validated to show they possess an immune response comparable to *Ae. aegypti* mosquitoes (Barletta, Silva et al. 2012).		
AF5	Single cell clone of *Ae. aegypti* cells originally derived from Aag2s and found to have a similar immune response to Aag2s (Varjak, Maringer et al. 2017).		
HFt	Human Foetal Foreskin Fibroblast cells immortalized by stable expression of human telomerase, as described by Smith, Goddard et al. (2013). HFt cells were gifted from Steven McFarlane (MRC-University of Glasgow Centre for	DMEM supplemented with 10% FBS and 5 µg/ml Hygromycin	37˚C, 5% CO_2

	Virus Research).		
A549-Npro	Human alveolar carcinoma cells, modified to contain an NPro which renders the cells IRF3 deficient and prevents them from producing an interferon response, as previously described (Hilton, Moganeradj et al. 2006, Perez-Cidoncha, Killip et al. 2014). Gifted from Dr Claire Donald (MRC-University of Glasgow Centre for Virus Research).	DMEM supplemented with 10% FBS, and 0.5 µg/ml Puromycin	37˚C, 5% CO_2
HEK-293T	Human embryonic kidney cells that express a mutant version of the SV40 large T antigen (DuBridge, Tang et al. 1987).	DMEM supplemented with 10% FBS	
Vero-E6	African green monkey kidney epithelial cells (Yasumura and Kawakita 1963).	DMEM supplemented with 10% FBS	
BHK	Baby Hamster kidney cells originally cultured by Macpherson and Stoker (1962).	GMEM supplemented with 10% FBS and 10% TPB	

2.1.1.2. Cell culture reagents utilised

Table 2-2 List of cell culture reagents used in this study

Name	Source	Catalogue number
2.5% Trypsin (10X)	Gibco	15090-046
Avicel RC dispersible microcrystalline cellulose (Avicel)	FMC BioPolymer	RC-591NF
Dharmacon DhermaFECT 2	GE Healthcare	T-2002-02
Dimethyl sulphoxide (DMSO)	Sigma	D2660
Dulbecco's Modified Eagle Medium (DMEM)	Gibco	41966-029
Fetal Bovine Serum (FBS)	Gibco	10270-106
Glasgow's Minimum Essential Medium (GMEM)	Gibco	21710-025
Hexadimethrine bromide (Polybrene)	Sigma-Aldrich	H9268
Leibovitz's-L15	Gibco	31415-029
Lipofectamine2000	Invitrogen	11668027
Lipofectamine LTX with PLUS reagent	Invitrogen	10964021
Poly-D-Lysine Hydrobromide	Sigma-Aldrich	P7405
Puromycin	Sigma-Aldrich	P8833
Sodium Bicarbonate	Gibco	25080-060
Tryptose Phosphate Broth (TPB)	Gibco	18050-039
Versene in PBS	E&O laboratories	BM0400

2.1.1.3. Viruses

Table 2-3 Viruses used in this study

Virus	Description
SFV-eGFP	Semliki Forest virus modified to encode an eGFP within the nsP3 protein, as described by Tamberg, Lulla et al. (2007). The plasmid was kindly gifted by Dr Esther Schnettler (Bernhard Nocht Institute for Tropical Medicine).
SFV-Ffluc	Semliki Forest virus modified to encode a Firefly luciferase (Ffluc) reporter protein within the nsP3 protein, as previously described (Tamberg, Lulla et al. 2007). The plasmid was kindly gifted by Dr Esther Schnettler (Bernhard Nocht Institute for Tropical Medicine).
ZIKV PE243	A clinical strain of ZIKV originally isolated from a patient in Recife (Brazil) from the 2016 outbreak, as described Donald, Brennan et al. (2016). The virus was grown and gifted by Dr Claire Donald (MRC-University of Glasgow).
ZIKV-nl	A clinical strain of ZIKV containing a NanoLuciferase reporter protein. The modified polyprotein contains a duplicated copy of the capsid protein flanked by a foot-and-mouth-disease virus 2A autoprotease, as previously described Mutso, Saul et al. (2017), Royle, Donald et al. (2017). The virus was produced and gifted by Jamie Royle (MRC-University of Glasgow Centre for Virus Research) subsequent stocks were grown by the author.

BUNV	A wild type strain of Bunyamwera virus, as described by Bridgen and Elliott (1996), gifted by Dr Xiaohong Shi (MRC – University of Glasgow Centre for Virus Research)
BUNV-nl	A strain of Bunyamwera virus modified to contain a NanoLuciferase (nl) reporter protein within the cytoplasmic domain of NSm, producing a fusion NSm-nl protein. As described by Dietrich, Shi et al. (2017), gifted by Dr Xiaohong Shi (MRC – University of Glasgow Centre for Virus Research).

2.1.2. Antibodies

Table 2-4 Antibodies used in this study

Target	Origin	Source	Primary or secondary	Dilution used
SUMO1	Rabbit	Abcam – AB32058	Primary	1:1000
SUMO2/3	Mouse	Abcam – AB81371	Primary	1:1000
Ubc9	Goat	Abcam – AB21193	Primary	1:1000
Actin	Rabbit	Sigma Aldrich –A5060	Primary	1:1000
SAE2	Rabbit	Bethyl – A302-925A	Primary	1:1000
PIAS1	Rabbit	LSBio – LS-B9173	Primary	1:1000
PIAS2α	Rabbit	Millipore – ABS447	Primary	1:1000
GFP	Rabbit	Abcam – AB290	Primary	1:1000
ZIKV NS3	Rabbit	A kind gift from Andres Merits (University of Tartu, Estonia) (Mutso, Saul et al. 2017)	Primary	1:1000
BUN N	Rabbit	A kind gift from Dr Xiaohong Shi (MRC – University of Glasgow Centre for Virus Research) (Weber, Dunn et al. 2001)	Primary	1:5000
Mouse primary	Goat with fluorophore	Thermo Scientific - SA535521	Secondary	1:10000

antibodies	conjugate			
Rabbit primary antibodies	Goat with fluorophore conjugate	Thermo Scientific – SA535571	Secondary	1:10000
Goat primary antibodies	Donkey with fluorophore conjugate	Li-Cor – 926-32214	Secondary	1:10000
Rabbit primary antibodies	Goat with peroxidase conjugate	Sigma Aldrich – A0545	Secondary	1:5000

2.1.3. Plasmids

Table 2-5 Plasmids used in this study

Name	Description	Source
pACYC-*Aa*SAE2/1	Bacterial dual expression vector containing the *Ae. aegypti* SAE1/2 activating heterodimer.	This study
pET28a-*Hs*SUMO1	Bacterial expression vector containing the sequence for *Hs*SUMO1	cDNA obtained from Professor Ron Hay, plasmids were a kind gift from Dr Chris Boutell
pET28a-*Hs*SUMO2	Bacterial expression vector containing the sequence for *Hs*SUMO2	cDNA obtained from Professor Ron Hay, plasmids were a kind gift from Dr Chris Boutell
pET28a-*Hs*SUMO3	Bacterial expression vector containing the sequence for *Hs*SUMO3	cDNA obtained from Professor Ron Hay, plasmids were a kind gift from Dr Chris Boutell
pET28a-*Hs*Ubc9	Bacterial expression vector containing the sequence for *Hs*Ubc9	cDNA obtained from Professor Ron Hay, plasmids were a kind gift from Dr Chris Boutell
pET28a-*Aa*SUMO	Bacterial expression vector containing the sequence for *Aa*SUMO	Dr Sue Jacobs, unpublished data

pET28a-SUMO chimaera	Bacterial expression vector containing the sequence for SUMO chimaera	Synthesised by GENEWIZ, cloned in this study
pET28a-SUMO chimaera K11R	Bacterial expression vector containing the sequence for SUMO chimaera with a mutated lysine -> arginine at position 11	Synthesised by GENEWIZ, cloned in this study
pET45b-*Aa*Ubc9	Bacterial expression vector containing the sequence for *Aa*Ubc9	This study
pET45b-*Aa*PIAS	Bacterial expression vector containing the sequence for *Aa*PIAS	Synthesised by GENEWIZ, cloned in this study
pET45b-*Aa*PIAS C371A	Bacterial expression vector containing the sequence for *Aa*PIAS with a cysteine -> alanine mutation at position 371	Synthesised by GENEWIZ, cloned in this study
pET45b-*Aa*Ubc9 C93S	Bacterial expression vector containing the sequence for *Aa*Ubc9 with a mutated cysteine -> serine at position 93	This study
pGEX-*Hs*SAE1/2	Bacterial expression vector containing the sequence for *Hs*SAE1/2 as described in (Tatham, Jaffray et al. 2001)	cDNA obtained from Professor Ron Hay, plasmids were a kind gift from Dr Chris Boutell
pCMV.DR.8.91	Lentivirus helper vector that expresses the reverse transcriptase polymerase, capsid protein (gag), and regulatory proteins (Rev and	A kind gift from Professor Rodger Everett (MRC – University of Glasgow Centre for

	Tat) as described in (Everett, Rechter et al. 2006)	Virus Research)
pCMV-SFV4.eGFP	Plasmid encoding Semliki Forest Virus containing an internal eGFP reporter protein as described in (Tamberg, Lulla et al. 2007)	A kind gift from Dr Esther Schnettler (Bernhard Nocht Institute for Tropical Medicine)
pCMV-SFV4.Ffluc	Plasmid encoding Semliki Forest Virus containing an internal Firefly luciferase reporter protein as described in (Tamberg, Lulla et al. 2007)	A kind gift from Dr Esther Schnettler (Bernhard Nocht Institute for Tropical Medicine)
pVSV-G	Lentivirus helper vector that expresses the VSV envelope protein, used in the production of lentivirus vectors as described in (Everett, Rechter et al. 2006)	A kind gift from Professor Rodger Everett (MRC – University of Glasgow Centre for Virus Research)
shCtrl	Plasmids encoding a short hairpin RNA against a non-targeted control sequence (5'-TTATCGCGCATATCACGCG-3')	A kind gift from Dr Chris Boutell (Everett, Rechter et al. 2006).
pLKO-shSUMO1	Plasmids encoding a short hairpin RNA against SUMO1	A kind gift from Dr Kristen Conn, unpublished data, from MISSION shRNA lentivirus vector collection (Sigma-

		Aldrich)
pLKO-shSUMO2/3	Plasmids encoding a short hairpin RNA against SUMO2/3	A kind gift from Dr Kristen Conn, unpublished data, from MISSION shRNA lentivirus vector collection (Sigma-Aldrich)
pLKO-shPIAS1	Plasmids encoding a short hairpin RNA against PIAS1 (5'-TTGTAAGTCGTAAGGCATGGG-3') as described in Brown, Conn et al. (2016)	A kind gift from Dr Kristen Conn

2.1.4. Primer sequences

Table 2-6 Oligonucleotide sequences used in this study

Primer	Use	Sequence (5'-3')
pET-Ubc9 F	Cloning	CCGGACCGGTTCCGGAATTGCGATCGC
pET-Ubc9 R	Cloning	CGCGCTCGAGCTACTCCGTGGCAGCCATGG
Ubc9 C93S Int F1	Site directed mutation	AACCGTCTCTCTGTCGC
Ubc9 C93S Int R1	Site directed mutation	GCGACAGAGAGACGGTT
AaSAE2 F	Cloning	GCACTGCAGGAAACAATAGC
AaSAE2 R	Cloning	CTCAGCTCCCGCTTCCGGATCC
AaSAE2 F1	Cloning	TCTCCGGATACTGCGGATCC
AaSAE2 R1	Cloning	GAATGATGTTTCCCGCCATGG
AaSAE2 F2	Cloning	GCTTTGAAGTCAAATCCATGG
AaSAE2 R2	Cloning	CAATGTGTACTCTTACC
AaSAE1 F	Cloning	ACCGCAGACGCCGCCTTG
AaSAE1 R	Cloning	GATATTAAAGTATATACG
AaSAE1 F1	Cloning	GAACGAACCGTGCGGAAGCTTC
AaSAE1 R1	Cloning	CTGAGCCCGAGACAAAGAAGCTTC
AaPIAS F for pET45b	Cloning	CCGGACCGGTATGAGAAAAACGCGG
AaPIAS R for pET45b	Cloning	CGCGGCGGCCGCTCATATCTTGG
pET28-AaSUMO F	Cloning	GGCGCATATGTCTGAAGAAAAAAAGG
pET28-AaSUMO R	Cloning	TATCCTCGAGTTATCCGCCTGTCTG

pET28-SUMO chimera F	Cloning	ATTGCATATGTCCGAGGAGAAGCC
Q_AaSUMO_F	Q-PCR	CGCCAATTTTCAGCACAC
Q_AaSUMO_R	Q-PCR	CGGATCCCTTCGAGTCC
Q_AaUbc9_F	Q-PCR	CGGCGAGGAGCGAAAAG
Q_AaUbc9_R	Q-PCR	TTCTTTCCTGGAATAG
Q_AaPIAS_F2	Q-PCR	GACAATCTTGTTATCGATGGCT
Q_AaPIAS_R	Q-PCR	GCGCTTCAATGGGAGATC
Q_LacZ_F	Q-PCR	CCGGCTGTGCCGAAAT
Q_LacZ_R	Q-PCR	GCGGCTGATGTTGAACTGG
Q_Ago2_F	Q-PCR	GAGCAAACAAATATCCCA
Q_Ago2_R	Q-PCR	TGGTGTCGCTTTTGGAC
Q_AeS7_F	Q-PCR	CCAGGCTATCCTGGAGTTG
Q_AeS7_R	Q-PCR	GACGTGCTTGCCGGAGAAC
Q_BUNV_Lprt_F_cRNA strand	Q-PCR	GACACCCCTGAGCTAGAGGAGC
Q_BUNV_Lprt_R_cRNA strand	Q-PCR	CCACCTCTGTCTCTGCTCTGGC
Q_SFV_Stru_F	Q-PCR	GCCGAAAACGCAGCCCAAG
Q_SFV_Stru_R	Q-PCR	GGCGTACCCAGTGACCTTTCCTT
Q_ZIKV_NS3_F	Q-PCR	ATCTGTATGGAGGTGGGTGC
Q_ZIKV_NS3_R	Q-PCR	CTCTCCCTCAATGGCTGCTA
T7-AaSUMO F	dsRNA synthesis	taatacgactcactatagggTCCGAATCGGAGCACATTAA
T7-AaSUMO R	dsRNA synthesis	taatacgactcactatagggCATGTTCCATGGCTTGTACG

T7-AaUbc9 F	dsRNA synthesis	taatacgactcactatagggATGTCCGGAATTGCGATCGC
T7-AaUbc9 R	dsRNA synthesis	taatacgactcactatagggGGATCCTTGATGTTCGGTTCGT
T7_AaPIAS_F_3	dsRNA synthesis	taatacgactcactatagggAAcAGGAGGATTACTTCCCACC
T7_AaPIAS_R_3	dsRNA synthesis	taatacgactcactatagggGCAGACGGGACAGTTCCAAG
Ago2 T7 F	dsRNA synthesis	taatacgactcactatagggGCCCTCAACAAGAAACACC
Ago2 T7 R	dsRNA synthesis	taatacgactcactatagggGGCGTTGATCTTGAGCCA
ßGal T7 F	dsRNA synthesis	taatacgactcactatagggGTCGCCAGCGGCACCGCGCCTTTC
ßGal T7 R	dsRNA synthesis	taatacgactcactatagggCCGGTAGCCAGCGCGGATCATCGG

2.1.5. Reagents, chemicals, buffers, and kits

2.1.5.1. Commercial kits

Table 2-7 Commercial kits used in this study

Name	Source	Catalogue number
EndoFree Plasmid Maxi Kit	Qiagen	12362
Fast SYBR Green Master mix	Applied Biosystems	4385612
Firefly Luciferase kit	Promega	E1500
MEGAScript RNAikit	Ambion	AM1626
Micro BCA™ Protein Assay Kit	Thermo Scientific	23235
NanoLuciferase kit	Promega	N1110
PureLink HiPure Plasmid Filter Maxiprep Kit	Invitrogen	K210017
QIAEX II® Gel Extraction Kit	Qiagen	20021
QIAprep Spin Miniprep Kit	Qiagen	27106
QIAquick PCR Purification Kit	Qiagen	28106
Rneasy Plus Mini Kit	Qiagen	74136
TaqMan Reverse Transcription reagents	Applied Biosystems	N8080234

2.1.5.2. Buffers made in house

Table 2-8 List of buffers made in house and used throughout the study

Name	Component
3x BM	30% SGB (v/v), 30% Glycerol (v/v), 8 M urea, 6.5% SDS (w/v), 100 mM DTT
3xBM -DTT	30% SGB (v/v), 30% Glycerol (v/v), 8 M urea, 6.5% SDS (w/v)
Blocking buffer (FBS)	5% filtered FBS in PBS
Blocking buffer (milk)	5% Skimmed Milk Powder in PBST
Coomassie Brilliant Blue Stain	0.12% Coomassie Brilliant Blue powder, 50% Methanol, 10% Acetic acid in water
Coomassie destain Solution	5% Methanol, 7% Acetic acid in water
Coomassie fix solution	50% Methanol, 10% Acetic acid in water
DNA loading buffer	65% Sucrose (w/v), 10 mM Tris, 10 mM EDTA
Fixing buffer	1.8% Formaldehyde, 0.1% NP40 in PBS
PBST	0.05% Tween-20 in PBS
Stacking Gel Buffer (SGB)	0.5 M Tris, 0.4% SDS (w/v), pH6.8
TAE Buffer (50x)	40 mM Tris, 1 mM EDTA, 5 mM sodium acetate (pH7.6)
Trypsin-versene	2.5% trypsin (v/v) in versene

2.1.5.3. Reagents used

Table 2-9 Reagents used in the study

Name	Source	Catalogue / CAS number
100bp DNA ladder	Promega	G571A
1kb DNA ladder	Promega	G210A
2-Propanol	Sigma-Aldrich	24137
2-Mercaptoethanol	MERCK	8.05740.0250
Acetic Acid	VWR Chemicals	20104.334
Amersham Protran 0.2 µm NC blotting membrane	GE Healthcare	10600001
Agar	E&O laboratories	BM5280
Agarose	Sigma-Aldrich	A9539
Ampicillin	Melford	A0104
Bovine Serum Albumin (BSA)	BioRad	500-0207
CellLyse	Sigma-Aldrich	C2978
Chloramphenicol	Sigma-Aldrich	C0378
Coomassie Brilliant Blue	BioRad	161-0400
d-Desthiobiotin	Sigma-Aldrich	D1411
Deoxynucleotides (dATP/dGTP/dCTP/dTTP)	Sigma-Aldrich	DNTPCA10
DL-Dithiothreitol (DTT)	Sigma-Aldrich	43819
Ethylenediaminetetraacetic acid (EDTA)	VWR International	60-00-4
Ethanol	Fisher Chemicals	64-17-5
Ethidium Bromide	Sigma-Aldrich	E1510
Formaldehyde solution (36.5-38%)	Sigma-Aldrich	F8775
Glycerol	Fisher Chemicals	56-81-5
Gurr Giemsa	VWR Chemicals	350864X
His-select® Nickel Affinity Gel	Sigma-Aldrich	P6611
Imidazole 99+% (titration)	Sigma-Aldrich	10250
Isopropyl-thio-ß-D-galactoside	GibcoRBL	15529-019

(IPTG)		
Hygromycin B	Invitrogen	10687010
Kanamycin	Sigma-Aldrich	60615
KPL True Blue Peroxidase Developing Solution	Sera Care	5510-0030
Luria-Bertani (LB) Broth	E&O laboratories	BM5300
Methanol	Fisher Chemicals	67-56-1
PageRuler™ Prestain NIR Protein Ladder	Thermo Scientific	26635
Phosphate Buffered Saline (PBS)	Sigma-Aldrich	D1408
Protease inhibitor cocktail tablets, EDTA Free	Roche	11 873 580 001
Magnesium Chloride ($MgCl_2$)	VWR Chemicals	25108.260
Nonidet P-40 (NP40) Substitute	Sigma-Aldrich	9016-45-9
NuPAGE™ MES SDS running buffer (20X)	Invitrogen	NP0002
NuPAGE™ Sample Reducing Agent (10X)	Invitrogen	NP0004
NuPAGE™ Transfer Buffer	Invitrogen	NP0006-1
NuPAGE™ 4-12% Bis-Tris Gel 10x12 well	Invitrogen	NP0322BOX
NuPAGE™ 4-12% Bis-Tris Gel 10x15 well	Invitrogen	NP0323BOX
Skimmed Milk Powder	Marvel	
Slide-A-Lyzer® MINI Dialysis Unit MWCO 3500	Thermo Scientific	69552
S.O.C. Media	Invitrogen	15544-034
Sodium Chloride	VWR Chemicals	27810.295
Sodium dodecyl sulfate solution (SDS)	Sigma-Aldrich	05030
Strep.Tactin Superflow™ Agarose	Novagen	71592
Tris	Roche	10 708 976 001
Triton-X-100	Promega	H5142

Tween 20	Millipore	655204
Urea	Sigma-Aldrich	U0631

2.1.6. Enzymes

All restriction enzymes and corresponding buffers were obtained from NEB. Phusion High-fidelity DNA polymerase and T4 DNA Ligase were obtained from NEB.

2.1.7. Reagents used for prokaryotic work

2.1.7.1. Bacterial strains and culture media

Two strains of chemically competent *Escherichia coli* (*E. coli*) were used in this study. DH5α (Invitrogen) were used in plasmid DNA amplification and cloning. The strain BL21(DE3) (New England Biolabs) was used in protein expression. All bacterial cultures were grown in a Luria-Bertani (LB) medium overnight, and spread onto agar plates containing the relevant antibiotic selection for the plasmid. Concentrations were: Ampicillin 100 µg/ml, Kanamycin 50 µg/ml, Chlormphenicol 50 µg/ml

2.1.6.2. Buffers for protein purification from bacterial extracts

The reagents used for protein purification can be found in **Table 2-9.**

<u>6xHis epitope tag purification buffer:</u>

Used for *Aa*SUMO, *Aa*Ubc9, *Aa*Ubc9 C93S, *Aa*PIAS, *Aa*PIAS C371A, *Hs*SUMO1, *Hs*SUMO2, *Hs*SUMO3, *Hs*Ubc9, *Hs*SAE1/2, SUMO chimaera, and SUMO chimaera K11R;

50 mM Tris (pH 7.0), 250 mM NaCl, 5% Glycerol, 2.5 mM $MgCl_2$, 10 mM 2-Mercaptoethanol, 30 mM Imidazole, 0.1% Triton-x-100, Protease Inhibitor Cocktail Tablet. Final pH 7.5.

<u>6xHis tag elution buffer:</u>

50 mM Tris (pH 7.0), 250 mM NaCl, 5% Glycerol, 2.5 mM $MgCl_2$, 10 mM 2-Mercaptoethanol, 350 mM Imidazole, 0.1% Triton-x-100, Protease Inhibitor Cocktail Tablet. Final pH 7.5.

6xHis tag dialysis buffer:

50 mM Tris (pH7.0), 150 mM NaCl, 5% Glycerol, 2 mM $MgCl_2$, 1 mM DTT

Strep.II tag purification buffer:

Used for *Aa*SAE1/2;

50 mM Tris (pH 7.0), 50 mM NaCl, 1 mM $MgCl_2$

Strep.II tag elution buffer:

50 mM Tris (pH 7.0), 50 mM NaCl, 1 mM $MgCl_2$, 2.5 mM d-Desthiobiotin (pH 8.5)

Strep.II tag dialysis buffer:

50 mM Tris (pH7.0), 150 mM NaCl, 5% Glycerol, 2 mM $MgCl_2$, 1 mM DTT

2.2. Methods

2.2.1. Cloning and DNA manipulation

2.2.1.1. DNA quantitation

The Nanodrop 2000 spectrophotometer (Thermo Scientific), was used to quantify DNA or RNA when necessary measuring absorbance at 260 and 280 nm.

2.2.1.2. Polymerase Chain Reaction (PCR) amplification

PCR was utilised for the amplification of nucleic acids. A total of 50 µl volume was used for each reaction, and occurred in a PCR Thermal Cycler (Techne TC-312). Each reaction contained 10 µl 5x Phusion® HF buffer (1x), 1 µl Phusion® DNA polymerase (1 U), 0.5 µl dNTPs (5 µM), 10 µM forward primer, 10 µM reverse primer, and approximately 50-100 ng template DNA or cDNA, made up with nuclease free water. Reactions were prepared on ice. Standard reactions were cycled as noted (**Table 2-10**). For dsRNA synthesis, the oligonucleotides contained an additional T7 sequence (5'-taatacgactcactataggg-3'), consequently the reaction cycle was modified (**Table 2-11**). Furthermore, for the production of T7-SUMO for dsRNA production, the concentration of oligonucleotides was decreased to 500 nM forward or reverse primer.

Table 2-10 Standard PCR cycle

Stage	Temperature (˚C)	Duration	
Initial denaturation	98	3 minutes	
Denaturation	98	30 seconds	Cycle 35 times
Oligo annealing	T_M -5	45 seconds	
Extension	72	30 seconds -> 1 minute	
Final extension	72	5 minutes	

Table 2-11 T7 PCR cycle

Stage	Temperature (˚C)	Duration	
Initial denaturation	98	3 minutes	
Denaturation	98	30 seconds	Cycle 6 times
Oligo annealing	T_M -10	45 seconds	
Extension	72	30 seconds	
Denaturation	98	30 seconds	Cycle 35 times
Oligo annealing	T_M -5	45 seconds	
Extension	72	30 seconds	
Final extension	72	5 minutes	

2.2.1.3. Restriction endonuclease digestion

A total volume of 20 µl of reaction mixture was made up for each digestion, containing 1 µl restriction enzyme (1 U/µl), 2 µl 10x required buffer, and plasmid DNA (up to 1 µg), made up in DNase-free water. The restriction enzymes and required buffers were purchased from New England Biosciences (NEB). Reactions were incubated for 1-2 hours at 37 ˚C prior to being analysed by agarose gel electrophoresis and extracted for further use (**Section 2.2.1.4**).

2.2.1.4. Agarose gel electrophoresis

All DNA products, and dsRNA products, were analysed by agarose gel electrophoresis in 1% agarose gels prepared with 1x TAE buffer containing ethidium bromide at 0.5 µg/ml. Samples were mixed with DNA loading dye at a 1:5 ratio, and the gels were resolved at 60 V for between 30 minutes – 2 hours, depending on the size of the product and distance required between bands. DNA ladder markers were used alongside samples to provide reference about the concentration and fragment size. After resolution, samples were visualised by an ultraviolet (UV) transilluminator. Short wave UV was used for imaging and long wave UV was used for gel extraction. Fragments were isolated with a scalpel and DNA isolated with the QIAEX II® Gel Extraction Kit (**Section 2.1.5.1**), following manufacturers guidance.

2.2.1.5. DNA Ligation

Digested fragments of the vector backbone and insert were examined on a 1% agarose gel and quantified by Nanodrop spectrophotometer to confirm expected size and assess concentration (**Section 2.2.1.1; Section 2.2.1.4**). The products were ligated together at a ratio of 7:1 insert fragment to vector backbone. Ligation reactions occurred in 10 µl volumes with 1 µl T4 DNA ligase and 1 µl DNA ligase buffer (**Section 2.1.6**). Samples were incubated overnight at 15 ˚C.

2.2.1.6. Transforming competent bacteria

E. coli DH5α's, used for DNA isolation and amplification, were transformed in 50 µl aliquots. Either 10 µl of ligated product (**Section 2.2.1.5**) or 100 ng plasmid DNA was gently mixed with the competent bacteria and left to incubate on ice for 30 minutes. The competent bacteria were then heat shocked at 42 ˚C for 45 seconds, and cooled briefly on ice. The bacteria were subsequently grown in 300 µl S.O.C medium for 45 minutes without any antibiotic present at 37 ˚C, and plated onto antibiotic selective plates. Bacterial plates were incubated overnight at 37 ˚C.

E. coli BL21 (DE3)'s, used for protein isolation, were transformed in 20 µl aliquots. Approximately 100 ng plasmid DNA was mixed with the competent bacteria and left to incubate on ice for 30 minutes. The competent bacteria were subsequently heat shocked at 42 ˚C for 30 seconds, and briefly cooled on ice. The bacteria were then grown in 300 µl S.O.C. Medium for 45 minutes without any antibiotic, and plated onto antibiotic selective plates overnight at 37 ˚C.

2.2.1.7. Growing bacterial cultures of *E. coli* DH5α

After competent DH5α were transformed with a plasmid of interest (**Section 2.2.1.6**), individual colonies were selected to be grown in LB Broth (**Table 2-9**). For small scale plasmid isolation colonies were grown o/n in 5 ml LB aliquots containing the relevant antibiotic with constant shaking. For large scale plasmid isolation, individual colonies were grown for 3 hours in 5 ml aliquots before being transferred to pre-warmed 350 ml batches of LB broth, containing the relevant antibiotic and allowed to grow o/n at 37 ˚C with constant shaking.

2.2.1.8. Isolation and amplification of DNA using kits

Small scale isolation

Colonies of DH5α were grown as specified (**Section 2.2.1.7**). To isolate the plasmid DNA, 3 ml of culture was centrifuged in an Eppendorf tube at 13,000 rpm for 3 minutes (Eppendorf benchtop centrifuge). The supernatant was removed and plasmid DNA was extracted using the QIAprep® Spin Miniprep Kit (**Table 2-7**) following manufacturers protocol. Following isolation, plasmid DNA was analysed by restriction digest and agarose gel electrophoresis, to confirm correct insert, and sequenced to confirm the gene sequence was correct.

Large scale isolation

Colonies of DH5α were grown as specified (**Section 2.2.1.7**). To isolate plasmid DNA, colonies were centrifuged at 3500 rpm for 30 minutes (Megafuge 16R, Thermoscientific). The supernatant was subsequently removed, and DNA was extracted using the EndoFree® Plasmid Maxi Kit, if the samples were to be used for mammalian transfection (**Table 2-7**). Samples that were intended to be used for further cloning, or bacterial transfection, were isolated using the PureLink HiPure Plasmid Filter Maxiprep Kit (**Table 2-7**).

2.2.1.9. Sequencing by commercial companies

DNA samples to be sequenced were sent to Source Bioscience for processing by Sanger sequencing. Samples were sequenced with primers provided by the company and data was subsequently analysed with VectorNTI® software (Life Technologies).

2.2.1.10. Site directed mutagenesis of plasmid DNA by PCR

The gene of interest (*Aa*Ubc9) was amplified using two pairs of forward and reverse primers, one pair at the 5' and 3' ends of the gene, and a complementary pair of internal primers which contained the Guanosine-Cytidine base pair mutation at position 278 to change the codon from 5'-TGT-3' (Cysteine) in to a 5'-TCT-3' (Serine). Two PCR reactions were initially needed which amplified the 5' and 3' halves of the gene. The next step involved combining the 5' and 3' halves and conducting a third PCR using the external 5' and 3' primers again, as described in (Heckman and Pease 2007) (**Table 2-10**).

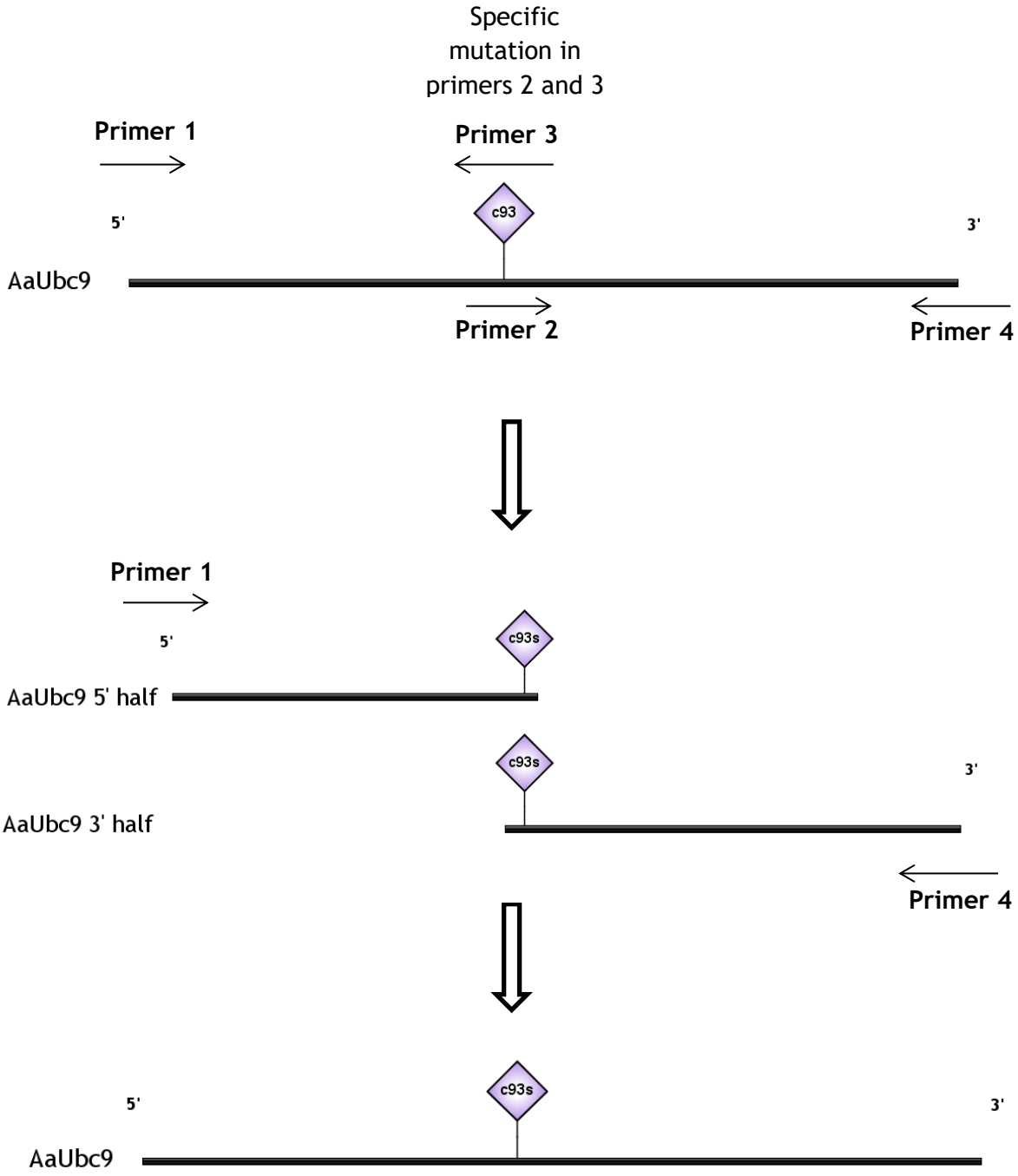

Figure 2.1 Schematic of site directed mutagenesis protocol for *Aa*Ubc9

The gene of interest was amplified using forward and reverse primers (1 and 4). Mutants are produced from two internal primers (2 and 3) which contain the genetic changes encoding the amino acid change Cysteine – Serine at position 93. In the first set of PCR reactions, primers 1 and 3 are used together, and primers 2 and 4 are used as a separate PCR reaction. Equal concentrations of the products are then combined to produce a template for the third PCR, which were undertaken using primers 1 and 4. Primers 1 and 4 also contained restriction endonuclease sites for future cloning into plasmid vectors.

2.2.1.11. dsRNA synthesis for cell culture

Total RNA was extracted from *Ae. aegypti* A20 cell culture, using RNAeasy Plus Kit, following the manufacturer's instructions (**Table 2-7**; **Section 2.2.6.4**), and cDNA was synthesised with random hexamer primers to use as a template for the PCR reaction (**Section 2.2.6.5; Section 2.2.1.2**). As the kit uses T7 DNA-dependent RNA polymerase, all the genes of interested used required the addition of a T7 gene sequence (5'-taatacgactcactataggg-3') which was included in the primer sequences (**Table 2-6**). Between 700 ng – 1 µg of purified T7-PCR product was used to produce dsRNA using the MEGAScript RNAi Kit (**Table 2-7**). The dsRNA synthesis occurred following the manufacturers guidance. The optional step of pre-heating the elution solution to 95 ˚C was undertaken in order to increase yields. Concentration of dsRNA was measured as described (**Section 2.2.1.1**), and purity of product was checked by agarose gel electrophoresis (**Section 2.2.1.4**).

2.2.1.12. dsRNA synthesis for adult *Ae. aegypti*

Total RNA was extracted from *Ae. aegypti* A20 cell culture, using RNeasy Plus Kit, following manufacturer's guidance (**Table 2-7; Section 2.2.6.4**). cDNA was synthesised with random hexamer primers to use as a template for the PCR reaction (**Section 2.2.6.5; Section 2.2.1.2**). As the kit uses T7 DNA-dependent RNA polymerase, all the genes of interested used required the addition of a T7 gene sequence (5'-taatacgactcactataggg-3') which was included in the primer sequences (**Table 2-6**). Between 10 - 15 µg of purified T7-PCR product was used to produce dsRNA using reagents from a MEGAScript RNAi Kit (**Table 2-7**). The initial reaction to synthesise dsRNA was set up as shown in **Table 2-12**, and the reaction was allowed to continue o/n at 37 ˚C. The following day RNA was annealed together for 5 minutes at 75 – 80 ˚C and left to cool at room temperature (RT). To remove DNA and any single stranded RNA which did not anneal, the sample was subjected to nuclease digestion; the reaction was set up as shown in **Table 2-13**. The reaction occurred at 37 ˚C for 1 hour. The dsRNA was subsequently purified by suspending the dsRNA in a binding buffer, as

described in **Table 2-14** binding the dsRNA to a column and centrifuging at 12400 rpm for 1 minute at 4 ˚C (Eppendorf benchtop centrifuge). Elution solution was pre-heated to 95 ˚C to maximise yields. dsRNA was then centrifuged at 4 ˚C at 12,400 rpm for 5 minutes and transferred to another RNase free Eppendorf tube in order to remove the salt pellet. The concentration and purity was checked to ensure there would be enough dsRNA in the final volume to treat mosquitoes with 2 µg dsRNA / mosquito (**Section 2.2.1.1; Section 2.2.1.4**). The dsRNA was vortexed with 1/10 volumes Sodium Acetate and 3 volumes 100% ethanol, the mixture was incubated at -80 ˚C for 2 hours. The sample was centrifuged again (30 minutes, 4 ˚C, 13,000 rpm) supernatant was discarded and the pellet was washed with 1 ml 70% ethanol, followed by another 10 minute centrifuge at 4 ˚C (13,000 rpm). The wash was removed and the pellet was allowed to air dry for 2 minutes before resuspension in nuclease free H_2O at 60 ˚C. The dsRNA was checked again by making a 1/50 dilution, quantifying on the nanodrop and resolving on an agarose gel (**Section 2.2.1.1; Section 2.2.1.4).**

Table 2-12 Components in a nuclease digestion for mosquito depletion

Component	Total for nuclease digestion
dsRNA solution	300 µl
Nuclease free H_2O	To total volume of 750 µl
10X Digestion buffer	75 µl
DNase I	30 µl
RNase	30 µl

Table 2-13 dsRNA synthesis reaction for mosquito depletion

Component	Total for dsRNA synthesis for mosquito depletion
DNA template	10-15 µg
Nuclease free H_2O	To total volume of 300 µl
10x T7 reaction	30 µl
ATP solution (75mM)	30 µl
GTP solution (75mM)	30 µl
CTP solution (75mM)	30 µl
UTP solution (75mM)	30 µl
T7 enzyme mix	30 µl

Table 2-14 dsRNA binding solution for mosquito depletion

Component	Total for dsRNA purification
dsRNA solution	750 µl
Nuclease free H_2O	2.25 ml
10X binding buffer	750 µl
100% Ethanol	3.75 ml

2.2.2. Purification of recombinant proteins

2.2.2.1. Expression in recombinant BL21 (DE3)

After competent *E. coli* BL21 (DE3) cells were transformed with a bacterial expression plasmid of interest (**Section 2.2.1.6**), 5 independent colonies were selected to be grown together o/n in LB broth with the relevant antibiotic at 37 ˚C with constant shaking as starter cultures. The starter cultures were used to set up larger pre-warmed cultures of 200-250 ml supplemented with the relevant antibiotic. The larger cultures were grown for 2 hours at 37 ˚C with constant shaking, and then transferred to a shaking 30 ˚C incubator, and protein expression was induced with the addition of 0.1 mM IPTG for 4-5 hours (**Table 2-9**).

2.2.2.2. Purification of 6xHis tagged proteins

BL21 (DE3) cells were initially transformed, and grown to express the protein of interest (**Section 2.2.1.6**; **Section 2.2.2.1**). Bacterial pellets containing bacterial expression plasmids which encode *Hs*SUMO1, *Hs*SUMO2, *Hs*SUMO3, *Hs*Ubc9, *Hs*SAE1/2, *Aa*SUMO, *Aa*Ubc9, *Aa*Ubc9 C93S, *Aa*PIAS, *Aa*PIAS C371A, SUMO chimaera, or SUMO chimaera K11R, were re-suspended in 25 ml 6xHis purification buffer (**Section 2.1.6.2**). The bacteria were lysed by probe-sonication (45 pulses, 30 Amps), and cell debris was centrifuged at 13000 xg for 10 minutes (Thermo Scientific Evolution RC) and filtered through a 0.45 µm filter (Sartorius). His-select Nickel Affinity Gel (Ni-NTA beads) (**Table 2-9**) were spin washed twice in 1ml 6xHis purification buffer by centrifugation at 6000 rpm for 30 seconds, and re-suspended in 300 µl 50% (w/v) purification buffer. The samples were tumbled end-over-end for 90 minutes at RT, washed twice in 10 ml 6xHis purification buffer, centrifuged at 1500 xg for 5 minutes (Eppendorf benchtop centrifuge), and washed a further three times in 1 ml 6xHis purification buffer. Proteins were eluted in 750 µl 6xHis elution buffer in three fractions (**Section 2.1.6.2**). Dialysis of protein samples occurred with slide-a-

lyser MINI dialysis units (Thermo Scientific), in 6xHis dialysis buffer for four hours (**Section 2.1.6.2**).

2.2.2.3. Purification of Strep.II tagged proteins

Bacterial pellets containing bacterial expression plasmids which encode *Aa*SAE1/2 were re-suspended in 2 ml Strep.II tag purification buffer (**Section 2.1.6.2**). Samples were then lysed by digital sonicator (7 repeats, 50% intensity, 30 seconds, 4 ˚C, Branson Digital Sonifier) and cell debris was centrifuged at 14000 xg for 10 minutes at 4 ˚C (Thermo Scientific Evolution RC). The samples were then filtered with a 0.45 µm filter, tumbled end-over-end for 90 minutes at RT, and washed three times with 1 ml Strep.II tag purification buffer. Samples were then eluted in three fractions of 600 µl Strep.II tag elution buffer, and dialysed o/n at 4 ˚C in Strep.II tag dialysis buffer (**Section 2.1.6.2**).

2.2.2.4. Quantification of proteins by BSA titration

Samples were resolved on a NuPAGE™ 4-12% Bis-Tris Gel alongside a prediluted BSA titration and coomassie stained, protein concentration was determined on the Li-Cor Odyssey Imaging System (**Table 2-9**; **Section 2.2.6.1; Section 2.2.6.2**; Li-Cor Odyssey CLx).

2.2.3. *In vitro* assays of recombinant proteins

2.2.3.1. SUMOylation assays

SUMOylation assays were carried out in 50 mM Tris (pH7.0), 50 mM NaCl, and 5 mM ATP. The reactions analysed by Western blot consisted of 50 ng SUMO, 50 ng Ubc9, and 50 ng SAE1/2 and 10 ng PIAS, where applicable, and occurred at either 28 ˚C or 37 ˚C, as indicated. Reactions analysed by Coomassie stain consisted of 300 ng SUMO, 100 ng Ubc9, 100 ng SAE1/2, and 20 ng PIAS where applicable. Reactions were allowed to continue for the desired length of time until the reaction was terminated by the addition of 3XBM (**Table 2-8**). Thioester-formation assays were terminated with 3XBM –DTT (**Table 2-8**). Samples were boiled at 95 ˚C for 10 minutes and resolved by SDS-PAGE before being transferred to a nitrocellulose membrane for analysis by Western blot (**Section 2.2.6.1; Section 2.2.6.3**).

Assays conducted for Mass Spectrum analysis by collaborators were conducted using 5 µg SUMO, 500 ng Ubc9, 500 ng SAE1/2, and 50 ng PIAS when required. Reactions were conducted at 28 ˚C for 1 hour and terminated with NuPAGE™ Sample Reducing Agent (**Table 2-9**). Samples were subsequently boiled for 10 minutes at 95 ˚C prior to being shipped to collaborators (Dr Michael Tatham, and Professor Ron Hay, University of Dundee) on dry ice.

2.2.4. Cell culture methods

2.2.4.1. Maintenance, growth, and passaging of cells

Mammalian cell cultures were sustained in T75 tissue culture flasks, unless otherwise stated (Nunc Fisher Scientific UK Ltd). Cells were maintained in appropriate media (**Table 2-1**) at 37 ˚C with 5% CO_2. When cells were approximately 90% confluent they were washed 2 - 3 times with 5 ml versene, and incubated with 2 ml trypsin-versene until the cells detached (**Table 2-8**). An aliquot of detached cells were re-suspended in 5 ml of the appropriate media before being seeded in a new flask or counted prior to seeding (**Section 2.2.4.2**).

Ae. aegypti cell cultures were sustained in T25 tissue culture flasks (Nunclon Delta surface Thermo scientific). Cells were maintained in L15 media at 28 ˚C with no CO_2 (**Table 2-1**), when cells were approximately 90% confluent they were knocked off into 2 ml of media using a Cell Scraper (Corning incorporated costar). An aliquot of cells were either re-suspended in 5 ml media in a new flask or counted and seeded for future experiments (**Section 2.2.4.2**).

2.2.4.2. Seeding of cells

The number of cells was determined using a Neubauer haemocytometer counting chamber using a light microscope. Mammalian cells were seeded in 6-, 12-, or 24-well plates. HFt cells were seeded at 1.5 x 10^5 cells / well in a 24-well plate, A549-Npros were seeded in 12 well plates at 3 x 10^5 cells / well, and BHK cells were seeded in 6 well plates at 5 x 10^5 cells / well.

Ae. aegypti cell culture were seeded in 24-well plates at 5 x 10^5 cells / well, after the wells had been treated with Poly-D-Lysine Hydrobromide. Briefly, Poly-D-Lysine Hydrobromide was diluted in sterilised PBS, the wells were incubated with 500 µl Poly-D-Lysine at room temperature for 30 minutes before the Poly-D-Lysine was aspirated off.

All cells in 24-well plates were covered with 1 ml of appropriate media, 12-well plates were covered in 1.5 ml media and cells in 6-well plates were covered with a total volume of 3 ml media. Cells were incubated in the required conditions overnight prior to future experiments.

2.2.4.3. Transfection of mammalian cells

Two different mammalian cell lines were transfected with plasmids:

BHK

3 x 10^5 BHK cells were seeded per well of a 6 well plate, each well was transfected with 2 µg pCMV-SFV4.eGFP or pCMV-SFV4.Ffluc using Lipofectamine2000 following manufacturers guidance (**Section 2.2.4.2; Section 2.2.4.3**; **Table 2-2; Table 2-5**). Conditioned media was added to transfection media after 4 hours and at the end of the day the transfection media was removed and fresh media was added. Cells were then incubated at 37 ˚C during propagation of virus stocks (**Section 2.2.5.1**).

HEK-293T

HEK-293T cells were seeded at a concentration of 2 X 10^6 cells in a 60 mm dish. Cells were incubated o/n at 37 ˚C in 5% CO_2 in 5 ml media, 3 µg of pLKO plasmid expressing a non-target control, SUMO1-targeting, SUMO2/3-targeting, or PIAS1-targeting short hairpin RNA (called shCtrl, shSUMO1, shSUMO2/3, or shPIAS1, respectively), along with the helper plasmids pVSV-G (3 µg) and pCMV-DR8.91 (3 µg) (**Table 2-5**) were combined with 250 µl of serum-free DMEM. PLUS reagent (8 µl) was added to the plasmid mixture and incubated for 15 minutes at room temperature. Simultaneously, 12 µl of Lipofectamine was also mixed with 250 µl serum-free DMEM, and left to incubate at room temperature for 15 minutes. After the incubation was completed, the serum-free DMEM with PLUS reagent, and serum-free DMEM with Lipofectamine were mixed together and allowed to

incubate together for a further 15 minutes at room temperature. Conditioned media was removed, and HEK-293T cells were incubated with the transfection media for 4 hours at 37 ˚C. A 50:50 mix of fresh and conditioned media was then replaced and incubated o/n at 37 ˚C. When CPE was observed (approximately 2 days post transfection), cell supernatant containing released lentiviral particles were harvested, and filtered through a 0.45 µm filter. Samples were then immediately used (**Section 2.2.4.4**).

2.2.4.4. Lentivirus transduction of cells

60 mm dishes of HFt cells at 4 x 10^5 cells / dish were seeded (**Section 2.2.4.2**). Filtered lentivirus (3.5 ml) was mixed with polybrene (3.5 µl) for each target (**Table 2-2**). The filtered lentivirus with polybrene was subsequently added to each dish, the cells were allowed to incubate o/n at 37 ˚C. The following day, the media was removed and fresh media supplemented with 1 µg/ml Puromycin, and 50 µg/ml of Hygromycin was applied to select for successfully transduced cells. The cells were passaged under continuous selection pressure, (5 µg/ml of Hygromycin, and 0.5 µg/ml of Puromycin). mRNA and protein expression was assessed by q-PCR and Western blotting (**Section 2.2.6.3**; **Section 2.2.6.6**).

2.2.4.5. dsRNA transfection of mosquito cells

AF5 cells were seeded in 24 well plates at 2.5 x 10^5 cells / well, and left to incubate o/n at 28 ˚C. Target dsRNA (300 ng) was transfected with 2 µl DharmaFECT2 (**Table 2-2**) per well following manufacturer's instructions. Cells were incubated at 28 ˚C for 72 hours prior to infection (**Section 2.2.5.5**).

2.2.5. Virology

2.2.5.1. Propagation of SFV

BHK cells were transfected with either the plasmid pCMV-SFV4.Ffluc, or pCMV-SFV4.eGFP (as described in **Section 2.2.4.3**), and incubated at 37 ˚C until CPE was observed, at which point the supernatant containing SFV was collected and centrifuged at 3000 rpm at 4 ˚C for 10 minutes, 1 ml of this p0 stock was used to infect a T175 flask of BHKs. The flask was incubated at 37 ˚C for 2-4 days until CPE was observed. Supernatant was then collected, centrifuged again at 3000 rpm at 4 ˚C for 10 minutes; virus was then aliquoted and stored at -80 ˚C for titration and future experiments.

2.2.5.2. Propagation of BUNV

An aliquot of both wild type BUNV and BUNV possessing a NanoLuciferase reporter protein was provided by Dr Xiaohong Shi (MRC – University of Glasgow Centre for Virus Research), this was used to infect a monolayer of 80-90% confluent BHK cells at a low MOI (0.01 - 0.001) (**Table 2-1; Table 2-3**). Upon observation of CPE (approximately 4 - 5 days post infection), supernatant was harvested and centrifuged at 3000 rpm at 4 ˚C for 10 minutes. Virus was aliquoted and stored at -80 ˚C for titration and future experiments.

2.2.5.3. Propagation of ZIKV

An aliquot of a clinical strain of ZIKV (PE243) and ZIKV possessing a NanoLuciferase reporter protein was provided by Dr Claire Donald (MRC – University of Glasgow Centre for Virus Research) and Jamie Royle (MRC – University of Glasgow Centre for Virus Research), respectively (**Table 2-3**). This virus was used to infect a roller bottle containing 60-70% confluent Vero cells at a low MOI (0.01 – 0.001) (**Table 2-1**). Media pH was maintained during this time by the addition of Sodium Bicarbonate (**Table 2-2**). Upon observation of CPE,

approximately 7 – 12 days post infection, virus was harvested and supplemented with an additional 10% FBS, aliquoted and stored at -80 ˚C for titration and future experiments.

2.2.5.4. Determining viral titre

Viral titre was determined by either lytic plaque formation or Immunocytochemistry (ICC) plaque staining. For the three viruses used; SFV and BUNV were titrated by lytic plaques, ZIKV was titrated by ICC. All titration involved 10-fold serial dilutions of the virus from stock concentrations. Titrations were calculated by determining the number of plaque forming units per ml (pfu/ml) of virus supernatant using the following formula:

$$pfu\ /ml = Number\ of\ plaques \times Dilution\ factor$$

Lytic plaques

BHK cells were seeded in 12 well plates at 2.5 x 10^5 cells / well and left to incubate o/n at 37 ˚C (**Table 2-1**). SFV or BUNV were serially diluted in serum-free GMEM and used to infect the cultured cells (**Section 2.2.5.5**). Infected cells were overlaid with an Avicel overlay (**Table 2-2**), and incubated for 48 hours (SFV) or 96 hours (BUNV). Overlay was removed by gently washing 2 - 3 times with 1 ml room temperature 1x PBS until all the Avicel had been removed. The cells were simultaneously fixed and stained with Giemsa (**Table 2-9**), and the number of lytic plaques counted under a plate microscope.

ICC plaque assay

A549-NPro cells were seeded in 12 well plates at 3 x 10^5 cells / well and left to incubate o/n at 37 ˚C. ZIKV was serially diluted in serum-free DMEM and used to

infect cultured cells (**Section 2.2.5.5**). Cells were then overlaid with an Avicel overlay and incubated for 72 hours at 37 ˚C (**Table 2-2**). Overlay was removed by gently washing 2 – 3 times with 1 ml room temperature 1xPBS until the Avicel had been removed. The cells then underwent an Immunocytochemistry (ICC) - staining (**Section 2.2.6.7**) and the number of plaques counted under a plate microscope.

2.2.5.5. Infection of cultured cells

Media was aspirated and an appropriate volume of virus stock was then diluted in 100 – 500 µl of serum-free media, depending on the size of the well. Virus was absorbed by incubating the cells under the relevant conditions for 1 hour (**Table 2-1**). The plates were rocked and rotated every 10 - 15 minutes to ensure even distribution of the virus across the cell monolayer. Finally, the cells either had the media replaced if a luciferase assay was being conducted (**Section 2.2.7**), or an Avicel overlay made up to 0.6% if a plaque assay was being conducted (**Table 2-2**).

2.2.6. Analytical techniques

2.2.6.1. Sodium dodecyl sulfate – Polyacrylamide gel electrophoresis

If cells were being used for SDS-PAGE and Western blotting, cells were washed twice with PBS before whole lysates were harvested in 3x BM diluted in water to 1.5x BM (**Table 2-8**). Samples from protein assays were terminated in 3x BM and therefore could instantly be resolved by SDS-PAGE. All samples were boiled for 10 minutes at 95 ˚C prior to loading. Wells were loaded with 10-15 µl of sample, and a PageRuler pre-stained NIR protein ladder was used as a reference marker for molecular mass. Proteins were resolved on Novex 4-12% Bis-Tris gels using NuPAGE MES (1x) running buffer (**Table 2-9**). Gels were resolved at 210 volts until the dye front reached the bottom of the gel. Resolved SDS-PAGE gels were then Coomassie stained (**Section 2.2.6.2**) or transferred to a nitrocellulose membrane for Western blotting (**Section 2.2.6.3**).

2.2.6.2. Coomassie staining of SDS-PAGE gels

Gels required for Coomassie staining analysis were fixed with Coomassie fix solution for 5 minutes (**Table 2-8**). The Coomassie fix solution was washed off with distilled water, and Coomassie Brilliant Blue Stain was added to the gel (**Table 2-8**). This was incubated together for 3 minutes before being washed off with distilled water again. The gel was then briefly rinsed in 100% Methanol, and left in Coomassie destain solution at room temperature with constant shaking until bands were visible (**Table 2-8**).

2.2.6.3. Western blotting

Resolved SDS-PAGE gels were transferred to an Amersham protran 0.2 µm nitrocellulose blotting membrane in 1x NuPage transfer buffer and 10% Methanol at 30 V for 60 mins. The membranes were blocked in blocking buffer (5% FBS) at

RT for 1 hour (**Table 2-8**). The required primary antibody was diluted in blocking buffer (5% FBS), and incubated on the blotting membrane at room temperature for 1 hour or o/n at 4 ˚C with constant shaking (**Table 2-4; Table 2-8**). The membrane was washed 3 times for 5 minutes each in PBST at room temperature. Secondary antibody was incubated with the membrane at room temperature for 1 hour (**Table 2-4**). The membrane was then washed 3 times for 5 minutes each with PBST, 2 times with PBS, and rinsed 4 times with distilled water. Western blots were imaged and quantified using a LiCor Odyssey Imaging System.

2.2.6.4. RNA extraction

Cells were seeded at 2 x 10^5 cells / well and left to incubate overnight in the required conditions (**Table 2-1; Section 2.2.4.2**). RNA extraction occurred following the RNeasy Plus Mini Kit (Qiagen) following manufacturers guidance (**Table 2-7**). Cells were harvested in 350 µl Buffer RLT Plus, and stored at -20 ˚C until processing.

2.2.6.5. Complementary DNA (cDNA) synthesis

Extracted RNA was used as a template for cDNA synthesis by reverse transcription of mRNA using the TaqMan™ Reverse Transcription Reagents kit and the provided random hexamer primers (**Table 2-7**). Purified RNA underwent reverse transcription in a final volume of 20 µl of reaction mix, consisting of a final concentration of 1x RT buffer, 1.75 mM $MgCl_2$, 0.5 mM each dNTP, 1 U / µl RNase Inhibitor, 2.5 U / ml MultiScribe™ RT, 2.5 µM Random Hexamers, and 1 µl template RNA (under 1 µg / reaction). The solution was made up to 20 µl in nuclease-free water. The RNA template was incubated at 25 ˚C for 10 minutes, to anneal primers, 37 ˚C for 60 minutes for extension, and 95 ˚C for 5 minutes to inactivate the reverse transcriptase.

2.2.6.6. Quantitative polymerase chain reaction (q-PCR)

SYBR Green

Ae. aegypti mRNA expression was analysed in triplicate using a SYBR Green Master mix with gene specific primers (**Table 2-6**). Each reaction occurred in a 20 µl volume, consisting of 10 µl SYBR Green, 1 µl each Forward and Reverse primer, and 0.3 µl cDNA template, made up with nuclease-free water. Samples were initially denatured at 95 ˚C for 20 seconds, prior to 40 cycles of 3 second denaturation at 95 ˚C, and 30 second anneal / extend stage at 60 ˚C. Previously validated ribosomal S7 was used as an endogenous control (**Table 2-6**) (McFarlane, Arias-Goeta et al. 2014). q-PCR was conducted on an Applied Biosystems 7500 Fast-Real Time PCR system using MicroAmp plates and Optical Adhesive covers (Applied Biosystems). Results were subsequently analysed using Applied Biosystems 7500 Software v2.0.5.

Primer-probes

Primer probe analysis was conducted on mammalian cells with targeted gene expression being depleted (**Section 2.2.4.4**). Here, the reactions occurred comprising of 1 µl gene specific primer-probe mix, 10 µl Taqman Fast universal mix, 2 µl cDNA, to a total volume of 20 µl with nuclease-free water (**Table 2-7**). Samples were initially denatured at 95 ˚C for 20 seconds, prior to 40 cycles of 3 second denaturation at 95 ˚C, and 30 second anneal / extend stage at 60 ˚C. Commercial GAPDH (4333764F) was used as an endogenous control; commercial primer probes to SUMO1 (4331182 (Hs02339312_g1)), SUMO2/3 (4331182 (Hs02743873_g1)), and PIAS1 (4331182 (Hs00184008_m1)) were all obtained from Thermo Fisher Scientific. Q-PCR was conducted on an Applied Biosystems 7500 Fast-Real Time PCR system using MicroAmp plates and Optical Adhesive covers (Applied Biosystems). Results were subsequently analysed using Applied Biosystems 7500 Software v2.0.5.

2.2.6.7. ICC-staining plaque assay

Cells undergoing an ICC-staining plaque assay had the Avicel overlay washed off 2 – 3 times in 1x PBS. Cells were then simultaneously fixed and permeabilized in Fixing buffer (**Table 2-8**). Cells were washed twice in PBST and blocked in blocking buffer (5% milk) for 30 minutes at room temperature with constant shaking (**Table 2-8**). Cells were incubated for 60 minutes at room temperature with the primary antibody of interest diluted in blocking buffer (5% milk) (**Table 2-8**). Cells were washed twice for 5 minutes each in PBST, and incubated for 2 hours with a relevant IgG-peroxidase secondary antibody. Three 5 minute washes with PBST were performed following the secondary antibody and True Blue Peroxidase stain was added and incubated until the colour was developed (**Table 2-9**). Plates were washed three times with PBST, once with PBS and once with distilled H_2O. Plates were allowed to dry prior to plaques being counted under a light microscope.

2.2.6.8. In Cell Western Blot (ICWB)

Throughout ICWB experiments, all reagents were filter sterilised with a 0.45 µm filter. All incubation steps occurred in the dark, and at no point were the plates allowed to come into contact with blue roll.

Experiments which required an ICWB were seeded on glass bottom 24 well plates (Greiner Bio-one) at 1 x 10^5 cells / well. Cells were infected, and incubated with an Avicel overlay for the duration of the experiment (**Section 2.2.5.5**). The Avicel overlay was washed off 3-4 times in 1x PBS, filtered with a 0.45 µm filter (**Table 2-2**). Cells were then simultaneously fixed and permeabilized in filtered Fixing buffer (**Table 2-8**). Cells were washed twice in filtered 1x PBST, and blocked in filtered blocking buffer (5% FBS) for 1 hour at room temperature with constant shaking (**Table 2-8**). Cells were subsequently incubated for 1 hour at room temperature with the primary antibody of interest diluted in blocking buffer (5% FBS) and filtered. Cells were washed 4 times for 15 minutes each in 500 µl filtered PBST, and incubated for 2 hours with the relevant Celltag 700 (1:5000)- IgG fluorophore secondary antibody made up in filtered blocking buffer

(5% FBS) (**Table 2-4**). Wells were washed 5 times for 15 minutes in 1ml filtered PBST, followed by 3 washes of 15 minutes in 1ml filtered PBS, and 2 times for 30 minutes in 1ml filtered H_2O. Plates were allowed to dry prior to being scanned on the LiCor, with scanning offset to 4 μm. Staining area was assessed by LiCor Image Studio Lite.

2.2.7. Reporter assays

2.2.7.1. Firefly-luciferase reporter assay

Upon completion of experiments using SFV4-Ffluc, media was aspirated off. When HFt cells were infected they were washed twice with PBS and lysed with 50 µl of 1x Cell Culture Lysis Reagent (CCLR) (Promega). When AF5 cells were used, 50 µl of 1x CCLR was immediately added to the cells. Following manufacturer's instructions, samples were vortexed, for 15 seconds and transferred to a fresh Eppendorf tube. Luciferase Assay Reagent (50 µl) was then mixed with 10 µl sample and the samples were tested using a Glomax luminometer (Promega) following manufacturer's instructions (**Table 2-7**). Readings were produced in relative light units and were recorded (**Section 2.2.8.3**).

2.2.7.2. NanoLuciferase reporter assay

Upon completion of experiments using ZIKV-Nl or BUNV-NL, media was aspirated off. When HFt cells were infected they were also washed twice with PBS. Samples were incubated directly with 50 µl Nano-Glo® Luciferase Assay Substrate + Buffer mix (Promega) (**Table 2-7**). Samples were transferred to an Eppendorf tube, and incubated at room temperature for 3 minutes prior to being tested in a GloMax luminometer (Promega) following manufacturer's guidance. Readings were produced in relative light units and were recorded (**Section 2.2.8.3**).

During mosquito analysis, samples were provided by collaborators of mosquitoes which had been treated with dsRNA to LacZ as a non-target control, or dsRNA to SUMO and subsequently fed blood containing ZIKV-NL at $1x10^7$ pfu/ml, supplemented with 2 mM ATP. Samples had already been lysed with glass beads by the collaborators (Floriane Almire, and Dr Emilie Pondeville, University of Glasgow), so 10 µl sample was mixed with 50 µl Nano-Glo® Luciferase Assay Substrate + Buffer (**Table 2-7**).

2.2.7.3. Protein quantification assay

Samples that needed to be quantified prior to mass spectrometry were harvested in CellLyse lysis buffer (**Table 2-9**). Samples were then sonicated using a digital sonicator (7 repeats, 50% intensity, 30 seconds, 4 ˚C, Branson Digital Sonifier), and a Micro BCA Protein Assay Kit (**Table 2-7**) was utilised to quantify the concentration of protein against a standard curve of known BSA concentrations, following manufacturer's instructions. Samples were diluted 1:5, 1:10, and 1:20 and quantified using a Nanodrop 2000 spectrophotometer (Thermo Scientific) measuring absorbance at 562 nm.

2.2.8. Bioinformatics

2.2.8.1. Joined Advanced SUMOylation site and SIM Analyser (JASSA)

Annotated amino acid sequences were obtained from UniProt for the proteins of interest. These amino acid sequences were then analysed through JASSA which is an online tool (http://www.jassa.fr/) that predicts sites likely to be SUMO modified (Beauclair, Bridier-Nahmias et al. 2015). The results were then annotated and presented using Illustrator for Biological Sequences (Ren, Wen et al. 2009, Liu, Xie et al. 2015). Some sites were also modelled to demonstrate location of the potential site of SUMO modification (**Section 2.2.8.2**).

2.2.8.2. Modelling software

Annotated amino acid sequences were obtained from UniProt for the proteins of interest. Viral proteins which had already been analysed with JASSA (**Section 2.2.8.1**), and the resolved structures available were then downloaded and analysed by the modelling programme Chimera 1.10.1 (Pettersen, Goddard et al. 2004).

Models of *Ae. aegypti* SUMOylation pathway proteins were conducted by obtaining the sequence of the proteins from UniProt, and predicting the tertiary structure with either Phyre2 or Chimera 1.10.1 (Pettersen, Goddard et al. 2004, Kelley and Sternberg 2009). The models predicted with Chimera were then plotted against the resolved structure of the *H. sapiens* SUMOylation proteins (Pettersen, Goddard et al. 2004).

2.2.8.3. Amino acid alignment

Amino acid alignment was conducted using the online software T-COFFEE (http://tcoffee.crg.cat/) (Notredame, Higgins et al. 2000). These results were then plotted and exported with BOXSHADE (http://sourceforge.net/projects/boxshade/).

2.2.8.4. Statistical analysis

Statistical analysis and graphs were produced with GraphPad 7.02. 2-Way ANOVAs, or Mann-Whitney U-tests were used to determine statistical significance (indicated in figures).

2.2.9. Cloning strategies used in this study

All cloning conducted used procedures detailed in **Section 2.2.1** using oligonucleotides detailed in **Table 2-6**. Specific approaches to cloning components of the *Ae. aegypti* SUMOylation pathway into vectors are described in this section. The correct construction was confirmed by restriction endonuclease digestion (**Section 2.2.1.3**) and sequencing (**Section 2.2.1.9**). Unless stated otherwise, genes were cloned from cDNA originally extracted from A20 cells by Dr Sue Jacobs (**Table 2-1**).

2.2.9.1. Cloning of pACYC-*Aa*SAE1/2

The pACYCDuet-1 vector is a bacterial expression vector that allows dual expression of two proteins following induction with IPTG. The vector is designed with chloramphenicol resistance, and a 6xHis tag in the N-terminal of one protein, and an S-tag on the C-terminal of the second protein (**Figure 2.3**). cDNA from A20 cells was used as a template with the primers *Aa*SAE2 F, *Aa*SAE2 R, *Aa*SAE2 F1, *Aa*SAE2 R1, *Aa*SAE2 F2, *Aa*SAE2 R2 (**Table 2-6**). *Aa*SAE2 is a large gene (approximately 2000 bp), consequently *Aa*SAE2 was cloned in three sections of approximately 650 bp, 450 bp, and 800 bp, and further PCRs were conducted to ensure the template was complete. Primers were designed to bind to the gene as depicted (**Figure 2.2**). The restriction endonuclease sites EcoRI and NotI were used to ligate the insert into the vector backbone.

*Aa*SAE1 was cloned with the primers *Aa*SAE1 F, *Aa*SAE1 R, *Aa*SAE1 F1, and *Aa*SAE1 R1 (**Table 2-6**). *Aa*SAE1 is also a large gene (approximately 1000 bp); consequently the gene was cloned in two parts of approximately 250 bp and 750 bp. An additional stop codon was inserted at the C-terminal to prevent the S-tag from being translated. *Aa*SAE1 was ligated into MCS2 on NdeI and XhoI.

A Strep.II tag was synthesised (Dundee Cell Products) of the sequence 5'-TGGAGCCACCCGCAGTTCGAAAAG-3' which was ligated to replace the 6xHis tab between the NcoI and EcoRI sites on the N-terminal of *Aa*SAE2.

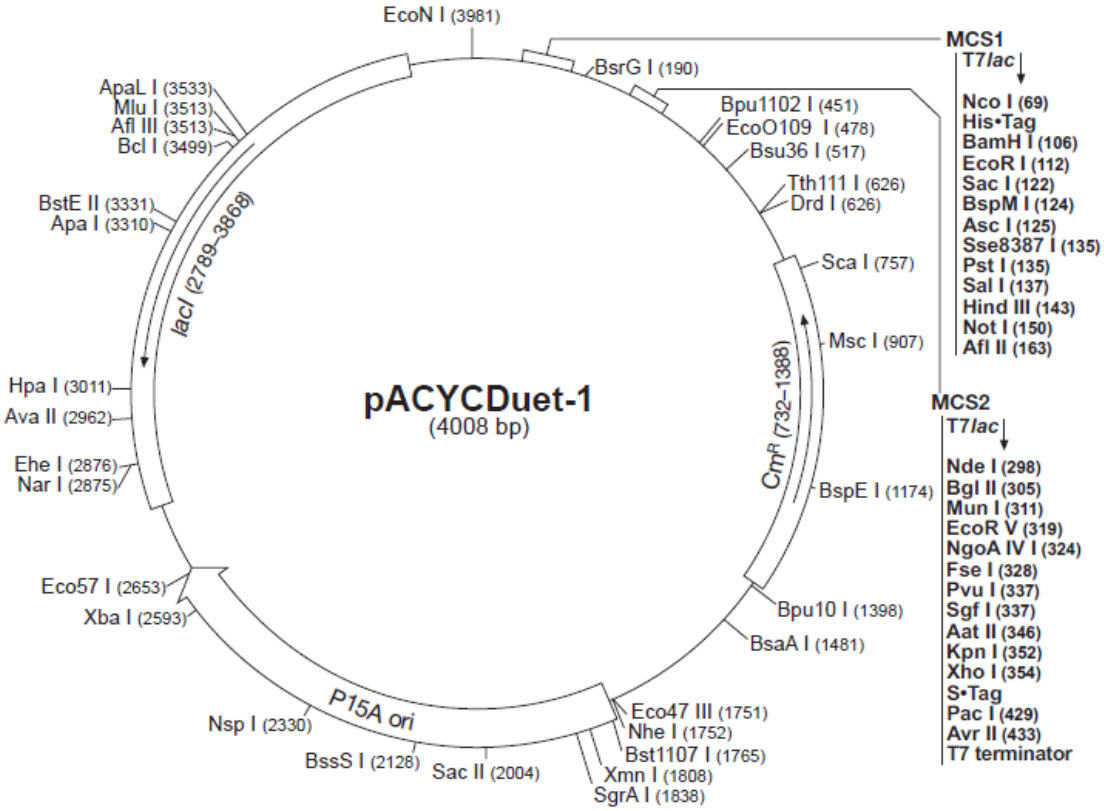

Figure 2.2 pACYCDuet-1 expression plasmid map

The plasmid map of pACYADuet-1, with cloning sites and other regions of interest shown. The plasmid expresses resistance to chloramphenicol. Image from Novagen.

Figure 2.3 *Aa*SAE2 primer binding sites

Image depicts the primer binding sites for cloning of *Aa*SAE2

2.2.9.2. Cloning of pET28a-SUMO chimaera and pET28a-SUMO chimaera K11R

The SUMO chimaera and SUMO chimaera K11R mutant were synthesised (GENEWIZ), and digested and ligated into the pET28 bacterial expression vector on the sites NdeI and XhoI, using the primers pET28-AaSUMO R and pET28-SUMO chimaera F (**Section 2.1.6; Section 2.2.1.3; Section 2.2.1.5**; **Table 2-6**; **Figure 2.4**).

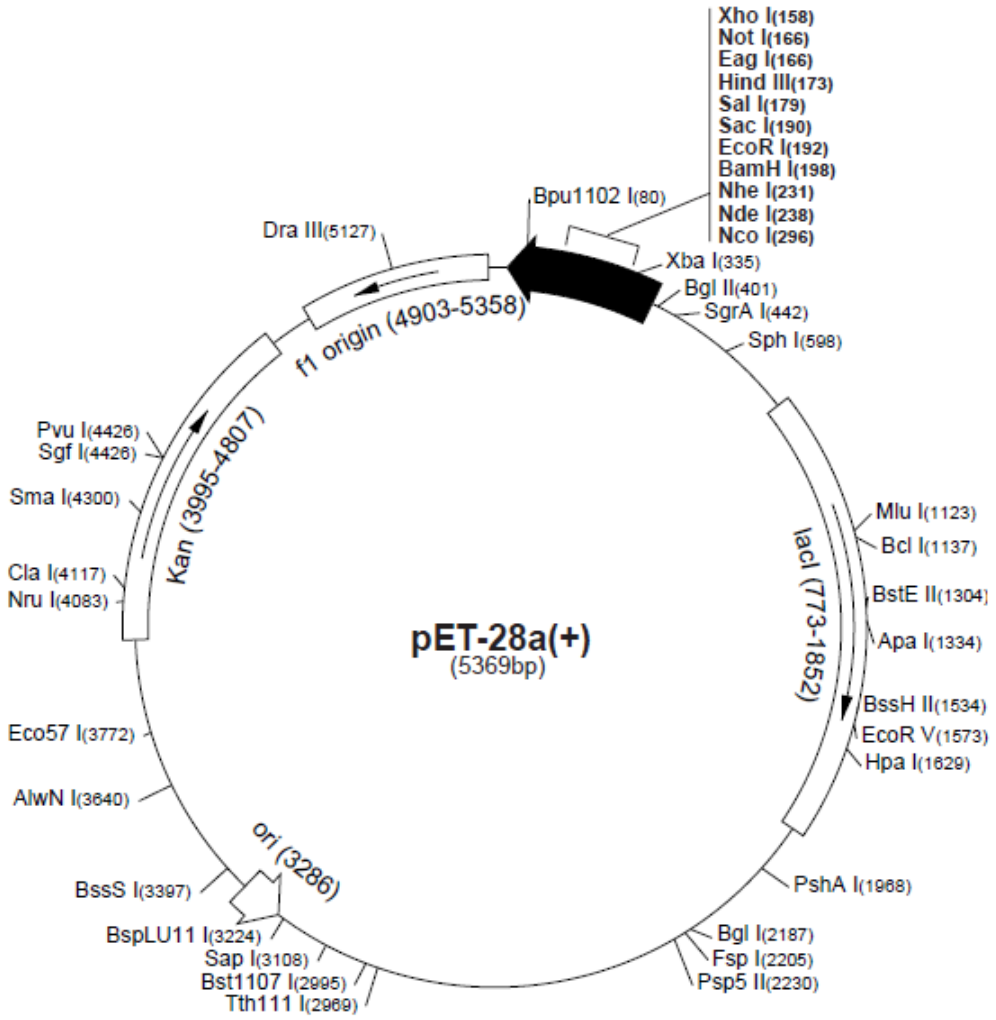

Figure 2.4 pET28a vector map

The plasmid map of pET-28a, with cloning sites and other regions of interest shown. The plasmid expresses resistance to kanamycin. The image is from Novagen.

2.2.9.3. Cloning of pET45b-*Aa*Ubc9 and pET45b-*Aa*Ubc9 C93S

*Aa*Ubc9 was cloned from A20 cDNA extracted by Dr Sue Jacobs (Unpublished data), using the primer sequences pET-Ubc9 F and pET-Ubc9 R (**Table 2-6**). This was cloned into the pET45b bacterial expression vector which contains an ampicillin resistance gene (**Figure 2.5**) on the AgeI and XhoI restriction sites. *Aa*Ubc9 C93S was produced using site directed mutagenesis by PCR described (**Section 2.2.1.10**) using the Ubc9 C93S Int F1 and Ubc9 C93S Int R1 primers (**Table 2-6**). *Aa*Ubc9 C93S was subsequently amplified with pET-Ubc9 F and pET Ubc9 R primers and cloned into the pET45b vector on the AgeI and XhoI restriction sites. Sequencing confirmed the mutation was present (**Section 2.2.1.9**).

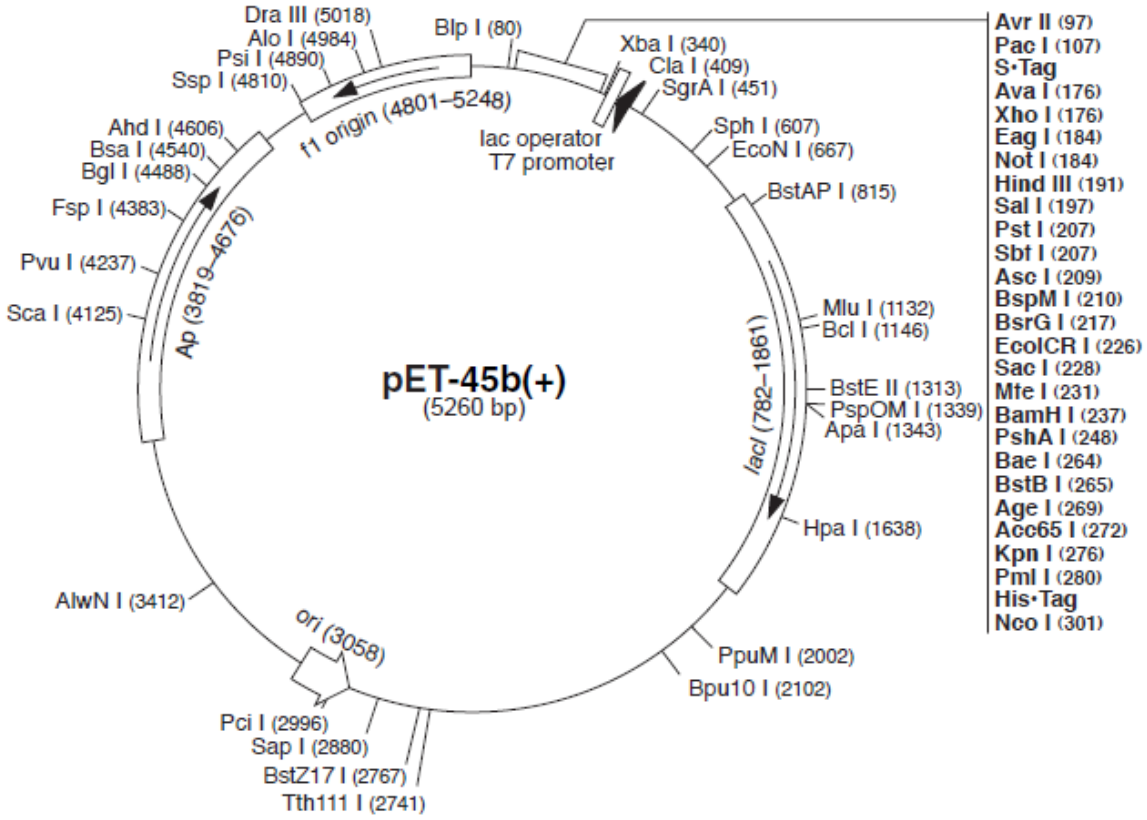

Figure 2.5 pET45b vector map

The plasmid map of pET-45b, with cloning sites and other regions of interest shown. The plasmid expresses resistance to ampicillin. The image is from Novagen.

2.2.9.4. Cloning of pET45b-*Aa*PIAS and pET45-*Aa*PIAS C371A

*Aa*PIAS and *Aa*PIAS C371A were synthesised (GENEWIZ) and amplified by PCR with the primers *Aa*PIAS F for pET45b and *Aa*PIAS R for pET45b (**Table 2-6**). The primers contained AgeI and NotI restriction sites for cloning into the pET45b vector (**Figure 2.5**).

2.2.9.5. Cloning of pET28a-*Aa*SUMO

Using pET28 vector (**Figure 2.4**), *Aa*SUMO was cloned from a plasmid of pET45-*Aa*SUMO (produced by Dr Sue Jacobs, unpublished data) using the primer sequences pET28-*Aa*SUMO F and pET28-*Aa*SUMO R (**Table 2-6**). PCR products were digested in NdeI and XhoI for ligation into the pET28 vector.

3. Conservation of the SUMOylation pathway between *Ae. aegypti* and *H. sapiens*

3.1. Overview

A limited amount of research has been conducted on the *Aa*SUMOylation pathway. Two previous studies have utilised a bioinformatics approach to compare the conservation of SUMO orthologues between invertebrate and vertebrate species. Choy *et al.*, (2013) compared the amino acid sequence of ubiquitin and ubiquitin-like proteins between four vector species. They found *Ae. aegypti* and *Anopheles gambiae (An. gambiae*) to both possess two SUMO orthologues, whereas *Culex quinquefasciatus* (*C. quinquefasciatus*) and *Ixodes scapularis* (*I. scapularis*) only possess one each (Choy, Severo et al. 2013). Urena *et al.*, (2015) compared the SUMO amino acid sequence from a range of insect species to mammalian SUMO homologues, including that of *H. sapiens*. They were able to determine that all insect SUMO proteins appear to lack a SUMO Conjugation Motifs (SCM) important for poly-SUMO chain formation (Urena, Pirone et al. 2016). However, neither study determined if constituent proteins of the SUMO pathway were expressed, or investigated their respective biochemical properties to orthologous proteins. Consequently, the biological activity of these proteins within insect vectors remains to be characterised.

Arboviruses are required to replicate efficiently in the vertebrate and invertebrate cells. Consequently, any divergence in biological activity of the SUMOylation pathways of *Ae. aegypti* and *H. sapiens* could result in different physiological consequences between species. It was hypothesised that if there is a high degree of conservation between the SUMOylation pathways, then any interaction between arboviruses and the SUMOylation pathway will likely be conserved between the two species.

A limited amount of research has currently been conducted on the interactions between arboviruses and the SUMOylation pathway in either *H. sapiens* or *Ae. aegypti*. Consequently, a bioinformatics approach was initially undertaken to determine if arboviral proteins contained sites amenable to SUMO modification. It was hypothesised that if SUMO modification was crucial for viral replication, SCM (ψ-K-x-[E/D]) sites would likely be conserved between closely related viral strains, and potentially between different virus family members. This strategy potentially increases the risk of false positives as it does not take protein folding

into account, or may miss genuine targets that require SUMO E3 ligases for modification independently of SCMs. However, this methodology serves as an initial indication of how likely viral proteins were to be targets of SUMO modification, and consequently, how likely the SUMOylation pathway is to affect arboviral replication.

In this chapter, the degree of conservation of the SUMOylation pathway between *Ae. aegypti* and *H. sapiens* were compared, and the antibody binding for the constituent parts of the SUMOylation pathways investigated. Furthermore, for each component of the SUMOylation pathway, mass spectrometry analysis was conducted to provide experimental evidence of protein expression. The arboviral proteins which could represent targets of SUMO modification for BUNV, SFV, and ZIKV have been determined.

3.2. Conservation of the SUMOylation pathway

3.2.1. Conservation of SUMO

The annotated *Ae. aegypti* genome sequence revealed the presence of two SUMO homologues, which we named *Aedes aegypti* SUMOa (*Aa*SUMOa; Q16EQ3) and *Aedes aegypti* SUMOb (*Aa*SUMOb; Q16I57). These were compared to the sequence of *Homo sapiens* SUMO 1-3 (*Hs*SUMO1-3; P63165; P61956; P55854). The highest degree of amino acid identity was found with either *Aa*SUMOa or *Aa*SUMOb with *Hs*SUMO3 (**Figure 3.1A**). Interestingly, however, neither *Aa*SUMOa nor *Aa*SUMOb contained an internal SCM like *Hs*SUMO3. This indicates that *Aa*SUMOa and *Aa*SUMOb are unlikely to efficiently form poly-SUMO chains in contrast to its closest *Hs*SUMO orthologue.

In order to determine any substantial differences in the tertiary structure of the SUMO homologues, the structure of *Aa*SUMOa was modelled using Phyre2 (**Figure 3.1B**) (Kelley and Sternberg 2009). The structural alignment with the resolved structure of *Hs*SUMO3 was additionally compared with the programme Chimera 1.10.1 (Pettersen, Goddard et al. 2004, Xu, Plechanovova et al. 2014). As demonstrated in **Figure 3.1C**, there was a high degree of structural similarity observed between *Aa*SUMOa and *Hs*SUMO3, with the only difference observed in the highly flexible N-terminal region. Together, **Figure 3.1B** and **Figure 3.1C** demonstrate that multiple programmes predict a highly conserved tertiary structure. Antibody binding was also tested, this demonstrated that the antibody raised to *Hs*SUMO2/3 could be utilised as a tool to detect *Aa*SUMO conjugated HMW proteins (**Figure 3.1D**). Unfortunately, unconjugated SUMO was not detected in this assay (data not shown) and therefore we cannot confirm the predicted molecular weight of the protein (~15 kDa). As the amino acid sequence identity between *Aa*SUMOa and *Aa*SUMOb is high, it was predicted that any biochemical differences would be conserved between the two homologous proteins. Furthermore, as there was no direct evidence to specifically support *Aa*SUMOb expression (**Table 3-1**); the focus of the rest of the study was on *Aa*SUMOa.

A

```
AaSUMOa     1 MSEEKKD-SKGSES-EH-----INLKVLGQDNAVVQFKIKKHTPLRKLMNAYCDRAGLSM
AaSUMOb     1 MSTDKKDQPKAAES-EH-----INLKVLGQDNAVVQFKIKKHTPLKKLMNAYCDRSGLSM
HsSUMO3     1 MSEEKPKEGVKTEN-DH-----INLKVAGQDGSVVQFKIKRHTPLSKLMKAYCERQGLSM
HsSUMO2     1 MADEKPKEGVKTENNDH-----INLKVAGQDGSVVQFKIKRHTPLSKLMKAYCERQGLSM
HsSUMO1     1 MSDQEAKPSTEDLG-DKKEGEYIKLKVIGQDSSEIHFKVKMTTHLKKLKESYCQRQGVPM

AaSUMOa    54 QVVRFRFDGQPINENDTPTTLEMEEGDTIEVYQQQTGG
AaSUMOb    55 QVVRFRFDGQPITENDSPTTLEMEEGDTIEVYQQQTGG
HsSUMO3    55 RQIRFRFDGQPINETDTPAQLEMEDEDTIDVFQQQTGG
HsSUMO2    56 RQIRFRFDGQPINETDTPAQLEMEDEDTIDVFQQQTGG
HsSUMO1    60 NSLRFLFEGQRIADNHTPKELGMEEEDVIEVYQEQTGG
```

B

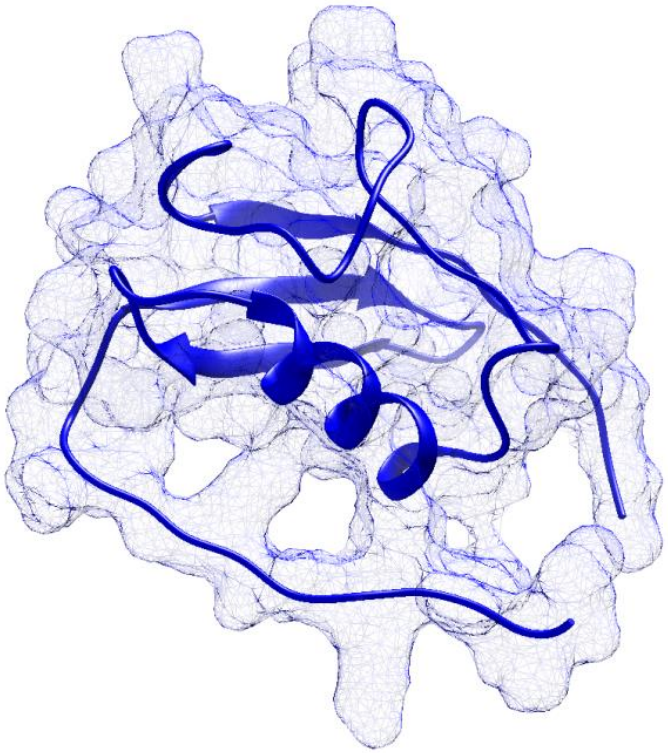

C

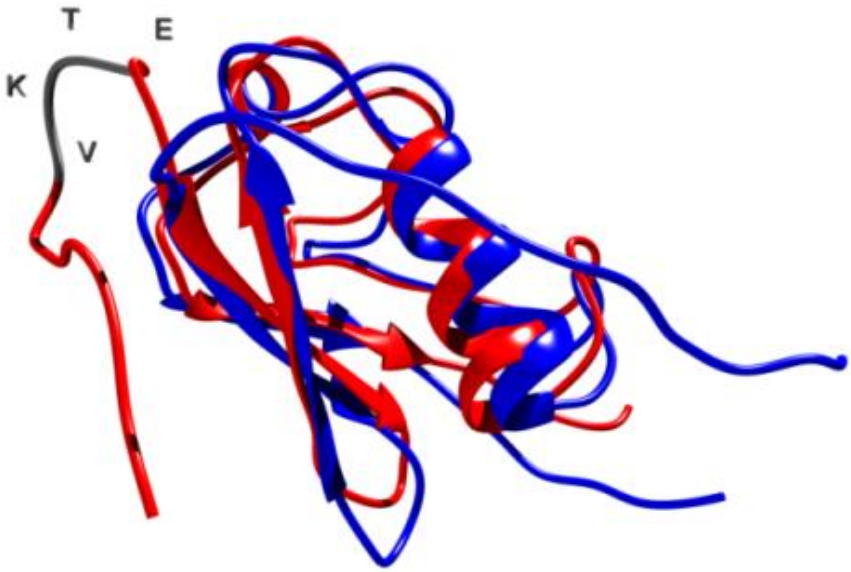

Continued on next page

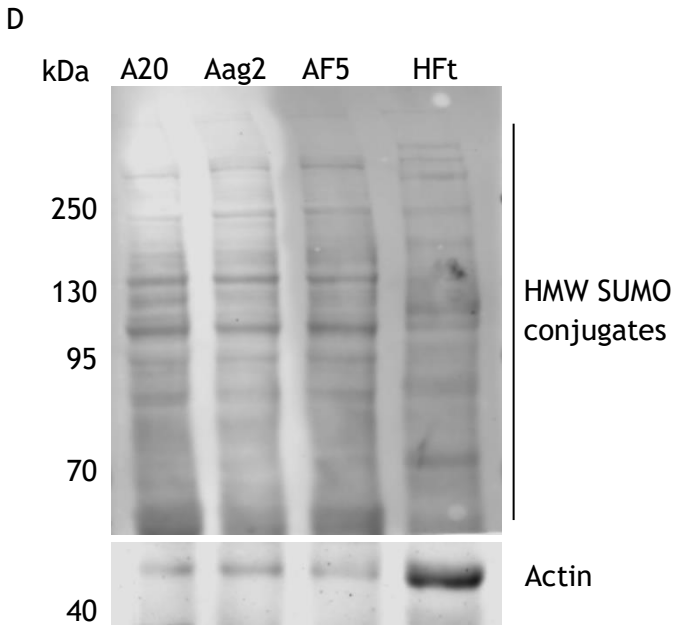

Figure 3.1 Conservation of SUMO between *Ae. aegypti* and *H. sapiens*.

(**A**) The annotated amino acid sequence of the two SUMO proteins in *Ae. aegypti* was compared to the sequence of *H. sapiens* SUMO3, *Hs*SUMO1 and *Hs*SUMO2 was included for comparison. Dashed box indicates the conjugation motif on *Hs*SUMO2/3. (**B**) Modelling the predicted structure of *Aa*SUMOa with Phyre2, (**C**) and comparing the resolved structure of *Hs*SUMO3 (PDB ID: 2MP2) to the predicted structure of *Aa*SUMOa modelled with Chimera, demonstrated structural conservation between the orthologous proteins. (**D**) 2.5 x 10^5 *Ae. aegypti* cells (A20, Aag2, AF5) or 1 x 10^5 *H. sapiens* cells (HFt; positive control) were seeded and incubated overnight. Cells were lysed into 100 µl and 10 µl cell lysate was resolved by SDS-PAGE and a Western blot was conducted with antibodies to *Hs*SUMO2/3 (upper blot). A Western blot probing for the expression of Actin was also conducted (lower blot) as a loading control. Molecular weight markers indicated.

3.2.2. Conservation of Ubc9

The annotated genome sequence of *Aa*Ubc9 was compared to the published sequence of *Hs*Ubc9. This demonstrated a high degree of amino acid identity, at 85%. Including the conservation of C93 (indicated with a '#'), which is important for the function of Ubc9 as a conjugation enzyme in *H. sapiens*. Furthermore, the 'PAQA' sequence is conserved (indicated by a bar) between *Hs*Ubc9 and *Aa*Ubc9, which has been shown to be the residues responsible for efficient recognition of SCM sites (Bernier-Villamor, Sampson et al. 2002). Interestingly, however, the D^{100} is not conserved between *Hs*Ubc9 and *Aa*Ubc9. This amino acid, along with K^{101} has been shown to slow the rate of thioester bond formation, which indicates that *Aa*Ubc9 may form thioester bonds at a greater rate than *Hs*Ubc9 (**Figure 3.2A**) (Tatham, Chen et al. 2003). The predicted tertiary structure of *Aa*Ubc9 was produced using multiple programmes, and a comparison of the structure of *Aa*Ubc9 against the resolved structure of *Hs*Ubc9 was conducted (**Figure 3.2B**; **Figure 3.2C**) (Giraud, Desterro et al. 1998). Once again, multiple programmes confirmed the conservation of secondary (α-helix and ß-sheets) and tertiary structure of the protein. Antibody binding was assessed, and one antibody was found which cross reacted between species which resolved at the expected molecular weight of ~20 kDa (**Figure 3.2D**).

A

```
HsUbc9     1 MSGIALSRLAQERKAWRKDHPFGFVAVPTKNPDGTMNLMNWECAIPGKKGTPWEGGLFKL
AaUbc9     1 MSGIAIARLGEERKAWRKDHPFGFVARPVKNADGTLNLMTWECAIPGKKGTPWEGGLYKL

                                                #       **
HsUbc9    61 RMLFKDDYPSSPPKCKFEPPLFHPNVYPSGTVCLSILEEDKDWRPAITIKQILLGIQELL
AaUbc9    61 RMIFKDDYPTSPPKCKFEPPLFHPNVYPSGTVCLSLLDEEKDWRPAITIKQILLGIQDLL

HsUbc9   121 NEPNIQDPAQAEAYTIYCQNRVEYEKRVRAQAKKFAP-S
AaUbc9   121 NEPNIKDPAQAEAYTIYCQNRLEYEKRVRAQARAMAATE
```

B

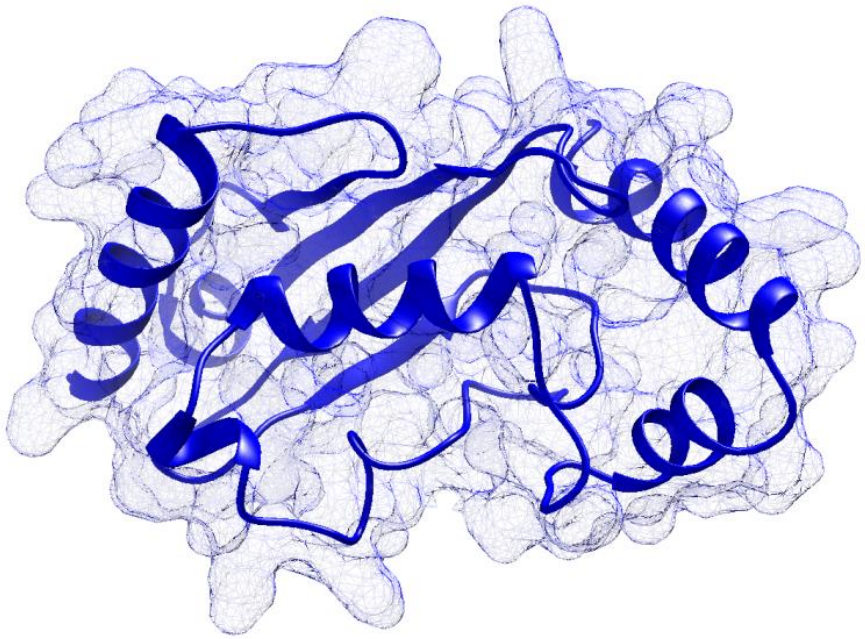

C

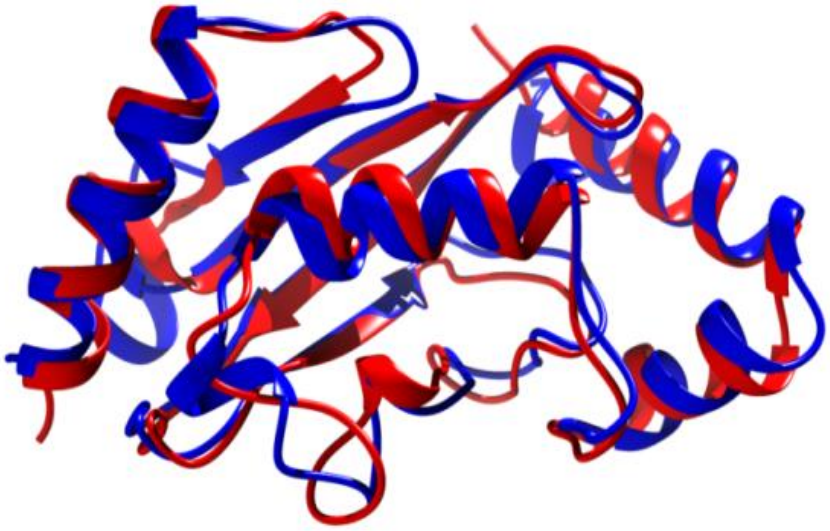

Continued on next page

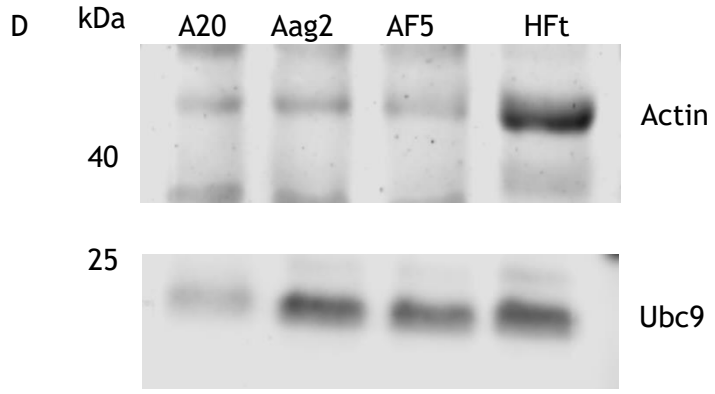

Figure 3.2 Conservation of Ubc9 between *Ae. aegypti* and *H. sapiens*.

(**A**) The annotated amino acid sequence of the Ubc9 in *Ae. aegypti* was compared to the sequence of *H. sapiens* Ubc9, they were found to share 85% amino acid identity, catalytically active Cys^{93} is represented by a '#', the residues which help regulate thioester bond formation Asp^{100} and Lys^{101} are indicated by '*', and the amino acids PAQA, which has a high affinity for SCM sites are indicated by a bar. (**B**) Modelling the predicted structure of *Aa*Ubc9, (**C**) and comparing it to the resolved structure of *Hs*Ubc9 (PDB ID: 1A3S), indicated structural conservation between the orthologues. (**D**) 2.5 x 10^5 *Ae. aegypti* cells (A20, Aag2, AF5) or 1 x 10^5 *H. sapiens* cells (HFt; positive control) were seeded and incubated overnight. Cells were lysed into 100 µl and 10 µl cell lysate was resolved by SDS-PAGE and a Western blot was conducted with antibodies to *Hs*Ubc9 (lower blot). A Western blot probing for the expression of Actin was also conducted (upper blot) as a loading control. Molecular weight markers indicated.

3.2.3. Conservation of SAE1/2

The amino acid sequence of *Aa*SAE1 and *Aa*SAE2 was taken from the annotated sequence of *Ae. aegypti*, and compared to the amino acid sequence of *H. sapiens* SAE1/2 activating heterodimer (**Appendix A: Amino acid sequence comparison between *Hs* and *AaSAE1*/2, and *Hs* and *AaPIAS***). The amino acid identity between *Hs*SAE1/2 and *Aa*SAE1/2 was lower than other components of the SUMOylation pathway, at 42% identity for SAE2, and 50% amino acid identity between the SAE1 orthologues. Structural models of the *Aa*SAE1/2 heterodimer and structural comparisons with the *Hs*SAE1/2 activating heterodimer revealed that even with an amino acid identity of 42% and 50%, the tertiary structure was still well conserved between species (Lois and Lima 2005) (**Figure 3.3A**; **Figure 3.3B**). Due to the reduced amino acid identity, the antibody available against *Hs*SAE2 did not appear to detect *Aa*SAE2 at the predicted molecular size of ~80 kDa (**Figure 3.3C**). There is a distinct band detected when *Ae. aegypti* cell lysate was tested at approximately 130 kDa (*, **Figure 3.3C**), however this is a far larger protein than *Aa*SAE2 is predicted to be, and far larger than recombinant *Aa*SAE2 resolved at (**Figure 4.2**).

A

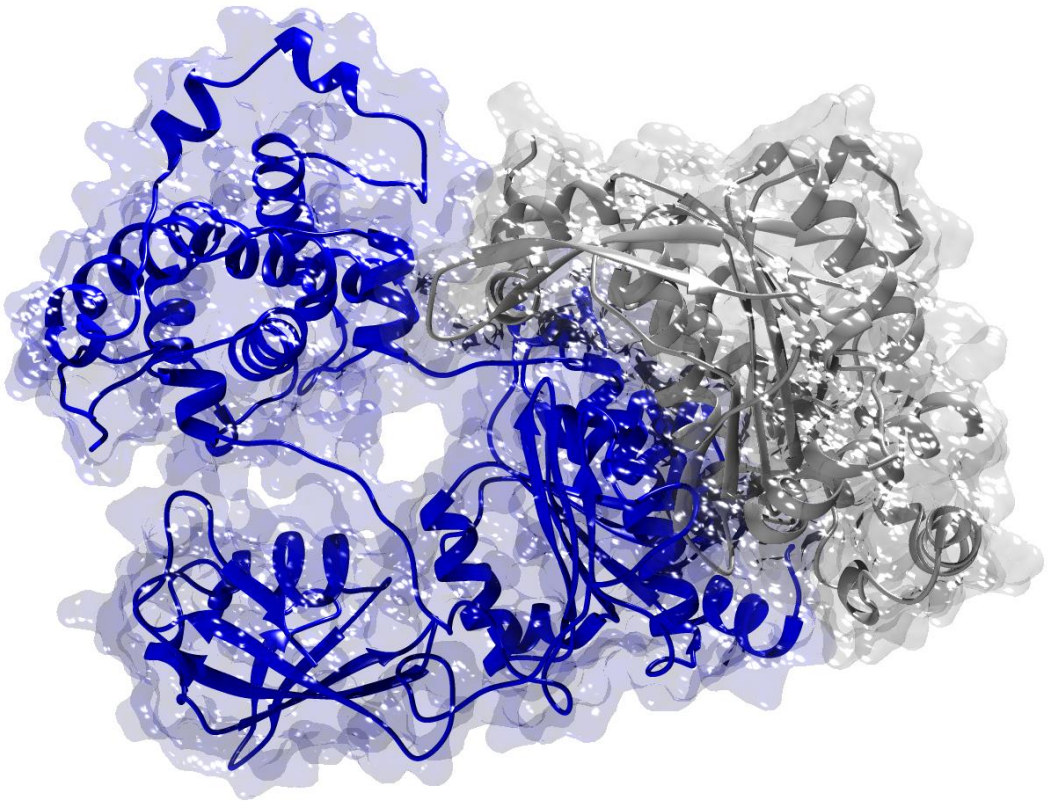

B

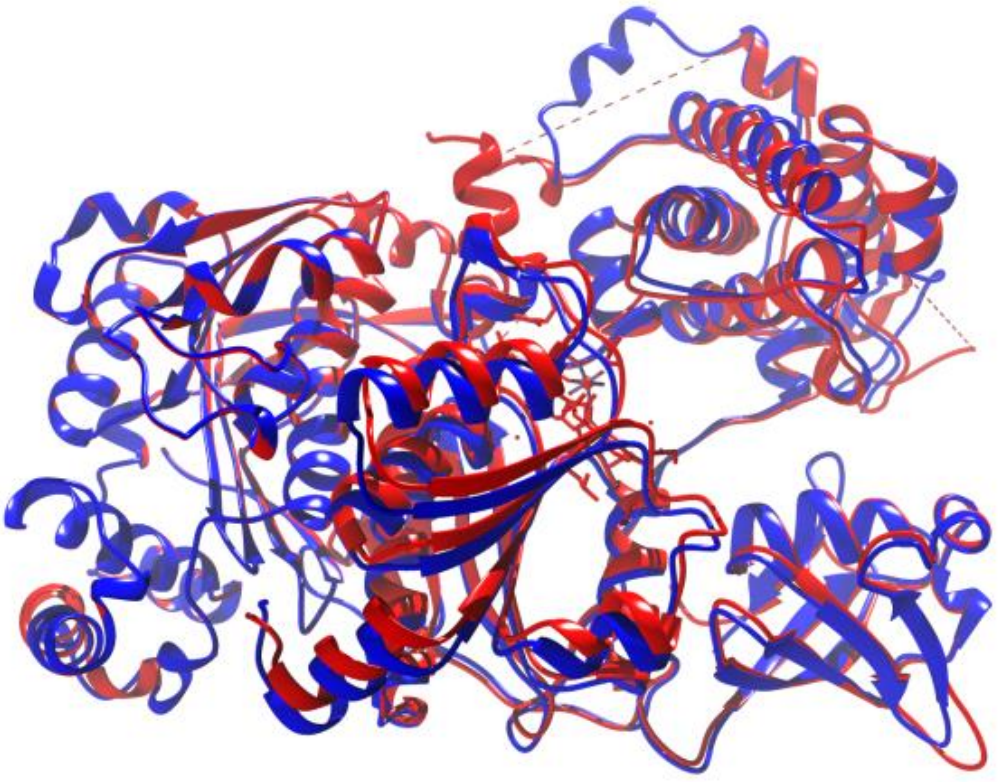

Continued on next page

C

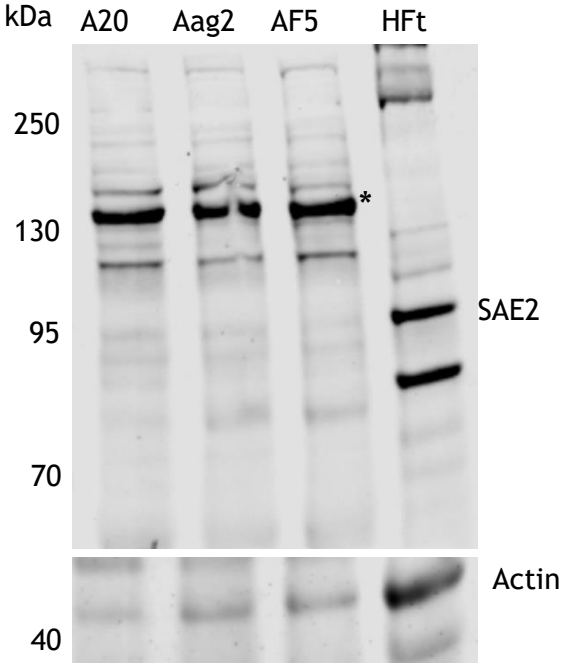

Figure 3.3 Conservation of SAE1/2 between *Ae. aegypti* and *H. sapiens*.

(**A**) Modelling the predicted structure of *Aa*SAE1/2, (**B**) and comparing it to the resolved structure of *Hs*SAE1/2 (PDB ID: 1Y8Q), indicated a high degree of structural conservation between the orthologues. (**D**) 2.5 x 10^5 *Ae. aegypti* cells (A20, Aag2, AF5) or 1 x 10^5 *H. sapiens* cells (HFt; positive control) were seeded and incubated overnight. Cells were lysed into 100 µl and 10 µl cell lysate was resolved by SDS-PAGE and a Western blot was conducted with antibodies to *Hs*SAE2 (upper blot). A Western blot probing for the expression of Actin was also conducted (lower blot) as a loading control. Molecular weight markers indicated.

3.2.4. Conservation of PIAS

*Aa*PIAS was located in the *Ae. aegypti* annotated genome and compared to the five *H. sapiens* PIAS homologues. There was a relatively low level of amino acid identity, in comparison to the other parts of the SUMOylation pathway: between 32-37% (**Appendix A: Amino acid sequence comparison between *Hs* and *AaSAE1*/2, and *Hs* and *AaPIAS*; Figure 3.4A**). However, when the amino acid identity of the SP-RING domain was compared between *Aa*PIAS and *Hs*PIAS1-4, the degree of amino acid identity increased to 65-70% (**Figure 3.4A**). Furthermore, the active C371 was identified, predicted to be responsible for the ligase activity of the protein (**Figure 3.4B**). Structural modelling was conducted, and a comparison was conducted with *Hs*PIAS2-α (**Figure 3.4C**; **Figure 3.4D**). Again, two different programmes predicted the overall structure of the protein was conserved, and the SP-RING domain of the PIAS orthologues has been indicated on the models. As the amino acid identity was predicted to be greatest throughout the entire protein with *Hs*PIAS2-α, an antibody to *Hs*PIAS2-α was used in an attempt to detect *Aa*PIAS. Unfortunately, the antibody did not cross-react between the two species (**Figure 3.4E**). There is a faint band at the same molecular size as *Hs*PIAS2-α (~85 kDa), however as it is not a distinct band, this could be non-specific, and it does not resolve at the expected molecular weight of AaPIAS (~70 kDa).

A

	% Amino acid identity	
	*Aa*PIAS whole protein	*Aa*PIAS SP-RING Domain
*Hs*PIAS1	35	70
*Hs*PIAS2-α	37	69
*Hs*PIAS2-β	36	69
*Hs*PIAS3	34	68
*Hs*PIAS4	32	65

B

Continued on next page

C

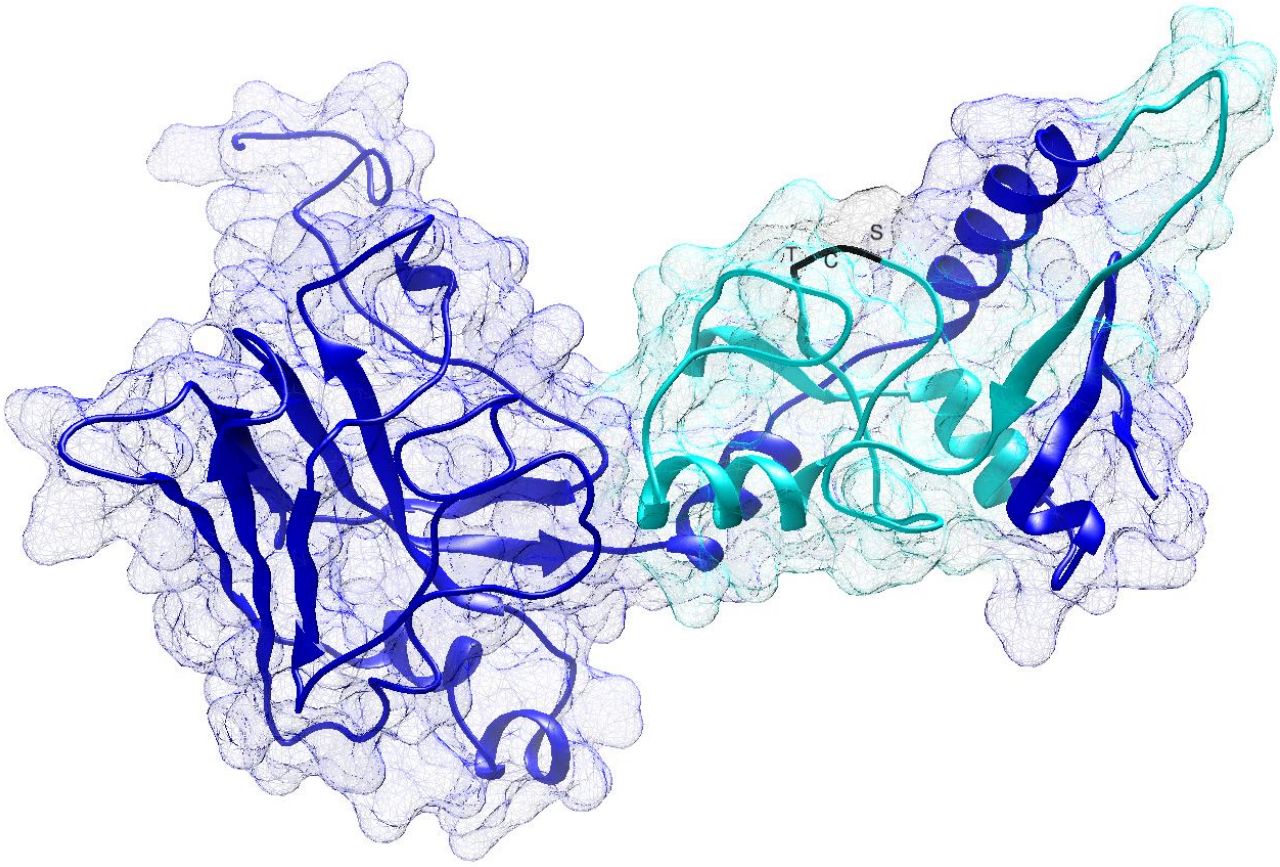

D

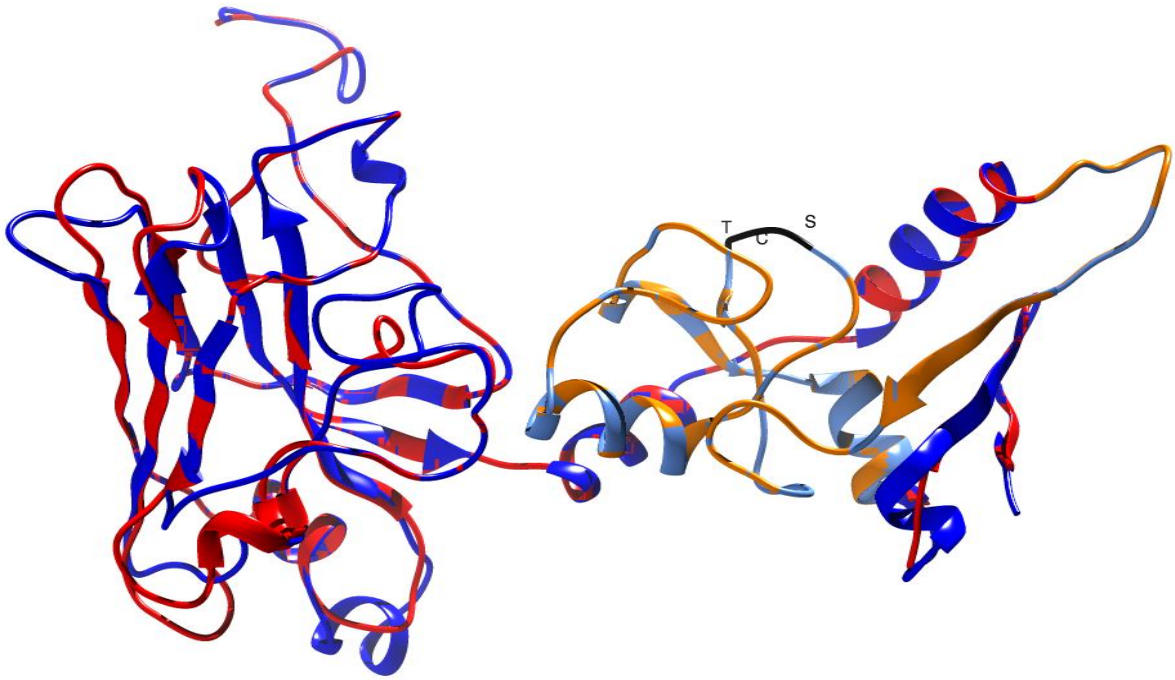

Continued on next page

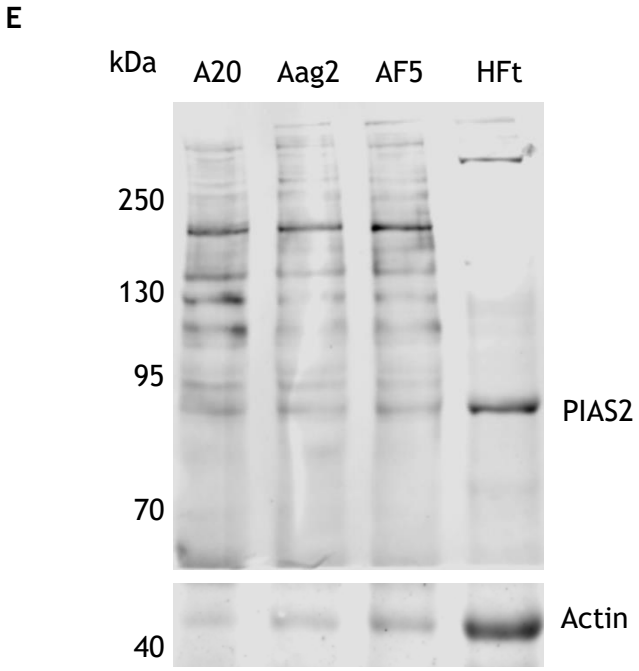

Figure 3.4 Conservation of PIAS between *Ae. aegypti* and *H. sapiens*.

(**A**) The annotated amino acid sequence of the *Ae. aegypti* PIAS was compared to the sequence of *H. sapiens* PIAS1-4, they were found to share 32-37% amino acid identity, although the catalytically active SP-RING domain contains 65-70% amino acid identity between the orthologues. (**B**) A schematic of the *Aa*PIAS protein indicating the SP-RING domain and the catalytically active C371. (**C**) Modelling the predicted structure of *Aa*PIAS using Phyre2, the SP-RING domain is highlighted in light blue, and the catalytically active C371, along with the flanking T370, and S372 are indicated; (**D**) the predicted structure of *Aa*PIAS, made with Chimera 1.10.1 was compared to the resolves structure of *Hs*PIAS2-α (PBD ID: 4FO9), The SP-RING domain of both orthologues are indicated in orange (*Hs*PIAS2-α), and silver (*Aa*PIAS), and the catalytically active C371 and flanking proteins are again indicated. (**E**) 2.5 x 10^5 *Ae. aegypti* cells (A20, Aag2, AF5) or 1 x 10^5 *H. sapiens* cells (HFt; positive control) were seeded and incubated overnight. Cells were lysed into 100 µl, 10 µl was resolved by SDS-PAGE and a Western blot was conducted with antibodies to *Hs*PIAS2-α (upper blot). A Western blot probing for the expression of Actin was also conducted (lower blot) as a loading control. Molecular weight markers indicated.

3.2.5. Confirmation of pathway expression

In order to confirm the *Aa*SUMOylation pathway was expressed, *Ae. aegypti* cells were assessed by LC-MS mass spectrometry for the presence of peptides to specific SUMO component proteins of the *Aa*SUMOylation pathway. Samples were prepared and quantified (as described **Section 2.2.7.3**), and sent to collaborators in Dundee University for analysis by mass spectrometry (**Table 3-1**). These data demonstrate that core component proteins of the *Aa*SUMOyaltion pathway are constitutively expressed in *Ae. aegypti* cells. q-PCR analysis was also conducted on *Aa*SUMO, *Aa*Ubc9, and *Aa*PIAS on different tissues from *Ae. aegypti* mosquitoes (**Figure 5.1**). This also confirmed that the components of the SUMOylation pathway were expressed in different *Ae. aegypti* tissues.

In the **Table 3-1**, the 'Protein' subheading indicates which protein the peptide sequence ('Amino acid sequence') is identified in. 'Sequence unique to protein' indicates if throughout the entire genome, the peptide sequence is only encoded in the 'Protein' identified, or if the peptide sequence is also encoded in other proteins. 'Length' details the number of amino acids in the peptide sequence, and 'Start / End amino acid position' indicates the position of the amino acid sequence within the protein.

Table 3-1 The SUMOylation pathway specific peptide sequences identified from *Ae. aegypti* cells by mass spectrometry.

Protein	Amino acid sequence	Sequence unique to protein	Length	Start amino acid position	End amino acid position
SUMOa/b	KLMNAYCDR	no	9	40	48
	LMNAYCDR	no	8	41	48
	VLGQDNAVVQFK	no	12	20	31
SUMOa	AGLSMQVVR	no	9	49	57
	SEEKKDSKGSESEHINLK	yes	18	2	19
Ubc9	CKFEPPLFHPNVYPSGTVCLSLL DEEKDWRPAITIK	no	36	75	110
	DDYPTSPPK	no	9	66	74
	DHPFGFVAR	no	9	19	27
	DHPFGFVARPVK	no	12	19	30
	DWRPAITIK	no	9	102	110
	FEPPLFHPNVYPSGTVCLSLLDEE KDWRPAITIK	no	34	77	110
	GTPWEGGLYK	no	10	50	59
	KDHPFGFVAR	no	10	18	27
	KDHPFGFVARPVK	no	13	18	30
	KGTPWEGGLYK	no	11	49	59
	MIFKDDYPTSPPK	no	13	62	74
	NADGTLNLMTWECAIPGKK	no	19	31	49
	QILLGIQDLLNEPNIK	no	16	111	126

	QILLGIQDLLNEPNIKDPAQAEAYTIYCQNR	no	31	111	141
SAE1	ADTEELPK	no	8	108	115
	AQQLNPMVELK	no	11	97	107
	AQQLNPMVELKADTEELPK	no	19	97	115
	AVTLLDDQVVK	no	11	60	70
	AVTLLDDQVVKEADFCSQFLAPQDSLR	no	27	60	86
	EADFCSQFLAPQDSLR	no	16	71	86
	FRDDEKRDPLYSER	no	14	240	253
	GFDVVCVIGANTEQLLR	no	17	123	139
	ILIAGVNGLGAEIAK	no	15	37	51
	KTDDFFKGFDVVCVIGANTEQLLR	no	24	116	139
	LWGLDSQK	no	8	23	30
	LWGLDSQKR	no	9	23	31
	NVILSGVK	no	8	52	59
	RSGPALPLLR	no	10	226	235
	SGPALPLLR	no	9	227	235
	TELVTSTVK	no	9	191	199
	TELVTSTVKR	no	10	191	200
	TKTELVTSTVK	no	11	189	199
	TKTELVTSTVKR	no	12	189	200
	TLSYPAYQVLLDFDYK	no	16	201	216
	TLSYPAYQVLLDFDYKAQSYAR	no	22	201	222

	TNRAEASLSR	no	10	87	96
	VEANGIELTEQEAELYDR	yes	18	2	19
SAE2	AAQIVGVFEPELQEK	yes	15	2	16
	ALNMLNPDVILDGK	no	14	467	480
	AQIFNIPR	no	8	357	364
	AQIFNIPRK	no	9	357	365
	ARVSNDDDDDDLIVIN	no	16	627	642
	ASTSNNGAVDDDDDMCIVEEDAEKPSTSDAGAGPSSSGSEKR	no	42	573	614
	AYHDSITTSNYGVNFFQQFNLVLNALDNR	no	29	93	121
	CYVCAAKPEVTLK	no	13	436	448
	DESSFDIVADPDSLKPK	no	17	534	550
	DPGRDESSFDIVADPDSLKPK	no	21	530	550
	EDEDQKTDDVQPSTSGQNGNSK	yes	22	551	572
	ELRDDILIK	no	9	458	466
	ESALSFNPNVK	no	11	80	90
	GLTQCYECTPK	no	11	156	166
	GTIVISSEEGETDCNNDK	no	18	481	498
	GTIVISSEEGETDCNNDKK	no	19	481	499
	GTIVISSEEGETDCNNDKKLEDLQIVDGCILK	no	32	481	512
	HAMDFVAACANIR	no	13	344	356
	HLFNQLFGESNEDEDVSPDTADPEAGAEAGESALAAEANEK	no	41	193	233

	HLFNQLFGESNEDEDVSPDTADPEAGAEAGESALAAEANEKGNVDR	no	46	193	238
	ILVVGAGGIGCEILK	no	15	22	36
	KLEDLQIVDGCILK	no	14	499	512
	LAEGDHLVWDKDDK	no	14	330	343
	LAEGDHLVWDKDDKHAMDFVAACANIR	no	27	330	356
	LCLTADVPLIESGTAGYNGQVELIKR	no	26	130	155
	LEDLQIVDGCILK	no	13	500	512
	LFYDDINYLLSMSNLWK	no	17	259	275
	NLVLSGFQDIEIIDLDTIDVSNLNR	no	25	37	61
	NQLFVPDR	no	8	420	427
	NTPSEPIHCIVWAK	no	14	179	192
	QFLFHKEHVGK	no	11	62	72
	SMAGNIIPAIATTNAITAGVVVMHAFR	no	27	372	398
	SRTPPNPAKWDALEEDGEAAPTDTVLR	no	27	276	302
	TLNPPNPK	no	8	428	435
	TPPNPAKWDALEEDGEAAPTDTVLR	no	25	278	302
	TPPNPAKWDALEEDGEAAPTDTVLRDQK	no	28	278	305
	TWAQQCGYDPEK	no	12	243	254
	TWAQQCGYDPEKIFNK	no	16	243	258
	VDDFVQNYELTVTVIHK	no	17	513	529

	VFGESITALKK	no	11	315	325
	VLSLTESAK	no	9	306	314
	VSNDDDDDDLIVIN	no	14	629	642
	WDALEEDGEAAPTDTVLR	no	18	285	302
	WDALEEDGEAAPTDTVLRDQK	no	21	285	305
PIAS	GGQVHANGIVPIPYPEATPNPGYPIHPDVK	no	30	126	155
	GYAAACYLVR	no	10	297	306
	IEHTIQVQLR	no	10	212	221
	IQEGSFFFHLTPQQATDIATNR	no	22	183	204
	KPTWNCPVCDK	no	11	389	399
	LAFFDVLATLLKPATLVPSNTTQR	no	24	159	182
	LCPLPNPIPTNKPGVEPK	no	18	247	264
	LSSEDNEIQLHK	no	12	421	432
	NVNKIEHTIQVQLR	no	14	208	221
	QAAEFTELKDLVHQLR	no	16	6	21
	RPPRPVNITPNVK	no	13	265	277
	TNDSCTLDTPSKPVQK	no	16	442	457
	VEVVSDDIEIITTDPPK	no	17	458	474
	VPQGMYQQQYANAVQNDNR	no	19	107	125
	VSDLQQLLGENNISR	no	15	22	36
	VSLVCPLGK	no	9	351	359

3.2.6. Summary

This analysis demonstrates that the SUMOylation pathway is conserved in *Ae. aegypti*. Sequence analysis has shown a high conservation of the protein (summarised in **Figure 3.5**), and importantly, revealed the catalytically functional residues of the proteins are present, shown for *Aa*PIAS in **Figure 3.4B**). Modelling the structure of the *Aa*SUMOylation proteins has revealed that they are very similar to their *H. sapiens* orthologues. Western blot analysis of *Ae. aegypti* cell lysate has also demonstrated that there are HMW SUMO conjugates in *Ae. aegypti*, demonstrating that the pathway is active. Antibody cross reaction also helps to demonstrate the amino acid sequence identity of the SUMO and Ubc9 orthologues. Finally, mass spectrometry analysis has also demonstrated that components of the *Aa*SUMOylation pathway which we can't detect by western blot (*Aa*SAE1/2, and *Aa*PIAS), are expressed in *Ae. aegypti*.

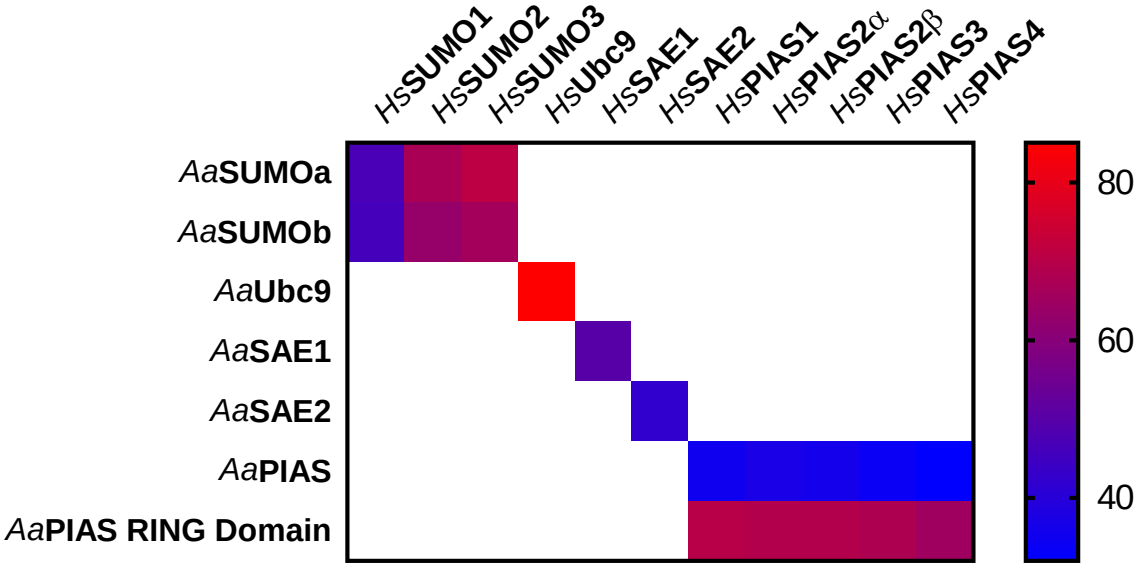

Figure 3.5 A heatmap of amino acid identity between the *Aa* and *Hs* SUMOylation pathways

The amino acid sequence of the *Aa*SUMOylation and *Hs*SUMOylation pathways were compared. Heatmap generated with Graphpad Prism 7.02, red demonstrates a greater percentage amino acid identity.

3.3. Viral proteins contain SUMO conjugation motifs

It is hypothesised that any direct effect of SUMOylation on arbovirus replication in either *H. sapiens* or *Ae. aegypti* would likely be dependent on SUMO modification of viral proteins. Approximately 74% of experimentally confirmed SUMO modifications occur at SCMs (Yavuz and Sezerman 2014). Consequently, polyprotein sequences from different arbovirus families were analysed for the presence of SCM motifs to determine the potential relevance of SUMO modification in the regulation of arboviral replication.

The published amino acid sequence of the proteins was analysed by the Joined Advances SUMOylation site and SIM Analyser (JASSA), an online SCM prediction tool (Beauclair, Bridier-Nahmias et al. 2015). Sites representing 'Strong Consensus' sequences were identified and are indicated with a bubble. 'Weak Consensus' sequences are depicted as vertical lines on the schematics. SCMs which are in a forward orientation are indicated in aqua, while sites in an inverse orientation are indicated in orange.

3.2.1. SCM sites on BUNV proteins

The Bunyamwera virus genome transcribes four proteins, these four proteins were analysed by JASSA to determine if they contained SCM sites. Multiple lysine residues were identified as potential targets of SUMO modification (**Figure 3.6**). Three of the 'Strong Consensus' sequences were located on the envelopment polyprotein, which is cleaved into the glycoproteins Gn and Gc, a non-structural protein NSm is also produced by the envelopment polyprotein. The three inverse 'Strong Consensus' sites ('EKKP'; 'ETKV', and 'EPKI') are all located on the Gc glycoprotein. The other three sites, also inverse SCMs, were located on the RNA-directed RNA polymerase (RDRP) L protein ('DYKV'; 'DGKV', and 'EHKV'). Very few sites were identified as being capable of SUMO modification on the Nucleoprotein and non-structural NSs protein, none of which were identified as a 'Strong Consensus' sequences. As the structure of the Gc glycoprotein, and the RDRP has not currently been resolved, no further analysis was conducted.

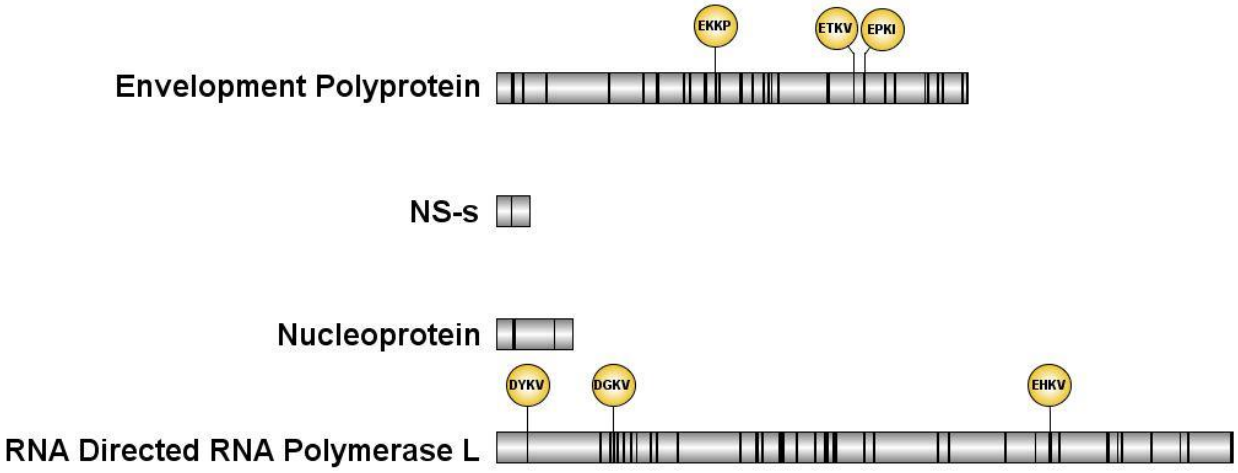

Figure 3.6 Predicted SUMO conjugation motifs on BUNV proteins

The annotated amino acid sequence of BUNV proteins were assessed by JASSA for the presence of SUMO conjugation motifs. Sites predicted as being a 'Strong Consensus' sequence are represented as bubbles. 'Weak Consensus' sequences are annotated as vertical lines. Of the four proteins produced by the BUNV genome, only two possess 'Strong Consensus' motifs, located on the Envelopment polyprotein and the RNA Directed RNA Polymerase L.

3.2.2. SCM sites on SFV proteins

The two polyprotein sequences from SFV and CHIKV were also analysed for the presence of SCMs with JASSA. SFV contained many sites amenable to SUMO modification, 10 of which were in the classical 'Strong Consensus' sequence (**Figure 3.7A**). Of these, seven were located on the non-structural polyprotein. Within the non-structural polyprotein, one site with the sequence 'VKGE' is located on the non-structural protein nsP1. Two SCM sites were found on nsP2 ('VKRE'; 'ERKI'), and a further two SCM sites were located on nsP3 ('EKKI'; 'VKCE'). Finally, the last two predicted SCMs were found on nsP4 ('DVKI'; 'EVKI'). The three remaining 'Strong Consensus' sequences were located on the structural polypeptide; two of which were found within the capsid (which overlap each other in the sequence 'VKHEGKV') and one was located in the Envelope glycoprotein E2 ('EGKP') (**Figure 3.7A**).

The resolved structure of the capsid protein was analysed to determine where the predicted SCM was located (**Figure 3.7B; Figure 3.7C; Figure 3.7D**). It was hypothesised that if the SCM was located on an internal section of the protein, it would be inaccessible as a target for SUMO modification. The resolved capsid structure revealed that the predicted SCM was found on a readily accessible part of the monomer, at the interface where monomers form multimers. As the resolved structure was not available for the Envelope glycoprotein E2 or the nsP1-4 proteins, the analysis was not continued for other potential SCMs in SFV.

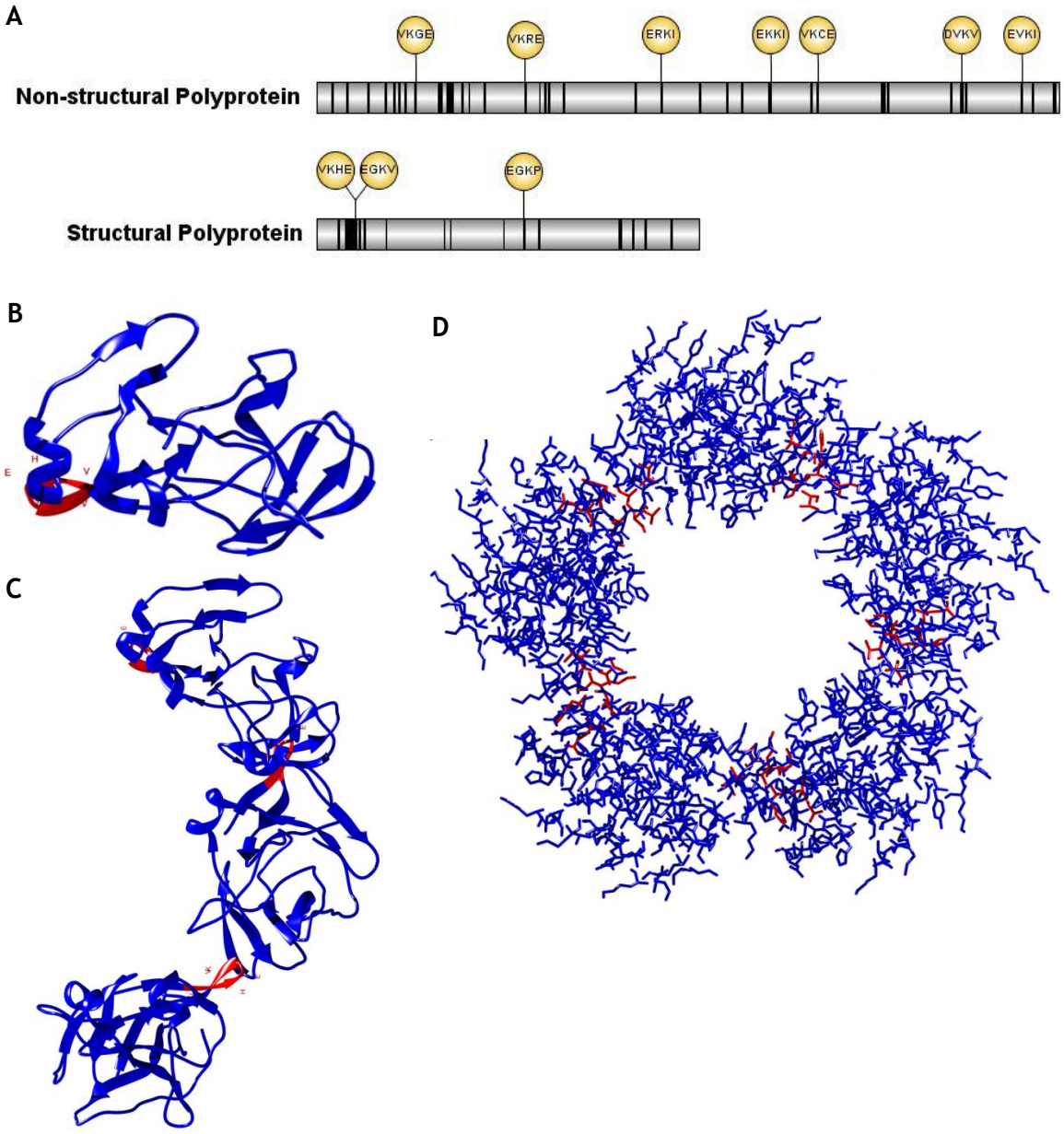

Figure 3.7 Predicted SUMO conjugation motifs on SFV polyproteins

The annotated amino acid sequence of SFV polyproteins were assessed by JASSA for the presence of SUMO conjugation motifs. (**A**) Sites predicted as being a 'Strong Consensus' sequence are represented as bubbles, 'Weak Consensus' sequences are annotated as vertical lines. Of the two polyproteins produced by the SFV genome, both possess multiple 'Strong Consensus' motifs. (**B**) The resolved structure of the Capsid (PDB ID: 1DYL) monomer, (**C**) trimer, (**D**) and a fully formed Capsid multimer are shown with the predicted 'Strong Consensus' motif indicated in red (Mancini, Clarke et al. 2000).

3.3.5. SCM sites on CHIKV proteins

Further JASSA analysis with CHIKV indicated three potential SCMs on the structural polyprotein, and one further potential SCM on the non-structural polyprotein (**Figure 3.8A**). As the 'VKHEGKV' region was found to be conserved from SFV to CHIKV in the capsid protein this indicated that the site has an important and conserved role between alphaviruses. The other potential SCM site found on the structural polyprotein was a 'PKGE' motif located on the Spike Glycoprotein E2 (**Figure 3.8B**). This SCM appears to not be readily accessible, as it is located within a fold of the protein, and therefore unlikely to be exposed for SUMO modification. The potential SCM on the non-structural polyprotein ('VKGE') was located on the nsP2. As the resolved structure of nsP2 was available this was modelled where the 'VKGE' region was located and it was found to be also located on an exposed region of the protein (**Figure 3.8C**).

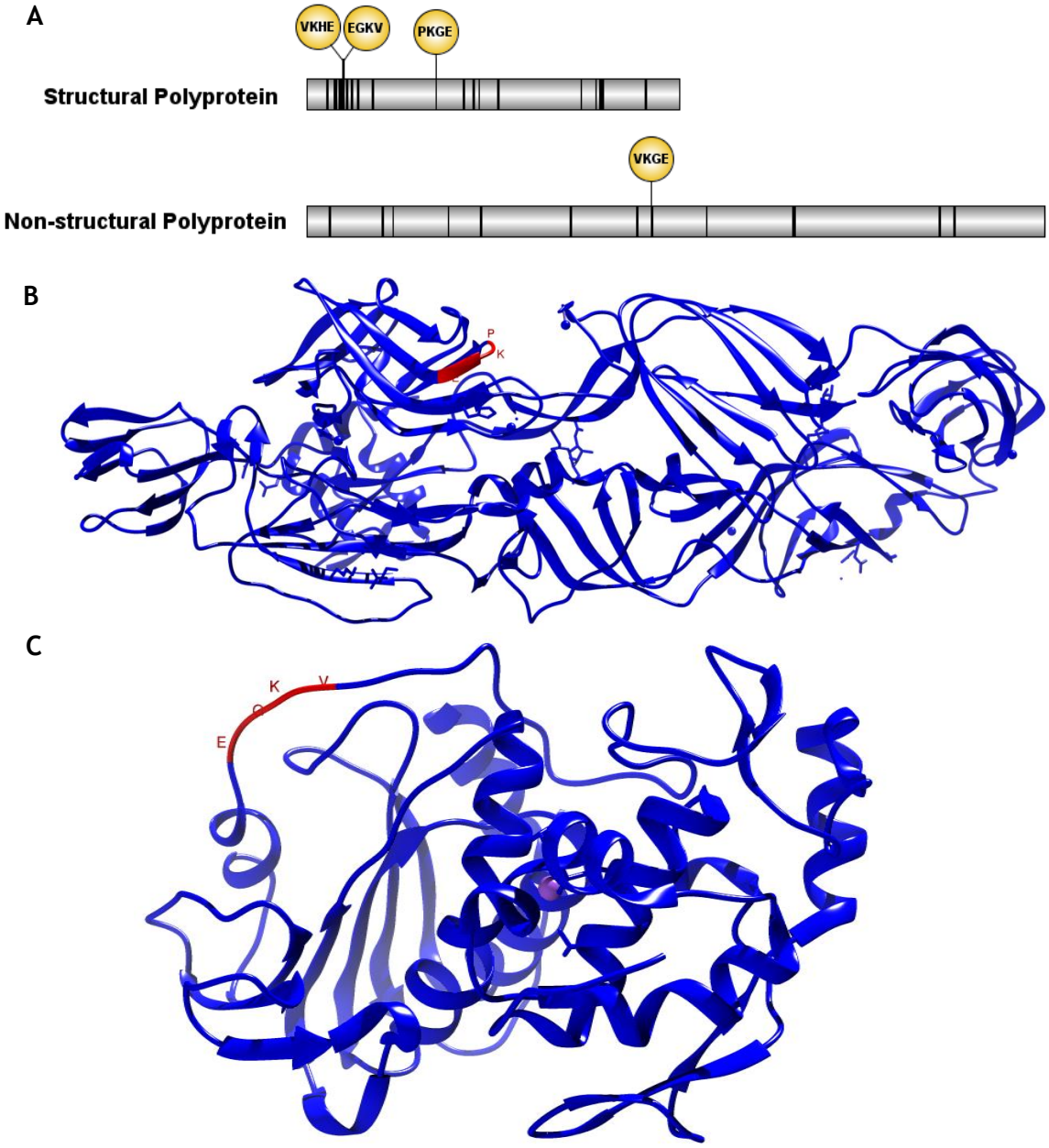

Figure 3.8 Predicted SUMO conjugation motifs on CHIKV polyproteins

The annotated amino acid sequence of CHIKV polyproteins were assessed by JASSA for the presence of SUMO conjugation motifs. (**A**) Sites predicted as being a 'Strong Consensus' sequence are represented as bubbles, other 'Weak Consensus' sequences are annotated as vertical lines on the polyproteins. Of the two polyproteins produced by the CHIKV genome, there are a total of four 'Strong Consensus' motifs. (**B**) The 'Strong Consensus' motifs identified in **A** were assessed for which protein they are located on, using the resolved structure of CHIKV Envelope glycoprotein E2 (PDB ID: 3N43) (Voss, Vaney et al. 2010), (**C**) and nsP2 (PDB ID: 3TRK), the SUMO conjugation motifs were identified and indicated in red.

3.3.6. SCM sites on ZIKV proteins

The analysis was also conducted on flaviviruses. Here, analysis of Zika virus identified three potential SCMs on the polyprotein (**Figure 3.9A**). One ('IKVE') was located on the small envelope protein. However, while the sequence was found on the strain of ZIKV used in these studies (PE243; **Table 2-3**) this was not conserved between strains and therefore was not examined further. Another potential SCM ('VKQD') identified on NS3 was also not conserved between different ZIKV strains, and therefore no further examinations were conducted. The final potential SCM ('VKYE') was located on NS5. This SCM was found to be conserved, and so the potential SCM site was modelled on the resolved structure of NS5. This was found to be on an exposed region of the protein, indicating a potential site for SUMO modification (**Figure 3.9B**).

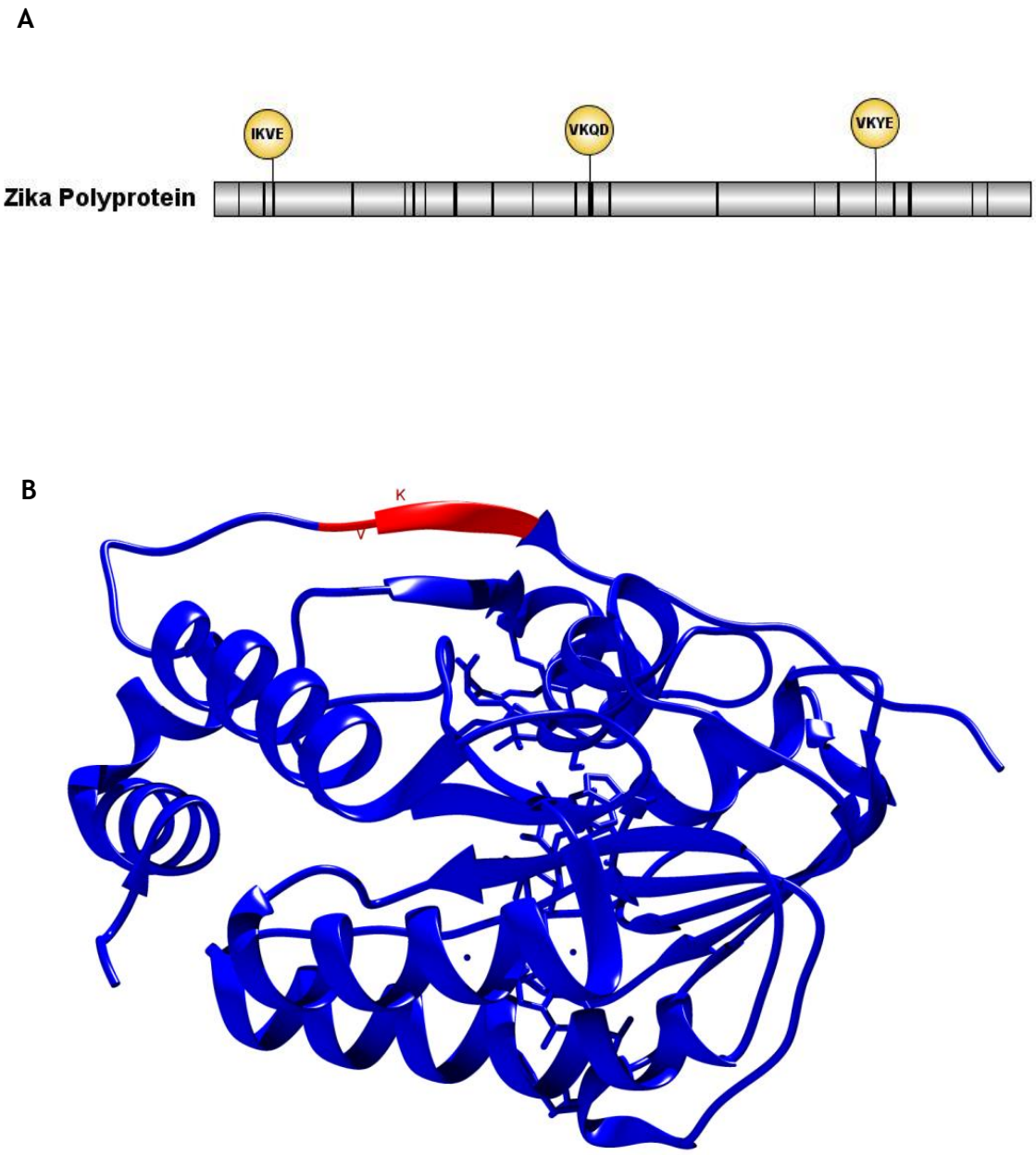

Figure 3.9 Predicted SUMO conjugation motifs on the ZIKV polyprotein

The annotated amino acid sequence of ZIKV polyprotein was assessed by JASSA for the presence of SUMO conjugation motifs. (**A**) The 3 sites predicted to be a 'Strong Consensus' sequence are represented as bubbles, other 'Weak Consensus' sequences are annotated as vertical lines on the polyprotein. There are three 'Strong Consensus' sequences located on the ZIKV polyprotein. (**B**) The 'Strong Consensus' motifs identified in **A** were assessed for which protein they are located on, using the resolved structure of ZIKV NS5, the SUMO conjugation motifs were identified and indicated in red (PDB ID: 5KQR) (Coloma, Jain et al. 2016).

3.3.7. SCM sites on DENV proteins

Previous studies have suggested an interaction between DENV and the SUMOylation pathway in *H. sapiens* (Chiu, Shih et al. 2007, Su, Tseng et al. 2016, Feng, Deng et al. 2018). DENV-2, the serotype utilised in previous studies which contain a large number of resolved structures to the proteins, was analysed revealing four potential SCM sites (**Figure 3.10A**). Of these four sites, two, 'VKWD' and 'PKNE', were not conserved from the proteins NS2b and NS3, respectively. 'VKKD', also located on NS3, was conserved and the resolved structure was available (**Figure 3.10B**). This indicated that the lysines in the 'VKKD' SCM are likely to be exposed, and consequently accessible for SUMO modification. Finally, the inverted 'PFKE' is located on the Non-structural protein 4B, however, the structure of the protein has not been resolved, and consequently, no further analysis was conducted on this site.

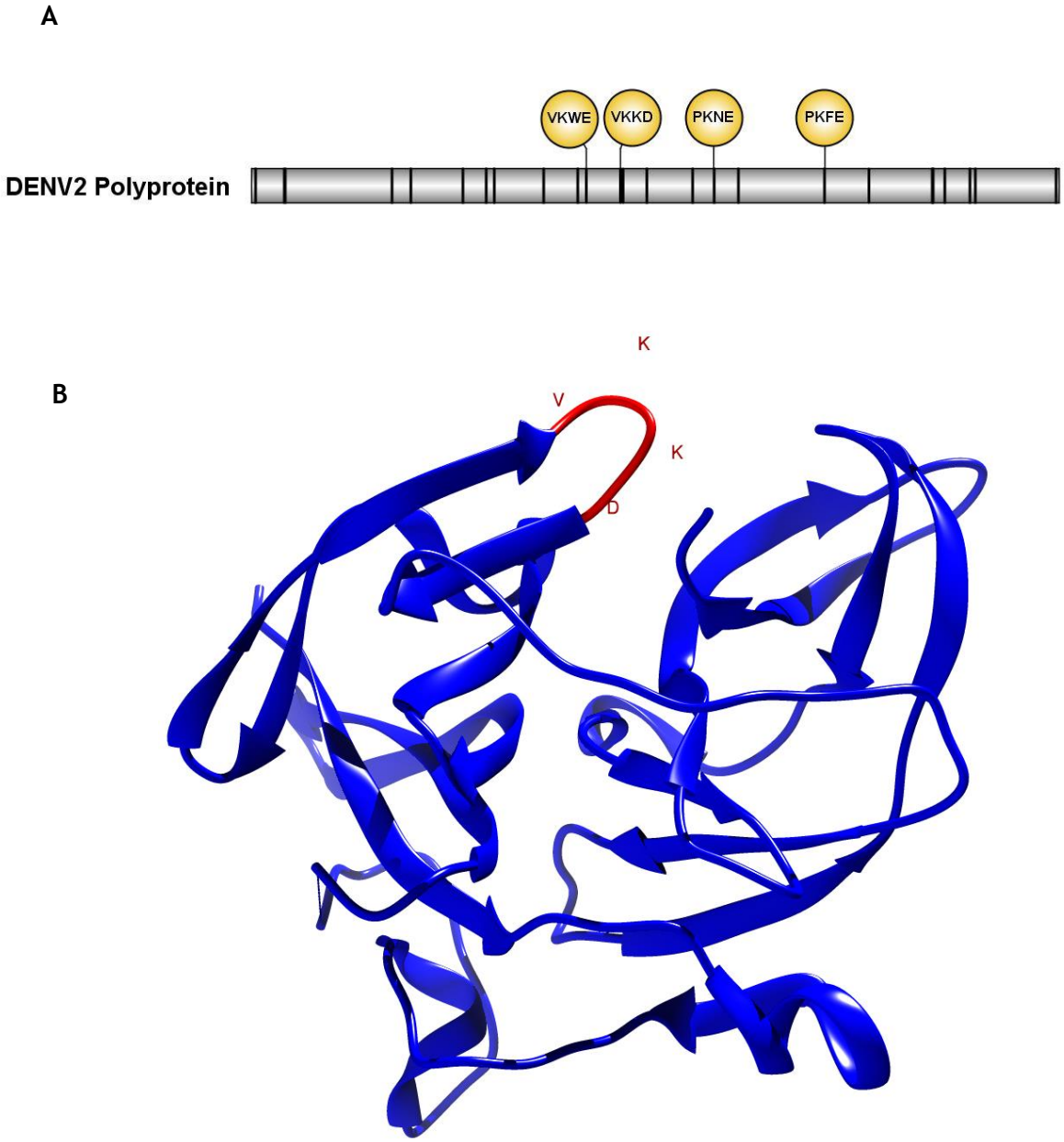

Figure 3.10 Predicted SUMO conjugation motifs on the DENV-2 virus polyprotein

The annotated amino acid sequence of DENV polyprotein was assessed by JASSA for the presence of SUMO conjugation motifs. (**A**) The 4 sites predicted to be a 'Strong Consensus' sequence are represented as bubbles, other 'Weak Consensus' sequences are annotated as vertical lines on the polyprotein. (**B**) The 'Strong Consensus' motifs identified in **A** were assessed for which protein they are located on, using the resolved structure of DENV-2 NS3, the SUMO consensus motifs were identified and indicated in red (PDB ID: 4M9K) (Yildiz, Ghosh et al. 2013). Other 'Strong Consensus' motifs were either not conserved, or the resolved structures were not available for analysis.

3.3.8. Summary

As summarised in Table 3-2, there are many potential sites of SUMO modification in arboviral proteins. While the resolved structure of many of these proteins is not available, for those which have been resolved indicate the SCM is frequently in an exposed location and consequently a potential target for SUMO modification. Su, Tseng et al. (2016) found that DENV-2 NS5 was a target of SUMO modification, unfortunately, this protein was not identified by this analysis, which is discussed further in **Section 3.4** and may indicate that the list does not represent all potential targets of SUMO modification in the arboviral proteins, suggesting a potential role for E3 ligase specificity.

Table 3-2 Summary of the SCM sequences found on the relevant proteins of different arboviruses

Virus	Protein	Resolved structure	SCM sequence	Exposed: Y/N
BUNV	Gc glycoprotein	Not available	EKKP / ETKV / EPKI	
	RDRP	Not available	DYKV / DGKV / EHKV	
SFV	Capsid protein	Present (PDB ID: 1DYL)	VKHEGKV	Y
	Envelope glycoprotein	Not available	EGKP	
	nsP1	Not available	VKGE	
	nsP2	Not available	VKRE / ERKI	
	nsP3	Not available	EKKI / VKCE	
	nsP4	Not available	DVKI / EVKI	
CHIKV	Capsid protein	Present (as shown with SFV)	VKHEGKV	Y
	Spike glycoprotein	Present (PDB ID: 3N43)	PKGE	N
	nsP2	Present (PDB ID: 3TRK)	VKGE	Y
ZIKV	Small envelope protein		IKVE	Not conserved
	NS3		VKQD	Not conserved
	NS5	Present (PDB ID: 5KQR)	VKYE	Y
DENV	NS2b		VKWD	Not conserved
	NS3	Not conserved / Present (PDB ID: 4M9K)	PKNE / VKKD	Y
	NS4b	Not available	PFKE	

3.4. Discussion

All viruses manipulate the cell they infect in order to replicate efficiently. Unlike most other viruses, arboviruses need to manipulate two distinct cell types, the vertebrate and invertebrate host species. The SUMOylation pathway has previously been reported to influence arbovirus replication; however the studies to date only investigate the interaction of the SUMOylation pathway on Dengue Virus Serotype 2 (Chiu, Shih et al. 2007, Su, Tseng et al. 2016, Feng, Deng et al. 2018). The studies by Chiu, Shih et al. (2007), Su, Tseng et al. (2016) and Feng, Deng et al. (2018) have also only been conducted in mammalian cells and found both pro-viral and anti-viral roles for the SUMO pathway. Consequently, while there is an understanding of interactions occurring in mammalian cells, nothing is known about any interactions between the SUMOylation pathway and arboviruses in *Ae. aegypti*. There are also a very limited number of studies investigating the *Ae. aegypti* SUMOylation pathway, and previous studies have only looked at the amino acid sequence homology (Choy, Severo et al. 2013, Urena, Pirone et al. 2016). Consequently, as an initial step, the *Aa*SUMOylation pathway was analysed for its similarity to the *Hs*SUMOylation pathway.

The analysis conducted here agrees with previous bioinformatic studies which demonstrate that the SUMO protein is conserved between *H. sapiens* and *Ae. aegypti* (**Figure 3.1**). Studies by Urena, Pirone et al. (2016), and Choy, Severo et al. (2013) both demonstrate that *Ae. aegypti* possesses the gene sequence of two SUMO homologues (Choy, Severo et al. 2013, Urena, Pirone et al. 2016). The study by Urena, Pirone et al. (2016) has also demonstrated that, based on the amino acid sequence, both *Aa*SUMO proteins lack the SCM and should be unable to efficiently form poly-SUMO chains, work which agrees with the studies conducted here. Neither study, however, proceeded to investigate the tertiary structure of the *Aa*SUMO proteins, nor did they examine if the proteins were expressed. Consequently, we show the novel findings that the SUMO protein shares a highly conserved tertiary structure, and demonstrated that the *Aa*SUMOa protein in *Ae. aegypti* is expressed (**Table 3-1**; **Figure 3.1**). Our mass spectrometry analysis failed to identify peptide sequences specific to *Aa*SUMOb. This could be because the *Aa*SUMOb protein could be expressed in specific

tissues which weren't studied, or *Aa*SUMOb may lack a promoter sequence and so may be a pseudogene.

Choy, Severo et al. (2013) also produced a phylogenetic tree of the annotated ubiquitin, ubiquitin-like conjugating enzymes, and activating enzymes, from a range of vector species. As their study focused on the generation of phylogenetic trees demonstrating how related the enzymes are between vector species, they did not look at the structure of the proteins. Here, we also demonstrate a shared amino acid identity, and proceed to show a similar tertiary structure of the predicted structure of *Aa*Ubc9 with the resolved structure of *Hs*Ubc9. This was also demonstrated with the predicted structure of *Aa*SAE1/2 plotted against the resolved structure of *Hs*SAE1/2. Finally, we validate the expression of *Aa*SUMOa, *Aa*Ubc9, *Aa*SAE1, and *Aa*SAE2, by mass spectrometry and Western blot (**Figure 3.2**; **Figure 3.3**; **Table 3-1**).

More studies have been conducted on *Aa*PIAS, due to its widely known role as a regulator of the JAK-STAT pathway. Zou, Souza-Neto et al. (2011) analysed the amino acid sequence of *Aa*PIAS and found conserved domains, including the SAP, PINIT, RING-finger like domain, and the Serine/Threonine-rich domain. Zou, Souza-Neto et al. (2011) also performed depletion studies and showed *Aa*PIAS to be expressed in *Ae. aegypti*, we demonstrate *Aa*PIAS to have a conserved tertiary structure and confirm *Aa*PIAS expression by mass spectrometry (**Figure 3.4**; **Table 3-1**).

We have demonstrated that the pathway is conserved, and that the proteins are expressed in *Ae. aegypti*. Consequently, we assessed the potential effect of SUMO modification on arboviral proteins. For this a bioinformatics based approach was initially adopted. Previous studies have found predictive algorithms to be a suitable method of identifying potential sites of SUMO modification within cellular and viral proteins, and therefore the JASSA programme was utilised to help identify potential sites of SUMO modification on arboviral proteins (Handu, Kaduskar et al. 2015, Estruch, Graham et al. 2016, Iribarren, Di Marzio et al. 2018).

Representative model and clinically important arboviruses from three arboviral families were selected for analysis. All the arbovruses studied are known to be transmitted by *Ae. aegypti*. BUNV, a negative-strand RNA *orthobunyavirus*, was found to possess six potential SCM sites in the three proteins, and one polyprotein, which BUNV initially translates (**Figure 3.6**). Unfortunately, the resolved structure of the proteins was unavailable, and consequently, the analysis does not examine the location of the SCM sites on the proteins.

JASSA analysis was also conducted on the alphavirus SFV, a positive-stranded RNA virus which appears to have 10 SCM sites throughout the two polyproteins it translates. Two sites were identified on the resolved capsid protein. These SCMs were located on an external surface, at the site where capsids form multimers (**Figure 3.7**). As SUMO modification has previously been reported to have roles in directing protein sub-cellular localisation (Matunis, Wu et al. 1998, Duprez, Saurin et al. 1999, Sachdev, Bruhn et al. 2001), this could potentially indicate a role for SUMO modification whereby SUMO modification transports the capsid monomers to the same location where they form multimers. Alternatively, it could indicate a role for SUMO in binding to the capsid monomers preventing the formation of multimers. CHIKV, another alphavirus, was also analysed (**Figure 3.8**). Interestingly, two SCM sites in the capsid protein were conserved between SFV and CHIKV, which indicates a potentially important and conserved role for this region of the capsid protein. Other sites which were indicated as possessing SCMs were the Envelope glycoprotein E2 and the non-structural nsP2 protein. The SCM site on the Envelope glycoprotein does not appear to be readily accessible, and therefore unlikely to be a site of SUMO modification. The SCM on nsP2, however, is on the surface of the protein, and consequently could represent a target for SUMO modification (**Figure 3.8**).

The polyprotein produced from the flavivirus ZIKV was assessed and found to contain three predicted SCM sites (**Figure 3.9**). Of these three, only one was located on a protein which had a resolved structure (NS5). This SCM was located on the surface of the protein, indicating that it is accessible for SUMO modification. The NS5 protein from many flaviviruses is well reported to localise to the nucleus of cells, a site of abundant SUMO modification within cells (Buckley, Gaidamovich et al. 1992, Miller, Sparacio et al. 2006, Hou, Cruz-Cosme

et al. 2017). DENV-2 was also assessed and found to possess four potential SCMs (**Figure 3.10**). The resolved structure was available for NS3. Here, the SCM was also found on a region of the protein accessible for SUMO modification. Previous studies have demonstrated DENV NS5 to be SUMO modified at the N-terminal (Su, Tseng et al. 2016). The JASSA analysis conducted here does not predict DENV NS5 to possess a 'Strong Consensus' SCM. Interestingly, however, the study by Su, Tseng et al. (2016) could not identify one lysine residue which was predominantly SUMO modified, and consequently hypothesised that SUMO could 'float' in the N-terminal binding with any available lysine, as even after all 12 N-terminal lysines were mutated, there was still SUMO binding to NS5. The analysis here does identify many 'Weak Consensus' sequences at the N-terminal of NS5 which may be the SUMO modified section of NS5 that Su, Tseng et al. (2016) identified (**Figure 3.10**). Alternatively, it could indicate a necessity for E3 SUMO ligase activity in order to modify NS5.

This work could be extended further to look at a bioinformatics comparison on the SENPs, which haven't been addressed in this study. Furthermore, other non-PIAS E3 ligases may be translated by *Ae. aegypti*, which could also influence the *Aa*SUMOylation pathway, but have not been studied here. The analysis here could also extend to other strains of clinically important arboviruses, such as Japanese Encephalitis Virus, or Western Equine Encephalitis Virus, which may indicate how well conserved, and how important a SCM is on any individual arboviral protein.

4. Biochemical analysis of the *Ae. aegypti* and *H. sapiens* SUMOylation pathways

4.1. Overview

Biochemical studies of the *H. sapiens* (*Hs*) SUMOylation pathway have revealed that the different *Hs*SUMO homologues possess different biological functions within the cell. For instance, *Hs*SUMO1 promotes ocular lens cell differentiation, while *Hs*SUMO2/3 inhibits this cell differentiation. This is due to the SUMO isoforms having different effects on the stability of transcription factors (Gong, Ji et al. 2014). As *Hs*SUMO2/3 possess an internal SCM at lysine 11 (Lys11; K11), both are capable of efficiently forming poly-SUMO chains, while *Hs*SUMO1 cannot. The formation of poly-SUMO chains is reported to have a variety of effects on proteins, including altering protein localisation, protein stability, and protein-protein interactions (Hardeland, Steinacher et al. 2002, Joseph, Tan et al. 2002, Pfander, Moldovan et al. 2005, Mullen and Brill 2008, Tatham, Geoffroy et al. 2008). As *Hs*SUMO1 does not contain an internal SCM, *Hs*SUMO1 modifications generally occurs as mono-SUMOylation, or as a chain terminator events (Wang, Pan et al. 2002).

*Aa*SUMOa and –b both lack an internal SCM. Consequently, the amino acid sequence suggests *Aa*SUMOa/b should share a biochemical function more equivalent to *Hs*SUMO1 than *Hs*SUMO3. This chapter investigates the biochemical function of the *Aa*SUMOylation pathway component enzymes to determine if *Aa*SUMO can form poly-SUMO chains in the absence of an SCM, utilising *in vitro* biochemical assays (Bencsath, Podgorski et al. 2002, Prudden, Pebernard et al. 2007, Vethantham and Manley 2009, Boutell and Davido 2015, Yang, Campbell et al. 2018).

The core components of the *Aa*SUMOylation machinery were expressed using a bacterial expression system and purified as recombinant proteins, and *in vitro* biochemical studies conducted to investigate the biochemical properties of individual *Aa*SUMOylation pathway component enzymes. Our data demonstrates that *Aa*SUMO is biochemically more similar to *Hs*SUMO1 than *Hs*SUMO2/3 due to the lack of an internal SCM. Interestingly, however, when a catalytically active *Aa*PIAS was included, *Aa*SUMO efficiently formed poly-SUMO chains. The formation of *Aa*SUMO chains being *Aa*PIAS dependent indicates a potential regulatory mechanism for poly-SUMO chain formation in *Ae. aegypti*. We also

demonstrate that the biochemical activity of the SUMOylation proteins is highly conserved and functionally interchangeable between *Ae. aegypti* and *H. sapiens*.

4.2. Purification of the *Aa*SUMOylation pathway

In order to determine the biochemical properties of the *Aa*SUMOylation pathway, the constituent proteins were cloned into vectors in frame with affinity tags. A bacterial expression system was adopted to purify recombinant proteins as bacteria do not possess a SUMOylation pathway. This reduces the likelihood of by-products being co-purified with biochemical activity that could influence *in vitro* SUMOylation assays. Many previous studies have utilised affinity tagged recombinant proteins for biochemical assays to characterise the biochemical propertied of the proteins demonstrating the validity for use in these studies (Derewenda 2004, Arnau, Lauritzen et al. 2006, Alontaga, Bobkova et al. 2012).

Constituent proteins from the *Hs*SUMOylation pathway were previously cloned into bacterial expression vectors in frame with either GST- or His-tags on the N-termini of the proteins (**Table 2-5**). Corresponding proteins from the *Aa*SUMOylation pathway were also cloned into bacterial expression vectors (**Section 2.2.9**). *Aa*SUMO, *Aa*Ubc9, *Aa*PIAS, and respective catalytically inactive mutants, and the SUMO chimaera were cloned to contain an in frame His-tag on the N-termini. Purification of *Aa*SAE1/2 required an N-termini Strep.II tag on *Aa*SAE2, as a His-tag resulted in dissociation of the heterodimer. It was hypothesised that *Aa*SAE1/2 was unable to be purified by Ni-affinity chromatography due to the presence of non-conserved Histidine residues in *Aa*SAE1 at positions 179/279/297/310, and *Aa*SAE2 at position 66, which are located at the interaction interface of *Aa*SAE1/2 (**Appendix B: Purification of *AaSAE1*/2**).

Purification of recombinant proteins yielded predominantly pure samples, although some contained significant breakdown products (**Figure 4.1; Figure 4.2**). Additionally, a catalytically inactive *Aa*Ubc9 (*Aa*Ubc9 C93S), and *Aa*PIAS C371A, a chimaeric SUMO, and a chimaeric SUMO K11R mutant were also purified by Ni-affinity chromatography (**Section 2.2.9; Appendix C**: **Purified *AaUbc9* C93S, the SUMO chimaera, and the SUMO chimaera K11**). A chimaeric SUMO protein, and K11R mutant, was produced to demonstrate that the lack of Lysine within an SCM in *Aa*SUMO was responsible for lack of efficient poly-SUMO chain formation. If the addition of an SCM within *Aa*SUMO did not resulted in the

efficient conjugation of poly-SUMO chains it would suggest another component of the *Aa*SUMOylation pathway was preventing poly-*Aa*SUMO chain formation.

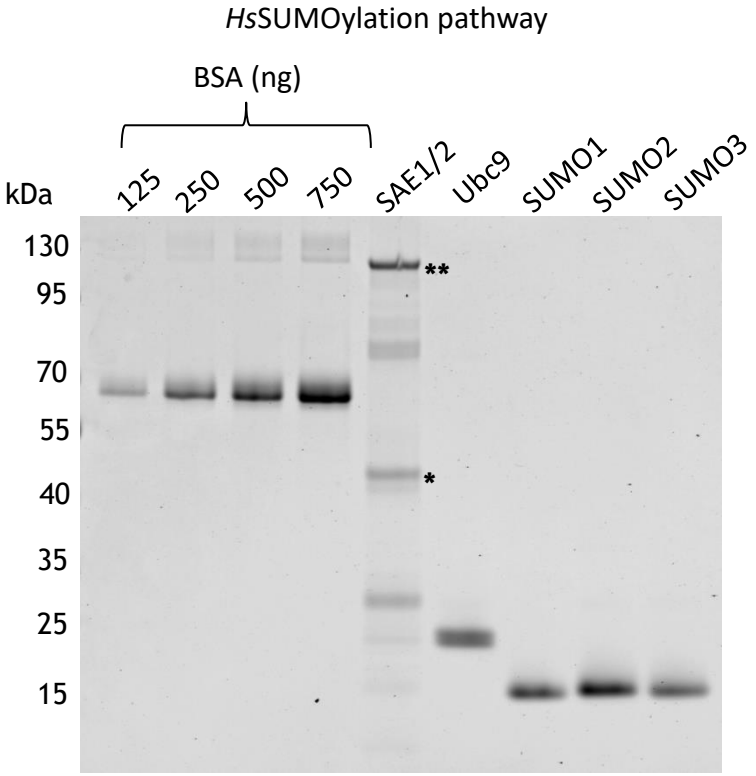

Figure 4.1 Recombinant *H. sapiens* SUMOylation proteins

Core proteins of the *H. sapiens* SUMOylation system were purified through Ni-affinity chromatography and resolved by SDS-PAGE with standardised concentrations of BSA. The gel was stained with Coomassie brilliant blue. Molecular weights indicated. * = His-SAE1, ** = GST-SAE2

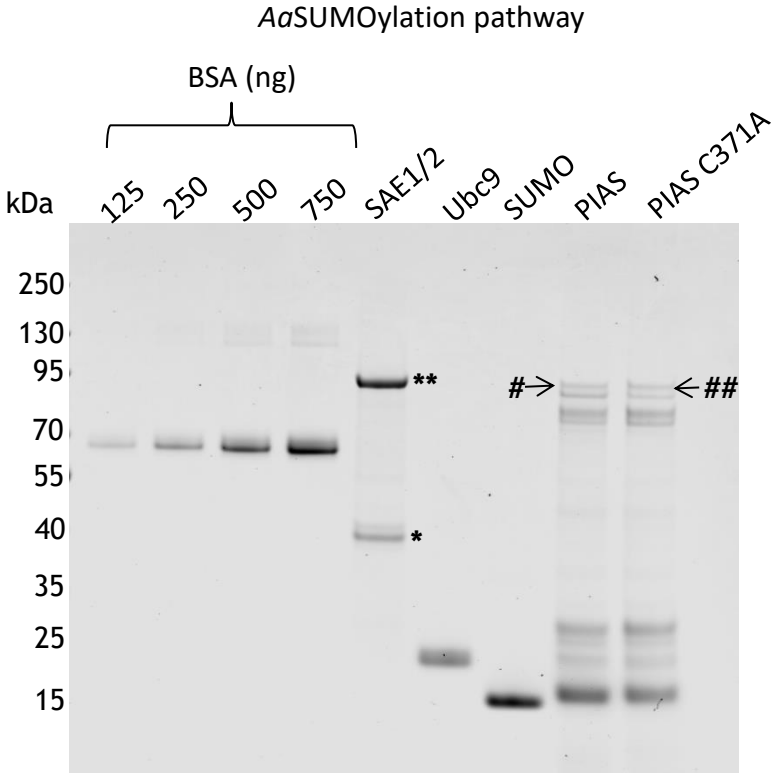

Figure 4.2 Recombinant *Ae. aegypti* SUMOylation enzymes

Core proteins of the *Ae. aegypti* SUMOylation system were purified through Ni-, or Biotin-affinity chromatography (SAE1/2). The proteins were resolved by SDS-PAGE with standardised concentrations of BSA. The gel was stained with Coomassie brilliant blue. Molecular weights indicated. * = SAE1, ** = Strep.II-SAE2, # = His-*Aa*PIAS, ##=His-*Aa*PIAS C371A.

4.3. Comparison of the biochemical properties of the *Ae. aegypti* and *H. sapiens* SUMOylation pathways

4.3.1. Recombinant *Aa*Ubc9 forms a thioester bond with SUMO at a similar rate to recombinant *Hs*Ubc9

Ubc9 is known to form a thioester bond with the terminal glycine residue of SUMO (Ubc9~SUMO) prior to modifying target substrates (Schwarz, Matuschewski et al. 1998, Tatham, Kim et al. 2003). The sequence similarity demonstrated 85% amino acid sequence identity (**Figure 3.2A**). Interestingly, previous work has implicated Asp^{100} and Lys^{101} as amino acids which influence the rate of thioester formation in *Hs*Ubc9. The presence of these amino acids has been shown to slow down the rate of thioester formation, but increase the rate of SUMO transfer to the substrate protein (Tatham, Chen et al. 2003). *Aa*Ubc9 encodes a Glu^{100} instead of an Asp^{100} (**Figure 3.2**), which led us to hypothesise that the rate at which *Aa*Ubc9 forms thioester bonds should occur at a slightly faster rate compared to *Hs*Ubc9.

Biochemical assays were conducted utilising recombinant proteins (300 ng *Hs*SUMO3, 100 ng *Hs*SAE1/2, and 100 ng *Hs* or *Aa*Ubc9). The proteins were mixed together in the presence of ATP, and incubated at 37˚C for the time course specified. The reactions were terminated with 3x BM –DTT (**Table 2-8**), which maintains the thioester bond. As indicated in **Figure 4.3A**, Ubc9~SUMO thioester conjugate resolved at the expected molecular weight. Furthermore, the addition of a catalytically inactive Ubc9, containing a C93S mutation, prevented thioester bond formation and therefore ensures that the band at the expected molecular weight represents Ubc9~SUMO. The formation of Ubc9~SUMO thioester was quantified, normalising to the background reading of the Coomassie stained gel at T0. Ubc9~SUMO thioester bond formation between *Hs*SUMO and either *Hs* or *Aa*Ubc9 occurred at approximately the same rate (**Figure 4.3B**). These data demonstrate that thioester bond formation between *Hs*SUMO3 and *Aa*Ubc9 occurs at a similar rate to *Hs*SUMO3 and *Hs*Ubc9, likely due to the high degree of

amino acid identity between the two Ubc9 orthologue proteins, indicating that these enzymes are biochemically indistinguishable *in vitro*.

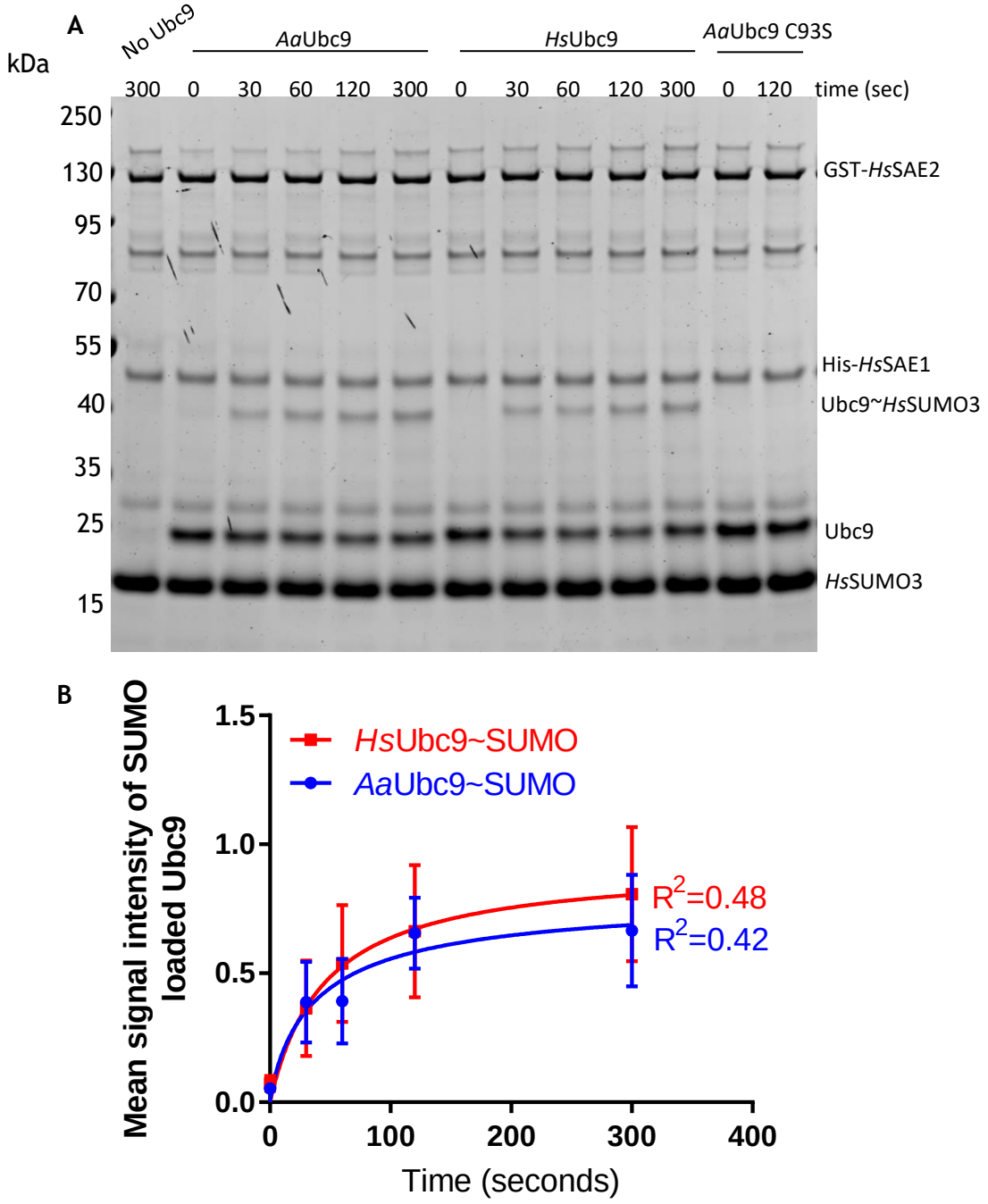

Figure 4.3 Comparison of *Hs*Ubc9 and *Aa*Ubc9 rate of thioester formation

Non-reducing biochemical Ubc9~SUMO thioester formation assays were conducted with 300 ng SUMO, 100 ng SAE1/2, 100 ng of either *Aa* or *Hs*Ubc9 in the presence of ATP and terminated at the specified time points. (**A**) Coomassie stained gel of the biochemical assay with either *Aa*Ubc9~ or *Hs*Ubc9~*Hs*SUMO3 indicated. One reaction containing no Ubc9, and a functionally inactive *Aa*Ubc9 mutant were included as controls. Molecular weight and other recombinant proteins are indicated. (**B**) Mean signal intensity of Ubc9~*Hs*SUMO3 from (**A**), with standard error bars shown. Curve plotted is nonlinear fit of data, as a specific binding with hill slope, with R^2 values shown, produced with GraphPad Prism 7.02, N=3.

4.3.2. Recombinant *Aa*SUMO is more biochemically comparable to *Hs*SUMO1 than *Hs*SUMO3 in an *in vitro* biochemical assay

The *Hs*SUMOylation pathway has been shown to be biochemically capable of forming poly-SUMO chains *in vitro* (Tatham, Jaffray et al. 2001). Using SAE2 and SUMO as substrates of SUMO modification, our assay compared the biochemical activity of the *Aa*SUMOylation pathway with the *Hs*SUMOylation pathway. Here, 50 ng of SAE1/2, 50 ng of Ubc9, and 50 ng of SUMO were incubated together at 28 ˚C. The reaction was terminated at the time points indicated with 3x BM (**Table 2-8**), the samples were resolved on an SDS-PAGE gel and a Western blot was conducted with antibodies raised against *Hs*SUMO2/3, and *Hs*SUMO1 when required.

*Aa*SUMO doesn't efficiently form mid-tier chains or HMW poly-SUMO chains, compared to *Hs*SUMO3 (**Figure 4.4A**). The biochemical activity of *Aa*SUMO is more comparable to that of *Hs*SUMO1 (**Figure 4.4B**). However, *Aa*SUMO does appear to be conjugated to *Aa*SAE2 slightly more efficiently compared to *Hs*SUMO1 conjugated to *Hs*SAE2. The signal intensity of the HMW SUMO conjugates was quantified and normalised to unconjugated SUMO at T0. When the biochemical activity of the three SUMO proteins was compared, *Aa*SUMO was observed to conjugate slightly more efficiently than *Hs*SUMO1, but far less efficiently than *Hs*SUMO3. The efficiency of SUMO conjugate formation of *Aa*SUMO is therefore more similar to that of *Hs*SUMO1 than *Hs*SUMO3 (**Figure 4.4C**).

The assays comparing the biochemical activity of *Aa*SUMO with *Hs*SUMO3 (**Figure 4.5A**) and *Hs*SUMO1 (**Figure 4.5B**) were also conducted at 37 ˚C, in order to determine if the lower temperature was altering the efficiency of the *Hs*SUMOylation pathway. However, as demonstrated in **Figure 4.5C**, *Aa*SUMO remained more biochemically comparable to *Hs*SUMO1, than *Hs*SUMO3, regardless of temperature. Collectively, these data indicate that *Aa*SUMO is biochemically more comparable to *Hs*SUMO1 than *Hs*SUMO3. This is likely due to the lack of an internal SCM, which is lacking in both *Hs*SUMO1 and *Aa*SUMO.

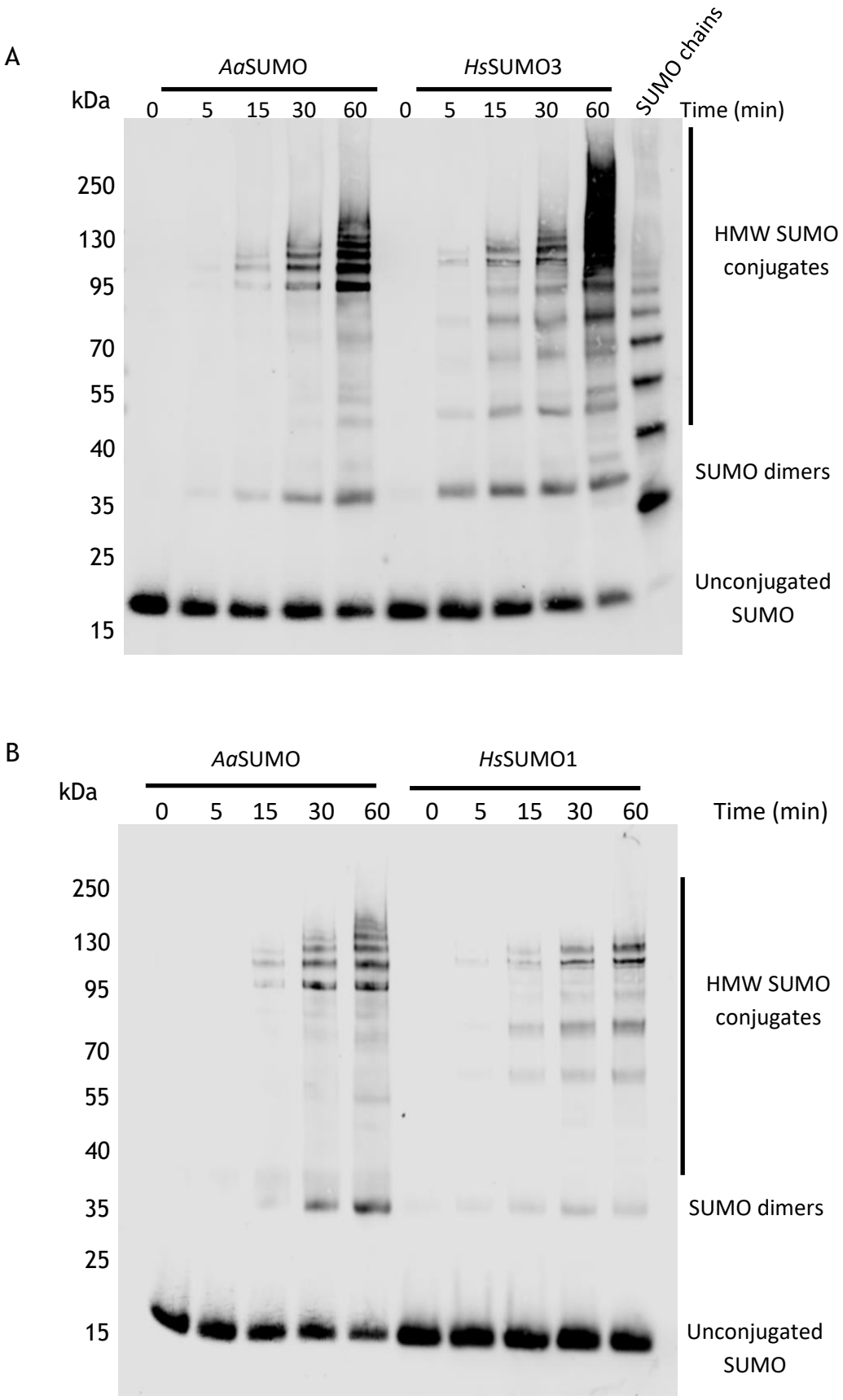

Continued on next page

C

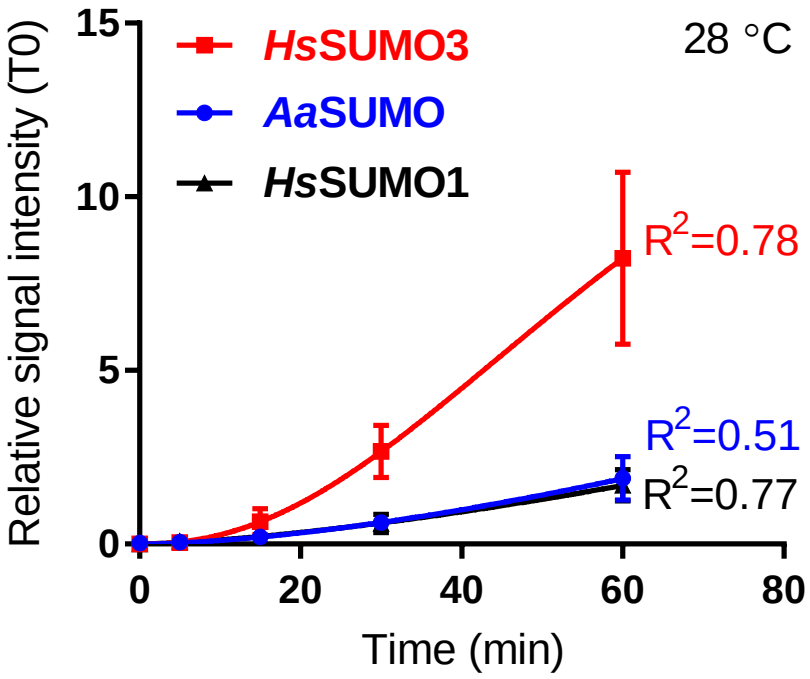

Figure 4.4 Comparison of *Aa* and *Hs* SUMOylation pathways activity at 28 ˚C

Biochemical reactions comparing the activity of 50 ng SUMO, SAE1/2, and Ubc9 from the *Aa* and *Hs* SUMOylation pathways were incubated together at 28 ˚C prior to the reaction being terminated after the specified periods of time. (**A**) Comparison of the build-up of SUMO-SUMO dimers and HMW SUMO conjugates of either *Aa*SUMO or *Hs*SUMO3. Commercial poly-SUMO2 chains were also included to indicate sizes of SUMO chains. An antibody to *Hs*SUMO2/3 was used to probe for *Aa* and *Hs*SUMO3 expression. (**B**) Comparison of the build-up of either *Aa*SUMO or *Hs*SUMO1 conjugates. Antibodies to *Hs*SUMO2/3 and *Hs*SUMO1 were utilised to probe for *Hs*SUMO1 and *Aa*SUMO expression over time. (**C**) Graphical view of the build-up of SUMO-SUMO dimers and HMW SUMO conjugates from both (**A**) and (**B**), signal intensity quantified using a LiCor. Curve is Specific binding with hill slope nonlinear fit of data, mean, standard error, and R^2 values shown, produced with GraphPad Prism 7.02. N≥3.

A

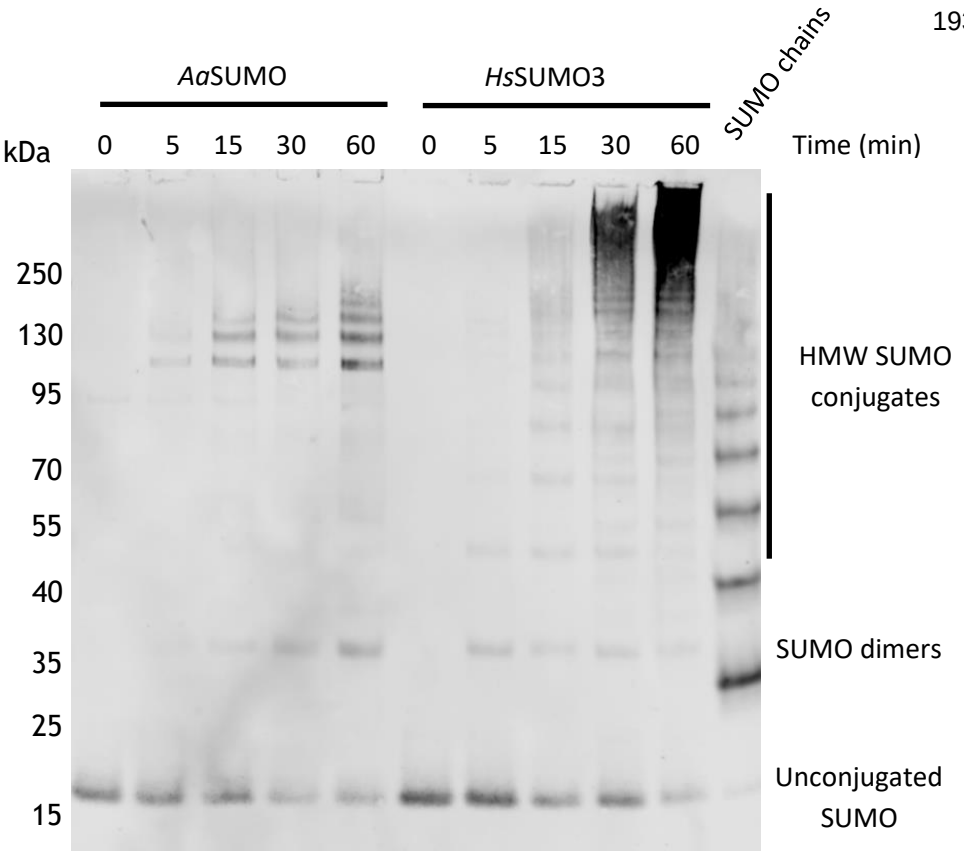

B

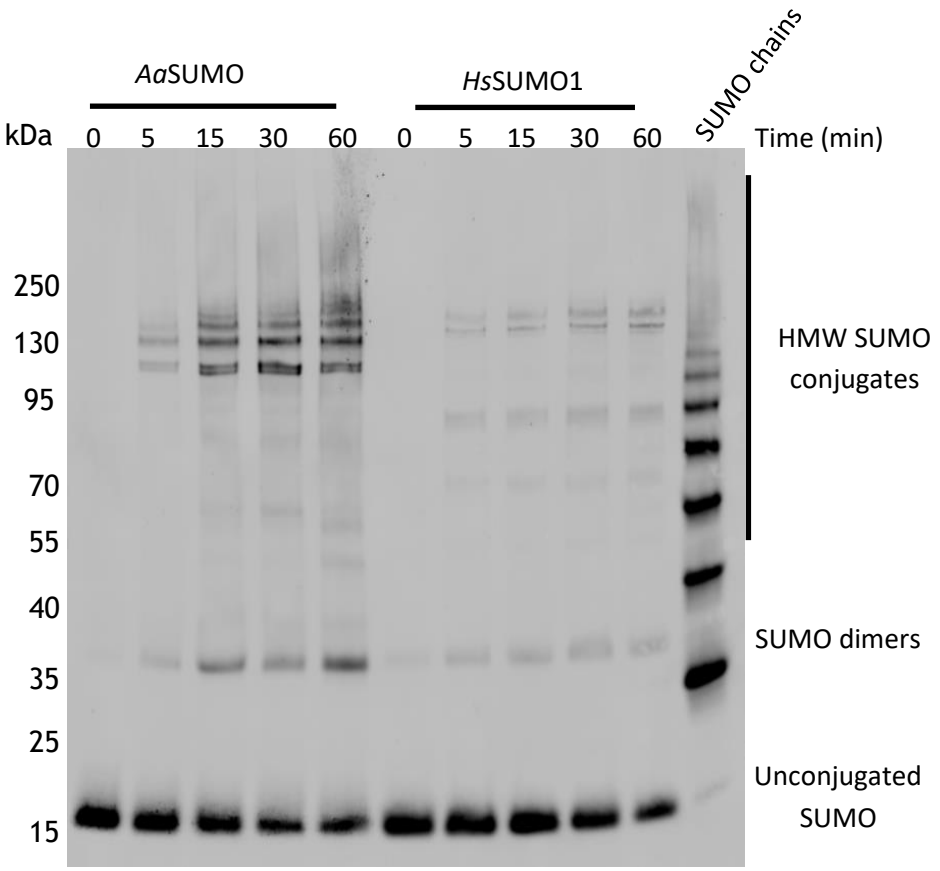

Continued on next page

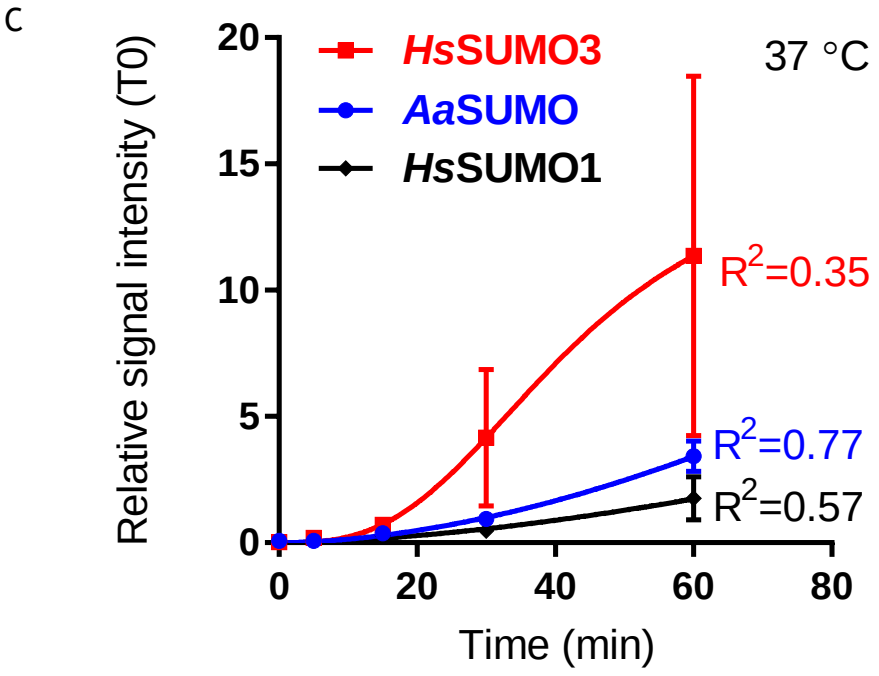

Figure 4.5 Comparison of *Aa* and *Hs* SUMOylation pathways activity at 37 ˚C

Biochemical reactions comparing the activity of 50 ng SUMO, SAE1/2, and Ubc9 from the *Aa* and *Hs* SUMOylation pathways were incubated together at 37 ˚C prior to the reaction being terminated after the specified periods of time. (**A**) Comparison of the build-up of SUMO-SUMO dimers and HMW SUMO conjugates of either *Aa*SUMO or *Hs*SUMO3. Commercial poly-SUMO2 chains were also included to indicate sizes of SUMO chains. An antibody to *Hs*SUMO2/3 was used to probe for *Aa* and *Hs*SUMO3 expression. (**B**) Comparison of the build-up of either *Aa*SUMO or *Hs*SUMO1 conjugates. Commercial poly-SUMO2 chains were also included to indicate sizes of SUMO chains. Antibodies to *Hs*SUMO2/3 and *Hs*SUMO1 were utilised to probe for *Hs*SUMO1 and *Aa*SUMO expression over time. (**C**) Graphical view of the build-up of SUMO-SUMO dimers and HMW SUMO conjugates from both (**A**) and (**B**) signal intensity quantified using a LiCor. Curve is Specific binding with hill slope nonlinear fit of data, mean, standard error, and R^2 values shown, produced with GraphPad Prism 7.02. N≥3.

4.3.3. A chimaeric SUMO protein efficiently forms HMW SUMO conjugates

This work has demonstrated a biochemical difference between the *Aa*SUMO protein and *Hs*SUMO3 utilising a combination of both bioinformatics and biochemical assays (**Section 3.2.1; Section 4.3.2**). The lack of efficient *Aa*SUMO poly-SUMO chain formation was hypothesised to be due to the lack of an internal SCM in *Aa*SUMO. A chimaeric SUMO protein was synthesised made from the N-terminal of *Hs*SUMO3 and the C-terminal of *Aa*SUMO. The N-terminal of the chimaeric protein consisted of the sequence MSEEKPKEGVKTEN, from *Hs*SUMO3, containing the SCM VKTE (shown in aqua). The C-terminal consisted of amino acid residues 14-91 from *Aa*SUMO. This resulted in a SUMO protein which could efficiently form poly-SUMO chains. A mutant chimaeric SUMO protein was also synthesised and purified which contained a K11R mutation, ablating the internal SCM (**Figure 4.6A**). This ensured *Aa*SUMO possessed the SCM and a control which cannot efficiently form poly-SUMO chains.

A similar biochemical experiment was set up utilising 50 ng chimaeric or K11R mutant SUMO protein, 50 ng Ubc9, and 50 ng SAE1/2. The samples were resolved on an SDS-PAGE gel, and probed with an antibody to *Hs*SUMO2/3 (**Figure 4.6B**). As demonstrated, the chimaeric SUMO formed HMW SUMO conjugates more efficiently than the K11R mutant chimaera. The signal intensity was quantified, normalised to the concentration of unconjugated SUMO at T0. The resulting graph demonstrates that the SUMO chimaera formed HMW conjugates far more efficiently than the SUMO chimaera K11R mutant, due to the presence of the lysine within the SCM (**Figure 4.6C**).

Together, these data demonstrate that a K11 within an SCM is necessary for the efficient formation of poly-*Aa*SUMO chains.

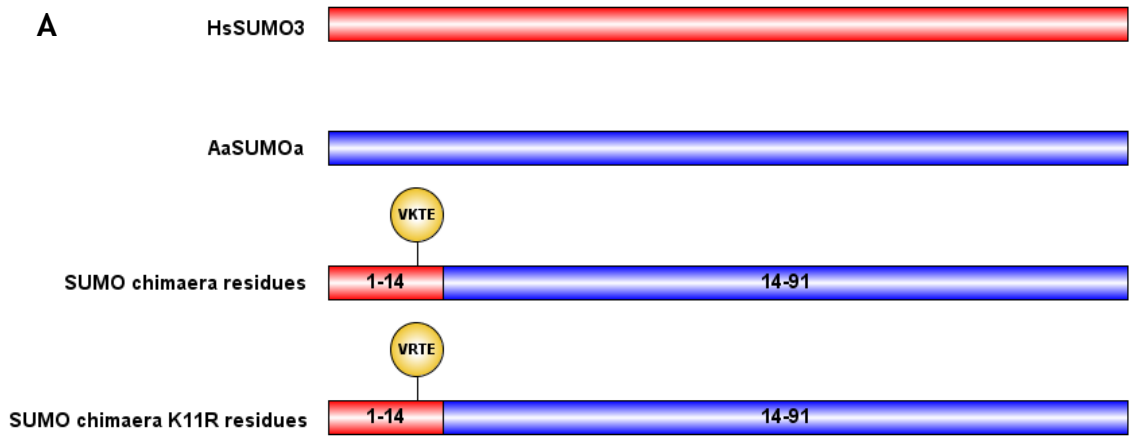

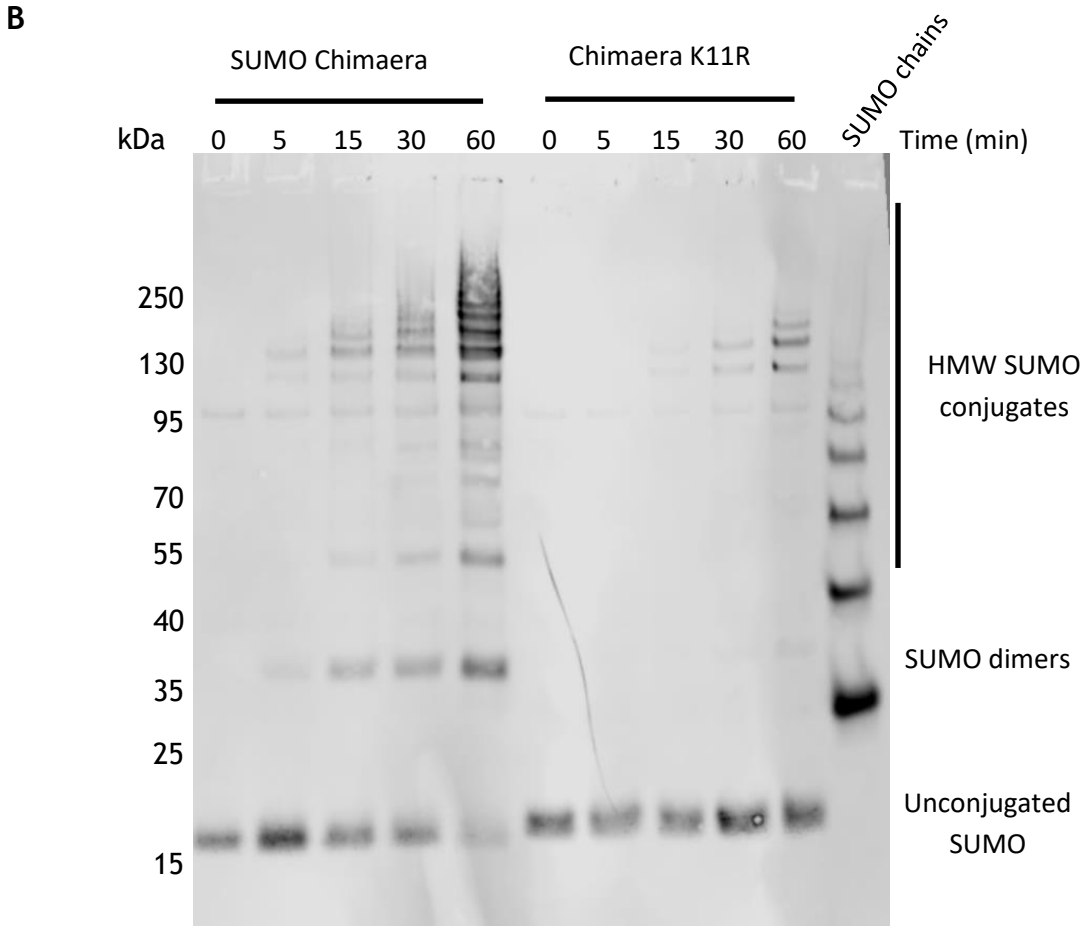

Continued on next page

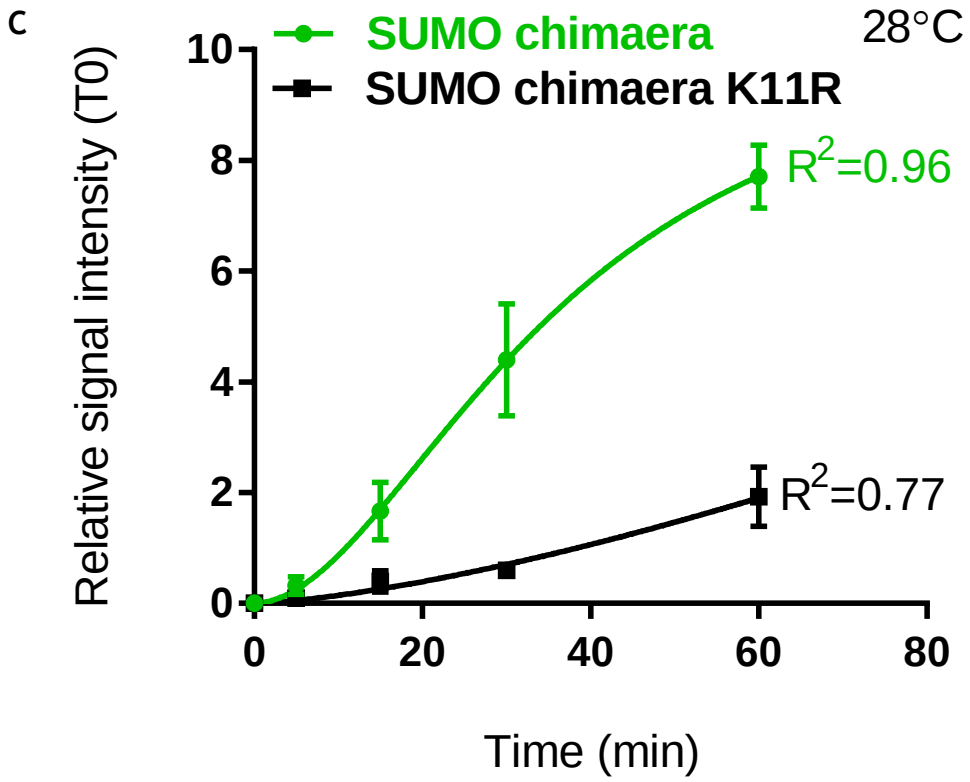

Figure 4.6 Comparison of SUMO chimaera with a K11R chimaera mutant

Biochemical reactions comparing the activity of 50 ng SUMO chimaera, SUMO chimaera K11R, SAE1/2, and Ubc9 from the *Aa*SUMOylation pathway was incubated together at 28 ˚C prior to the reaction being terminated after the specified periods of time. (**A**) A schematic of the SUMO chimaera, and SUMO chimaera K11R mutant which demonstrates what the protein is made from and where the K11R mutation is. (**B**) Comparison of the build-up of SUMO-SUMO dimers and HMW SUMO conjugates when the SUMO chimaera was used compared to the SUMO chimaera K11R mutant at time points indicated post initiation of reaction. An antibody to *Hs*SUMO2/3 was used to probe for SUMO expression. Commercial poly-SUMO2 chains were also included to indicate sizes of SUMO chains. Molecular mass markers are shown. (**C**) Signal intensity of SUMO conjugates from (**B**) was detected with a LiCor, normalised to unconjugated SUMO at T0. Mean results were plotted on a graph with standard error bars, n≥3, nonlinear fit of data was plotted as Specific binding with hill slope with R^2 values shown produced with GraphPad Prism 7.02.

4.3.4. *Aa*PIAS enhances rate of HMW SUMO conjugate formation

In *H. sapiens*, the family of PIAS proteins are well reported to efficiently increase the rate of poly-SUMO chain formation (Eisenhardt, Chaugule et al. 2015). This is due to the catalytically active SP-RING domain. *Aa*PIAS shares a relatively well conserved SP-RING domain and a conserved catalytically active Cys^{371} (**Section 3.2.4).** Consequently, we sought to identify if PIAS shared a similar biochemical function in the SUMOylation pathway of *Ae. aegypti* as in *H. sapiens*. Wild type and catalytically inactive mutant *Aa*PIAS (*Aa*PIAS C371A; CA) were cloned into a bacterial expression vector and purified (**Figure 4.2**). Upon addition of 10 ng of *Aa*PIAS or *Aa*PIAS C371A to the SUMOylation assay mixture at 28 ˚C, there was a rapid build-up of HMW SUMO conjugates in a SP-RING dependent manner (**Figure 4.7A**). Assays were quantified and plotted (**Figure 4.7B**). These data demonstrate that biochemically active *Aa*PIAS is required to efficiently form poly-*Aa*SUMO chains *in vitro*.

Equivalent reaction samples were sent for mass spectrometry analysis by collaborators at the University of Dundee (**Section 2.2.3.1; Figure 4.8A**). Mass spectrometry analysis revealed that every *Aa*SUMOa lysine residue can act as an acceptor site for SUMO modification *in vitro* (**Figure 4.8B**), with the most prominent lysine residues being K5/6/9/40 (**Figure 4.8C**). These residues are predominantly located around the N-terminus of *Aa*SUMO (**Figure 4.8D**). Further analysis of the effect of *Aa*PIAS on the formation of SUMO dimers or poly-SUMO chains indicated that *Aa*PIAS does not appear to influence acceptor site preference (**Figure 4.8E**), but rather rate of accumulation (**Figure 4.7A**).

Together this demonstrates that *Aa*SUMO is capable of forming poly-SUMO chains, but it only efficiently occurs in the presence of an *Aa*PIAS. This could potentially indicate an additional level of regulation on the formation of poly-SUMO chains in *Ae. aegypti*, compared to *H. sapiens*. Although the formation of poly-SUMO chains in *Ae. aegypti* mosquitoes has not been investigated, and the potential biological effects of poly-SUMO chain formation indicates an exciting new avenue of research.

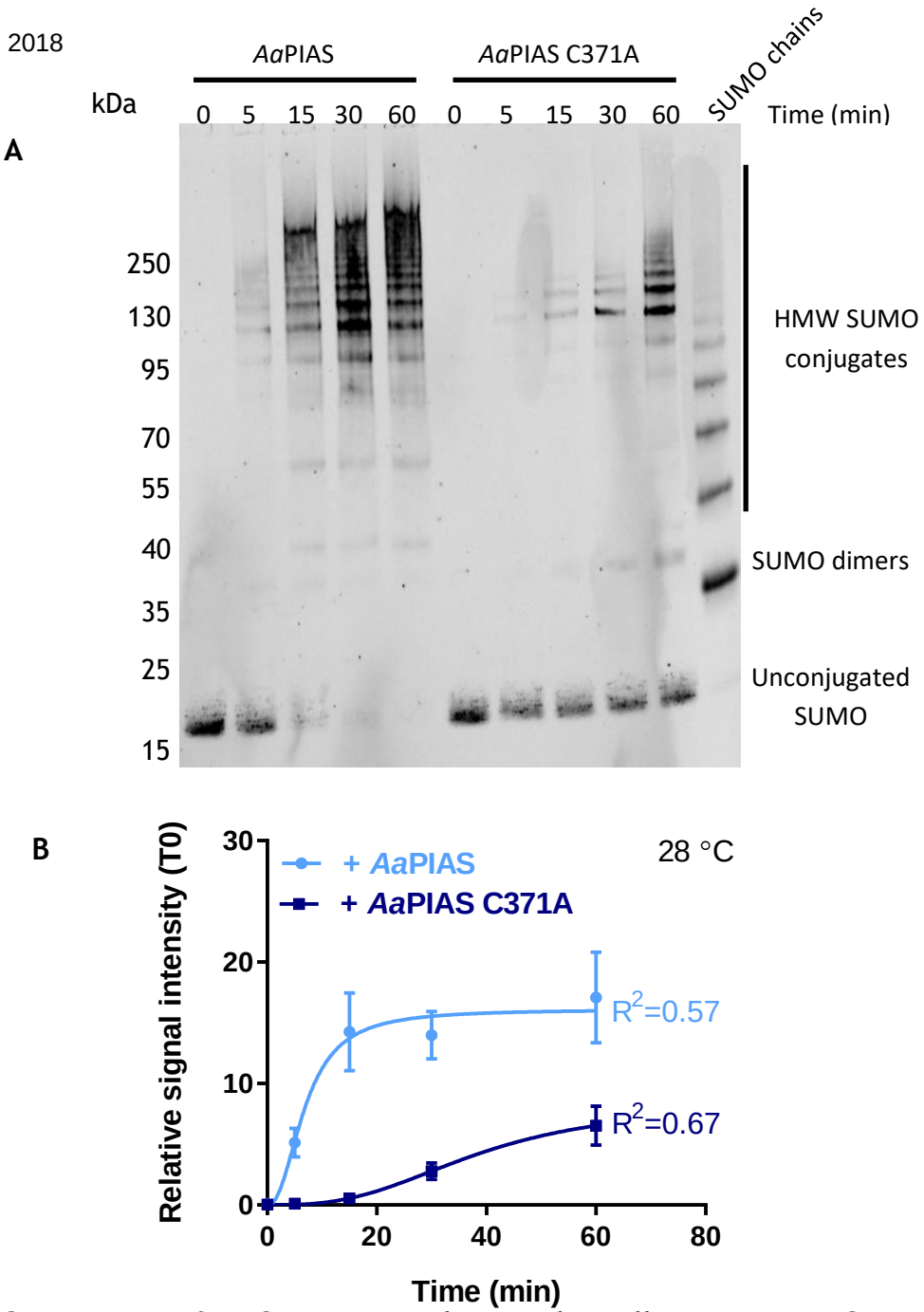

Figure 4.7 Comparison of PIAS activity with a catalytically inactive PIAS mutant

Biochemical reactions comparing the activity of 50 ng SUMO, SAE1/2, Ubc9, and 10 ng *Aa*PIAS or *Aa*PIAS C371A from the *Aa*SUMOylation pathway was incubated together at 28 ˚C prior to the reaction being terminated after the specified periods of time. (**A**) A representative biochemical assay demonstrating the difference in the build-up of HMW SUMO conjugates when the *Aa*PIAS was used against the *Aa*PIAS C371A mutant at time points of 0, 5, 15, 30, or 60 minutes post initiation of the reaction at 28 ˚C. Membranes were probed with an antibody to *H. sapiens* SUMO2/3 for expression of SUMO. Commercial poly-SUMO2 chains were also included to indicate sizes of SUMO chains. Molecular weight is indicated. (**B**) Signal intensity of SUMO-SUMO dimers and HMW SUMO conjugates from (**A**) was quantified with a LiCor, normalised to unconjugated SUMO at T0. Mean of n≥3 repeats calculated and plotted as a nonlinear curve with specific binding with hill slope by Graphpad Prism 7.02, with standard error and R^2 values indicated.

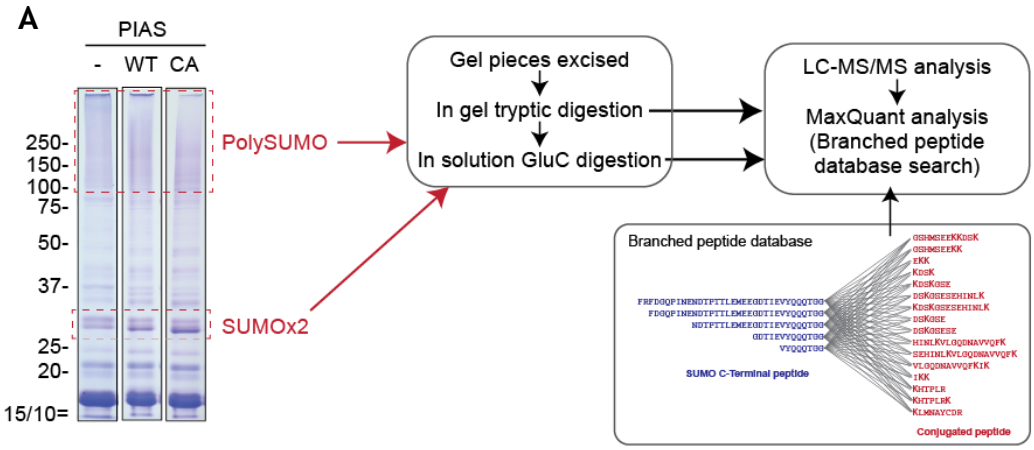

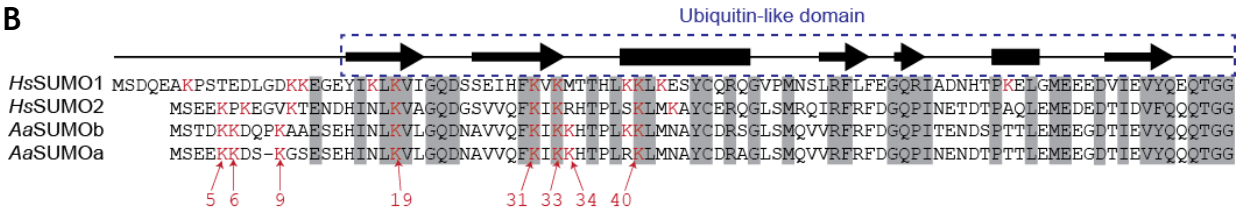

C

	K5	K6	K9	K19	K31	K33	K34	K40
Total branched peptide intensity	$8.72x10^9$	$5.28x10^9$	$4.94x10^9$	$0.14x10^9$	$0.30x10^9$	$3.46x10^9$	$0.16x10^9$	$11.99x10^9$
Number of branched peptide evidences	6	5	8	2	1	4	3	5
Average Andromeda score	120.26	158.21	119.04	89.80	105.28	137.91	88.97	138.86

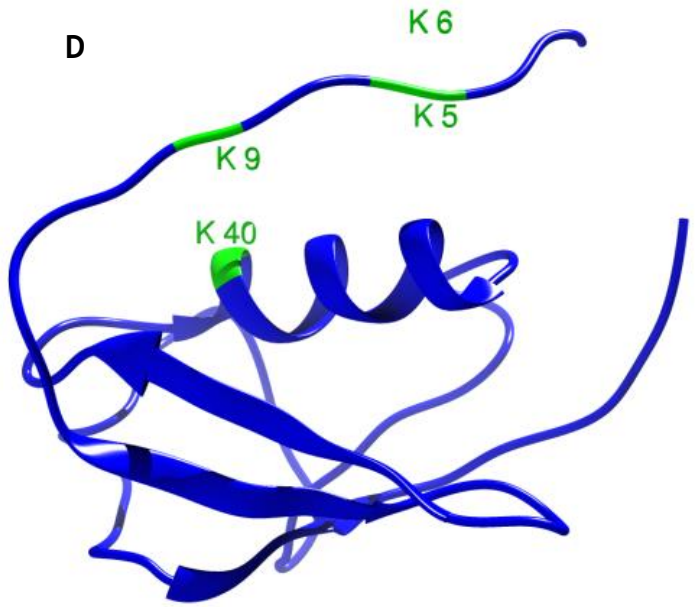

Continued on next page

E

	% Total branched peptide intensity by slice							
	K5	K6	K9	K19	K31	K33	K34	K40
No PIAS (SUMOx2)	17	19	9	0	0	8	0	47
No PIAS (PolySUMO)	20	16	2	0	0	8	0	54
WT PIAS (SUMOx2)	22	17	5	2	0	16	0	37
WT PIAS (PolySUMO)	29	12	16	0	1	10	1	30
CA PIAS (SUMOx2)	16	23	16	1	0	7	0	37
CA PIAS (PolySUMO)	9	30	23	0	0	12	0	25

Figure 4.8 Mass spectrometry analysis reveals which lysine's SUMO is binding to.

Biochemical assays were conducted prior to being sent to collaborators at the University of Dundee for analysis by mass spectrometry. (**A**) Coomassie gel showing *in vitro* conjugation assay products from reactions either lacking *Aa*PIAS (-) or including an active (WT) or inactive (CA) *Aa*PIAS. Schematic that explains the sample processing and mass spectrometry analysis using a branched peptide database. (**B**) Sequence alignment of the *Ae. aegypti* and *H. sapiens* SUMO orthologues. Sequence identity is shown by grey boxes and SUMO-1 secondary structure shown above with arrow showing strands, and box showing helices. The ubiquitin-like domain is indicated by the broken blue box. *Aa*SUMOa lysine residues are shown in red and the position indicated. (**C**) Summary of mass spectrometry data associated with identified SUMO-SUMO branched peptides from the samples shown in (**A**). Data are aggregated for all samples and separated by lysine acceptor. (**D**) A model of the *Aa*SUMOa protein with the lysine residues which are most likely to be SUMO modified, as identified in (**C**) indicated. (**E**) Slice-specific peptide intensity data separated by lysine acceptor. Data are % total intensity of all branched peptides found in each slice.

4.4. Biochemical activity of the pathways is conserved between species

As the orthologous proteins are well conserved at an amino acid and structural level, we hypothesised that the biochemical activity of the proteins should be sufficiently conserved to enable the individual *Ae. aegypti* SUMOylation proteins to substitute for *H. sapiens* SUMOylation pathway constituent proteins. If so, this would demonstrate that the proteins share a high degree of biochemical conservation as well. The assays were conducted at 37 ˚C as described in **Section 2.2.3.1**.

4.4.1. *Aa*SUMO can be utilised by the *Hs*SUMOylation pathway

*Aa*SUMOa shares 68% amino acid identity with *Hs*SUMO2, and possesses a similar tertiary structure (**Section 3.2.1**). In order to determine if *Aa*SUMO is capable of being conjugated by the *Hs*SUMOylation pathway, 100 ng SAE1/2, 100 ng Ubc9, and 300 ng either *Aa*SUMO, or *Hs*SUMO2 were incubated together. Additional samples were also included which lacked either SUMO, or *Hs*Ubc9, to demonstrate that the HMW bands represent genuine SUMO conjugates. The samples were terminated at the specified times, resolved by SDS-PAGE, and the gel was Coomassie stained (**Figure 4.9**). This analysis revealed that *Aa*SUMO can be utilised by the *Hs*SUMOylation machinery, to be conjugated to the GST-*Hs*SAE2, although conjugation of *Aa*SUMO does not appear to be as efficient as *Hs*SUMO2. This is likely explained by the lack of SCM on *Aa*SUMO, as previously described (**Section 4.3.2; Section 4.3.3**).

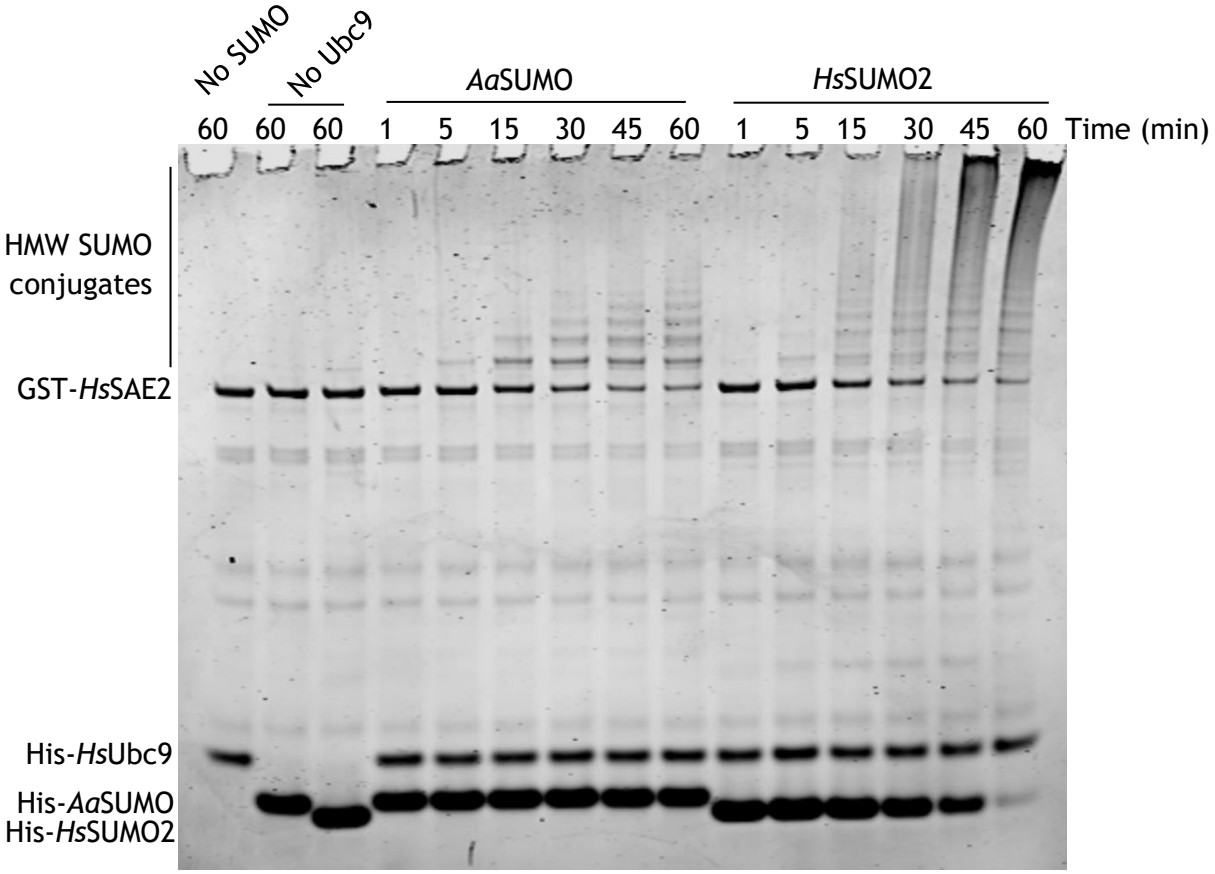

Figure 4.9 *Aa*SUMO is biochemically active with *Hs*SUMOylation machinery

100 ng *Hs*Ubc9, 100 ng *Hs*SAE1/2, and 300 ng either *Aa*SUMO or *Hs*SUMO2 were incubated together at 37 ˚C for varying lengths of time. Samples including no SUMO or no Ubc9 were included as controls. The reaction was terminated and the samples were resolved on an SDS-PAGE gel. The gel was stained by Coomassie and demonstrates that over time there is a build-up of HMW SUMO conjugates when *Aa*SUMO was incubated. This shows that the *Aa*SUMO protein is functionally interchangeable with *Hs*SUMO. N=2.

4.4.2. *Aa*Ubc9 can be utilised in the *Hs*SUMOylation pathway with *Hs*SUMO2

*Aa*Ubc9 shares 85% amino acid identity with *Hs*Ubc9, a conserved active site (C93), and a conserved tertiary structure (**Figure 3.2**). As a consequence, it was hypothesised that *Aa*Ubc9 should be able to efficiently conjugate *Hs*SUMO2 after activation by *Hs*SAE1/2. The biochemical conservation of *Aa*Ubc9 was tested against *Hs*Ubc9, to determine if *Aa*Ubc9 is able to be substituted for *Hs*Ubc9 in the *Hs*SUMOylation pathway. An experiment utilising 300 ng *Hs*SUMO2, 100 ng *Hs*SAE1/2, and either 100 ng *Aa*Ubc9 or *Hs*Ubc9 was set up, the reactions were terminated at the times stated, samples were then resolved by SDS-PAGE, and Coomassie stained. *Aa*Ubc9 was found to be capable of efficiently conjugating *Hs*SUMO2 to GST-*Hs*SAE2 (**Figure 4.10**).

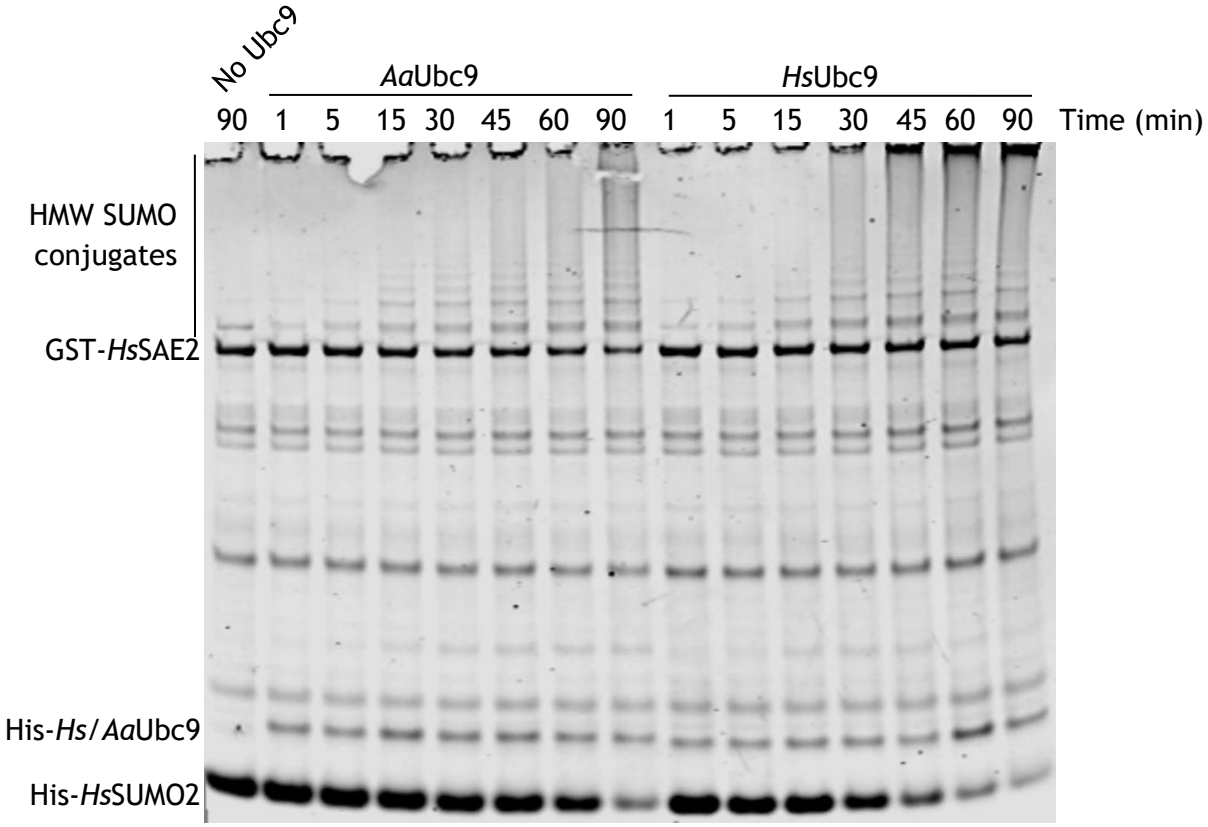

Figure 4.10 *Aa*Ubc9 is biochemically active with *Hs*SUMOylation machinery

300 ng *Hs*SUMO2, 100 ng *Hs*SAE1/2, and 100 ng either *Aa*Ubc9 or *Hs*Ubc9 were incubated together at 37 ˚C for varying lengths of time. A sample including no Ubc9 was included as a control. The reaction was terminated and the samples were resolved on an SDS-PAGE gel. The gel was stained by Coomassie and demonstrates that over time there is a build-up of HMW SUMO2 conjugates when *Aa*Ubc9 was incubated. This shows that *Aa*Ubc9 is functionally interchangeable with *Hs*Ubc9. N=2.

4.4.3. *Aa*SAE1/2 utilise in *Hs*SUMOylation pathway

Due to the relatively low degree of amino acid identity between *Hs*SAE1/2 and *Aa*SAE1/2 (50% and 42%, for SAE1 and SAE2 respectively) compared to the rest of the SUMOylation pathway (**Section 3.2.3**), it was unlikely that *Aa*SAE1/2 would work to the same efficiency as *Hs*SAE1/2 when used in the *Hs*SUMOylation pathway. However, the active Cys^{173} is still conserved (**Appendix A: Amino acid sequence comparison between *Hs* and *AaSAE1*/2, and *Hs* and *AaPIAS***), and the tertiary structure of the proteins is also well conserved (**Section 3.2.3**), therefore it was hypothesised that *Aa*SAE1/2 could still activate *Hs*SUMO orthologues. An experiment utilising either 100 ng *Aa*SAE1/2 or *Hs*SAE1/2, with 300 ng *Hs*SUMO2, and 100 ng *Hs*Ubc9 was conducted and terminated at specified times. The samples were then resolved by SDS-PAGE, and Coomassie stained. The results reveal that *Aa*SAE1/2 is capable of activating *Hs*SUMO2 that *Aa*SAE2 can act as a substrate for *Hs*SUMO2 modification (**Figure 4.11**).

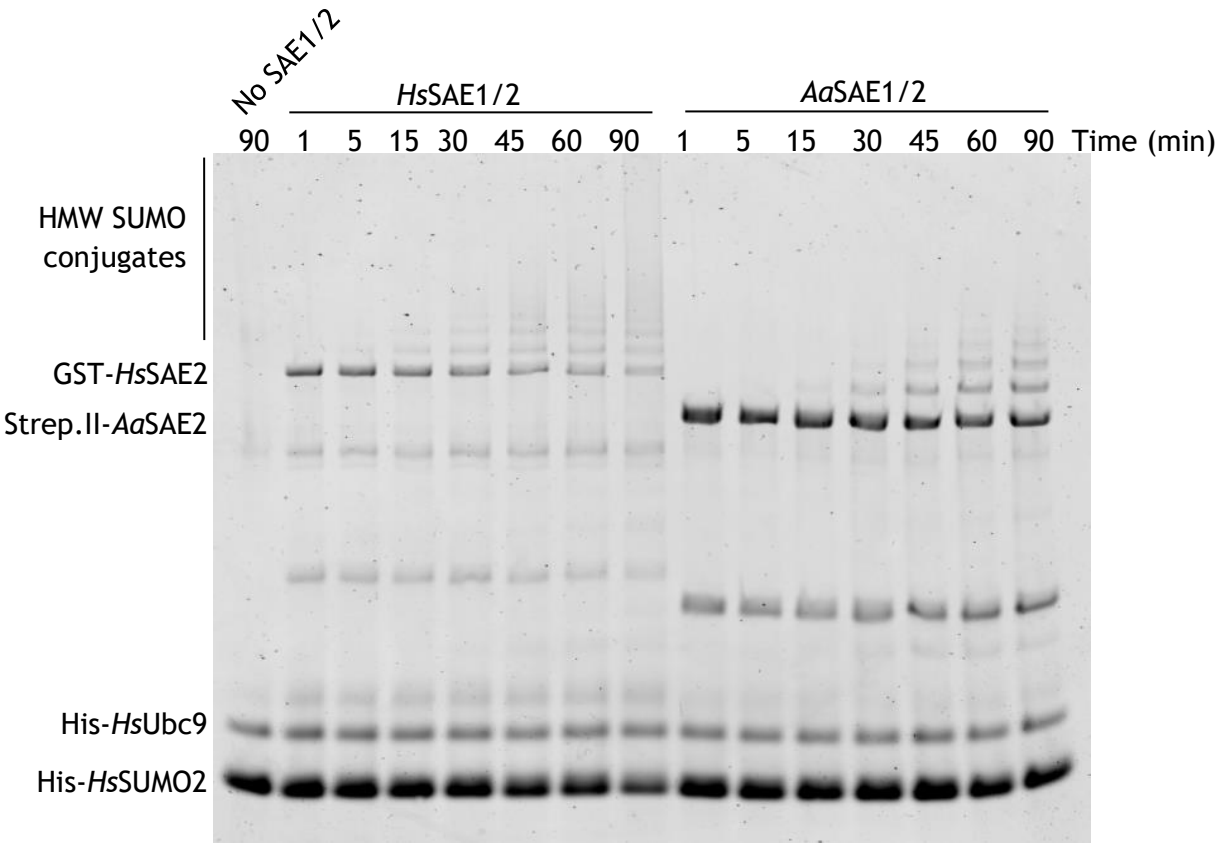

Figure 4.11 *Aa*SAE1/2 is biochemically active with *Hs*SUMOylation machinery

300 ng *Hs*SUMO2, 100 ng *Hs*Ubc9, and 100 ng either *Aa*SAE1/2 or *Hs*SAE1/2 were incubated together at 37 ˚C for varying lengths of time. A sample including no SAE1/2 was included as a control. The reaction was terminated and the samples were resolved on an SDS-PAGE gel. The gel was stained by Coomassie and demonstrates that over time there is a build-up of HMW SUMO2 conjugates when *Aa*SAE1/2 was incubated. This shows that the *Aa*SAE1/2 heterodimer is functionally interchangeable with the *Hs*SAE1/2 heterodimer. N=1.

4.4.4. *Aa*PIAS can enhance rate of *Hs*SUMO3 chain formation

*Aa*PIAS was also tested for its ability to be utilised by the *Hs*SUMOylation pathway. As described in **Section 3.2.4**, *Aa*PIAS only shares 32% - 37% amino acid identity with the orthologous proteins, however, the SP-RING domain does share a higher degree of amino acid identity (between 65% - 70%). The activity of *Aa*PIAS was tested against the activity of the catalytically inactive mutant. The experiment was conducted with 300 ng *Hs*SUMO2, 100 ng *Hs*Ubc9, 100 ng *Hs*SAE1/2 and either 20 ng *Aa*PIAS, or *Aa*PIAS C371A. Reactions were terminated at the specified times, resolved by SDS-PAGE, and Coomassie stained. *Aa*PIAS can be seen to efficiently form HMW conjugates, compared to *Aa*PIAS C371A, while utilising *Hs*SAE1/2, *Hs*Ubc9, and *Hs*SUMO2 (**Figure 4.12**). Within 15 minutes, the E3 ligase activity of *Aa*PIAS efficiently forms a build-up of HMW SUMO conjugates indicative of poly-SUMO chain formation. In the absence of a catalytically functional SP-RING domain, the same build-up of HMW SUMO conjugates is not present until the 90 minute time point. This also demonstrates that even though the overall amino acid identity between *Aa*PIAS and the *H. sapiens* orthologues is 32% - 37%, *Aa*PIAS is still able to interact with *Hs*SUMO2, *Hs*Ubc9, and *Hs*SAE2.

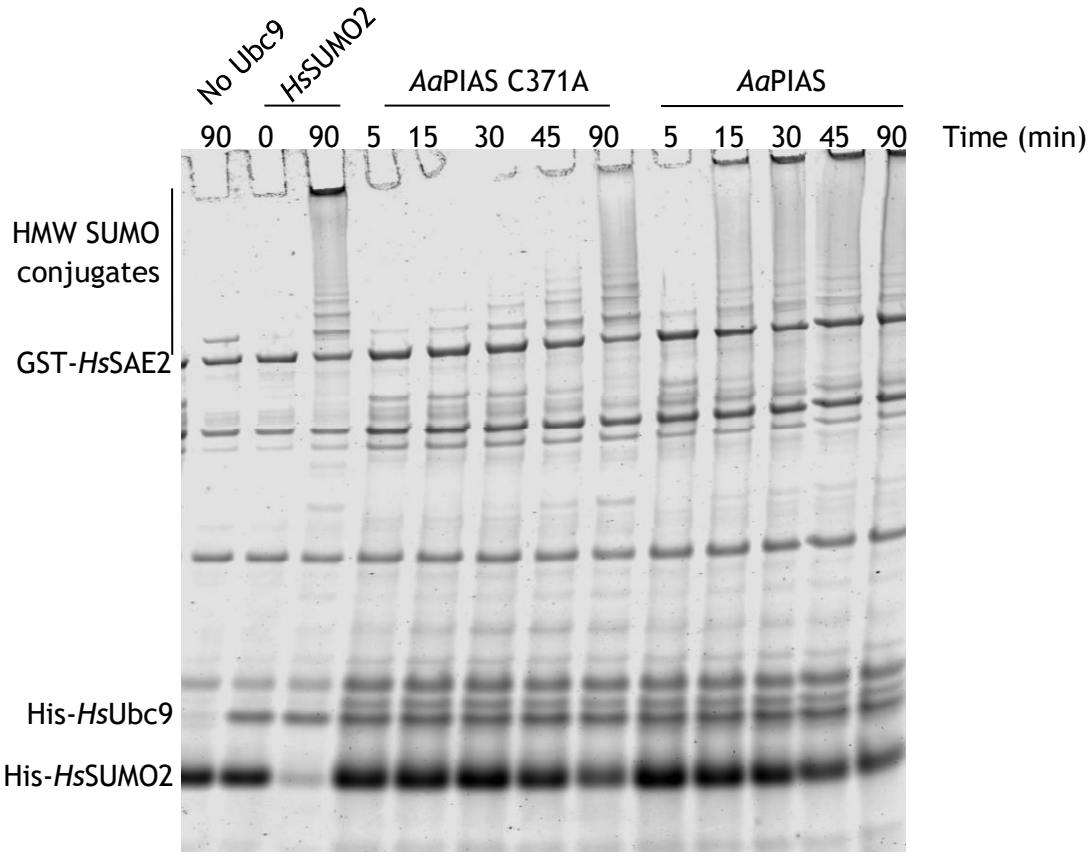

Figure 4.12 *Aa*PIAS is biochemically active with *Hs*SUMOylation machinery

300 ng *Hs*SUMO2, 100 ng *Hs*Ubc9, 100 ng *Hs*SAE1/2 and either 20 ng *Aa*PIAS, or *Aa*PIAS C371A, were incubated together at 37 ˚C for varying lengths of time. Samples including no Ubc9 and no PAIS were included as controls. The reaction was terminated and the samples were resolved on an SDS-PAGE gel. The gel was stained by Coomassie. This demonstrates that a functional SP-RING domain results in an efficient increase in HMW *Hs*SUMO2 conjugates. N=1.

4.5. Discussion

Protein modification by the SUMOylation pathway is known to have a wide variety of important biological functions in many species of eukaryotes. A large body of work has been produced in *H. sapiens* demonstrating the effect of mono- or poly-SUMO modification. Likewise, there has been a large body of work conducted in yeast (*Saccharomyces cerevisiae*; *S. cerevisiae*) and in *D. melanogaster*. This work has revealed important functions of SUMO modification, including protein sub-cellular localisation and protein stability (Desterro, Rodriguez et al. 1998, Miteva, Keusekotten et al. 2010).

It is well known that in the *Hs*SUMOylation pathway, Ubc9 forms a thioester bond with SUMO through the Sulphur atom in the R group of the cysteine amino acid (Tatham, Chen et al. 2003, Tatham, Kim et al. 2003). It was hypothesised that *Aa*Ubc9 would also form a thioester bond with SUMO, due to the conserved active site (C^{93}); a mutant which is incapable of forming thioester bonds was also purified as a control (**Appendix C: Purified *AaUbc9* C93S, the SUMO chimaera, and the SUMO chimaera K11**). As *Aa*Ubc9 encodes a Glutamic acid (E^{100}) instead of an Aspartic acid (D^{100}), we expected the rate of *Aa*Ubc9~SUMO formation to be up to 1.3-fold greater than *Hs*Ubc9~SUMO (Tatham, Chen et al. 2003). However, these results demonstrate that the C93 in *Aa*Ubc9 does form thioester bonds with SUMO at a comparable rate to *Hs*Ubc9 irrespective of the presence of E^{100} instead of D^{100} (**Section 4.3.1**). This is likely due to the similarity between the structure of Aspartic acid and Glutamic acid resulting in a predominantly similar phenotype.

As *Aa*SUMO is lacking an internal SCM, it was hypothesised it should not be able to efficiently form poly-SUMO chains (**Section 3.2.1**). Utilising the recombinant proteins described in **Section 4.2**, the ability of *Aa*SUMO to form poly-SUMO chains in an *in vitro* assay was assessed. When comparing the build-up of HMW SUMO conjugates between the *Aa*SUMOylation pathway and the *Hs*SUMOylation pathway, there are a range of similarities and differences with both *Hs*SUMO1 and *Hs*SUMO3 (**Figure 4.4; Figure 4.5**). These results show that conducting the assay at either 28 ˚C or 37 ˚C have no effect on the activity of the *Aa*SUMOylation pathway; we also found that *Aa*SUMO and *Hs*SUMO1 / *Hs*SUMO3

all form SUMO-SUMO dimers within 5-15 minutes, and all SUMO orthologues studied are capable of SUMO modifying SAE2. SUMO modification of SAE2 has previously been reported to result in the localisation of SAE2 out of the nucleus, and altering enzyme activity (Truong, Lee et al. 2012, Truong, Lee et al. 2012). As *Aa*SAE2 also appears to be a substrate for SUMO modification, it seems likely that SUMO modification of *Aa*SAE2 results in a similar phenotype, although further studies would be needed to confirm this *in vivo*. There are also notable differences in the biochemical activity of *Aa*SUMO and *Hs*SUMO3, demonstrated in **Figure 4.4** and **Figure 4.5**. This includes the ability of *Hs*SUMO3 to efficiently form mid-tier SUMO chains, and the formation of a 'smear', typically indicative of poly-SUMO chains, at the top of the blot of HMW SUMO conjugates. The mid-tier and HMW chains are also both absent when *Hs*SUMO1 is utilised. Together, this demonstrates that the biochemical activity of *Aa*SUMO is more comparable to *Hs*SUMO1, compared to *Hs*SUMO3. This also demonstrates that *Aa*SUMO cannot efficiently form poly-SUMO chains at either 28 ˚C or 37 ˚C. Furthermore, as the rate of Ubc9~SUMO thioester bond formation is equivalent between species, it rules out a lack of poly-SUMO chain formation being due to different activity of Ubc9, and further implicates the lack of SCM in the inability to form poly-SUMO chains. SUMO1 has been reported to form chains on low affinity sites when large concentrations of Ubc9 are added *in vitro*, and it is possible that any poly-*Hs*SUMO1 chains, or poly-*Aa*SUMO chains formed in this assay could be due to the concentration of Ubc9 (Matic, van Hagen et al. 2008). This could be confirmed by titrating in lower concentrations of Ubc9 and performing mass spectrometry analysis to determine if one lysine is predominantly modified.

To confirm that the SCM would result in the formation of poly-SUMO chains, a chimaeric SUMO protein was produced and purified, which contained the SCM from *Hs*SUMO3, replacing the first 14 amino acids of the *Aa*SUMO protein, including the SCM (**Section 4.3.3**). The chimaeric SUMO formed chains of HMW SUMO conjugates more efficiently than a chimaeric mutant which contained a mutation in lysine 11 (K11R), the primary substrate for SUMO chain formation (Tatham, Jaffray et al. 2001). The chimaeric protein is capable of efficiently forming HMW SUMO conjugates when compared to the chimaera K11R (**Figure 4.6**). This shows that the lack of a lysine within an internal SCM prevents SUMO chains from efficiently forming in *Ae. aegypti*.

Upon addition of the E3 ligase, *Aa*PIAS, however, there was a rapid build-up of HMW SUMO chains forming (**Figure 4.7**). The activity of *Aa*PIAS was compared to *Aa*PIAS C371A, which clearly demonstrated a rapid increase in HMW SUMO conjugates forming. The SP-RING domain of PIAS proteins are widely known to be the catalytically active site for enhancing SUMO conjugation (Hochstrasser 2001, Hay 2005). This work demonstrates that the *Aa*SUMOylation pathway is capable of forming poly-*Aa*SUMO chains, but only when an *Aa*PIAS is available. This indicates that the important biological functions of poly-SUMO chains are also utilised in *Ae. aegypti*. Previous work by Urena, Pirone et al. (2016), on *Blattella germanica* (*B. germanica*) and *D. melanogaster* suggested that insect SUMO proteins could not form poly-SUMO chains. The evidence here indicates that *Aa*SUMO can form poly-SUMO chains *in vitro*, but requires the presence of an *Aa*PIAS for this to occur efficiently. The *in vitro* biochemical evidence Urena, Pirone et al. (2016) presented on *B. germanica* did not include the activity of a PIAS protein. They also found that ectopic expression of *Hs*SUMO3 had a deleterious effect on *D. melanogaster* development, which suggests that poly-SUMO chain formation is tightly regulated in insects. Further mass spectrometry analysis also indicates that *Aa*SUMO can form chains on any internal lysine, although chains are predominantly formed on K5/6/9/40. These lysine residues are all expected to be located on a readily accessible region of the N-terminal of the protein (**Figure 4.8**).

Previous studies have looked at the conservation of the SUMOylation pathway by ectopically expressing tagged Drosophila SUMOylation proteins in human cells, and determining that they could be conjugated to human proteins (Lehembre, Badenhorst et al. 2000). In this study, we sought to further characterise the conservation of the *Aa*- and *Hs*-SUMOylation pathways in an *in vitro* based assay. Much previous work on the biochemistry of the *H. sapiens* and *S. cerevisiae* SUMOylation pathways have been conducted using *in vitro* biochemical assays (Tatham, Jaffray et al. 2001, Bencsath, Podgorski et al. 2002, Yang, Campbell et al. 2018). It was hypothesised that due to the shared amino acid sequence, tertiary structure, and enzyme active sites, the biochemical function of the proteins should be conserved as well (**Section 3.2.1; Section 3.2.2; Section 3.2.3; Section 3.2.4**). Biochemical conservation could be observed by substituting the orthologous proteins, as previously demonstrated (Urena, Pirone

et al. 2016). Here, we have demonstrated *in vitro* that *Aa*SUMO, *Aa*Ubc9, *Aa*SAE1/2, or *Aa*PIAS can function as a substitute for their *H. sapiens* orthologues (**Figure 4.9; Figure 4.10; Figure 4.11; Figure 4.12**). For Ubc9 and SAE1/2, there appears to be a difference in the activity of the enzymes. This could be due to deviation between reactions as only one repeat was undertaken. Other causes could be due to the buffering conditions during protein purification, which were originally optimised for the *Hs*SUMOylation pathway. *Hs*Ubc9 and *Hs*SAE1/2 also evolved to activate and conjugate the *Hs*SUMO proteins, so a difference in the activity may be due to a lower affinity between *Aa*Ubc9 or *Aa*SAE1/2 with *Hs*SUMO. This could be further explored by investigating the activity of the *Hs*SUMO proteins, *Hs*Ubc9, or *Hs*SAE1/2, in the *Aa*SUMOylation pathway, experiments that there was not time to conduct here.

Other ways this work could be extended is by examining the functional phenotype of SENPs. Previous work in *S. cerevisiae* has indicated that SENPs have different roles in maturing SUMO or in deSUMOylating proteins (Di Bacco, Ouyang et al. 2006, Eckhoff and Dohmen 2015). Further studies could also be conducted to perform a poly-SUMO chain pull down on *Ae. aegypti* cell lysate, to determine if *Ae. aegypti* produce poly-SUMO chains *in vivo*. Mass spectrometry analysis could then be conducted to attempt to determine which proteins are modified by, or interact with poly-SUMO chains. Furthermore, confirming these phenotypes with recombinant and endogenous *Aa*SUMOb would help to demonstrate if *Aa*SUMOb is biochemically and biologically similar to *Aa*SUMOa, or if there are undiscovered roles for the two proteins.

5. *Aa*SUMOylation pathway suppresses arbovirus replication

5.1. Overview

The SUMOylation pathway is known to regulate the expression of a variety of genes, including those involved in cellular immunity in species ranging from *H. sapiens* to *D. melanogaster*. For instance, the immune proteins 14-3-3ε, Imd, and STAT92E have all been shown to be a substrate of SUMO modification in *D. melanogaster* (Handu, Kaduskar et al. 2015). The function of SUMO modification of these proteins has not yet been determined; however it is likely that SUMOylation of STAT92E suppresses the activation of STAT, in a similar mechanism to SUMOylation of *H. sapiens* STAT proteins. Due to the importance of SUMOylation in the regulation of immune pathways, the SUMOylation pathway is a prominent target for virus manipulation in order to restrict the immune response and promote replication from the outset of infection. Moreover, previous work with arboviruses in *H. sapiens* cells suggests that various components of the SUMOylation pathway interact directly with DENV proteins to the benefit or detriment of viral replication. Studies by Chiu, Shih et al. (2007) suggest that Ubc9 can SUMO modify the viral E protein at various lysine residues, although no biological function of this modification was determined. Over-expression of Ubc9 has also been shown to suppress DENV replication, indicating an antiviral role for Ubc9 during DENV infection (Chiu, Shih et al. 2007). This was supported by more recent studies by Feng, Deng et al. (2018) who depleted Ubc9 by siRNAs and found an increase in viral RNA expression (Feng, Deng et al. 2018). In contrast to this, studies by Su, Tseng et al. (2016) have shown that the N-terminal of DENV NS5 is a substrate for SUMO modification, which stabilizes NS5 to suppress induction of STAT2 antiviral signalling. Consequently, this study indicates a proviral role for SUMO modification during DENV infection (Su, Tseng et al. 2016). To date, no virology has been conducted on the effect of the SUMOylation pathway on arbovirus replication in *Ae. aegypti*.

This chapter aims to address the expression pattern of the *Aa*SUMOylation pathway in different organs and cells within *Ae. aegypti*, and to determine if there is a biologically functional requirement for the *Aa*SUMOylation pathway during arboviral replication. Previous studies have investigated the expression of the SUMOylation pattern in a range of tissues of multiple species by q-PCR analysis and microscopy studies (Bohren, Nadkarni et al. 2004, Hu and Chen

2013, Bocksberger, Karch et al. 2014, Liang, Lee et al. 2016). These studies have revealed different patterns of expression of SUMO in different organs of invertebrates. For instance, in the salivary glands of *D. melanogaster*, SUMO is predominantly nuclear, localising to the chromosome arms, chromocentre, and chromosome telomeres within the nucleus (Nie, Xie et al. 2009, Bocksberger, Karch et al. 2014). To our knowledge, no studies have investigated the expression of SUMO in *Ae. aegypti*. Consequently, q-PCR and microscopy studies were conducted to reveal the ubiquitous, but differential, expression of SUMO in different *Ae. aegypti* tissues. dsRNA was utilised to deplete mRNA transcripts encoding *SUMO*, *Ubc9*, *PIAS*, or *LacZ* as a non-target negative control. Arboviral infections were conducted with arboviruses encoding an internal luciferase reporter protein to measure any effect on viral replication, as conducted previously (Tamberg, Lulla et al. 2007, Dietrich, Shi et al. 2017, Royle, Donald et al. 2017). q-PCR analysis was done on viral genome to ensure luciferase expression correlated with viral replication, and depletion of the SUMOylation pathway was not altering viral translation. These studies were conducted in mosquitoes *in vivo*, to determine the effect of SUMO depletion on the replication of ZIKV, and *in vitro* with BUNV, SFV, and ZIKV. Together, these studies reveal that the *Aa*SUMOylation pathway has an overall suppressive effect on arbovirus replication in a virus-dependent manner.

Throughout this chapter, *in vivo* experiments were conducted by Floriane Almire and Dr Emilie Pondeville.

5.2. Expression of the *Aa*SUMOylation pathway

SYBR Green q-PCR was undertaken to determine the level of transcript expression of *Aa*SUMO, *Aa*Ubc9, and *Aa*PIAS relative to the carcass in four tissues known to support arboviral replication. The midgut is known to be the first barrier to arboviral replication, as it constitutes the first cells arboviruses need to establish replication in. Haemocytes, the mosquito immune cells, can transport the arbovirus around the mosquito once they are infected and are believed to be a key amplifying site for arboviruses. The ovaries are the site of replication essential for vertical transmission of the arbovirus, and the salivary glands are the site of replication prior to being injected into a new host (Hardy, Houk et al. 1983).

Dissection of the female adult mosquitoes was conducted by Floriane Almire and Dr Emilie Pondeville. RNA extraction, and cDNA synthesis was undertaken by F. Almire. Mosquitoes were non-blood fed prior to harvesting and analysis. Throughout the course of this chapter, the mosquito midgut is referred to as the gut. The term tissues are used to mean both perfused mosquito cells (haemocytes) and dissected mosquito organs (salivary glands, gut, and ovaries).

5.2.1. Q-PCR analysis shows the *Aa*SUMOylation pathway is differentially expressed in *Ae. aegypti* tissues

Q-PCR analysis was conducted to examine the expression of mRNA transcripts in the tissues mentioned. Primers were designed to *SUMO*, *Ubc9*, or *PIAS* and primers to the ribosomal *S7* gene were used as an endogenous control to standardise expression of the gene of interest across tissues (**Table 2-6**). Melt curves were conducted to ensure primer dimers were not interfering with the analysis (**Appendix E: Melt curve analysis of q-PCR primers**). Results were normalised to the carcass, material which consists of the abdomen after the gut and ovaries have been removed. The results show that *SUMO*, *Ubc9*, and *PIAS* mRNA are all expressed throughout these *Ae. aegypti* tissues. These results show that the SUMOylation pathway is expressed in the haemocytes and the ovaries,

as approximately 20-25 fold more *SUMO* mRNA is expressed compared to the carcass (**Figure 5.1**). *SUMO* mRNA expression in the gut and salivary glands is also greater than the carcass, but only by approximately 3–6 fold.

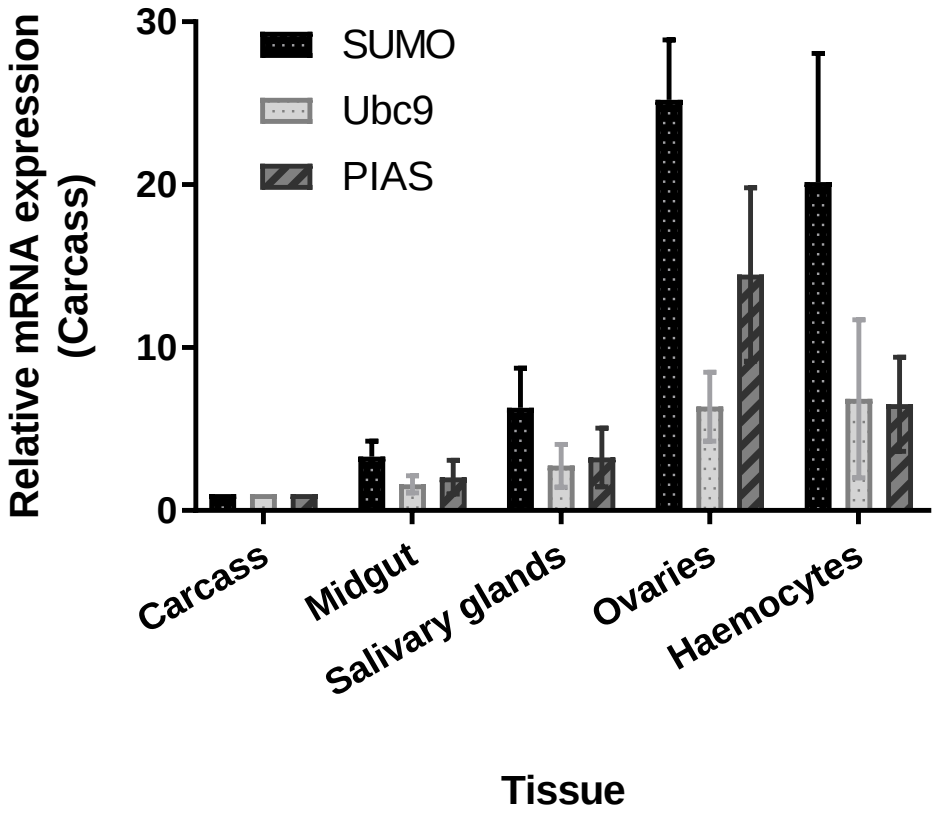

Figure 5.1 Q-PCR of SUMOylation pathway transcript expression in *Ae. aegypti* tissues

SYBR Green q-PCR was conducted on cDNA synthesised with random hexamers on RNA extracted from *Ae. aegypti* salivary glands, gut, ovaries, haemocytes, and carcass. Transcript expression of *SUMO*, *Ubc9*, and *PIAS* was examined. Levels of mRNA were normalised to ribosomal *S7*, using the threshold cycle (ΔΔCT) method and expressed relative to the carcass, which consists of the abdomen after the gut and ovaries have been removed. The results demonstrate the SUMOylation pathway is most abundantly expressed in the ovaries and haemocytes, but still have a higher level of expression in the salivary glands and gut relative to the carcass. Means of relative quantitation (RQ) and standard deviations (SD) shown, n=3, plotted with GraphPad Prism 7.02

5.2.2. *Aa*SUMO is expressed in all *Ae. aegypti* tissues studied

Confocal microscopy studies were conducted on the tissue samples. Here, DAPI stain is used to detect nucleic acids (blue), Phalloidin 488 stain is used to detect F-actin (green), and an antibody to SUMO2/3 are used to detect SUMO expression (red). Confocal microscopy was undertaken by Floriane Almire. Controls staining with no primary antibody were also performed for each replicate, where no signal was detected (**Appendix D: No primary antibody controls of SUMO expression in *Ae. aegypti* tissues**).

5.2.2.1. *Aa*SUMO is expressed in the haemocytes

Ae. aegypti haemocytes are known to be a key site of arboviral amplification within the vector species, and are therefore a crucial target for arboviral infection. Investigation into the expression of SUMO by confocal microscopy revealed that all forms of haemocytes studied express SUMO. Undifferentiated prohaemocytes (**Figure 5.2A**), and differentiated granulocytes (**Figure 5.2B**) both express SUMO in a predominantly punctate nuclear distribution. This punctate distribution is commonly found in *H. sapiens* cells due to extensive SUMO modification of PML nuclear bodies (PML-NB) (Kamitani, Nguyen et al. 1998).

AF5 cell culture was also assessed for SUMO expression. AF5 cells are derived from Aag2s, a larval *Ae. aegypti* haemocyte cell line (**Table 2-1**) (Barletta, Silva et al. 2012, Varjak, Maringer et al. 2017). These cells expressed a similar pattern of staining to the haemocytes isolated from *Ae. aegypti*, as punctate nuclear structures. Interestingly, these structures are more defined in AF5 cells than in the haemocytes. There was also some cells which did not express SUMO in nuclear punctate structures, these cells are likely to be expressing a diffuse nuclear staining pattern which was not detected under these conditions.

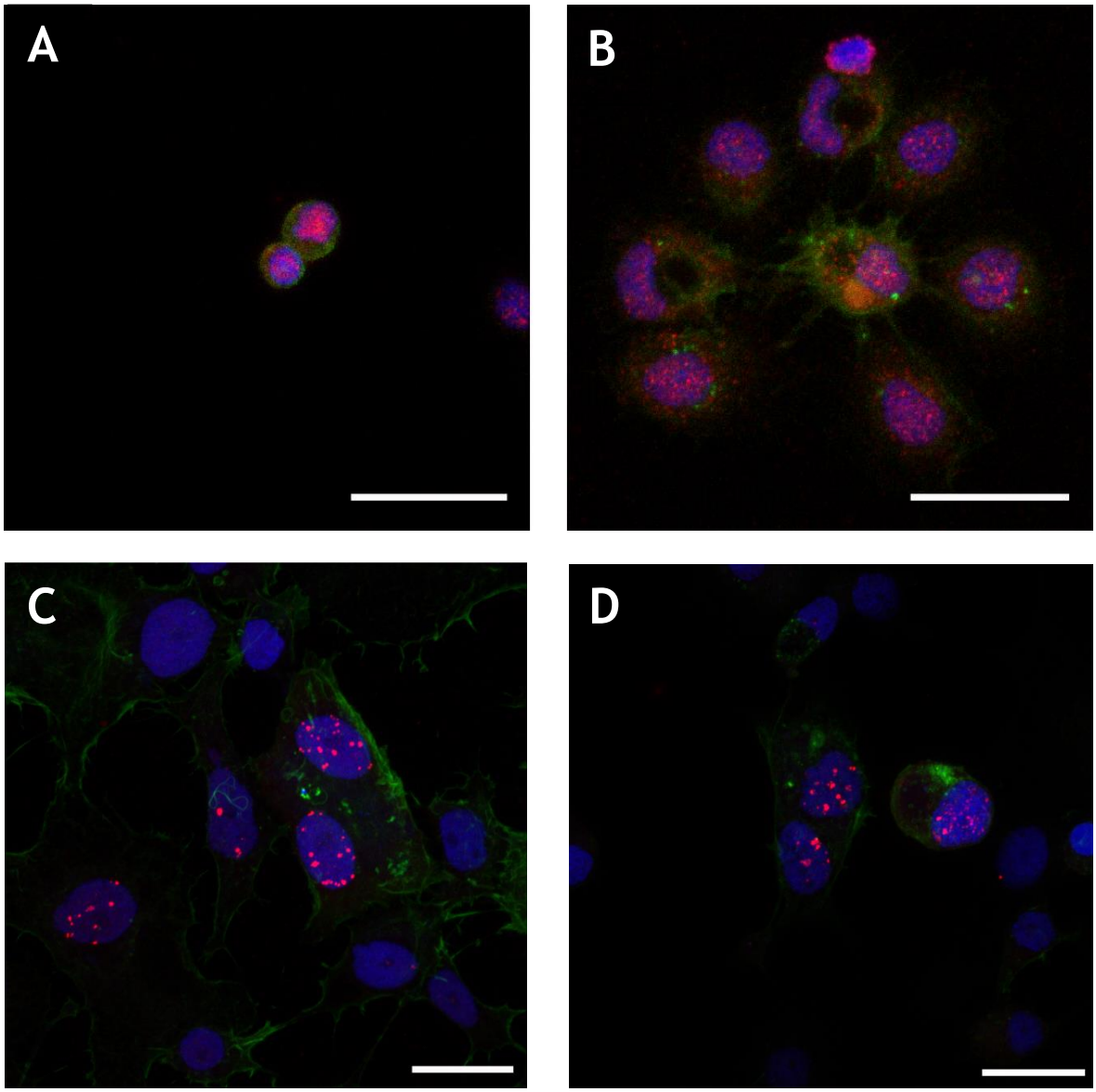

Figure 5.2 Confocal microscopy of SUMO expression in *Ae. aegypti* haemocytes

Haemocytes were extracted from adult *Ae. aegypti* and stained with DAPI (nuclei, in blue), phalloidin 488 (F-actin, in green), and αSUMO2/3 primary antibody (red). (**A**) Undifferentiated prohaemocytes and (**B**) differentiated granulocytes both displayed the greatest extent of SUMO staining within the nuclei. (**C, D**) $3x10^4$ AF5 cells were seeded in each well of an ibidi slide and incubated overnight. Images were taken on a Zeiss LSM 880 microscope with a 63X (**A** and **B**) or 40X (**C** and **D**) oil-immersion objective and are representative of n=≥3. Scale bar represents 20 μm.

5.2.2.2. *Aa*SUMO is expressed in the salivary glands

Ae. aegypti salivary glands are a key site for arboviral replication prior to infecting a naïve host. SUMO staining was therefore conducted on the salivary glands; however, the majority of the staining appears to be localised to fat bodies. The distal-lateral lobe (**Figure 5.3A**), proximal-lateral, and median lobe (**Figure 5.3B**) are imaged. Surrounding these organs are fat bodies (arrows), which express SUMO to the greatest levels.

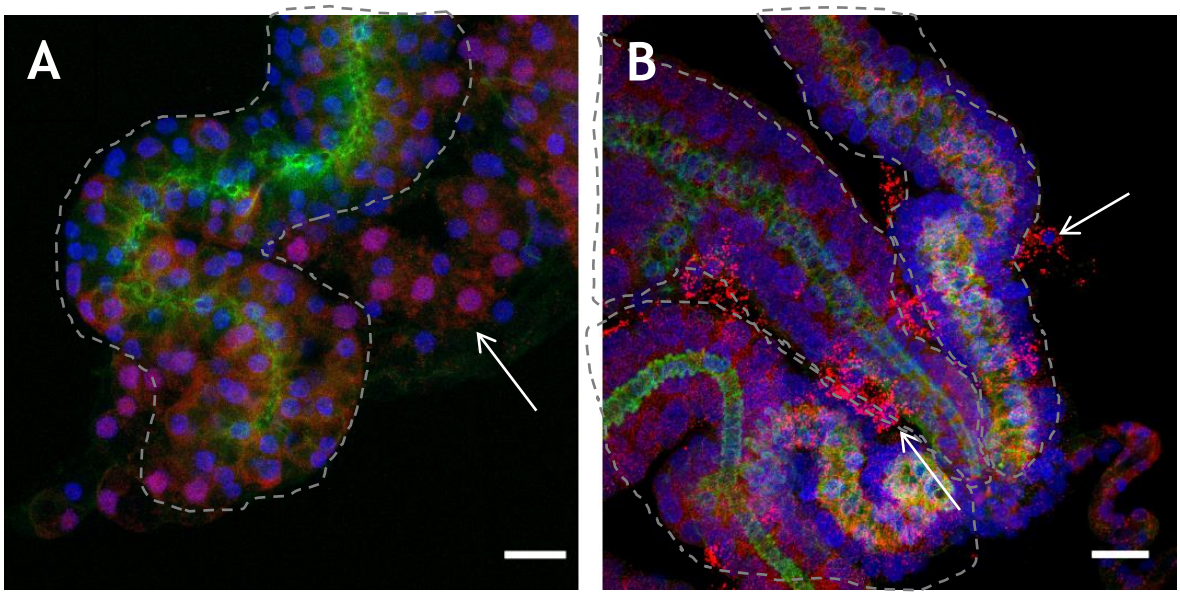

Figure 5.3 Confocal microscopy of SUMO expression in *Ae. aegypti* salivary glands

Salivary glands were extracted from adult *Ae. aegypti* and stained with DAPI (nuclei, in blue), phalloidin 488 (F-actin, in green), and αSUMO2/3 primary antibody (red). (**A**) Distal lateral lobe, (**B**) proximal-lateral lobes, and median lobe stained for SUMO expression (circled). Arrows indicate likely fat bodies. Images were taken on a Zeiss LSM 880 microscope with 40X oil-immersion objective and are representative n=≥3. Scale bar represents 20 μm.

5.2.2.3. *Aa*SUMO is expressed in the gut

The gut acts as the first site of arboviral infection in *Ae. aegypti,* and therefore acts as a prominent antiviral barrier to incoming arboviruses. Within the gut, SUMO appears to be predominantly localised to the nuclei of cells (**Figure 5.4**). Without cell specific markers it is impossible to be certain which cells of the midgut are being stained, however, they are likely to be a combination of stem cells, enteroendocrine cells, and enterocytes.

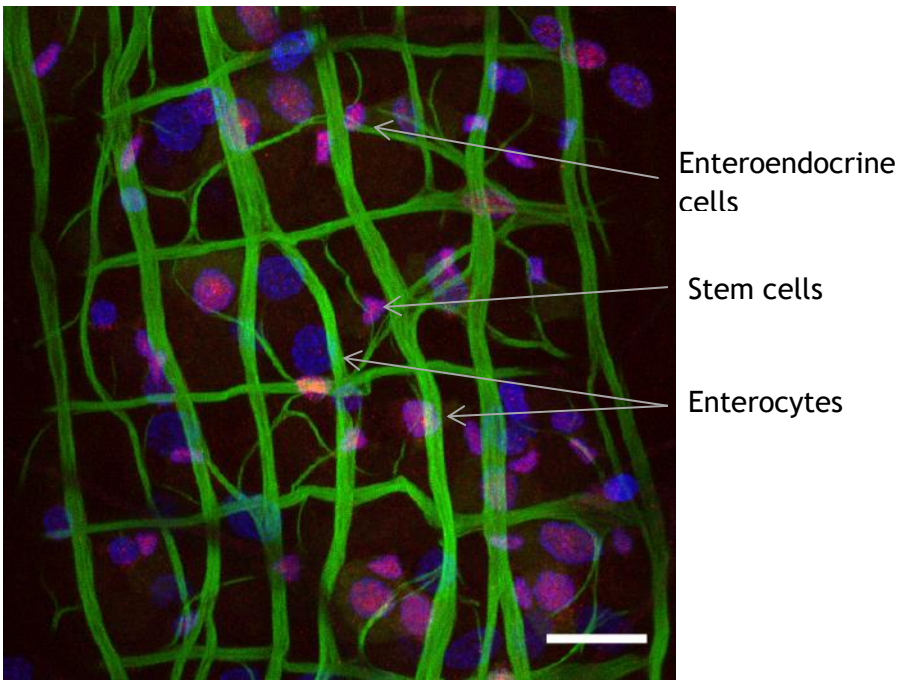

Figure 5.4 SUMO expression in the *Ae. aegypti* gut by confocal microscopy

The gut was extracted from adult female *Ae. aegypti* and stained with DAPI (nuclei, in blue), phalloidin 488 (F-actin, in green), and αSUMO2/3 primary antibody (red). A combination of stem cells, enteroendocrine cells, and enterocytes are shown and likely examples are indicated, with SUMO predominantly localised to the nucleus. Images were taken on a Zeiss LSM 880 microscope with 40X oil-immersion objective and are representative of n=≥3. Scale bar represents 20 μm.

5.2.2.4. *Aa*SUMO is expressed in the ovaries

Upon investigation of *Ae. aegypti* ovaries, SUMO was found to be expressed in differential patterns in different sites. In the oviduct, SUMO is expressed predominantly in the nuclei (**Figure 5.5A**). In the ovarian sheath, SUMO again appears to be primarily expressed in the nuclei, the DAPI stained nuclei which are not expressing punctate SUMO structures are likely epithelial somatic follicular cells, which surround the egg chamber but are located below the ovarian sheath (**Figure 5.4; Figure 5.5B**) (Dr Emilie Pondeville, personal communications). **Figure 5.5C** and **Figure 5.5D** show the primary vitellogenic follicle, and the germarium within an ovariole. Interestingly, within these tissues, SUMO expression is primarily cytoplasmic. The most abundant staining appears in the cytoplasm of the germarium and secondary follicles. Also within the germarium there is further staining of the nuclei of stem germ cells, which give rise to new follicles (Nicholson 1921). There is also prominent cytoplasmic SUMO expression in the follicular cells surrounding the future oocyte (**Figure 5.5C**). Within the nurse cells, there is a build-up of SUMO expression at the perinuclear region of the nuclei (arrows), similar to what has previously been observed in *D. melanogaster* ovaries (Hashiyama, Shigenobu et al. 2009). Furthermore, SUMO expression within the follicular cells surrounding the primary follicle is predominantly cytoplasmic. The differential expression of SUMO in the tissues studied here strongly indicates a cellular and tissue specific role for SUMO modification in *Ae. aegypti*.

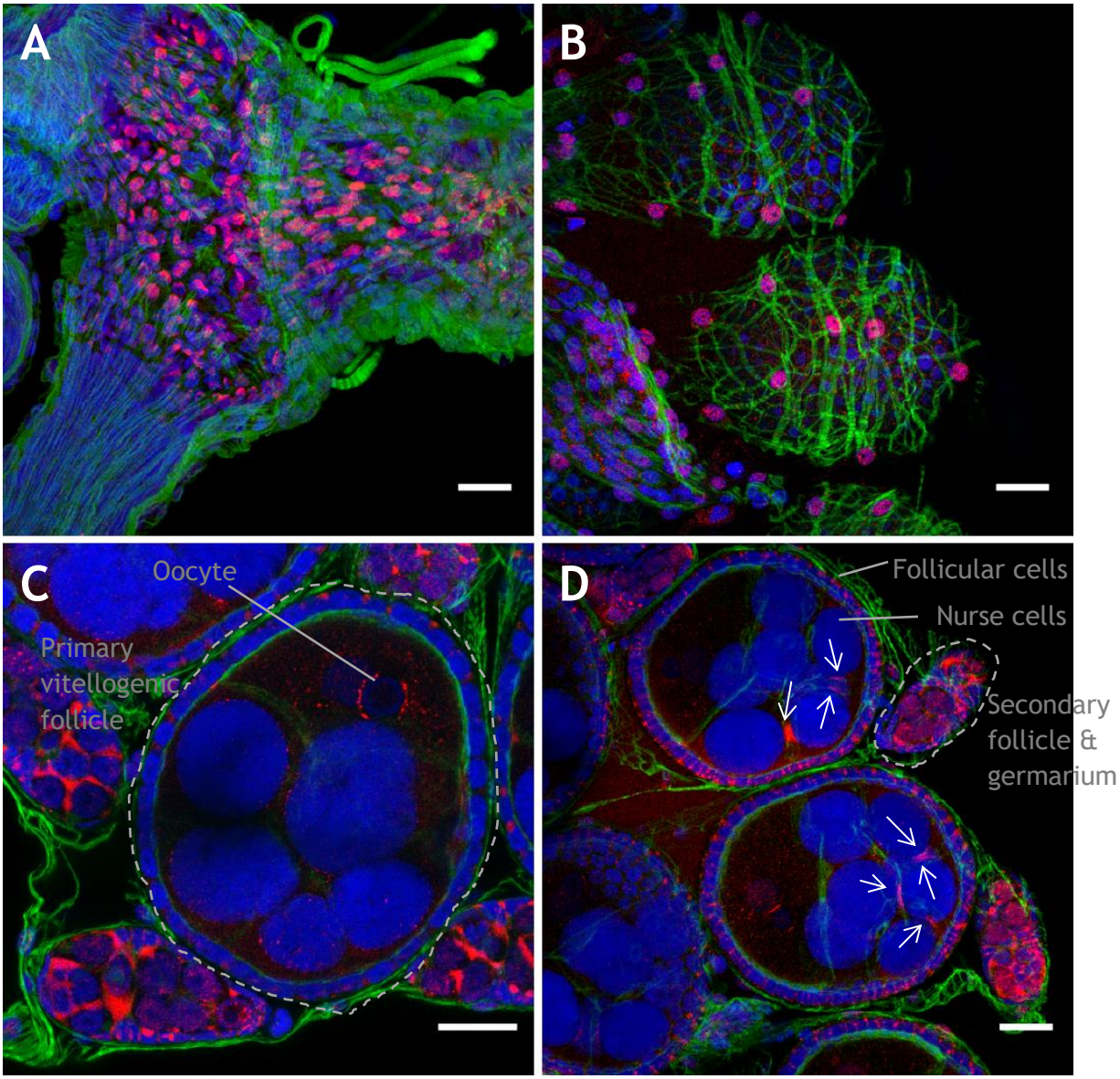

Figure 5.5 Expression of SUMO in *Ae. aegypti* ovaries

Ovaries were extracted from adult *Ae. aegypti* and stained with DAPI (nuclei, in blue), phalloidin 488 (F-actin, in green), and αSUMO2/3 primary antibody (red). (**A**) Oviduct, (**B**) ovarioles encased by the ovarian sheath, (**C, D**) and ovarioles containing the primary vitellogenic follicle (circled in **C**) and secondary follicle and germarium (circled in **D**). Within the ovaries, SUMO is found predominantly localised in the cytoplasm, while in the ovarian sheath, and oviduct SUMO is primarily localised in the nuclei. Arrows indicate SUMO signal accumulating in the perinuclear region of nurse cells. Images were taken on a Zeiss LSM 880 microscope with 40X oil-immersion objective and are representative of n=≥3. Scale bar represents 20 μm.

5.3. Depletion of *Aa*SUMO *in vivo* does not significantly enhance ZIKV replication

In order to determine the overall effect of *Aa*SUMO during arbovirus replication, *SUMO* mRNA expression was depleted through dsRNA knock down. A negative control dsRNA was also produced against the bacterial LacZ. dsRNA was injected into 10 female adult *Ae. aegypti*, which were subsequently harvested and assessed for *SUMO* mRNA expression by q-PCR. Two strains of *Ae. aegypti* were tested for depletion efficiency, Liverpool and Paea strains. A trial dsRNA knock down was conducted which resulted in no deaths amongst the mosquitoes (**Figure 5.6A**), and approximately 70% depletion in the Liverpool strain, and 92% depletion in the Paea strain (**Figure 5.6B**; **Figure 5.6C**). Experiments were continued with the Paea strain of *Ae. aegypti*, as these achieved a better level of depletion and are more susceptible to ZIKV infection *in vivo* (Dr Emilie Pondeville, personal communications). *Ae. aegypti* depleted of *SUMO* mRNA were then infected with ZIKV-nl (**Table 2-3**). Three biological replicates indicated a trend that *SUMO* mRNA depletion resulted in a greater replication of ZIKV, but the phenotype was not statistically significant (P=0.7969). This is likely due to the overall variance of ZIKV-nl in the mosquito population (**Figure 5.7A**), discussed further in **Section 5.6**.

To determine if there was a correlation between the samples expressing high or low levels of luciferase and *SUMO* mRNA depletion, three individual mosquitoes with the highest luciferase expression, and the three with the lowest luciferase expression from each replicate were combined and assessed. The dsSUMO treated samples (blue) had consistently lower *SUMO* mRNA expression by q-PCR than the dsLacZ control (brown) treated samples (**Figure 5.7B**). Notably, there was a wide variation in the basal expression of *SUMO* mRNA within the dsLacZ treated samples, indicating that *SUMO* mRNA expression varies between individuals. Analysis was also conducted on ZIKV RNA to ensure that the samples expressing high or low levels of luciferase correlated with levels of viral RNA replication. The samples with high concentrations of luciferase expression consistently had higher levels of viral RNA, compared to the samples expressing low concentrations of luciferase, indicating that the luciferase expression was an accurate indicator of viral replication (**Figure 5.7C**).

As stated, there appears to be a large degree of variation between SUMO expression between individual mosquitoes (**Figure 5.7B**). There are also other variables to consider within individuals treated with dsRNA, including the variation between which tissues are depleted of *SUMO* mRNA and which tissues are amplifying the arbovirus at the time point of harvest. For instance, if the dsRNA is targeting *SUMO* mRNA in the ovaries, salivary glands, and fat bodies, but haemocytes are the primary amplifying cell type, then any effect of SUMO depletion may be diminished (Xi, Ramirez et al. 2008, Ramirez, Souza-Neto et al. 2012, Carissimo, Pondeville et al. 2015).

As a consequence of the difficulty in controlling these variables *in vivo*, *in vitro* depletion studies were performed to directly assess the influence of SUMOylation on arbovirus replication. This approach enabled a greater range of arboviruses to be tested, and a greater selection of components in the SUMOylation pathway to be analysed for their respective biological phenotype.

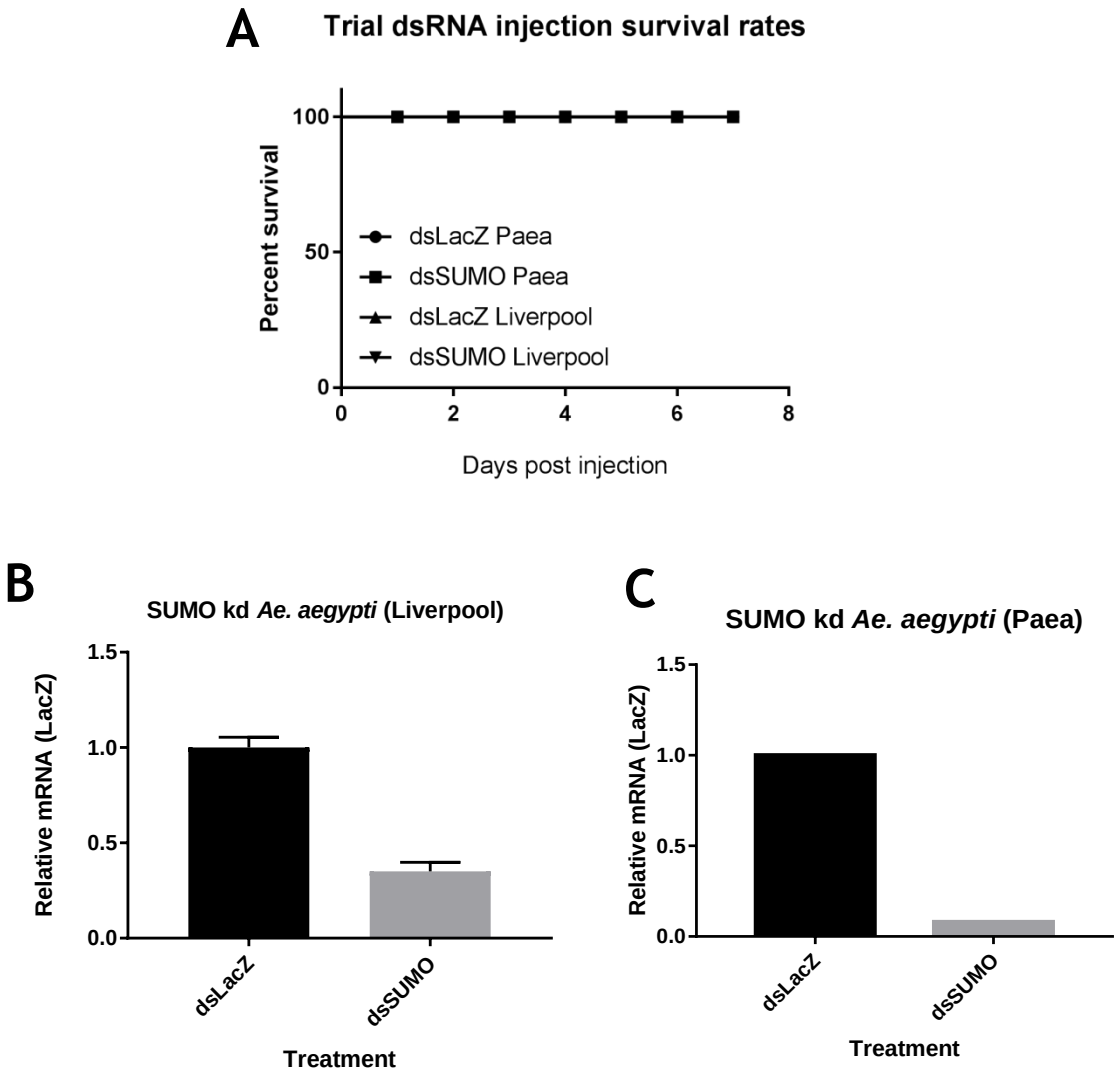

Figure 5.6 SUMO transcript expression levels achieved by q-PCR after dsRNA knockdown

(**A**) Survival rates of 10 female *Ae. aegypti* Liverpool or Paea strain mosquitoes treated with dsRNA to target SUMO or LacZ (negative control). (**B**) *Ae. aegypti* (Liverpool) *SUMO* mRNA levels were determined by SYBR Green q-PCR. Values were normalised to ribosomal *S7* using ΔΔCT and expressed relative to the normalised levels in the LacZ treated wells. Results represent RQ mean with RQ Min/Max shown. (**C**) *Ae. aegypti* (Paea) *SUMO* mRNA levels were determined by SYBR Green q-PCR by Floriane Almire. Values were normalised to ribosomal *S7* using Standard Curve, and expressed relative to the normalised levels in the LacZ treated wells. Results represent RQ mean. All graphs produced with GraphPad Prism 7.02 (n=1).

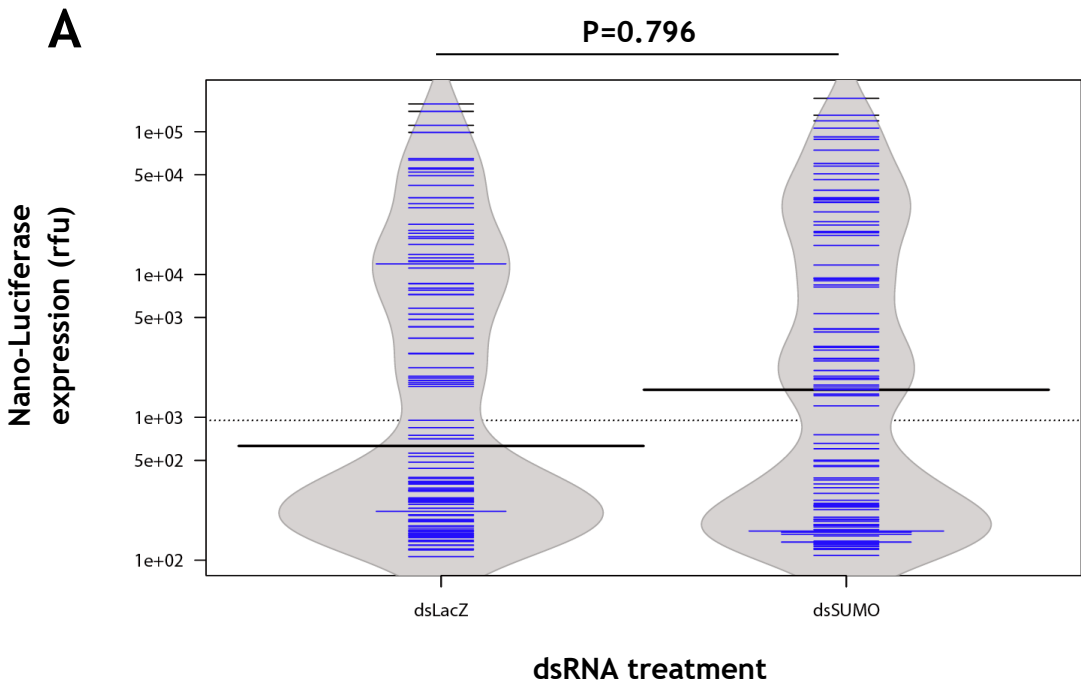

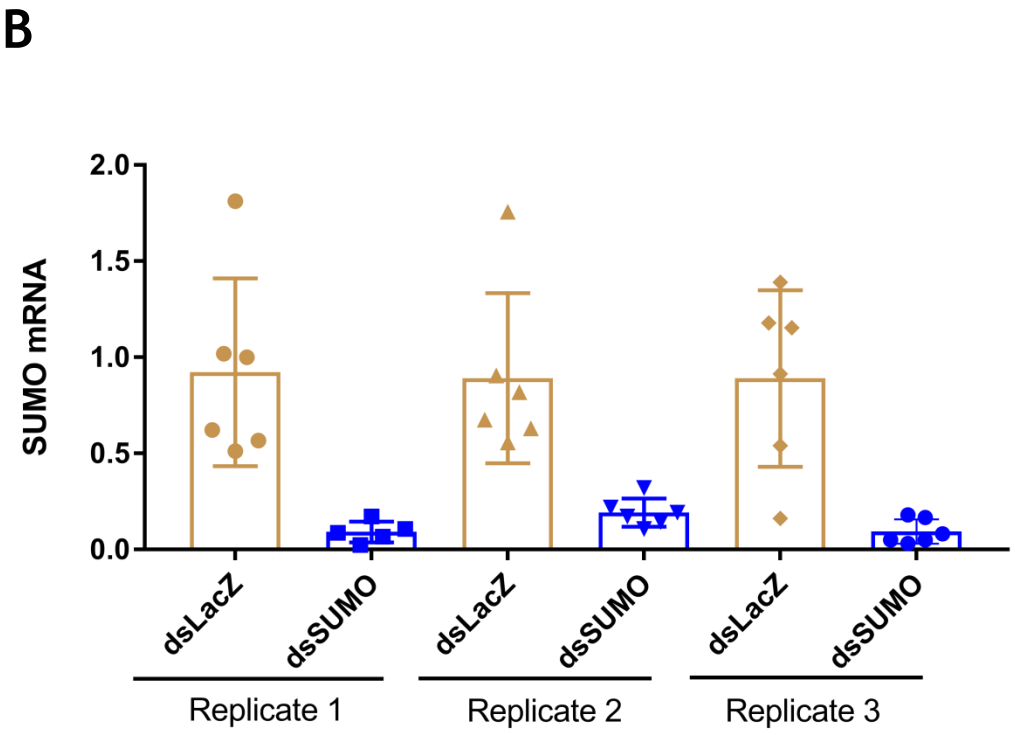

Continued on next page

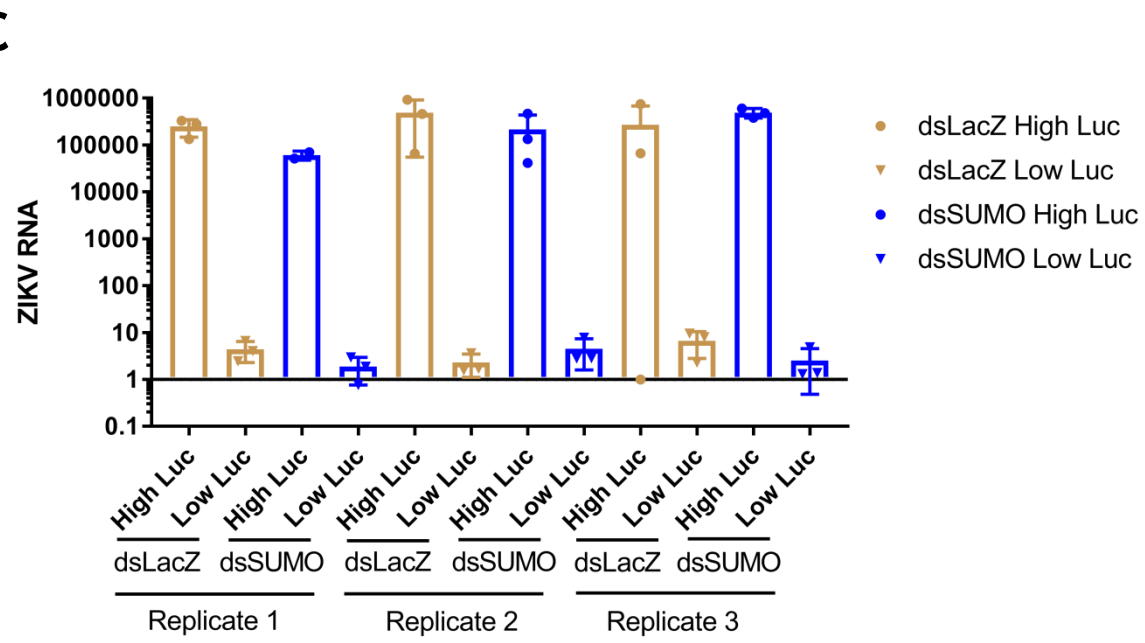

Figure 5.7 Effect of knocking down SUMO expression on ZIKV replication in *Ae. aegypti* mosquitoes

Female *Ae. aegypti* mosquitoes were treated with dsRNA to SUMO or LacZ and fed blood containing $1.04x10^7$ pfu/ml ZIKV-nl, supplemented with 2 mM ATP. Mosquitoes which fed were isolated and harvested for analysis 7 days post blood feeding. (**A**) Nano-Luciferase readings were analysed by a luminometer, and readings are indicated. Black lines show the medians; blue lines represent individual data points, lengths are proportional to frequency of occurrence; polygons represent the estimated density of the data. Mann-Whitney U statistical test was conducted on >100 mosquitoes from three independent experiments. (**B**) Samples expressing the three highest and three lowest luciferase readings were combined from the dsLacZ and dsSUMO treated conditions from each biological replicate were assessed for levels of depletion by SYBR Green q-PCR by Floriane Almire. RQ values indicated as individual points, the mean and standard deviation are shown. Samples were normalised to a dsLacZ treated sample at random. (**C**) The samples from (**B**) were assessed for relative levels of ZIKV RNA by SYBR Green q-PCR by Floriane Almire. Mean calculated from RQ values and standard deviation shown plotted on GraphPad Prism 7.02. Samples were normalised to the dsLacZ treated high luciferase sample from replicate 3.

5.4. dsRNA can deplete expression of the *Aa*SUMOylation pathway in AF5 cells

Due to the previously mentioned variables in mosquitoes we cannot control for, dsRNA was used to deplete *SUMO*, *Ubc9*, and *PIAS* mRNAs in AF5 cells. AF5 cells are a single cell clonal population of Aag2 cells, which are likely derived from haemocytes (Barletta, Silva et al. 2012). Haemocytes are known to be an amplifying tissue for arboviral replication and to express SUMO (Franz, Kantor et al. 2015) (**Figure 5.1; Figure 5.2**). Samples were treated with the desired dsRNA for 72 hours, followed by a 48 hour infection with an arbovirus encoding a luciferase protein at a low MOI (0.05 pfu/cell). Samples were subsequently harvested either for q-PCR or luciferase analysis. Q-PCR analysis confirmed that the mRNA transcripts were consistently depleted by 72% – 82% for the different mRNAs of interest by 72 hours post transfection (**Figure 5.8A**). One sample was taken to assess the effect of dsRNA treatment on SUMO and Ubc9 expression by Western blot. This demonstrated that there were fewer HMW SUMO conjugates in the samples treated with dsRNA to SUMO, Ubc9, or PIAS relative to the non-target control. Ubc9 did not appear to decrease in concentration by Western blot (**Figure 5.8B**).

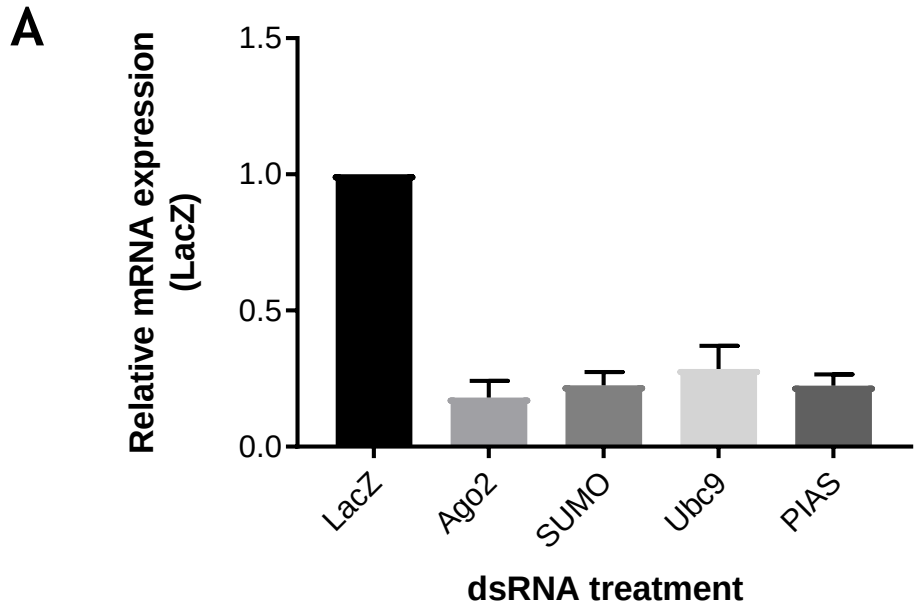

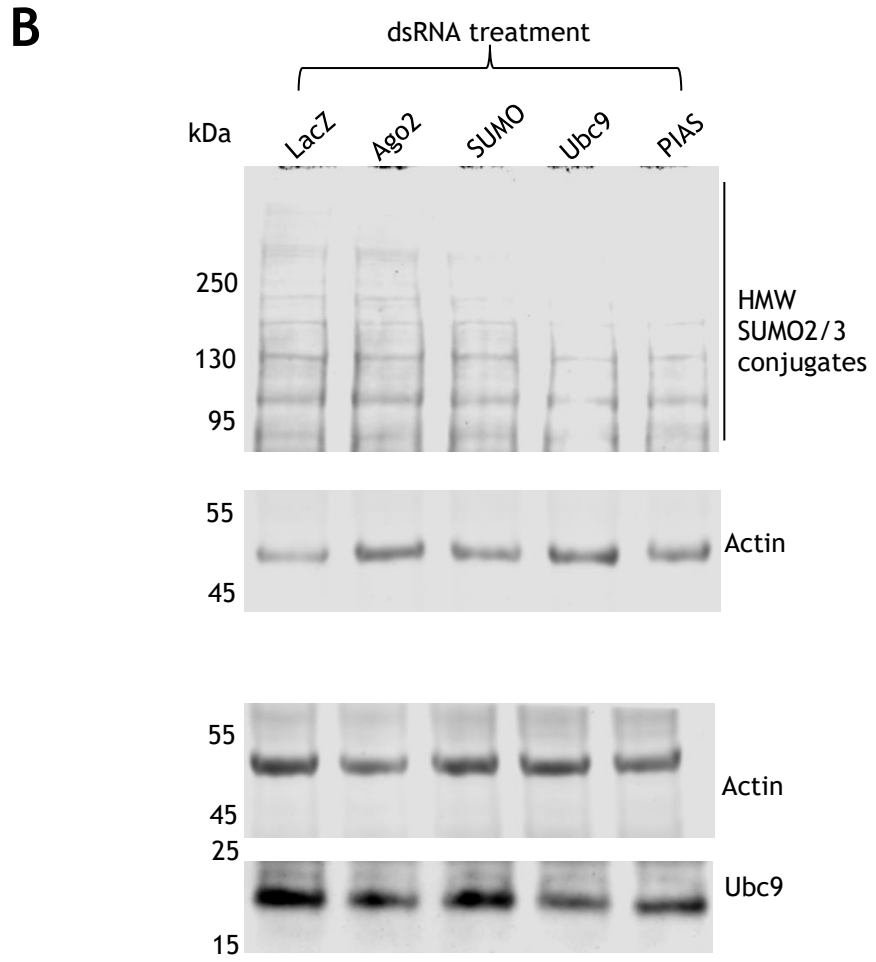

Continued on next page

Figure 5.8 Depletion of the *Aa*SUMOylation pathway by q-PCR and Western blot

AF5 cells were treated with dsRNA against the indicated cellular transcripts for 72 hours, followed by infection for 48 hours at an MOI of 0.05 pfu/cell. (**A**) Bar graph shows mRNA levels of *Ago2*, *SUMO*, *Ubc9*, and *PIAS*, determined by SYBR Green q-PCR. Values were normalised to ribosomal *S7* using ΔΔCT and expressed relative to the normalised levels in the non-target (LacZ) treated wells. Results represent RQ means, with SD bars shown, produced with GraphPad Prism 7.02 (n=15). (**B**) A representative Western blot was conducted to determine the effect of RNA depletion on protein expression. Membranes were probed with antibodies to SUMO2/3, Ubc9, or Actin as a loading control. Molecular mass markers are shown

5.5. Interaction of the *Aa*SUMOylation pathway and arboviruses *in vitro*

AF5 cells were treated with dsRNA to SUMO, Ubc9, PIAS, Ago2 as a positive control, or LacZ as a non-target control. Cells were infected with a virus encoding an internal luciferase protein as detailed in **Table 2-3**. SYBR Green q-PCR was also conducted to determine if depletion of the SUMO pathway was affecting viral translation or viral replication. Luciferase expression and viral RNA levels were normalised to the non-target LacZ control.

5.5.1. Depletion of the *Aa*SUMOylation pathway enhances replication of BUNV

In order to assess the effect of the *Aa*SUMOylation pathway on BUNV replication, depleted AF5 cells were infected at a low MOI (0.05) with BUNV-nl (**Table 2-3**). Nano-Luciferase readings were taken as five biological repeats, each in triplicate. These readings demonstrate that depletion of SUMO, Ubc9, or PIAS significantly enhances the replication of BUNV-nl by approximately two- to three-fold, on par with the positive control, Ago2 (**Figure 5.9A**). Q-PCR was conducted in parallel on the viral complementary RNA (cRNA). Only depletion of Ubc9 resulted in a statistically significant increase in BUNV cRNA levels, with a mean increase of approximately 2.2-fold, compared to between 1.2- and 1.6-fold increases when Ago2, SUMO, or PIAS was depleted (**Figure 5.9B**). These results indicate that depletion of components of the *Aa*SUMOylation pathway may be affecting viral transcription and translation differently. Alternatively, depletion of SUMO or PIAS may be weakly effecting viral replication, yet the depletion still has a significant effect on viral luciferase levels. This would also be true for the positive control, Ago2, which may alternatively indicate that the q-PCR may not be sensitive enough to detect the changes in viral cRNA levels.

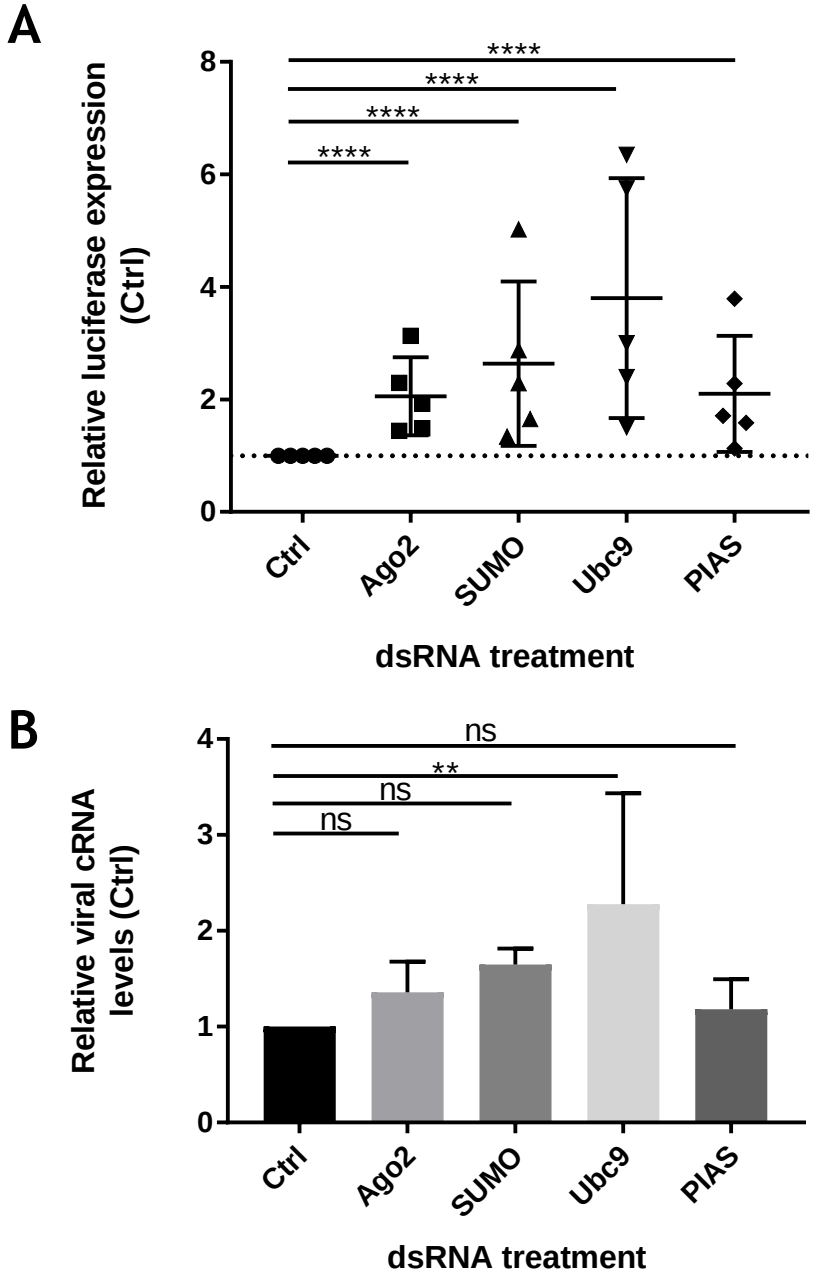

Figure 5.9 Effect of depletion of the *Aa*SUMOylation pathway on BUNV replication

AF5 cells were treated with dsRNA against SUMO, Ubc9, PIAS, Ago2 (positive control), or bacterial LacZ (non-target control; Ctrl) for 72 hours. Cells were then infected with BUNV-nl (MOI 0.05 pfu/cell) for 48 hours. (**A**) Samples were harvested and assessed for Nano-Luciferase expression, readings were normalised to the non-target control, triplicate samples were taken, n=5, mean and Standard deviation from biological repeats presented. (**B**) Viral complementary RNA (cRNA) levels were assessed by SYBR Green q-PCR. Values were normalised to ribosomal S7 using ΔΔCT and expressed relative to the normalised levels in the non-target control. Results represent RQ mean, with standard deviation bars shown (n=5). Graphs were produced with GraphPad Prism 7.02, two-way ANOVA statistics utilised, ns = not significant, ** indicates p=<0.01, **** indicates p= <0.001

5.5.2. Depletion of the *Aa*SUMOylation pathway enhances replication of SFV

In order to assess the effect of the *Aa*SUMOylation pathway on SFV replication, the depleted AF5 cells were infected at a low MOI (0.05 pfu/cell) with SFV-Ffluc (**Table 2-3**). Firefly-luciferase readings were taken as five biological repeats, each in triplicate. These readings demonstrate that depletion of SUMO, and especially Ubc9, but not PIAS, significantly enhanced the replication of SFV-Ffluc. Mean viral luciferase expression increased by two- and five-fold for SUMO and Ubc9 depleted cells, respectively, in comparison to the control (**Figure 5.10A**). Q-PCR was conducted on the viral RNA levels harvested. Here, q-PCR results demonstrated a similar, but more pronounced, phenotype as observed with the luciferase readings. Mean viral RNA levels increased by six- and ten-fold for SUMO and Ubc9 depleted cells, respectively, compared to the control. This demonstrates that depletion of SUMO or Ubc9, but not PIAS significantly enhanced replication of SFV-Ffluc (**Figure 5.10B**). This indicates that endogenous *Ae. aegypti* SUMO and Ubc9 both suppress the replication of SFV, while PIAS does not, although it is also possible that the *Aa*PIAS depletion levels need to be more thorough to see a significant effect.

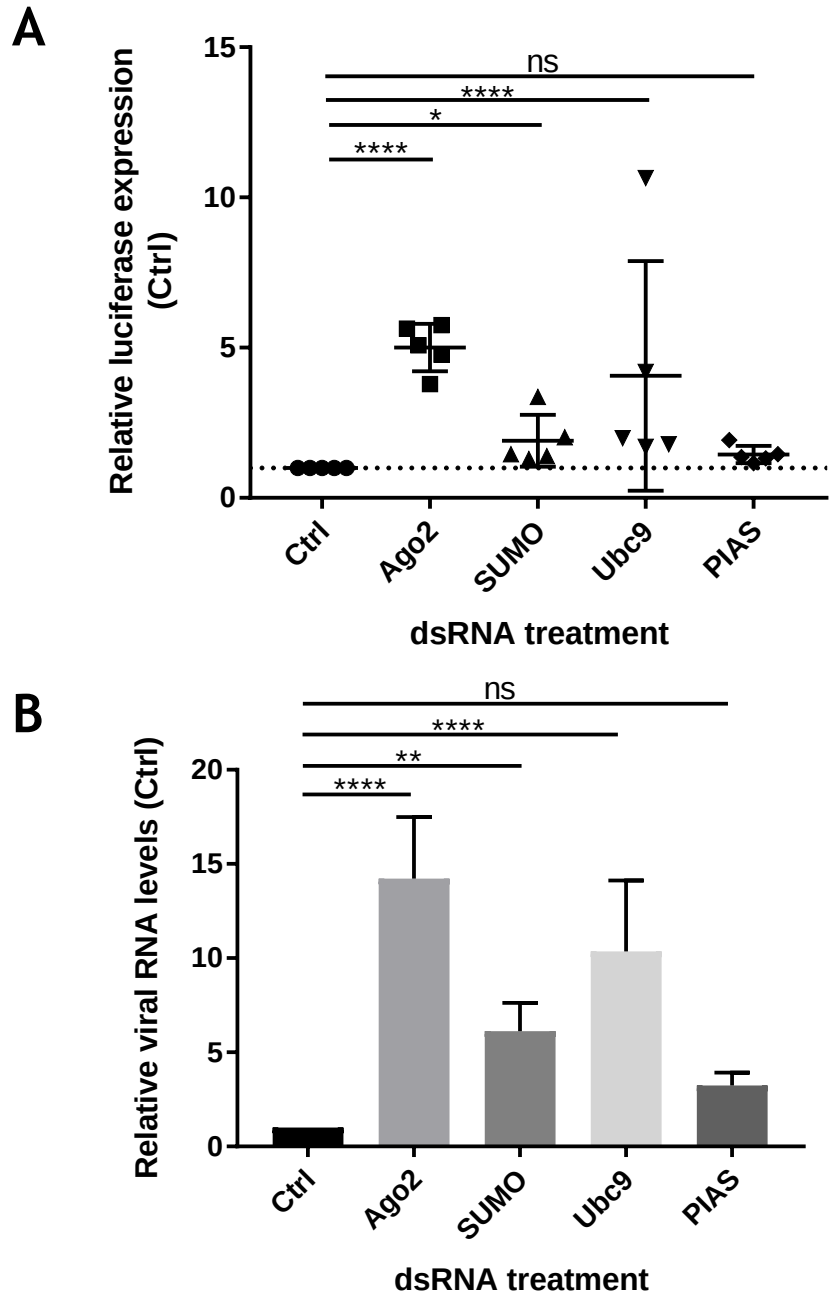

Figure 5.10 Effect of depletion of the *Aa*SUMOylation pathway on SFV replication

AF5 cells were treated with dsRNA against SUMO, Ubc9, PIAS, Ago2 (positive control), or bacterial LacZ (non-target control; Ctrl) for 72 hours. Cells were then infected with SFV-FFluc (MOI of 0.05) for 48 hours. (**A**) Samples were harvested and assessed for Firefly-Luciferase expression, readings were normalised to the non-target control, triplicate samples were taken, n=5, mean and standard deviation from biological repeats presented. (**B**) Viral RNA levels were assessed by SYBR Green q-PCR. Values were normalised to ribosomal S7 using ΔΔCT and expressed relative to the normalised levels in the non-target control. Results represent RQ mean, with standard deviation bars shown (n=5). Graphs were produced with GraphPad Prism 7.02, two-way ANOVA statistics utilised, ns indicates not significant, * indicates p=<0.05, ** indicates p=<0.01, **** indicates p= <0.001

5.5.3. Depletion of the *Aa*SUMOylation pathway enhances replication of ZIKV

When testing the effect of the *Aa*SUMOylation pathway on the replication of ZIKV, depleted AF5 cells were infected at a low MOI (0.05 pfu/cell) for 48 hours with ZIKV-nl (**Table 2-3**). Samples were then harvested for q-PCR or luciferase analysis. Nano-Luciferase expression demonstrates that depletion of SUMO, Ubc9, or PIAS resulted in a small, but consistent, increase in viral replication of approximately 1.5-fold (**Figure 5.11A**). When investigating the viral RNA levels by q-PCR, viral RNA levels also increased following depletion of the SUMOylation pathway. Interestingly, q-PCR had a higher proportional increase in viral RNA than observed by luciferase 1.5-fold up to a three-fold increase in viral RNA levels when PIAS was depleted (**Figure 5.11B**).

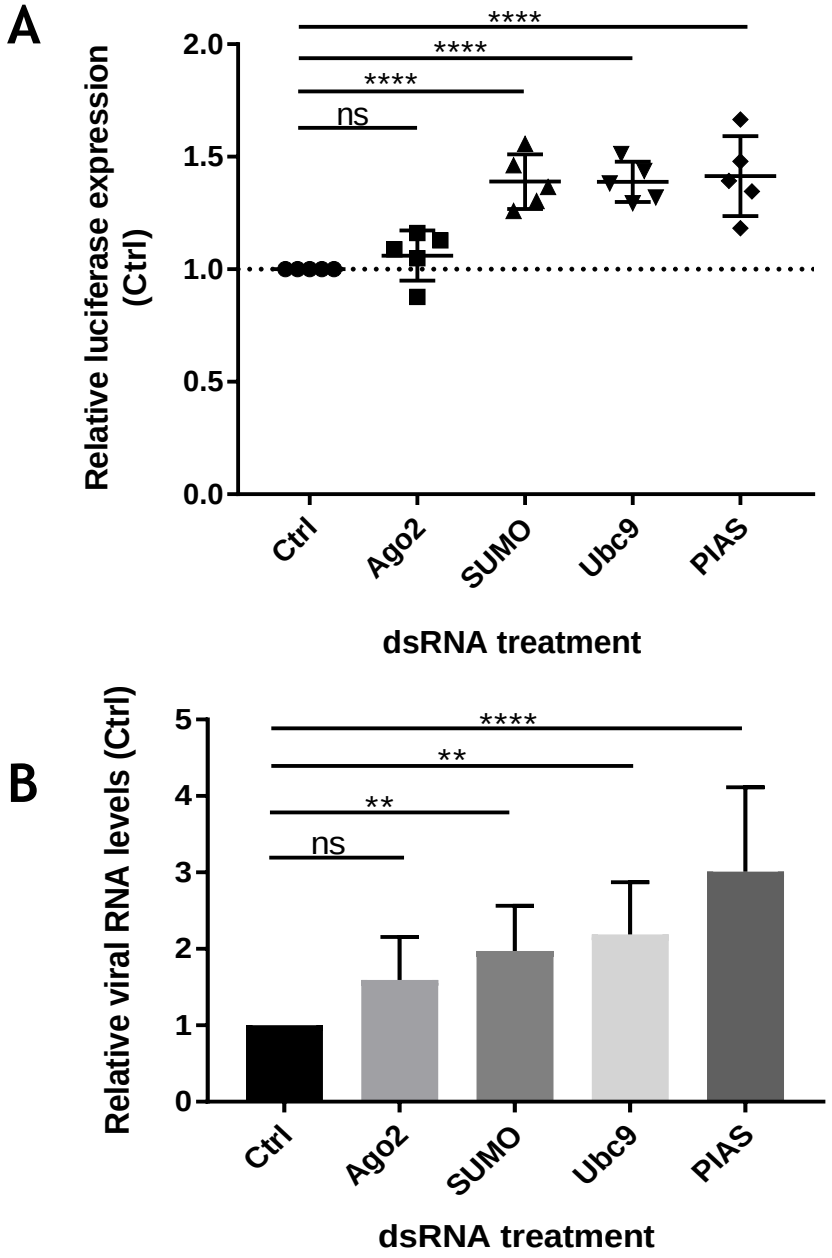

Figure 5.11 Effect of depletion of the *Aa*SUMOylation pathway on ZIKV replication

AF5 cells were treated with dsRNA against SUMO, Ubc9, PIAS, Ago2 (positive control), or bacterial LacZ (non-target control; Ctrl) for 72 hours. Cells were then infected with ZIKV-nl (MOI 0.05 pfu/cell) for 48 hours. (**A**) Samples were harvested and assessed for Nano-Luciferase expression, readings were normalised to the Ctrl, triplicate samples were taken, n=5 mean and standard deviation from biological repeats presented. (**B**) viral RNA levels were assessed by SYBR Green q-PCR. Values were normalised to ribosomal S7 using ΔΔCT and expressed relative to the normalised levels in the non-target control (n=5). Results represent RQ mean, with standard deviation bars shown (n=5). Graphs were produced with GraphPad Prism 7.02, two-way ANOVA statistics utilised, ns = not significant, ** indicates p=<0.01, **** indicates p= <0.001

5.6. Discussion

Component enzymes of the SUMOylation pathway are known to be differentially expressed in different tissues and organs from a range of species (Bohren, Nadkarni et al. 2004, Hu and Chen 2013, Liang, Lee et al. 2016). To date, however, little work has been reported in insects. Early studies in *D. melanogaster* indicated that SUMO and Ubc9 were expressed in a variety of tissues, although no comparison of relative expression levels have been reported (Lehembre, Badenhorst et al. 2000). Experiments by Hu and Chen (2013), in *Cynoglossus semilaevis* indicated that *Ubc9* mRNA was expressed to the greatest extent in the reproductive organs, followed by the blood cells. According to open source data from the Human Protein Atlas (https://www.proteinatlas.org/), in *H. sapiens*, Ubc9 protein is predominantly expressed in reproductive organs and tissues involved in the immune system (including the lymph nodes and tonsils). SUMO1, SUMO2, and SUMO3 are expressed to a relatively high level in tissues involved in the immune system, endocrine tissues, reproductive tissues, and adipose tissues (Uhlen, Oksvold et al. 2010, Uhlen, Fagerberg et al. 2015). We hypothesised that different organs in *Ae. aegypti* would have different requirements for SUMO modification and consequently, tissues would express varying levels of SUMO, Ubc9 and PIAS. Collectively, the data presented in this study does correlate with what has been previously reported, despite comparing vertebrate to invertebrates. We show that the SUMOylation pathway is expressed to the greatest extent in the reproductive organs (ovaries) and immune cells (haemocytes), whereas there is a relatively low level of SUMO expression in the gut, relative to the carcass (**Figure 5.1**). Consequently, we sought to assess the expression of SUMO in a range of *Ae. aegypti* tissues.

To our knowledge, there aren't any studies investigating the expression of SUMOylation pathway component proteins in *D. melanogaster* haemocytes. Consequently, comparisons are drawn with *H. sapiens* cells. In *H. sapiens* cells, SUMO expression is predominantly localised to the nucleus due to the extensive SUMO modification of PML-NBs (Kamitani, Nguyen et al. 1998). The staining seen in **Figure 5.2** displays a similar phenotype to *H. sapiens* cells, and could indicate a PML-like protein expressed in the nuclei that is also extensively SUMO-

modified. Studies on the expression of SUMO in the salivary glands of *D. melanogaster* found SUMO localised to the nuclei, likely localised to the chromosome arms, chromocentre, and chromosome telomere (Nie, Xie et al. 2009, Bocksberger, Karch et al. 2014). In our microscopy, we cannot confidently detect SUMO in the nuclei of salivary gland cells, due to the presence of fat bodies (Dr Emilie Pondeville, personal communications; **Figure 5.3**). However, it seems likely that SUMO would localise to the same region of the salivary glands, as they are relatively closely related insect species. Further studies would be needed to confirm this using specific cellular markers at a higher resolution. To our knowledge, no published studies exist investigating the expression of SUMO in the midgut of *D. melanogaster*. In the studies we have conducted, SUMO appears to be localised to the nucleus of specific cells (**Figure 5.4**). Without cell specific markers, it is impossible to say with certainty which cells have the greatest abundance of SUMO expression. However, due to the location and size of the nucleus, cells with the greatest abundance of SUMO expression are believed to be enterocytes, enteroendocrine cells, and stem cells (Dr Emilie Pondeville, personal communications).

Studies investigating the expression of SUMO during the development of *D. melanogaster* ovaries found that SUMO was primarily localised to the nuclei of the germ cells. After the ovaries had developed primary vitellogenic follicles, SUMO staining was predominantly localised to the nuclei of oocytes and also found at the perinuclear region of the nurse cells (Hashiyama, Shigenobu et al. 2009). In our samples, *Ae. aegypti* SUMO is primarily expressed in the cytoplasm of the ovarioles, although there is a similar accumulation of SUMO expression at the perinuclear region of the nurse cells and oocyte (**Figure 5.5**). There is also extensive cytoplasmic SUMO expression in the follicular cells, similar to what has previously been observed in *D. melanogaster*. The most predominant SUMO expression appears to be localised to the cytoplasm of the germarium, which were not analysed in *D. melanogaster*. The expression pattern of SUMO in *Ae. aegypti* ovaries strongly suggests that there is a shared biological function during egg development as in *D. melanogaster*. Previous studies have demonstrated that within *D. melanogaster* Ftz-f1, a nuclear receptor involved in lipid uptake, is only expressed in the presence of SUMO, and Ftz-f1 is itself a substrate of SUMO modification. Furthermore, Ftz-f1 has also been shown to be expressed in

the ovaries of *Ae. aegypti*, indicating that Ftz-f1 could be a substrate of SUMO modification in *Ae. aegypti* ovaries, although studies would be required to confirm this (Zhu, Chen et al. 2003, Talamillo, Herboso et al. 2013).

Some genes which alter in expression include genes involved in the antiviral immune response. For instance, 14-3-3ε, has been shown to be upregulated following a blood meal, 14-3-3ε is also a known target of SUMO modification in *D. melanogaster* (Bottino-Rojas, Talyuli et al. 2015, Handu, Kaduskar et al. 2015). Due to the known regulation of cellular immunity by SUMO in other species, it was hypothesised that SUMO modification could influence the replication of arboviruses in *Ae. aegypti*. Initially, these studies were attempted *in vivo*. However, while we were able to detect a trend that ZIKV replication increased following treatment with dsRNA, the trend was not statistically significant. Previous studies have encountered similar problems with not being able to detect a significant effect *in vivo* (Troupin, Londono-Renteria et al. 2016). This is potentially due to the virus upregulating the gene expression *in vivo* but not *in vitro*, or effect of the larger number of variables that are challenging to control or account for. For instance, as the dsRNA is injected into *Ae. aegypti* it is impossible to say which cells and tissues were depleted of SUMO to the greatest extent. As the midgut acts as the first site of arboviral replication in the mosquito, a greater depletion in the midgut may result in a more pronounced phenotype, compared to a greater depletion achieved in the salivary glands. This could be the case even if the overall level of *SUMO* mRNA appears to be depleted to a similar extent (**Figure 5.6**). Furthermore, the range of *SUMO* mRNA expression in the dsLacZ treated samples also indicates that the basal level of *SUMO* significantly varies between individual populations or individuals within the population of mosquitoes (**Figure 5.7B**). Consequently, there is no way of knowing which individuals in the control population may have more or less *SUMO* expression prior to infection, which may distort the statistical analysis of results.

The difficulty in controlling the variables in adult *Ae. aegypti* led to a greater emphasis on *in vitro* depletion and infection work. This also enabled other components of the *Aa*SUMOylation pathway to be examined for any effect on arboviral replication of SFV, BUNV, or ZIKV. Following successful depletion of

*Aa*SUMO, *Aa*Ubc9, or *Aa*PIAS, we show that depletion of the *Aa*SUMOylation pathway results in a significant increase in the expression of BUNV luciferase and RNA expression (**Figure 5.8**; **Figure 5.9**). Depletion of *Aa*SUMO and *Aa*Ubc9 also resulted in a significant increase in the replication of SFV (**Figure 5.10**). Interestingly, *Aa*PIAS depletion did not enhance replication of SFV, which indicates a virus specific role for *Aa*PIAS in suppressing arbovirus replication, although this could be due to the depletion not being effective enough for a phenotype to be observed with SFV. Alternatively, it could indicate that some substrates for SUMO modification do not require PIAS to enhance the rate of conjugation, or it could indicate that SUMO and Ubc9 are suppressing SFV replication independent of SUMO conjugation. When ZIKV was infected in cells depleted of *Aa*SUMO, *AaU*bc9, or *Aa*PIAS, ZIKV replication was significantly enhanced (**Figure 5.11**).

Due to potential differences in the protein half-life of *Aa*SUMO, *Aa*Ubc9, or *Aa*PIAS, we cannot say what levels of protein depletion were achieved for *Aa*PIAS, as we do not possess an antibody which cross reacts with *Aa*PIAS. By Western blot *Aa*Ubc9 does not appear to be depleted (**Figure 5.8B**), this is likely due to protein stability, as the mRNA levels have been depleted by ~70%. Furthermore, as a Western blot for SUMO was only conducted at the end of the experiment, after harvesting, it is unknown how efficiently *Aa*SUMO protein was depleted from cells.

Time limitations resulted in the mechanism of action not being determined. However, in *D. melanogaster* SUMO is well-known to modify proteins involved in cellular immunity, including 14-3-3ε, the Imd protein, Casp, STAT92E, or Hop (Bhaskar, Smith et al. 2002, Gronholm, Ungureanu et al. 2010, Handu, Kaduskar et al. 2015). Furthermore, previous studies in *Ae. aegypti* which depleted the expression of PIAS suggested that mosquitoes became more resistant to DENV infection. Five antimicrobial peptides (four Cecropin A-like genes and one Defensin 1-like gene), were found to be down-regulated in mosquito cell cultures which had JAK-STAT activated (by depleting PIAS expression) (Souza-Neto, Sim et al. 2009). The study by Souza-Neto, Sim et al. (2009) implicates a broad role for the JAK-STAT pathway in suppressing DENV replication, although they do not examine the possibility that PIAS is also acting as a SUMO E3 ligase on separate

immune proteins, as other antimicrobial peptides could be up-regulated when PIAS was endogenously expressed.

These results support the hypothesis that SUMO is differentially expressed in the *Ae. aegypti* tissues that we investigated. This is likely due to proteins expressed in specific tissues possessing different requirements for SUMO modification. *Aa*SUMOylation pathway expression is broadly in line with what has previously been reported in *H. sapiens* and *D. melanogaster*. Furthermore, due to differing effects from depletion of the *Aa*SUMOylation pathway on the arboviruses studied, the *Aa*SUMOylation pathway is capable of suppressing the replication of BUNV, SFV, and ZIKV, in a virus specific manner.

The underlying mechanism of suppression is not clear, and requires further investigation. Infected cell lysate was analysed by mass spectrometry (data not shown), however this proved unsuccessful in identifying any SUMO modified viral proteins. It was also unable to identify cellular substrates of SUMO modification that had changed in response to infection. Time constraints meant that this experiment was not repeated or optimised further, but future work could optimise this experiment to attempt to identify a mechanism of suppression. Experiments, such as cell viability assays, should be conducted to confirm cell health following depletion of the SUMOylation pathway. Further studies would also be required to determine if the SUMOylation pathway was having positive and negative roles at different stages of arbovirus replication, rather than just determine an overall phenotypic effect. If there was a pro-viral effect at any stage of the virus replication cycle, it could open opportunities for small molecule inhibitors to be developed. Other arboviruses and other vectors could also be studied to determine if the SUMOylation pathway has a broad antiviral effect on all arboviruses in their vector species. Future studies could also investigate the expression of SUMO in *Ae. aegypti* tissues following a blood meal. *In vivo*, the expression of proteins and the structure of tissue are well known to change following a blood meal; it would therefore be interesting to determine if SUMO expression also changes (Perrone and Spielman 1988, Kato, Dasgupta et al. 2002, Sodja, Fujioka et al. 2007). Finally, repeating the *in vivo* depletion studies and assessing how effective the depletion, along with viral levels in different

tissues could indicate a statistically significant, or tissue specific role for SUMO modification in arbovirus replication.

Collectively, the data presented here suggests that the SUMOylation pathway acts to suppress arbovirus replication. As no substrates were identified, we cannot say for certain if the suppression is due to SUMO modification of target proteins, or if the constituent proteins are interacting with the viral proteins through novel mechanisms. Although, as depletion of any component of the *Aa*SUMOylation pathway results in a significant increase in BUNV and ZIKV replication, it seems likely that SUMO conjugation, requiring the entire pathway, is suppressing replication of these viruses.

6. *Hs*SUMOylation pathway suppresses arbovirus expression

6.1. Overview

Published studies examining the role of host SUMOylation during arbovirus infection have focused on the influence of the *Hs*SUMOylation pathway during DENV infection, which found opposing roles for the *Hs*SUMOylation pathway. Chiu, Shih et al. (2007) found that over expression of Ubc9 had an antiviral effect on the replication of DENV, due to Ubc9 interacting with the E protein, potentially through Lys^{51} and Lys^{241} suggesting that Ubc9 was antiviral. This was supported by a recent study which used siRNAs to deplete expression of Ubc9 and found an increase in DENV viral RNA (Feng, Deng et al. 2018). Su, Tseng et al. (2016) however, conducted studies which used stably tranfected shRNAs to deplete expression of Ubc9, and found a decrease in DENV replication, suggesting a proviral effect of endogenous Ubc9. The mechanism they characterised indicated that SUMO2/3 modified the N-terminal of DENV capsid protein, promoting its stability and enhancing replication. Consequently, it is still unclear if SUMO conjugation has an overall proviral or antiviral role during flavivirus infection in *H. sapiens* cells. Furthermore, nothing is known about the influence of the *Hs*SUMOylation pathway on arboviruses from other viral families.

This chapter aims to determine if the *Hs*SUMOylation pathway is capable of influencing the replication of alphaviruses, flaviviruses, and orthobunyaviruses. A depletion system was utilised as for *Ae. aegypti* cells (**Section 5.4**) to determine the effect of the *Hs*SUMOylation pathway during arboviral replication. An immortalised Human fibroblast cell line (HFt) was utilised in these studies, as arboviruses are known to initially amplify in fibroblast cells at the inoculation site (Vogel, Kell et al. 2005). Furthermore, HFt's are known to possess a competent immune response to viral infection (Smith, Goddard et al. 2013). *SUMO1*, *SUMO2/3*, and *PIAS1* mRNA was targeted for depletion by lentiviral transduction and expression of targeted or non-targeting (control) short hairpin RNAs (shRNA). Utilisation of shRNA expressing lentiviruses is a well-established approach for targeting host SUMOylation proteins in human fibroblast cells (Brown, Conn et al. 2016, Conn, Wasson et al. 2016, Alandijany, Roberts et al. 2018). Viral luciferase assays were conducted as described in **Section 5.5**. In cell Western blot assays (ICWB) were conducted to monitor the initiation and development of ZIKV infection. ICWB has the advantage of being readily

quantifiable due to the use of near-infrared probes, more reproducible, and quicker than Western blots (Aguilar, Zielnik et al. 2010, Hoffman, Moerke et al. 2010). Cell stains can be utilised as a loading control to ensure a similar number of cells are present for each depleted cell line. ICWBs have also been used previously to determine the effect of depletion on viral plaque numbers (Sklan, Staschke et al. 2007).

6.2. Lentiviral transduction with shRNAs depletes expression of components of the SUMOylation pathway in HFt cells

Previous studies have utilised shRNA to target host mRNAs which decrease expression of components of the *Hs*SUMOylation pathway to determine the effect of that protein, either direct or indirect, on viral replication (Brown, Conn et al. 2016, Conn, Wasson et al. 2016, Su, Tseng et al. 2016). Only the study by Su, Tseng et al. (2016) utilises shRNAs targeting Ubc9 (also known as UBE2I) to determine the effect on DENV2 replication. Their study was conducted in alveolar adenocarcinoma (A549) cells.

Here, diploid HFt cells were stably transduced with lentiviruses expressing shRNAs targeting SUMO1, SUMO2/3, or PIAS1 (shSUMO1, shSUMO2/3, or shPIAS1, respectively). To ensure lentiviral transduction was not affecting the phenotype, parallel HFt cells were transduced with lentiviruses containing a non-targeting shRNA (shCtrl). At passage 3, samples were validated for mRNA abundance and protein expression by q-PCR and Western blot, respectively (**Figure 6.1A; Figure 6.1B; Figure 6.1C; Figure 6.1D**). All subsequent viral experiments were conducted on cells at passage 3 or 4 to ensure cells maintained a similar level of depletion over the course of the study. Q-PCR demonstrates that there is a reduced amount of targeted mRNA remaining. A total of 96% depletion was achieved when *SUMO1* was depleted relative to the shCtrl sample, while 80% and 79% depletion was achieved when *SUMO2/3* or *PIAS1* were depleted. Western blot also indicates that expression of all the proteins was reduced compared to the shCtrl sample.

A

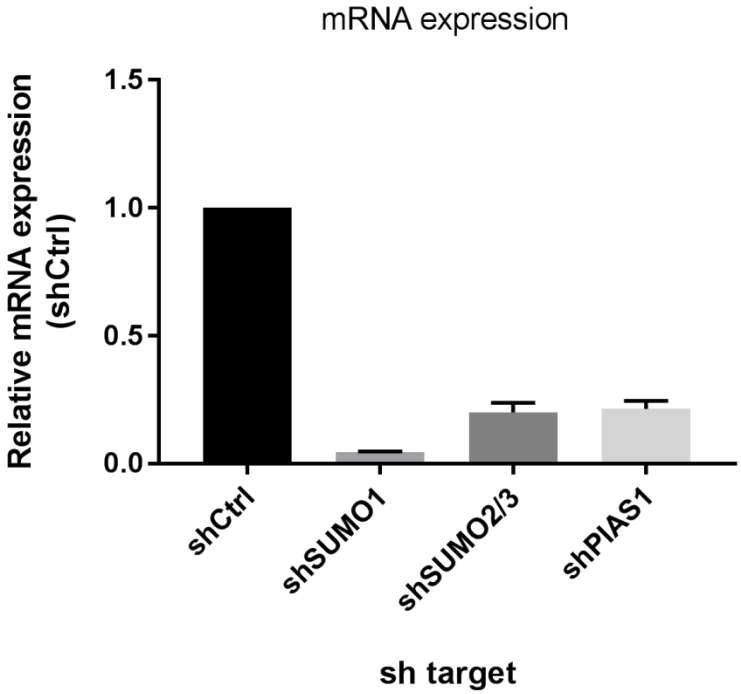
mRNA expression
Relative mRNA expression (shCtrl)
1.5
1.0
0.5
0.0
shCtrl
shSUMO1
shSUMO2/3
shPIAS1
sh target

B

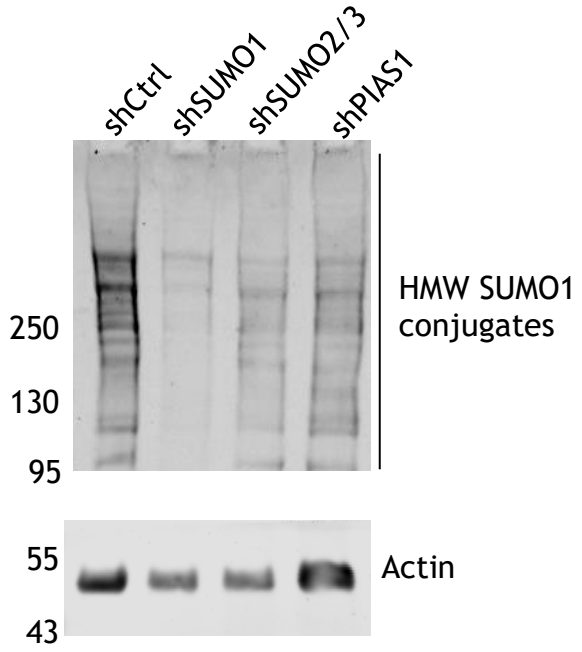
shCtrl
shSUMO1
shSUMO2/3
shPIAS1
HMW SUMO1 conjugates
250
130
95
55
43
Actin

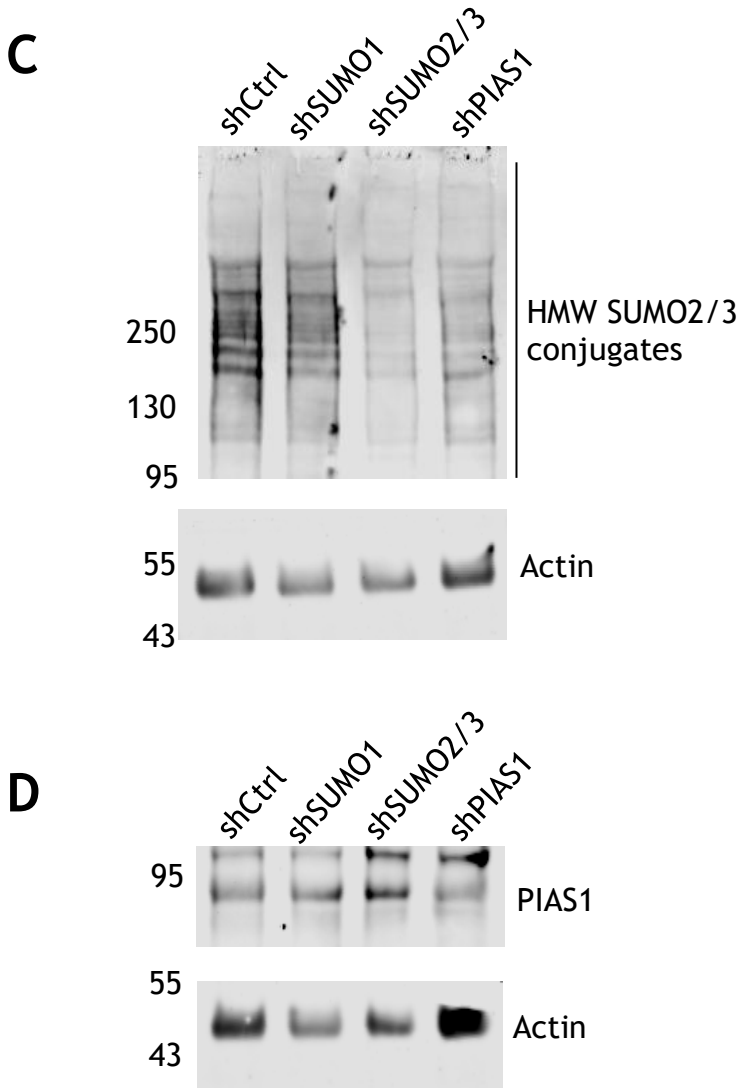

Figure 6.1 Depletion of SUMOylation pathway from HFt cells

HFt cells were transduced with lentivirus vectors expressing short-hairpin RNA (shRNA) targeting SUMO1 (shSUMO1), SUMO2/3 (shSUMO2/3), PIAS1 (shPIAS1), or a non-target control (shCtrl). (**A**) Bar graph shows mRNA levels of *SUMO1*, *SUMO2/3*, and *PIAS1* in the stably transduced lentivirus cell lines. Levels of mRNA were determined using TaqMan system of qPCR. Values were normalised to *GAPDH* mRNA as an endogenous control using cycle threshold (ΔΔCT), and expressed relative to shCtrl. Results represent the mean of three relative quantitation (RQ) plus standard deviation. Western blot for expression of (**B**) SUMO1, (**C**) SUMO2/3, (**D**) and PIAS1, with a loading control (lower blot) from whole cell lysates. Membranes were probed with antibodies to SUMO1, SUMO2/3, or PIAS1 to determine level of protein depletion, and antibodies to Actin as the loading control. Molecular weights indicated.

6.3. Depletion of components of the *Hs*SUMOylation pathway enhances arbovirus expression *in vitro*

As depletion of the *Aa*SUMOylation pathway increased the replication of BUNV, SFV, or ZIKV, it was hypothesised that the *Hs*SUMOylation pathway would also influence arbovirus replication, as this pathway is well conserved. To assess the effect of the *Hs*SUMOylation pathway on arbovirus replication, three parallel cell lines depleted of SUMO1, SUMO2/3, and PIAS1 were infected with arboviruses containing a luciferase reporter protein at a range of MOIs (0.5, 0.1, and 0.05) for 24 hours (SFV) or 48 hours (ZIKV and BUNV). Luciferase readings were taken over three biological repeats. When the cells were infected with BUNV-nl, luciferase expression increased significantly in cell lines depleted of SUMO1 or PIAS1 (**Figure 6.2A**). Interestingly, upon infection of the cells with SFV-Ffluc, neither SUMO1 nor SUMO2/3 depletion had a significant effect on Ffluc expression. However, depletion of PIAS1 led to a significant 8.4-fold increase in Ffluc expression (**Figure 6.2B**).

Studies of the flavivirus DENV, in *H. sapiens* cells have found contradictory roles for the *Hs*SUMOylation pathway (Chiu, Shih et al. 2007, Su, Tseng et al. 2016, Feng, Deng et al. 2018). ZIKV, another flavivirus, was shown to be suppressed by the *Aa*SUMOylation pathway (**Section 5.5.3**). It was therefore hypothesised that the *Hs*SUMOylation pathway would also influence ZIKV replication. Consequently, using *H. sapiens* HFt cells depleted of SUMO1, SUMO2/3, or PIAS1, the effect of the *Hs*SUMOylation pathway on ZIKV was determined. Luciferase assays of ZIKV-nl expression in cells depleted of PIAS1 resulted in a significant; approximately five fold, increase in luciferase expression (**Figure 6.2C**). This phenotype was corroborated by an ICWB conducted which showed more plaques forming in cells depleted of PIAS1 compared to the shCtrl treated cells (**Figure 6.2D**). Average plaque forming efficiency (PFE) experiments from ICWBs indicated that SUMO1 depleted cells have two plaques while PIAS1 depleted cells have approximately six plaques, while infected shCtrl cell monolayers didn't produce any plaques (**Figure 6.2E**). PFE and luciferase analysis on the effect of SUMO2/3 depletion on ZIKV expression shows no statistically significant effect. Although, luciferase

assays indicate that ZIKV expression in cells depleted of SUMO2/3 is lower than control cells (**Figure 6.2C**).

Collectively, these results indicate that the *Hs*SUMOylation pathway is capable of suppressing arbovirus replication. This predominantly occurs through the actions of *Hs*PIAS1. Depletion of PIAS1 results in a significant increase in the luciferase expression of all arboviruses studied here. This could be due to a shared mechanism, or through a mechanism which is specific to each arbovirus. Furthermore, depletion of SUMO1, but not SUMO2/3, suppresses the replication of BUNV, which shows that a target protein needs to be modified specifically by SUMO1. Due to time limitations these observations could not be pursued further.

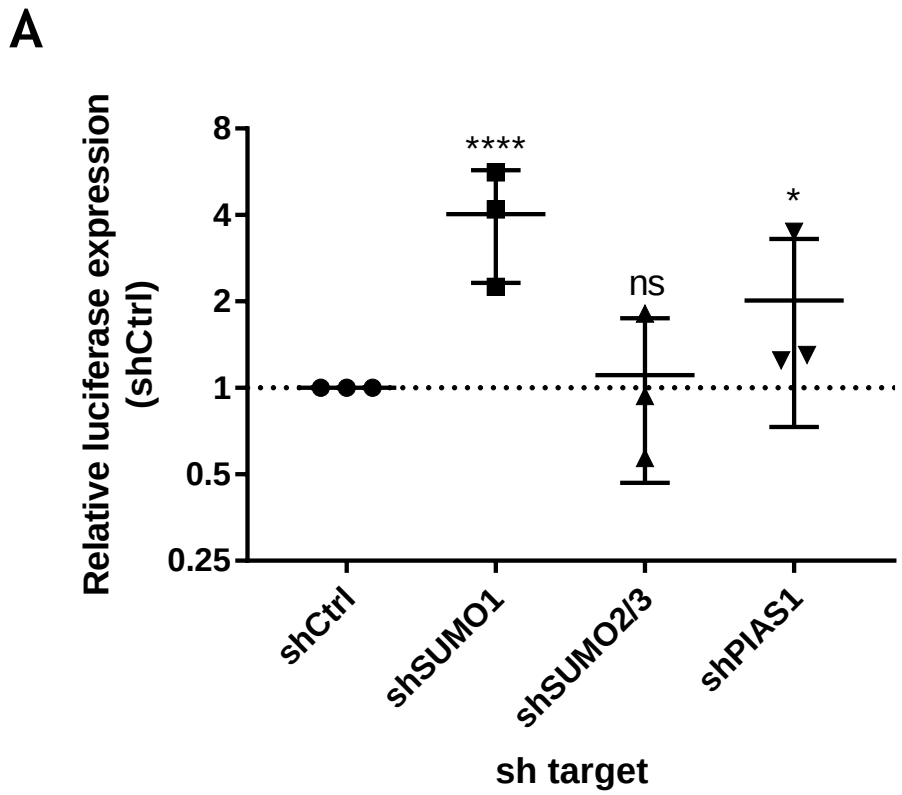

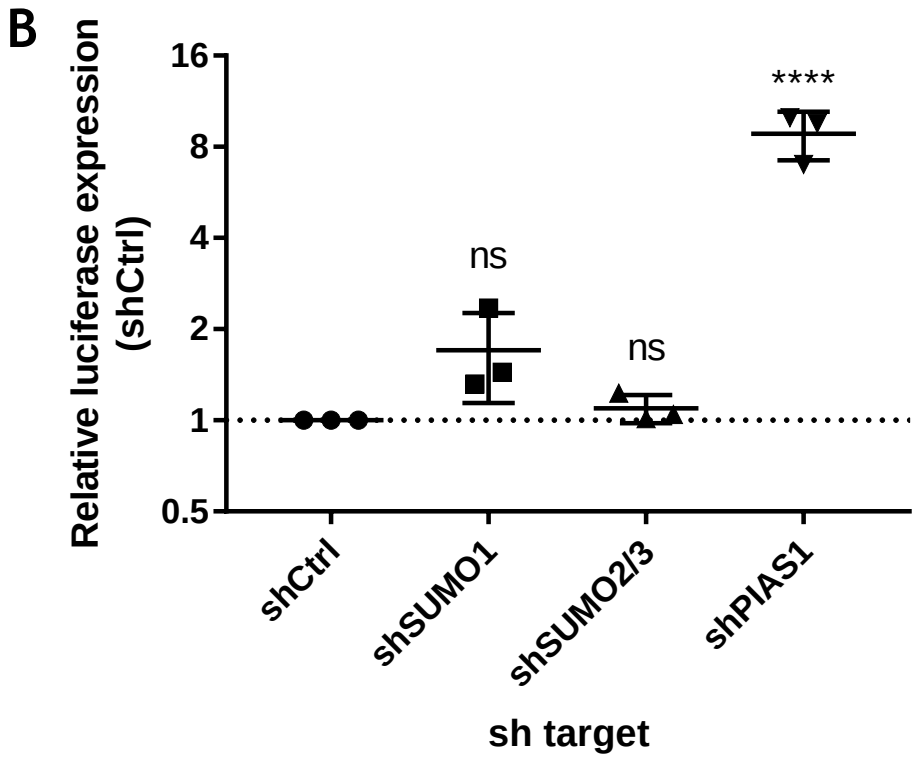

Continued on next page

C

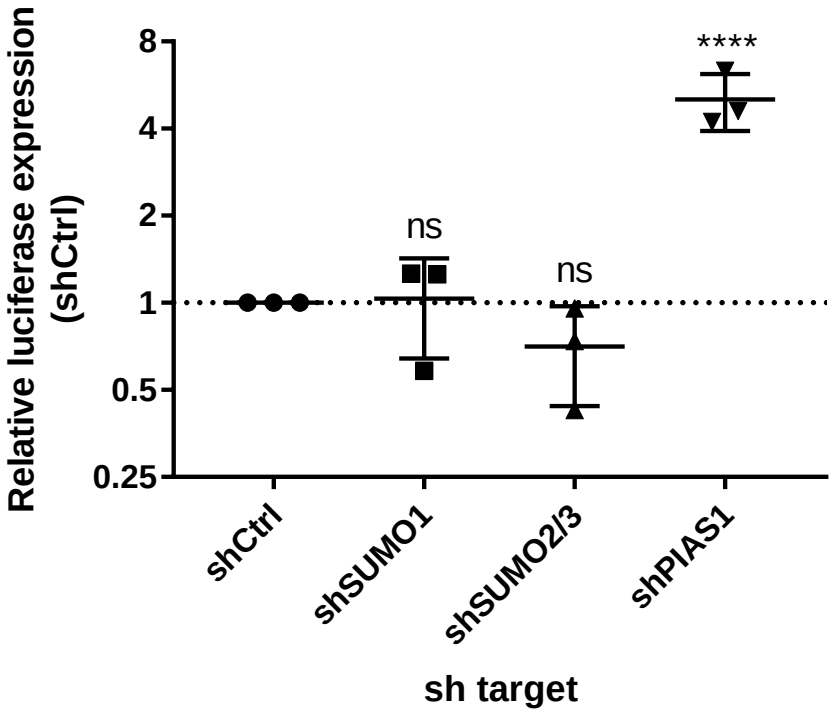

D

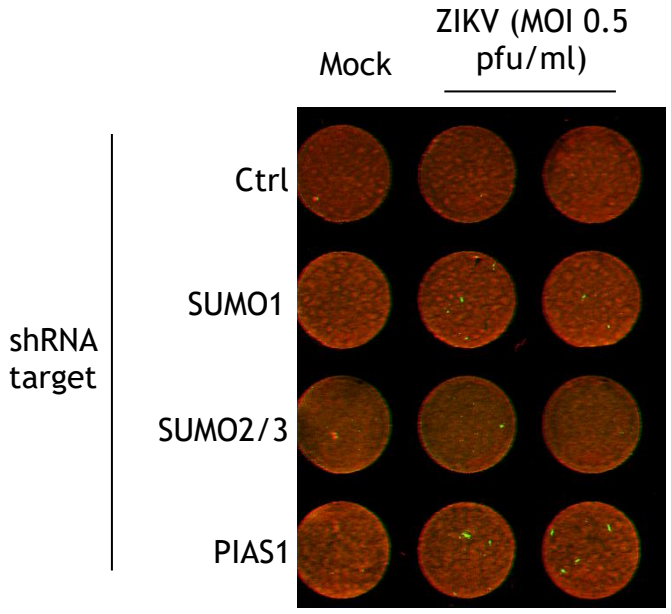

Continued on next page

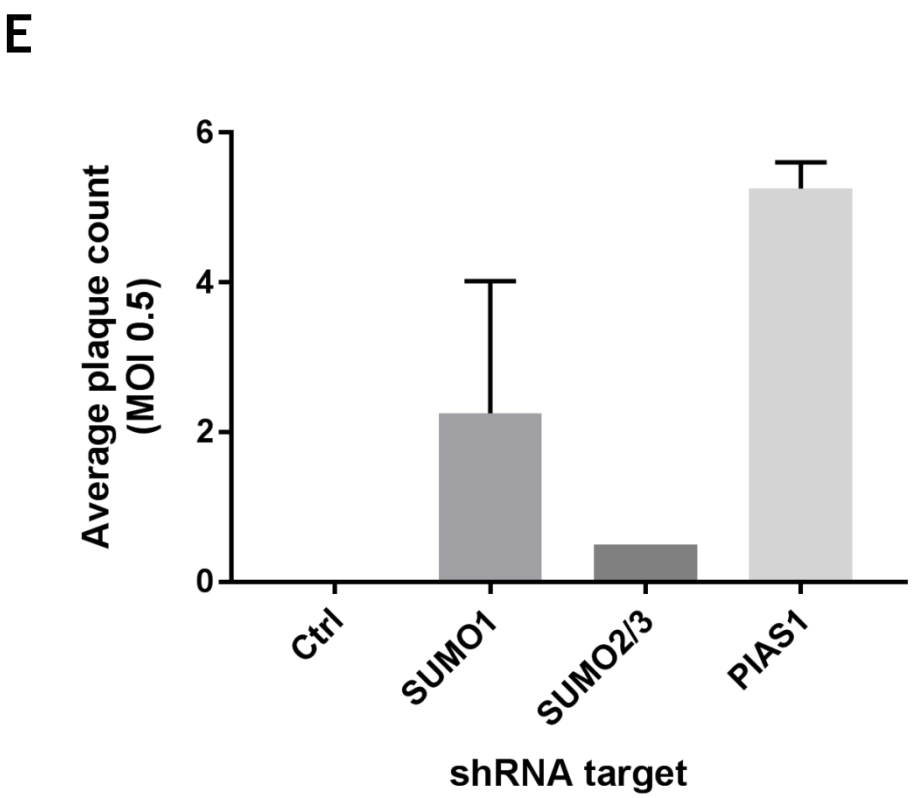

Figure 6.2 Effect of depletion of the *Hs*SUMOylation pathway on arbovirus expression

Cells were transduced with lentiviruses targeting *SUMO1*, *SUMO2/3*, *PIAS1* mRNA, or a non-target control (Ctrl). Cells were infected with either BUNV expressing a Nano-Luciferase reporter (BUNV-nl), SFV expressing a Firefly Luciferase reporter (SFV-Ffluc), a clinical strain of ZIKV (ZIKV-wt), or ZIKV expressing a Nano-Luciferase reporter (ZIKV-nl). Infections occurred at a MOI of 0.5, 0.1, or 0.05 for 48 hours (BUNV and ZIKV) or 24 hours (SFV) before the samples were harvested. (**A**) BUNV-nl, (**B**) SFV-Ffluc and (**C**) ZIKV-nl readings were normalised to the Ctrl samples, and the mean of five technical repeats was taken and plotted for each of the three biological replicates on a Log2 graph. Statistics were conducted on GraphPad Prism 7.02 using a 2-way ANOVA, ns indicates not significant; * = $p \leq 0.05$, **** = $p \leq 0.001$. (**D**) ICWB of cells depleted of the SUMOylation pathway and either mock infected, or infected with ZIKV-wt at an MOI of 0.5. Upon harvesting, cells were fixed and probed with antibodies against ZIKV NS3-protein (green) and CellTag 700 stain was included as a loading control (red). N=2. (**E**) The number of plaques produced in (**D**) was counted, and plotted in Graphpad Prism 7.02 showing the mean number of plaques and standard deviation. N=2.

6.4. Discussion

The *Hs*SUMOylation pathway has previously been shown to positively or negatively influence viral replication for a range of viruses (reviewed in Wilson (2012), Lowrey, Cramblet et al. (2017)). This may occur through direct modification of the viral proteins, or as a consequence of modifying other cellular proteins, for instance transcription factors. Previous studies indicate that the SUMOylation pathway has a proviral and antiviral effect on DENV replication. However, both of these studies interpreted the effect of SUMOylation based on Ubc9 (overexpression or depletion), and neither of these studies looked at other arboviruses. Consequently, our knowledge is limited as to the overall relevance of SUMOylation in the replication of arboviruses in human cells. Given that our previous data indicates that the *Aa*SUMOylation pathway can influence arbovirus replication from different arboviral families, and that the SUMOylation pathways are well conserved (**Section 3.2; Section 5.5**), we hypothesised that the *Hs*SUMOylation pathway should also influence the replication of these arboviruses.

This hypothesis was tested through the depletion of SUMO1, SUMO2/3, and PIAS1 from HFt cells, an immortalised *H. sapiens* fibroblast cell line which possesses a competent innate immune response (Smith, Goddard et al. 2013, Alandijany, Roberts et al. 2018). Depletion levels ranged from ~95% for SUMO1, to ~80% for SUMO2/3 or PIAS1 (**Figure 6.1**). When cells depleted of components of the SUMOylation pathway were infected with BUNV-nl, SUMO1 and PIAS1 depletion both appeared to significantly increase the luciferase expression. When PIAS1 was depleted, luciferase expression increased by two-fold, and when SUMO1 was depleted luciferase expression increased by four-fold (**Figure 6.2A**). Firefly-Luciferase data indicates that PIAS1 depletion also significantly enhances the expression of SFV, while depletion of SUMO1 and SUMO2/3 had no significant effect (**Figure 6.2B**). By luciferase analysis, cells infected with ZIKV after being depleted of PIAS1 experienced a significant increase in luciferase expression (**Figure 6.2C**). A similar phenotype is demonstrated by ICWB, as more plaques are visible in cells depleted of PIAS compared to the control (**Figure 6.2D**).

This work correlates with work by Guo, Chen et al. (2017), which found that replication of the flavivirus HCV was restricted by PIAS2. PIAS2 was found to reduce HCV core, NS3, and NS5A levels through the proteasome pathway (Guo, Chen et al. 2017). Furthermore, studies on PIAS1 and PIAS4 with Herpes Simplex Virus-1 (HSV-1) found that HSV-1 is also restricted by the PIAS1 and PIAS4 homologues (Brown, Conn et al. 2016, Conn, Wasson et al. 2016). Together, these studies indicate an antiviral role for the PIAS family of proteins independent of its role as an inhibitor of activated STAT, and negative regulator of innate immunity.

Furthermore, previous studies by Su, Tseng et al. (2016), suggest that SUMO modification of DENV NS5 increases protein stability, and therefore is proviral. The studies by Su, Tseng et al. (2016) were conducted by depleting Ubc9 expression. The experiments conducted here depleted expression of SUMO1 or SUMO2/3, and while the luciferase readings when SUMO2/3 was depleted were consistently lower than the non-target control sample (**Figure 6.2C**), the effect was not statistically significant. This could be due to a number of reasons, for instance the ~20% mRNA expression remaining in the SUMO2/3 depleted cells, may be enough to protect the viral protein from degradation. Alternatively, SUMO2/3 has previously been reported to be able to substitute for loss of SUMO1 function in the development of mice, consequently it is possible that in this assay SUMO1 is substituting for loss of SUMO2/3 (Zhang, Mikkonen et al. 2008). Furthermore, cells are known to possess a supply of unconjugated SUMO, therefore depletion levels need to be extensive enough to reduce both the supply of unconjugated SUMO and HMW SUMO conjugates. If depletion levels are not extensive enough, a biological phenotype of SUMO2/3 in arboviral infection may be missed. Other previous reports have utilised overexpression, or depletion of Ubc9 to implicate Ubc9 in being antiviral against DENV (Chiu, Shih et al. 2007, Feng, Deng et al. 2018). In order to confirm the validity of either previous study, future work would need a greater depletion of the individual SUMO homologues, Ubc9, and could include the activating enzyme, SAE1/2, to determine if it is the SUMO modification, or interaction with Ubc9 which is producing the pro- or anti-viral phenotype.

Further ICWB analysis was attempted for lentivirus-sh depleted cells which were infected with SFV-eGFP, or a wild type BUNV (data not shown). During this analysis all infections were left for 48 hours, this resulted in ZIKV plaques being visible, but small. It is likely that if the ZIKV infected cells were left for longer more plaques would be visible. Conversely, cultures infected with SFV-eGFP were lysed by the end of the infection period. Depleted cell cultures infected with BUNV did produce readily detectable plaques; however there was not a noticeable difference between the shCtrl and other treated cells, which would make drawing comparisons difficult.

Collectively, these data indicate that the *Hs*SUMOylation pathway is capable of suppressing the replication of a range of arboviruses. SUMO1 depletion significantly enhanced BUNV luciferase expression, while PIAS1 appears to have a wide ranging antiviral effect which is capable of suppressing BUNV, SFV, and ZIKV. Due to time limitations, the studies here are primarily relying on luciferase expression to infer replication, and consequently further studies investigating viral RNA are required to confirm these phenotypes alter viral replication. Other studies, such as mass spectrometry analysis to identify SUMO substrates and introducing lysine mutations, would also be required to decipher the underlying mechanism of action.

7. Discussion

7.1. Overview

This thesis had three initial objectives: to determine the homology between the *Ae. aegypti* and *H. sapiens* SUMOylation pathways; to characterise the biochemical properties of the *Ae. aegypti* SUMOylation pathway; and to determine if the SUMOylation pathway affected the replication of Semliki Forest Virus, Bunyamwera virus, or Zika virus within the transmitting vector species *Ae. aegypti*. Bioinformatic analysis indicated that the *Ae. aegypti* and *H. sapiens* SUMOylation pathways were well conserved. The biochemical properties of the *Aa*SUMOylation pathway demonstrated that there was significant overlap between homologous proteins of both species, to the extent that the *Aa*SUMOylation proteins were biochemically interchangeable with the *Hs*SUMOylation pathway. Furthermore, this analysis indicated that *Aa*SUMO required a catalytically active *Aa*PIAS in order to efficiently form poly-SUMO chains. Finally, it was identified that components of the *Ae. aegypti* and *H. sapiens* SUMOylation pathways can suppress arbovirus replication in an arbovirus dependent manner.

7.2. Conservation of the sequence, structure, biochemical function, and expression of the *Aa*- and *Hs*-SUMOylation pathways

The SUMOylation pathway is known to be important for a wide array of important biological processes throughout the cell, including cellular immunity, cell cycle progression, and the cell stress response. Consequently, SUMO modification is known to be well conserved between various species, including *H. sapiens*, *D. melanogaster,* and *S. cerevisiae* (Matunis, Coutavas et al. 1996, Lehembre, Badenhorst et al. 2000). Our mass spectrometry analysis of *Ae. aegypti* cell culture demonstrates that SUMO, along with the constituent proteins of the SUMOylation pathway are expressed (**Table 3-1**). Bioinformatics and computational modelling show that the amino acid sequence and tertiary structure of SUMO, the E2 conjugating enzyme (Ubc9), and activating heterodimer (SAE1/2), were well conserved (**Figure 3.2; Figure 3.3**).

There is only one known PIAS in *Ae. aegypti*, in contrast to five known *Hs*PIAS homologues. The *Hs*PIAS homologues can have different functions in the cell, as they are able to act as a ligase for SUMO conjugation on specific target proteins (Chung, Liao et al. 1997, Liu, Liao et al. 1998, Reindle, Belichenko et al. 2006). As there is only one *Aa*PIAS, it seems likely that there is not the same degree of E3-target protein specificity. More work has been conducted on *Aa*PIAS, than *Aa*SUMO, *Aa*Ubc9, or *Aa*SAE1/2, because of the biological homology of PIAS as an inhibitor of activated STAT. Previous studies have mapped the biologically functional domains of *Aa*PIAS, which identified the SP-RING domain, along with the SAP, PINIT, and S/T variable domains (Zou, Souza-Neto et al. 2011). Our work has also identified the SP-RING domain of *Aa*PIAS to be conserved, and found that *Aa*PIAS possessed a conserved tertiary structure, even though the amino acid sequence identity was only between 32% - 37% (**Figure 3.4**). Previous studies have also investigated the function of *Aa*PIAS as an inhibitor of the *Ae. aegypti* JAK-STAT pathway, and found that depletion of PIAS activated the JAK-STAT signalling, demonstrating a conserved biological function for PIAS in *Ae. aegypti* and *H. sapiens*. The greatest variation in biochemical activity came from the SUMO homologue. Although the amino acid sequence and predicted tertiary structure of SUMO is well conserved with *Hs*SUMO3, *Aa*SUMO lacks the SCM in the N-terminus of SUMO (**Figure 3.1**). As a consequence, *Aa*SUMO functions biochemically more similarly to *Hs*SUMO1. This aligns with previous reports, which found that most eukaryotic organisms express both SUMO1 and a SUMO2/3 paralogue. Insects, however, do not possess a SUMO1 paralogue, and the SUMO2/3 paralogue(s) lack the SCM (Choy, Severo et al. 2013, Urena, Pirone et al. 2016). This suggests that insect SUMO does not have the ability to efficiently form poly-SUMO chains without the presence of an E3 ligase, indicating an extra degree of regulation in insects.

The biochemical function of the homologous SUMOylation pathways is well conserved. The recombinant proteins are biochemically similar enough that they can substitute one another. *Hs*SAE1/2 and *Hs*Ubc9 can activate and conjugate *Aa*SUMO to form HMW SUMO conjugates (**Figure 4.9**). *Aa*SAE1/2 can also activate *Hs*SUMO2, and *Aa*Ubc9 is capable of conjugating *Hs*SUMO2 into HMW SUMO conjugates, to form poly-SUMO chains (**Figure 4.10; Figure 4.11**). These demonstrated that the biochemical properties of the SUMOylation pathways are

well conserved and function interchangeably. These studies were only undertaken to determine if the biochemical properties were conserved, consequently there is a low number of replicates. For these experiments, the analysis was conducted by Coomassie staining of SDS-PAGE gels. This has the advantage of being able to observe the relative abundance of all proteins within reaction mixtures. However, care must be taken to ensure the protein which is being observed is the protein of interest. Throughout this study, no work was conducted on *Ae. aegypti* deSUMOylating enzymes (SENPs), further studies are required to determine the structure, biological function, organ localisation, and number of *Aa*SENP homologues.

The expression pattern of SUMO throughout *Ae. aegypti* also indicates a conserved pattern of expression between species. Analysis of the open source Human Protein Atlas (https://www.proteinatlas.org/), and studies on the fish species *Cynoglossus semilaevis,* also indicate that the SUMO homologues and Ubc9 are abundantly expressed in the reproductive organs and immune related organs (Uhlen, Oksvold et al. 2010, Hu and Chen 2013, Uhlen, Fagerberg et al. 2015). Our data also shows that the *Aa*SUMOylation pathway is primarily expressed within the reproductive tissues and the haemocytes of adult female *Ae. aegypti* (**Figure 5.1**). Further work to develop greater insight into the expression of SUMO within different organs of *Ae. aegypti* could be conducted by dissecting the specific *Ae. aegypti* organs and conducting proteomic analysis to try to identify SUMO conjugated proteins. If SUMO modification of homologous proteins is conserved between species it would suggest a conserved biological function within organs.

7.3. Biochemical properties of the *Aa*SUMOylation pathway

Biochemical studies have previously been used to provide detailed biological insights into host SUMOylation pathways (Muller, Hoege et al. 2001, Tatham, Jaffray et al. 2001, Gong, Ji et al. 2014). Utilising affinity tag protein purification, the components of the *Aa*SUMOylation pathway have been purified

(**Figure 4.2**) and biochemically characterised for the first time. The assays revealed that the biochemical properties of the homologous pathways appear to be broadly similar. Ubc9 is capable of forming thioester bonds with SUMO at comparable kinetic rates (**Figure 4.3**). No studies were conducted to determine the rate of thioester formation on SAE2. This was because SAE1/2 has a known ability to autoSUMOylate (Truong, Lee et al. 2012). However, future studies could be conducted in parallel non-reducing and reducing environments to compare the rate of SAE2~SUMO thioester formation. The primary difference between the *H. sapiens* and *Ae. aegypti* SUMOylation pathway is from the biochemical properties conferred by *Aa*SUMO. *Aa*SUMO is biochemically more comparable to *Hs*SUMO1, as both lack an internal SCM, even though *Aa*SUMO shares more amino acid identity with *Hs*SUMO3 (**Figure 3.1; Figure 4.4**; **Figure 4.5**; **Figure 4.6**). Our studies show that *Aa*SUMO can still form chains, but this process only occurs efficiently when in the presence of an *Aa*PIAS (**Figure 4.7**). Poly-SUMO chain formation is widely known to be important for a myriad of cellular processes in species ranging from *H. sapiens* to *S. cerevisiae* (Tatham, Jaffray et al. 2001, Bylebyl, Belichenko et al. 2003, Ulrich 2008). The conserved ability to form poly-SUMO chains, as demonstrated by the formation of HMW SUMO conjugated proteins (**Figure 4.7**), indicates that poly-SUMO chains are likely to also have an important biological function in *Ae. aegypti*. Previous studies have shown the *D. melanogaster* SUMO (*Dm*SUMO) cannot form poly-SUMO chains due to the lack of SCM (Urena, Pirone et al. 2016). Here, we show that *Aa*SUMO cannot form poly-SUMO chains unless an E3 ligase, such as an *Aa*PIAS, is present (**Figure 4.7**). Consequently, based on our studies, it seems likely that insects including *Ae. aegypti* and *D. melanogaster* can form chains, but only under tightly regulated circumstances with the presence of an E3 ligase such as PIAS.

Mass spectrometry analysis of our samples indicated that poly-SUMO chains could form on any lysine residue on the *Aa*SUMO protein, although lysine 5, 6, 9, and 40 were primary acceptors for SUMO-SUMO conjugation (**Figure 4.8**). In *H. sapiens* and *S. cerevisiae*, the primary site of SUMO conjugation is within an SCM. It is likely that if this analysis was repeated including the SUMO chimaera, the Lysine 11 would be the primary site of SUMO conjugation as it is located in an SCM. Furthermore, *in vitro* assays can force the formation of poly-*Hs*SUMO1

chains by increasing the concentration of Ubc9 incubated in the assay (Matic, van Hagen et al. 2008). Perhaps one possible avenue for investigations would have been to titrate in lower concentrations of the SAE1/2 and Ubc9, to identify the lowest concentrations of protein required to conjugate SUMO in the timeframe of the assay. A lower concentration of SAE1/2 and Ubc9 would increase the chance of SUMO conjugating to substrates with a higher affinity, and may have helped to identify if there is a preference for a specific SUMO lysine. A pull down specific for SUMO-chains could also have conclusively proven poly-SUMO chain formation *in vivo*. Poly-SUMO chains are important in *H. sapiens* cells for a range of biological properties, including protein localisation, protein stability, and protein-protein interactions. If insects cannot form poly-SUMO chains *in vivo*, it raises many questions about how these functions are performed in insect cells.

7.4. The SUMOylation pathway is broadly antiviral to arboviruses

Many studies have implicated components of the SUMOylation pathway as having a proviral or antiviral effect through depletion experiments (Brown, Conn et al. 2016, Conn, Wasson et al. 2016, Su, Tseng et al. 2016, Guo, Chen et al. 2017, Feng, Deng et al. 2018). SUMO depletion experiments are crude, as they do not distinguish between different targets of SUMO modification, so it becomes hard to determine if a phenotype is directly or indirect (Lyst and Stancheva 2007). It does, however, demonstrate whether the SUMO pathway has an overall proviral or antiviral effect on arbovirus replication within the cell. Previous studies have also used dsRNA to deplete expression of targets proteins, such as Ago2, or PIWI4, in *Ae. aegypti* or *Ae. aegypti* cell culture to determine the effect of the target protein on arbovirus replication (Schnettler, Donald et al. 2013, McFarlane, Arias-Goeta et al. 2014, Dietrich, Shi et al. 2017, Varjak, Maringer et al. 2017).

Initially, in adult *Ae. aegypti* mosquitoes, *SUMO* mRNA was depleted by dsRNA injection, and the mosquitoes were infected with ZIKV-nl (**Figure 5.6**). No

significant effect was found on luciferase expression (**Figure 5.7**). However, there are a large number of variables which could not be controlled for that may alter the infectivity of ZIKV in the mosquitoes. These include variations in which tissues are being depleted and which are becoming infected. For instance, the dsRNA could be predominantly depleting *SUMO* mRNA in the ovaries and salivary glands, which together account for over 50% of *SUMO* mRNA (**Figure 5.1**). If, however, at the end of the experiment ZIKV was primarily replicating in the haemocytes and midgut, the SUMO levels would not have been altered in the relevant tissues. Consequently, we opted to deplete expression of *SUMO*, *Ubc9*, or *PIAS* in *Ae. aegypti* cell culture, where there are fewer variables, and subsequently infected with the alphavirus SFV, orthobunyavirus BUNV, or flavivirus ZIKV (**Figure 5.8**). Studies were later conducted in *H. sapiens* cells. Lentiviruses expressing short hairpin RNA was transfected into fibroblast cells, to deplete expression of *SUMO1*, *SUMO2/3*, or *PIAS1* (**Figure 6.1**). Following successful depletion, cells were infected with SFV, ZIKV, or BUNV and changes in luciferase readings were assessed.

When SFV replication was assessed in depleted *Ae. aegypti* cells, depletion of *Aa*SUMO or *Aa*Ubc9 resulted in a significant increase in viral luciferase expression and viral RNA levels, indicating that endogenous *Aa*SUMO and *Aa*Ubc9 suppress arbovirus replication. When *Aa*PIAS was depleted there was no significant effect on viral replication (**Figure 5.10**). There are many potential mechanisms this could be due to. The capsid protein of SFV contains two readily accessible overlapping SCMs (**Figure 3.7**). One possibility could be that the capsid monomers could be SUMO modified, interfering with the formation of the capsid during virus assembly. Depletion of SUMO or Ubc9 would hypothetically reduce the amount of SUMO conjugation on the capsid, and therefore reduce the amount of interference, increasing viral assembly and replication. This would need to be investigated experimentally. Mass spectrometry analysis could indicate if the capsid was a target of SUMO modification, and mutation of acceptor sites in the SFV capsid could demonstrate if SUMO modification was altering viral replication. Alternatively, many other proteins SFV encodes also contain an SCM, including the envelope glycoprotein, nsP1, nsP2, nsP3, or nsP4. SUMO binding to any of these proteins could alter viral protein activity or stability, this could also be investigated through mass spectrometry and

mutational studies to determine target, and function of SUMO modification. An alternative hypothesis would be that the increased replication is due to SUMO modification of immune proteins which could normally suppress SFV replication. As the SUMO pathway is suppressed, the immune proteins would not be modified, and SFV could theoretically replicate to higher titres. Again, this would need to be confirmed experimentally; potentially through mass spectrometry analysis of SUMO modified immune proteins in uninfected and infected cells. Interestingly, and in contrast to *Ae. aegypti*, *H. sapiens* cells depleted of SUMO1 or SUMO2/3 showed no significant effect on viral luciferase expression. However, there was a significant increase in viral luciferase when *Hs*PIAS1 was depleted (**Figure 6.2**). This could suggest that the SUMO modification hypothesised in *Ae. aegypti* does not occur in *H. sapiens*. Alternatively, the *H. sapiens* SUMO homologues could possess redundant or overlapping functional roles with each other. This could be examined experimentally by depleting expression of Ubc9 or SAE1/2, and determining if the SUMO conjugation alters viral luciferase expression.

When the effect of the depletion on BUNV replication was assessed, *Aa*SUMO, *Aa*Ubc9, or *Aa*PIAS depletion all increased the replication of BUNV (**Figure 5.9**). Furthermore, depletion of *Hs*SUMO1 or *H*sPIAS1 also increased luciferase expression of BUNV (**Figure 6.2**). This indicates a conserved role for the SUMOylation pathway in suppressing BUNV replication between host and vector species. As depletion of *Hs*SUMO2/3 did not result in a statistically significant increase in luciferase expression, modification specifically by *Hs*SUMO1 seems likely. Two potential targets of this modification are the Gc protein, or the RDRP, both of which contain three SCM sites (**Figure 3.6**). As the resolved structure of these proteins is not available, it is currently impossible to say if the SCMs are accessible to SUMO modification, or to postulate on a potential mechanism of action. Interestingly, SUMO1, Ubc9, PIAS1, and PIAS2β have all been implicated in the transport of the ribonucleocapsid (RNC) of other Bunyavirales (Seoul and Hantaan viruses) to the Golgi prior to viral packaging (Lee, Yoshimatsu et al. 2003, Maeda, Lee et al. 2003). Due to the overall antiviral effect on BUNV, the findings suggest that either BUNV RNC may be transported to the Golgi via a different mechanism to Hantaan virus or Seoul virus, or alternatively, modification by SUMO may still transport the RNC to be

packaged, but there may also be an overall more significant antiviral effect on another part of the virus replication cycle. This would result in the overall antiviral effect from SUMO1 that these studies show.

Depletion of *Aa*SUMO, *Aa*Ubc9, or *Aa*PIAS in *Ae. aegypti* resulted in a small but consistent significant increase in ZIKV replication (**Figure 5.11**). This could be due to modification of NS5, which contain a readily accessible SCM (**Figure 3.9**). Alternatively, as described for SFV, SUMO could be modifying immune related proteins which normally function to suppress ZIKV replication. As the *Aa*SUMOylation pathway has been depleted, cellular immune proteins may not be modified, and consequently ZIKV replication could increase. In contrast to this, in *H. sapiens* cells, *Hs*SUMO1 and *Hs*SUMO2/3 depletion did not have any significant effect on viral replication (**Figure 6.2**). This could be explained if the level of depletion in *H. sapiens* cells were not as effective as *Ae. aegypti*. Alternatively, there may be redundancy between the function of *Hs*SUMO1 and *Hs*SUMO2/3. Another possibility is that ZIKV could have evolved a mechanism to replicate without being affected by SUMO modification in *H. sapiens* cells, potentially due to the evolutionary divergence between the *Hs*SUMOylation and *Aa*SUMOylation pathways. The flavivirus DENV has been shown to be SUMO modified at the N-terminal of NS5 to increase protein stability, the study could not identify one specific lysine residue that was modified. Consequently, they hypothesised that SUMO 'floats' around the N-terminus of the protein and could modify any of the available lysine residues, as even mutation of all 12 lysine residues in the N-terminal resulted in a weak SUMOylated band (Su, Tseng et al. 2016). Our study does not provide evidence to support this mechanism occurring with ZIKV. However, it could be due to redundancy between *Hs*SUMO1 and *Hs*SUMO2/3 modification.

Surprisingly, regardless of the arbovirus utilised, when *Hs*PIAS1 was depleted there was a statically significant increase in viral luciferase expression (**Figure 6.2**). It seems likely that this indicates a novel biological antiviral function for PIAS1, independent of and in contrast to its reported function as an inhibitor of STAT and negative regulator of the IFN response (Liu, Liao et al. 1998, Liu, Mink et al. 2004). The majority of PIAS functions are related to SUMO, so it is likely that the antiviral activity found here is also related to SUMO modification

(Rytinki, Kaikkonen et al. 2009). This could occur through its activity as an E3 ligase, for instance by SUMO modifying a transcription factor, and activating it or altering the subcellular localisation, or by SUMO modifying a viral protein targeting it for proteasome degradation. PIAS2 was recently found to target the HCV core, NS3, and NS5A proteins for proteasome degradation in a ubiquitin independent manner, and therefore act as an antiviral protein during HCV infection (Guo, Chen et al. 2017). It is possible that PIAS1 acts in a similar mechanism against a range of arboviral proteins. Alternatively, PIAS1 has also been reported to associate with PML-NBs through SIM dependent mechanisms, resulting in the SUMO-1 modification of PML-NBs and enhancing the antiviral properties of this protein complex (Brown, Conn et al. 2016). Previous studies have found that PML-NBs suppress the replication of DENV2, and consequently it is possible that PML-NBs also suppress the replication of other arboviruses, and that this activity could be enhanced by PIAS1 mediated SUMO modification (Giovannoni, Damonte et al. 2015). PIAS4 has also been previously shown to be an intrinsic antiviral protein to HSV-1, through SIM-dependent and SIM-independent mechanisms, PIAS4 localises to sites of genome entry and to replication compartments, and suppress viral replication (Conn, Wasson et al. 2016).

Collectively, these results indicate that the interplay between the SUMOylation pathway in the host and vector, following arbovirus infection is context dependent. Future work should focus on determining the mechanism of action. This could be achieved through mass spectrometry analysis to determine if any viral proteins are being SUMO modified; it could also demonstrate other immune related proteins being SUMO modified in response to infection with an arbovirus. It is likely there is a combination of proviral and antiviral roles for SUMO modification during arbovirus replication. More studies should be conducted to decipher mechanisms to determine if there is a potential for genetically engineered mosquitoes which may help target any proviral roles for SUMO modification. In turn, this may help to restrict arboviral replication to reduce the burden of arboviral disease.

7.5. Concluding remarks

The SUMOylation pathway is a conserved and vital form of protein modification found in all eukaryotic organisms studied to date, including *Ae. aegypti*. The formation of poly-SUMO chains in *Ae. aegypti* requires an *Aa*PIAS, due to the lack of an internal SCM within *Aa*SUMO. This indicates an extra regulatory step for the *Aa*SUMOylation pathway, which is less prevalent in other species that express a SUMO with an internal SCM. Constituent *Aa*SUMOylation pathway enzymes are expressed throughout *Ae. aegypti*, albeit in a tissue dependent manner. The *Aa*SUMOylation pathway has also been shown to contribute to the suppression of arbovirus replication from three distinct viral families in an arbovirus dependent manner. Furthermore, work in *H. sapiens* cell lines indicates a novel and important function for PIAS1 in restricting the replication of a range of arboviruses.

8. References

Acheson, N. H. and I. Tamm (1967). "Replication of Semliki Forest virus: an electron microscopic study." Virology **32**(1): 128-143.

Adams, M. J., E. J. Lefkowitz, A. M. Q. King, B. Harrach, R. L. Harrison, N. J. Knowles, A. M. Kropinski, M. Krupovic, J. H. Kuhn, A. R. Mushegian, M. Nibert, S. Sabanadzovic, H. Sanfaçon, S. G. Siddell, P. Simmonds, A. Varsani, F. M. Zerbini, A. E. Gorbalenya and A. J. Davison (2017). "Changes to taxonomy and the International Code of Virus Classification and Nomenclature ratified by the International Committee on Taxonomy of Viruses (2017)." Archives of Virology **162**(8): 2505-2538.

Adebajo, A. O. (1996). "Rheumatic manifestations of tropical diseases." Curr Opin Rheumatol **8**(1): 85-89.

Adorisio, S., A. Fierabracci, I. Muscari, A. M. Liberati, E. Ayroldi, G. Migliorati, T. T. Thuy, C. Riccardi and D. V. Delfino (2017). "SUMO proteins: Guardians of immune system." Journal of Autoimmunity **84**: 21-28.

Aguilar, H. N., B. Zielnik, C. N. Tracey and B. F. Mitchell (2010). "Quantification of Rapid Myosin Regulatory Light Chain Phosphorylation Using High-Throughput In-Cell Western Assays: Comparison to Western Immunoblots." PLOS ONE **5**(4): e9965.

Aguilar, P. V., S. C. Weaver and C. F. Basler (2007). "Capsid Protein of Eastern Equine Encephalitis Virus Inhibits Host Cell Gene Expression." Journal of Virology **81**(8): 3866-3876.

Aguirre, S., A. M. Maestre, S. Pagni, J. R. Patel, T. Savage, D. Gutman, K. Maringer, D. Bernal-Rubio, R. S. Shabman, V. Simon, J. R. Rodriguez-Madoz, L. C. Mulder, G. N. Barber and A. Fernandez-Sesma (2012). "DENV inhibits type I IFN production in infected cells by cleaving human STING." PLoS Pathog **8**(10): e1002934.

Akhrymuk, I., S. V. Kulemzin and E. I. Frolova (2012). "Evasion of the innate immune response: the Old World alphavirus nsP2 protein induces rapid degradation of Rpb1, a catalytic subunit of RNA polymerase II." J Virol **86**(13): 7180-7191.

Akil, A., G. Wedeh, M. Zahid Mustafa and A. Gassama-Diagne (2016). "SUMO1 depletion prevents lipid droplet accumulation and HCV replication." Arch Virol **161**(1): 141-148.

Alagu, J., Y. Itahana, F. Sim, S.-H. Chao, X. Bi and K. Itahana (2018). "Tumor Suppressor p14ARF Enhances IFN-γ–Activated Immune Response by Inhibiting PIAS1 via SUMOylation." The Journal of Immunology **201**(2): 451-464.

Alandijany, T., A. P. E. Roberts, K. L. Conn, C. Loney, S. McFarlane, A. Orr and C. Boutell (2018). "Distinct temporal roles for the promyelocytic leukaemia (PML) protein in the sequential regulation of intracellular host immunity to HSV-1 infection." PLOS Pathogens **14**(1): e1006769.

Alontaga, A. Y., E. Bobkova and Y. Chen (2012). "Biochemical Analysis of Protein SUMOylation." Current protocols in molecular biology / edited by Frederick M. Ausubel ... [et al.] **CHAPTER**: Unit10.29-Unit10.29.

Alphey, L. (2014). "Genetic control of mosquitoes." Annu Rev Entomol **59**: 205-224.

Andersson, H., B. U. Barth, M. Ekstrom and H. Garoff (1997). "Oligomerization-dependent folding of the membrane fusion protein of Semliki Forest virus." J Virol **71**(12): 9654-9663.

Ang, F., A. P. Wong, M. M. Ng and J. J. Chu (2010). "Small interference RNA profiling reveals the essential role of human membrane trafficking genes in mediating the infectious entry of dengue virus." Virol J **7**: 24.

Anglero-Rodriguez, Y. I., P. Pantoja and C. A. Sariol (2014). "Dengue virus subverts the interferon induction pathway via NS2B/3 protease-IkappaB kinase epsilon interaction." Clin Vaccine Immunol **21**(1): 29-38.

Arbouzova, N. I. and M. P. Zeidler (2006). "JAK/STAT signalling in Drosophila: insights into conserved regulatory and cellular functions." Development **133**(14): 2605-2616.

Arif, B. M. and P. Faulkner (1972). "Genome of Sindbis virus." J Virol **9**(1): 102-109.

Arnau, J., C. Lauritzen, G. E. Petersen and J. Pedersen (2006). "Current strategies for the use of affinity tags and tag removal for the purification of recombinant proteins." Protein Expression and Purification **48**(1): 1-13.

Atasheva, S., A. Fish, M. Fornerod and E. I. Frolova (2010). "Venezuelan equine Encephalitis virus capsid protein forms a tetrameric complex with CRM1 and importin alpha/beta that obstructs nuclear pore complex function." J Virol **84**(9): 4158-4171.

Bardos, V. and E. Cupkova (1962). "The Calovo virus--the second virus isolated from mosquitoes in Czechoslovakia." J Hyg Epidemiol Microbiol Immunol **6**: 186-192.

Barletta, A. B., M. C. Silva and M. H. Sorgine (2012). "Validation of Aedes aegypti Aag-2 cells as a model for insect immune studies." Parasit Vectors **5**: 148.

Bartenschlager, R. and S. Miller (2008). "Molecular aspects of Dengue virus replication." Future Microbiology **3**(2): 155-165.

Bayer, P., A. Arndt, S. Metzger, R. Mahajan, F. Melchior, R. Jaenicke and J. Becker (1998). "Structure determination of the small ubiquitin-related modifier SUMO-1." J Mol Biol **280**(2): 275-286.

Bazan, J. F. and R. J. Fletterick (1989). "Detection of a trypsin-like serine protease domain in flaviviruses and pestiviruses." Virology **171**(2): 637-639.

Beauclair, G., A. Bridier-Nahmias, J. F. Zagury, A. Saib and A. Zamborlini (2015). "JASSA: a comprehensive tool for prediction of SUMOylation sites and SIMs." Bioinformatics **31**(21): 3483-3491.

Beckham, C. J. and R. Parker (2008). "P bodies, stress granules, and viral life cycles." Cell Host Microbe **3**(4): 206-212.

Bencsath, K. P., M. S. Podgorski, V. R. Pagala, C. A. Slaughter and B. A. Schulman (2002). "Identification of a Multifunctional Binding Site on Ubc9p Required for Smt3p Conjugation." Journal of Biological Chemistry **277**(49): 47938-47945.

Bentz, G. L., C. B. Whitehurst and J. S. Pagano (2011). "Epstein-Barr Virus Latent Membrane Protein 1 (LMP1) C-Terminal-Activating Region 3 Contributes to LMP1-Mediated Cellular Migration via Its Interaction with Ubc9." Journal of Virology **85**(19): 10144-10153.

Bernier-Villamor, V., D. A. Sampson, M. J. Matunis and C. D. Lima (2002). "Structural basis for E2-mediated SUMO conjugation revealed by a complex between ubiquitin-conjugating enzyme Ubc9 and RanGAP1." Cell **108**(3): 345-356.

Bernier-Villamor, V., D. A. Sampson, M. J. Matunis and C. D. Lima (2002). "Structural Basis for E2-Mediated SUMO Conjugation Revealed by a Complex between Ubiquitin-Conjugating Enzyme Ubc9 and RanGAP1." Cell **108**(3): 345-356.

Bernstein, E., A. M. Denli and G. J. Hannon (2001). "The rest is silence." Rna **7**(11): 1509-1521.

Bhaskar, V., M. Smith and A. J. Courey (2002). "Conjugation of Smt3 to Dorsal May Potentiate the Drosophila Immune Response." Molecular and Cellular Biology **22**(2): 492-504.

Bhatt, S., P. W. Gething, O. J. Brady, J. P. Messina, A. W. Farlow, C. L. Moyes, J. M. Drake, J. S. Brownstein, A. G. Hoen, O. Sankoh, M. F. Myers, D. B. George, T. Jaenisch, G. R. Wint, C. P. Simmons, T. W. Scott, J. J. Farrar and S. I. Hay (2013). "The global distribution and burden of dengue." Nature **496**(7446): 504-507.

Bhatt, S., P. W. Gething, O. J. Brady, J. P. Messina, A. W. Farlow, C. L. Moyes, J. M. Drake, J. S. Brownstein, A. G. Hoen, O. Sankoh, M. F. Myers, D. B. George, T. Jaenisch, G. R. W. Wint, C. P. Simmons, T. W. Scott, J. J. Farrar and S. I. Hay (2013). "The global distribution and burden of dengue." Nature **496**: 504.

Bhattacharyya, S., A. Zagorska, E. D. Lew, B. Shrestha, C. V. Rothlin, J. Naughton, M. S. Diamond, G. Lemke and J. A. Young (2013). "Enveloped viruses disable innate immune responses in dendritic cells by direct activation of TAM receptors." Cell Host Microbe **14**(2): 136-147.

Billoir, F., R. de Chesse, H. Tolou, P. de Micco, E. A. Gould and X. de Lamballerie (2000). "Phylogeny of the genus Flavivirus using complete coding sequences of arthropod-borne viruses and viruses with no known vector." Journal of General Virology **81**(3): 781-790.

Binari, R. and N. Perrimon (1994). "Stripe-specific regulation of pair-rule genes by hopscotch, a putative Jak family tyrosine kinase in Drosophila." Genes Dev **8**(3): 300-312.

Blair, C. D. and K. E. Olson (2015). "The role of RNA interference (RNAi) in arbovirus-vector interactions." Viruses **7**(2): 820-843.

Bocksberger, M., F. Karch and J.-M. Gibert (2014). "In vivo analysis of a fluorescent SUMO fusion in transgenic Drosophila." Fly **8**(2): 108-112.

Boggio, R., A. Passafaro and S. Chiocca (2007). "Targeting SUMO E1 to ubiquitin ligases: a viral strategy to counteract sumoylation." J Biol Chem **282**(21): 15376-15382.

Bohren, K. M., V. Nadkarni, J. H. Song, K. H. Gabbay and D. Owerbach (2004). "A M55V polymorphism in a novel SUMO gene (SUMO-4) differentially activates heat shock transcription factors and is associated with susceptibility to type I diabetes mellitus." J Biol Chem **279**(26): 27233-27238.

Borkent, A. (2014) "World Species of Biting Midges (Diptera: Ceratopogonidae)."

Bottino-Rojas, V., O. A. C. Talyuli, N. Jupatanakul, S. Sim, G. Dimopoulos, T. M. Venancio, A. C. Bahia, M. H. Sorgine, P. L. Oliveira and G. O. Paiva-Silva (2015). "Heme Signaling Impacts Global Gene Expression, Immunity and Dengue Virus Infectivity in Aedes aegypti." PLoS ONE **10**(8): e0135985.

Boutell, C. and D. J. Davido (2015). "A quantitative assay to monitor HSV-1 ICP0 ubiquitin ligase activity in vitro." Methods **90**: 3-7.

Bowden, T. A., D. Bitto, A. McLees, C. Yeromonahos, R. M. Elliott and J. T. Huiskonen (2013). "Orthobunyavirus Ultrastructure and the Curious Tripodal Glycoprotein Spike." PLOS Pathogens **9**(5): e1003374.

Bowen, M. D., S. G. Trappier, A. J. Sanchez, R. F. Meyer, C. S. Goldsmith, S. R. Zaki, L. M. Dunster, C. J. Peters, T. G. Ksiazek and S. T. Nichol (2001). "A Reassortant Bunyavirus Isolated from Acute Hemorrhagic Fever Cases in Kenya and Somalia." Virology **291**(2): 185-190.

Breakwell, L., P. Dosenovic, G. B. Karlsson Hedestam, M. D'Amato, P. Liljeström, J. Fazakerley and G. M. McInerney (2007). "Semliki Forest Virus Nonstructural Protein 2 Is Involved in Suppression of the Type I Interferon Response." Journal of Virology **81**(16): 8677-8684.

Bridgen, A. and R. M. Elliott (1996). "Rescue of a segmented negative-strand RNA virus entirely from cloned complementary DNAs." Proc Natl Acad Sci U S A **93**(26): 15400-15404.

Briese, T., B. Bird, V. Kapoor, S. T. Nichol and W. I. Lipkin (2006). "Batai and Ngari viruses: M segment reassortment and association with severe febrile disease outbreaks in East Africa." J Virol **80**(11): 5627-5630.

Brown, J. R., K. L. Conn, P. Wasson, M. Charman, L. Tong, K. Grant, S. McFarlane and C. Boutell (2016). "SUMO Ligase Protein Inhibitor of Activated STAT1 (PIAS1) Is a Constituent Promyelocytic Leukemia Nuclear Body Protein That Contributes to the Intrinsic Antiviral Immune Response to Herpes Simplex Virus 1." J Virol **90**(13): 5939-5952.

Brown, S., N. Hu and J. C. Hombria (2001). "Identification of the first invertebrate interleukin JAK/STAT receptor, the Drosophila gene domeless." Curr Biol **11**(21): 1700-1705.

Buckley, A., S. Gaidamovich, A. Turchinskaya and E. A. Gould (1992). "Monoclonal antibodies identify the NS5 yellow fever virus non-structural protein in the nuclei of infected cells." J Gen Virol **73 (Pt 5)**: 1125-1130.

Byk, L. A. and A. V. Gamarnik (2016). "Properties and Functions of the Dengue Virus Capsid Protein." Annual review of virology **3**(1): 263-281.

Bylebyl, G. R., I. Belichenko and E. S. Johnson (2003). "The SUMO Isopeptidase Ulp2 Prevents Accumulation of SUMO Chains in Yeast." Journal of Biological Chemistry **278**(45): 44113-44120.

Calisher, C. H. (1996). History, Classification, and Taxonomy of Viruses in the Family Bunyaviridae. The Bunyaviridae. R. M. Elliott. Boston, MA, Springer US**:** 1-17.

Campbell, C. L., T. Harrison, A. M. Hess and G. D. Ebel (2014). "MicroRNA levels are modulated in Aedes aegypti after exposure to Dengue-2." Insect Molecular Biology **23**(1): 132-139.

Cappadocia, L. and C. D. Lima (2018). "Ubiquitin-like Protein Conjugation: Structures, Chemistry, and Mechanism." Chemical Reviews **118**(3): 889-918.

Carissimo, G., E. Pondeville, M. McFarlane, I. Dietrich, C. Mitri, E. Bischoff, C. Antoniewski, C. Bourgouin, A. B. Failloux, A. Kohl and K. D. Vernick (2015). "Antiviral immunity of Anopheles gambiae is highly compartmentalized, with distinct roles for RNA interference and gut microbiota." Proc Natl Acad Sci U S A **112**(2): E176-185.

CDC. (2018). "La Crosse Encephalitis." Retrieved 22/06/2018, from https://www.cdc.gov/lac/tech/symptoms.html.

Chamberlain, R. W., R. H. Gogel and W. D. Sudia (1966). "Experimental vector studies with strains of St. Louis encephalitis virus isolated from mosquitoes during the 1964 epidemics." J Med Entomol **3**(3): 268-270.

Chambers, T. J., A. Grakoui and C. M. Rice (1991). "Processing of the yellow fever virus nonstructural polyprotein: a catalytically active NS3 proteinase domain and NS2B are required for cleavages at dibasic sites." Journal of Virology **65**(11): 6042-6050.

Chan, Y. K. and M. U. Gack (2016). "A phosphomimetic-based mechanism of dengue virus to antagonize innate immunity." Nat Immunol **17**(5): 523-530.

Chang, R. Y., T. W. Hsu, Y. L. Chen, S. F. Liu, Y. J. Tsai, Y. T. Lin, Y. S. Chen and Y. H. Fan (2013). "Japanese encephalitis virus non-coding RNA inhibits activation of interferon by blocking nuclear translocation of interferon regulatory factor 3." Vet Microbiol **166**(1-2): 11-21.

Chang, T.-H., S. Xu, P. Tailor, T. Kanno and K. Ozato (2012). "The Small Ubiquitin-like Modifier-Deconjugating Enzyme Sentrin-Specific Peptidase 1 Switches IFN Regulatory Factor 8 from a Repressor to an Activator during Macrophage Activation." The Journal of Immunology **189**(7): 3548-3556.

Chen, Y., T. Maguire, R. E. Hileman, J. R. Fromm, J. D. Esko, R. J. Linhardt and R. M. Marks (1997). "Dengue virus infectivity depends on envelope protein binding to target cell heparan sulfate." Nat Med **3**(8): 866-871.

Chieux, V., W. Chehadeh, J. Harvey, O. Haller, P. Wattré and D. Hober (2001). "Inhibition of Coxsackievirus B4 Replication in Stably Transfected Cells Expressing Human MxA Protein." Virology **283**(1): 84-92.

Chiu, M. W., H. M. Shih, T. H. Yang and Y. L. Yang (2007). "The type 2 dengue virus envelope protein interacts with small ubiquitin-like modifier-1 (SUMO-1) conjugating enzyme 9 (Ubc9)." J Biomed Sci **14**(3): 429-444.

Choe, K.-M., H. Lee and K. V. Anderson (2005). "Drosophila peptidoglycan recognition protein LC (PGRP-LC) acts as a signal-transducing innate immune receptor." Proceedings of the National Academy of Sciences of the United States of America **102**(4): 1122-1126.

Choy, A., M. S. Severo, R. Sun, T. Girke, J. J. Gillespie and J. H. Pedra (2013). "Decoding the ubiquitin-mediated pathway of arthropod disease vectors." PLoS One **8**(10): e78077.

Chu, P. W. G. and E. G. Westaway (1987). "Characterization of Kunjin virus RNA-dependent RNA polymerase: Reinitiation of synthesis in Vitro." Virology **157**(2): 330-337.

Chung, C. D., J. Liao, B. Liu, X. Rao, P. Jay, P. Berta and K. Shuai (1997). "Specific Inhibition of Stat3 Signal Transduction by PIAS3." Science **278**(5344): 1803-1805.

Chung, C. D., J. Liao, B. Liu, X. Rao, P. Jay, P. Berta and K. Shuai (1997). "Specific inhibition of Stat3 signal transduction by PIAS3." Science **278**(5344): 1803-1805.

Ciano, K., J. Saredy and D. Bowers (2014). "Heparan Sulfate Proteoglycan: An Arbovirus Attachment Factor Integral to Mosquito Salivary Gland Ducts." Viruses **6**(12): 5182.

Clarke, B. D., J. A. Roby, A. Slonchak and A. A. Khromykh (2015). "Functional non-coding RNAs derived from the flavivirus 3' untranslated region." Virus Res **206**: 53-61.

Cleaves, G. R. (1985). "Identification of dengue type 2 virus-specific high molecular weight proteins in virus-infected BHK cells." J Gen Virol **66 (Pt 12)**: 2767-2771.

Clements, A. N. (1992). "The biology of mosquitoes."

Coloma, J., R. Jain, K. R. Rajashankar, A. Garcia-Sastre and A. K. Aggarwal (2016). "Structures of NS5 Methyltransferase from Zika Virus." Cell Rep **16**(12): 3097-3102.

Conn, K. L., P. Wasson, S. McFarlane, L. Tong, J. R. Brown, K. G. Grant, P. Domingues and C. Boutell (2016). "Novel Role for Protein Inhibitor of Activated STAT 4 (PIAS4) in the Restriction of Herpes Simplex Virus 1 by the Cellular Intrinsic Antiviral Immune Response." J Virol **90**(9): 4807-4826.

Cortese, M., S. Goellner, E. G. Acosta, C. J. Neufeldt, O. Oleksiuk, M. Lampe, U. Haselmann, C. Funaya, N. Schieber, P. Ronchi, M. Schorb, P. Pruunsild, Y. Schwab, L. Chatel-Chaix, A. Ruggieri and R. Bartenschlager (2017). "Ultrastructural Characterization of Zika Virus Replication Factories." Cell Reports **18**(9): 2113-2123.

Costa, A., E. Jan, P. Sarnow and D. Schneider (2009). "The Imd Pathway Is Involved in Antiviral Immune Responses in Drosophila." PLOS ONE **4**(10): e7436.

Cubenas-Potts, C. and M. J. Matunis (2013). "SUMO: a multifaceted modifier of chromatin structure and function." Dev Cell **24**(1): 1-12.

Dang, Y., N. Kedersha, W. K. Low, D. Romo, M. Gorospe, R. Kaufman, P. Anderson and J. O. Liu (2006). "Eukaryotic initiation factor 2alpha-independent pathway of stress granule induction by the natural product pateamine A." J Biol Chem **281**(43): 32870-32878.

Dash, P. K., M. M. Parida, P. Saxena, A. Abhyankar, C. Singh, K. Tewari, A. M. Jana, K. Sekhar and P. L. Rao (2006). "Reemergence of dengue virus type-3 (subtype-III) in India: Implications for increased incidence of DHF & DSS." Virology Journal **3**(1): 55.

Davis, R. J. (1994). "MAPKs: new JNK expands the group." Trends Biochem Sci **19**(11): 470-473.

de Groot, R. J., W. R. Hardy, Y. Shirako and J. H. Strauss (1990). "Cleavage-site preferences of Sindbis virus polyproteins containing the non-structural proteinase. Evidence for temporal regulation of polyprotein processing in vivo." EMBO J **9**(8): 2631-2638.

De, I., S. G. Sawicki and D. L. Sawicki (1996). "Sindbis virus RNA-negative mutants that fail to convert from minus-strand to plus-strand synthesis: role of the nsP2 protein." J Virol **70**(5): 2706-2719.

de la Cruz-Herrera, C. F., M. Campagna, M. A. García, L. Marcos-Villar, V. Lang, M. Baz-Martínez, S. Gutiérrez, A. Vidal, M. S. Rodríguez, M. Esteban and C. Rivas (2014). "Activation of the Double-stranded RNA-dependent Protein Kinase PKR by Small Ubiquitin-like Modifier (SUMO)." Journal of Biological Chemistry **289**(38): 26357-26367.

Deddouche, S., N. Matt, A. Budd, S. Mueller, C. Kemp, D. Galiana-Arnoux, C. Dostert, C. Antoniewski, J. A. Hoffmann and J. L. Imler (2008). "The DExD/H-box helicase Dicer-2 mediates the induction of antiviral activity in drosophila." Nat Immunol **9**(12): 1425-1432.

Deller, J. J., Jr. and P. K. Russell (1968). "Chikungunya disease." Am J Trop Med Hyg **17**(1): 107-111.

DeLotto, Y. and R. DeLotto (1998). "Proteolytic processing of the Drosophila Spätzle protein by Easter generates a dimeric NGF-like molecule with ventralising activity." Mechanisms of Development **72**(1): 141-148.

Derewenda, Z. S. (2004). "The use of recombinant methods and molecular engineering in protein crystallization." Methods **34**(3): 354-363.

Desterro, J. M., M. S. Rodriguez and R. T. Hay (1998). "SUMO-1 modification of IkappaBalpha inhibits NF-kappaB activation." Mol Cell **2**(2): 233-239.

Desterro, J. M., M. S. Rodriguez, G. D. Kemp and R. T. Hay (1999). "Identification of the enzyme required for activation of the small ubiquitin-like protein SUMO-1." J Biol Chem **274**(15): 10618-10624.

Desterro, J. M. P., M. S. Rodriguez and R. T. Hay (1998). "SUMO-1 Modification of IκBα Inhibits NF-κB Activation." Molecular Cell **2**(2): 233-239.

Di Bacco, A., J. Ouyang, H. Y. Lee, A. Catic, H. Ploegh and G. Gill (2006). "The SUMO-specific protease SENP5 is required for cell division." Mol Cell Biol **26**(12): 4489-4498.

Dick, G. W., S. F. Kitchen and A. J. Haddow (1952). "Zika virus. I. Isolations and serological specificity." Trans R Soc Trop Med Hyg **46**(5): 509-520.

Dietrich, I., X. Shi, M. McFarlane, M. Watson, A.-L. Blomström, J. K. Skelton, A. Kohl, R. M. Elliott and E. Schnettler (2017). "The Antiviral RNAi Response in Vector and

Non-vector Cells against Orthobunyaviruses." PLOS Neglected Tropical Diseases **11**(1): e0005272.

Dietrich, I., X. Shi, M. McFarlane, M. Watson, A. L. Blomstrom, J. K. Skelton, A. Kohl, R. M. Elliott and E. Schnettler (2017). "The Antiviral RNAi Response in Vector and Non-vector Cells against Orthobunyaviruses." PLoS Negl Trop Dis **11**(1): e0005272.

Dominguez, G., C. Y. Wang and T. K. Frey (1990). "Sequence of the genome RNA of rubella virus: evidence for genetic rearrangement during togavirus evolution." Virology **177**(1): 225-238.

Donald, C. L., B. Brennan, S. L. Cumberworth, V. V. Rezelj, J. J. Clark, M. T. Cordeiro, R. Freitas de Oliveira Franca, L. J. Pena, G. S. Wilkie, A. Da Silva Filipe, C. Davis, J. Hughes, M. Varjak, M. Selinger, L. Zuvanov, A. M. Owsianka, A. H. Patel, J. McLauchlan, B. D. Lindenbach, G. Fall, A. A. Sall, R. Biek, J. Rehwinkel, E. Schnettler and A. Kohl (2016). "Full Genome Sequence and sfRNA Interferon Antagonist Activity of Zika Virus from Recife, Brazil." PLoS Negl Trop Dis **10**(10): e0005048.

Dong, S., A. M. Kantor, J. Lin, A. L. Passarelli, R. J. Clem and A. W. E. Franz (2016). "Infection pattern and transmission potential of chikungunya virus in two New World laboratory-adapted Aedes aegypti strains." Scientific Reports **6**: 24729.

DuBridge, R. B., P. Tang, H. C. Hsia, P. M. Leong, J. H. Miller and M. P. Calos (1987). "Analysis of mutation in human cells by using an Epstein-Barr virus shuttle system." Mol Cell Biol **7**(1): 379-387.

Duffy, M. R., T.-H. Chen, W. T. Hancock, A. M. Powers, J. L. Kool, R. S. Lanciotti, M. Pretrick, M. Marfel, S. Holzbauer, C. Dubray, L. Guillaumot, A. Griggs, M. Bel, A. J. Lambert, J. Laven, O. Kosoy, A. Panella, B. J. Biggerstaff, M. Fischer and E. B. Hayes (2009). "Zika Virus Outbreak on Yap Island, Federated States of Micronesia." New England Journal of Medicine **360**(24): 2536-2543.

Duprez, E., A. J. Saurin, J. M. Desterro, V. Lallemand-Breitenbach, K. Howe, M. N. Boddy, E. Solomon, H. de The, R. T. Hay and P. S. Freemont (1999). "SUMO-1 modification of the acute promyelocytic leukaemia protein PML: implications for nuclear localisation." J Cell Sci **112 (Pt 3)**: 381-393.

Dutuze, M. F., M. Nzayirambaho, C. N. Mores and R. C. Christofferson (2018). "A Review of Bunyamwera, Batai, and Ngari Viruses: Understudied Orthobunyaviruses With Potential One Health Implications." Frontiers in Veterinary Science **5**: 69.

Duval, D., G. Duval, C. Kedinger, O. Poch and H. Boeuf (2003). "The 'PINIT' motif, of a newly identified conserved domain of the PIAS protein family, is essential for nuclear retention of PIAS3L." FEBS Lett **554**(1-2): 111-118.

Eckhoff, J. and R. J. Dohmen (2015). "In Vitro Studies Reveal a Sequential Mode of Chain Processing by the Yeast SUMO (Small Ubiquitin-related Modifier)-specific Protease Ulp2." J Biol Chem **290**(19): 12268-12281.

Edwards, J. F., S. Higgs and B. J. Beaty (1998). "Mosquito feeding-induced enhancement of Cache Valley Virus (Bunyaviridae) infection in mice." J Med Entomol **35**(3): 261-265.

Eifan, S. A. and R. M. Elliott (2009). "Mutational Analysis of the Bunyamwera Orthobunyavirus Nucleocapsid Protein Gene." Journal of Virology **83**(21): 11307-11317.

Eisenhardt, N., V. K. Chaugule, S. Koidl, M. Droescher, E. Dogan, J. Rettich, P. Sutinen, S. Y. Imanishi, K. Hofmann, J. J. Palvimo and A. Pichler (2015). "A new vertebrate SUMO enzyme family reveals insights into SUMO-chain assembly." Nat Struct Mol Biol.

Elliott, R. M. (1989). "Nucleotide sequence analysis of the large (L) genomic RNA segment of Bunyamwera virus, the prototype of the family Bunyaviridae." Virology **173**(2): 426-436.

Elliott, R. M. (1989). "Nucleotide sequence analysis of the small (S) RNA segment of Bunyamwera virus, the prototype of the family Bunyaviridae." J Gen Virol **70 (Pt 5)**: 1281-1285.

Elsasser, S., R. R. Gali, M. Schwickart, C. N. Larsen, D. S. Leggett, B. Muller, M. T. Feng, F. Tubing, G. A. Dittmar and D. Finley (2002). "Proteasome subunit Rpn1 binds ubiquitin-like protein domains." Nat Cell Biol **4**(9): 725-730.

Epps, J. L. and S. Tanda (1998). "The Drosophila semushi mutation blocks nuclear import of bicoid during embryogenesis." Curr Biol **8**(23): 1277-1280.

Espada-Murao, L. A. and K. Morita (2011). "Delayed Cytosolic Exposure of Japanese Encephalitis Virus Double-Stranded RNA Impedes Interferon Activation and Enhances Viral Dissemination in Porcine Cells." Journal of Virology **85**(13): 6736-6749.

Estruch, S. B., S. A. Graham, P. Deriziotis and S. E. Fisher (2016). "The language-related transcription factor FOXP2 is post-translationally modified with small ubiquitin-like modifiers." Sci Rep **6**: 20911.

Everett, R. D. (2001). "DNA viruses and viral proteins that interact with PML nuclear bodies." Oncogene **20**: 7266.

Everett, R. D., S. Rechter, P. Papior, N. Tavalai, T. Stamminger and A. Orr (2006). "PML contributes to a cellular mechanism of repression of herpes simplex virus type 1 infection that is inactivated by ICP0." J Virol **80**(16): 7995-8005.

Falgout, B., R. Chanock and C. J. Lai (1989). "Proper processing of dengue virus nonstructural glycoprotein NS1 requires the N-terminal hydrophobic signal sequence and the downstream nonstructural protein NS2a." Journal of Virology **63**(5): 1852-1860.

Falgout, B., M. Pethel, Y. M. Zhang and C. J. Lai (1991). "Both nonstructural proteins NS2B and NS3 are required for the proteolytic processing of dengue virus nonstructural proteins." J Virol **65**(5): 2467-2475.

Feng, T., L. Deng, X. Lu, W. Pan, Q. Wu and J. Dai (2018). "Ubiquitin-conjugating enzyme UBE2J1 negatively modulates interferon pathway and promotes RNA virus infection." Virology Journal **15**: 132.

Fields, W. and M. Kielian (2013). "A key interaction between the alphavirus envelope proteins responsible for initial dimer dissociation during fusion." J Virol **87**(7): 3774-3781.

Flores, H. A. and S. L. O'Neill (2018). "Controlling vector-borne diseases by releasing modified mosquitoes." Nat Rev Microbiol **16**(8): 508-518.

Forrester, N. L., G. Palacios, R. B. Tesh, N. Savji, H. Guzman, M. Sherman, S. C. Weaver and W. I. Lipkin (2012). "Genome-scale phylogeny of the alphavirus genus suggests a marine origin." J Virol **86**(5): 2729-2738.

Fragkoudis, R., Y. Chi, R. W. C. Siu, G. Barry, G. Attarzadeh-Yazdi, A. Merits, A. A. Nash, J. K. Fazakerley and A. Kohl (2008). "Semliki Forest virus strongly reduces mosquito host defence signaling." Insect Molecular Biology **17**(6): 647-656.

Frank, C., I. Schoneberg and K. Stark (2011). "Trends in imported chikungunya virus infections in Germany, 2006-2009." Vector Borne Zoonotic Dis **11**(6): 631-636.

Franz, A. W. E., A. M. Kantor, A. L. Passarelli and R. J. Clem (2015). "Tissue Barriers to Arbovirus Infection in Mosquitoes." Viruses **7**(7): 3741-3767.

Fredericksen, B. L. and M. Gale, Jr. (2006). "West Nile virus evades activation of interferon regulatory factor 3 through RIG-I-dependent and -independent pathways without antagonizing host defense signaling." J Virol **80**(6): 2913-2923.

Fros, J. J., W. J. Liu, N. A. Prow, C. Geertsema, M. Ligtenberg, D. L. Vanlandingham, E. Schnettler, J. M. Vlak, A. Suhrbier, A. A. Khromykh and G. P. Pijlman (2010). "Chikungunya virus nonstructural protein 2 inhibits type I/II interferon-stimulated JAK-STAT signaling." J Virol **84**(20): 10877-10887.

Fros, J. J., E. van der Maten, J. M. Vlak and G. P. Pijlman (2013). "The C-terminal domain of chikungunya virus nsP2 independently governs viral RNA replication, cytopathicity, and inhibition of interferon signaling." J Virol **87**(18): 10394-10400.

Fu, J., Y. Xiong, Y. Xu, G. Cheng and H. Tang (2011). "MDA5 is SUMOylated by PIAS2beta in the upregulation of type I interferon signaling." Mol Immunol **48**(4): 415-422.

Fuscaldo, A. A., H. G. Aaslestad and E. J. Hoffman (1971). "Biological, physical, and chemical properties of Eastern equine encephalitis virus. I. Purification and physical properties." J Virol **7**(2): 233-240.

Gao, Y., N. R. Hannan, S. Wanyonyi, N. Konstantopolous, J. Pagnon, H. C. Feng, J. B. Jowett, K. H. Kim, K. Walder and G. R. Collier (2006). "Activation of the selenoprotein SEPS1 gene expression by pro-inflammatory cytokines in HepG2 cells." Cytokine **33**(5): 246-251.

Garmashova, N., R. Gorchakov, E. Frolova and I. Frolov (2006). "Sindbis Virus Nonstructural Protein nsP2 Is Cytotoxic and Inhibits Cellular Transcription." Journal of Virology **80**(12): 5686-5696.

Garmashova, N., R. Gorchakov, E. Volkova, S. Paessler, E. Frolova and I. Frolov (2007). "The Old World and New World alphaviruses use different virus-specific proteins for induction of transcriptional shutoff." J Virol **81**(5): 2472-2484.

Gaunt, M. W., A. A. Sall, X. de Lamballerie, A. K. Falconar, T. I. Dzhivanian and E. A. Gould (2001). "Phylogenetic relationships of flaviviruses correlate with their epidemiology, disease association and biogeography." J Gen Virol **82**(Pt 8): 1867-1876.

Geiss-Friedlander, R. and F. Melchior (2007). "Concepts in sumoylation: a decade on." Nat Rev Mol Cell Biol **8**(12): 947-956.

GenBank FJ042790.1. "Homo sapiens Sumo13 mRNA, complete cds." Retrieved 25.06.2018, from https://www.ncbi.nlm.nih.gov/nuccore/FJ042790.1.

Gérardin, J. A., E. A. Baise, G. A. Pire, M. P. P. Leroy and D. J. M. Desmecht (2004). "Genomic structure, organisation, and promoter analysis of the bovine (Bos taurus) Mx1 gene." Gene **326**: 67-75.

Giovannoni, F., E. B. Damonte and C. C. García (2015). "Cellular Promyelocytic Leukemia Protein Is an Important Dengue Virus Restriction Factor." PLoS ONE **10**(5): e0125690.

Girard, Y. A., K. A. Klingler and S. Higgs (2004). "West Nile virus dissemination and tissue tropisms in orally infected Culex pipiens quinquefasciatus." Vector Borne Zoonotic Dis **4**(2): 109-122.

Giraud, M. F., J. M. Desterro and J. H. Naismith (1998). "Structure of ubiquitin-conjugating enzyme 9 displays significant differences with other ubiquitin-conjugating enzymes which may reflect its specificity for sumo rather than ubiquitin." Acta Crystallogr D Biol Crystallogr **54**(Pt 5): 891-898.

Goldstein, G., M. Scheid, U. Hammerling, D. H. Schlesinger, H. D. Niall and E. A. Boyse (1975). "Isolation of a polypeptide that has lymphocyte-differentiating properties and is probably represented universally in living cells." Proc Natl Acad Sci U S A **72**(1): 11-15.

Gong, L., W. K. Ji, X. H. Hu, W. F. Hu, X. C. Tang, Z. X. Huang, L. Li, M. Liu, S. H. Xiang, E. Wu, Z. Woodward, Y. Z. Liu, Q. D. Nguyen and D. W. Li (2014). "Sumoylation differentially regulates Sp1 to control cell differentiation." Proc Natl Acad Sci U S A **111**(15): 5574-5579.

Gong, L., T. Kamitani, K. Fujise, L. S. Caskey and E. T. H. Yeh (1997). "Preferential Interaction of Sentrin with a Ubiquitin-conjugating Enzyme, Ubc9." Journal of Biological Chemistry **272**(45): 28198-28201.

Gong, L., S. Millas, G. G. Maul and E. T. Yeh (2000). "Differential regulation of sentrinized proteins by a novel sentrin-specific protease." J Biol Chem **275**(5): 3355-3359.

Gonzalez-Scarano, F., R. S. Janssen, J. A. Najjar, N. Pobjecky and N. Nathanson (1985). "An avirulent G1 glycoprotein variant of La Crosse bunyavirus with defective fusion function." J Virol **54**(3): 757-763.

Gottesman, S. (1989). "Genetics of Proteolysis in Escherichia-Coli." Annual Review of Genetics **23**: 163-198.

Grant, A., S. S. Ponia, S. Tripathi, V. Balasubramaniam, L. Miorin, M. Sourisseau, M. C. Schwarz, M. P. Sanchez-Seco, M. J. Evans, S. M. Best and A. Garcia-Sastre (2016). "Zika Virus Targets Human STAT2 to Inhibit Type I Interferon Signaling." Cell Host Microbe **19**(6): 882-890.

Gronholm, J., D. Ungureanu, S. Vanhatupa, M. Ramet and O. Silvennoinen (2010). "Sumoylation of Drosophila transcription factor STAT92E." J Innate Immun **2**(6): 618-624.

Groseth, A., C. Weisend and H. Ebihara (2012). "Complete Genome Sequencing of Mosquito and Human Isolates of Ngari Virus." Journal of Virology **86**(24): 13846-13847.

Grün, D., Y.-L. Wang, D. Langenberger, K. C. Gunsalus and N. Rajewsky (2005). "microRNA Target Predictions across Seven Drosophila Species and Comparison to Mammalian Targets." PLOS Computational Biology **1**(1): e13.

Guo, J., D. Chen, X. Gao, X. Hu, Y. Zhou, C. Wu, Y. Wang, J. Chen, R. Pei and X. Chen (2017). "Protein Inhibitor of Activated STAT2 Restricts HCV Replication by Modulating Viral Proteins Degradation." Viruses **9**(10): 285.

Guyatt, K. J., E. G. Westaway and A. A. Khromykh (2001). "Expression and purification of enzymatically active recombinant RNA-dependent RNA polymerase (NS5) of the flavivirus Kunjin." J Virol Methods **92**(1): 37-44.

Haddow, A. J., M. C. Williams, J. P. Woodall, D. I. Simpson and L. K. Goma (1964). "TWELVE ISOLATIONS OF ZIKA VIRUS FROM AEDES (STEGOMYIA) AFRICANUS (THEOBALD) TAKEN IN AND ABOVE A UGANDA FOREST." Bull World Health Organ **31**: 57-69.

Hamel, R., O. Dejarnac, S. Wichit, P. Ekchariyawat, A. Neyret, N. Luplertlop, M. Perera-Lecoin, P. Surasombatpattana, L. Talignani, F. Thomas, V. M. Cao-Lormeau, V. Choumet, L. Briant, P. Despres, A. Amara, H. Yssel and D. Misse (2015). "Biology of Zika Virus Infection in Human Skin Cells." J Virol **89**(17): 8880-8896.

Han, K.-J., L. Jiang and H.-B. Shu (2008). "Regulation of IRF2 transcriptional activity by its sumoylation." Biochemical and Biophysical Research Communications **372**(4): 772-778.

Handu, M., B. Kaduskar, R. Ravindranathan, A. Soory, R. Giri, V. B. Elango, H. Gowda and G. S. Ratnaparkhi (2015). "SUMO-Enriched Proteome for Drosophila Innate Immune Response." G3 (Bethesda) **5**(10): 2137-2154.

Hannoun, Z., G. Maarifi and M. K. Chelbi-Alix (2016). "The implication of SUMO in intrinsic and innate immunity." Cytokine & Growth Factor Reviews.

Hardeland, U., R. Steinacher, J. Jiricny and P. Schär (2002). "Modification of the human thymine-DNA glycosylase by ubiquitin-like proteins facilitates enzymatic turnover." The EMBO Journal **21**(6): 1456-1464.

Harding, H. P., I. Novoa, Y. Zhang, H. Zeng, R. Wek, M. Schapira and D. Ron (2000). "Regulated translation initiation controls stress-induced gene expression in mammalian cells." Mol Cell **6**(5): 1099-1108.

Hardy, J. L., E. J. Houk, L. D. Kramer and W. C. Reeves (1983). "Intrinsic factors affecting vector competence of mosquitoes for arboviruses." Annu Rev Entomol **28**: 229-262.

Harris, W. H. and C. W. Duval (1924). "STUDIES UPON THE ETIOLOGY OF DENGUE FEVER : I. EXPERIMENTAL TRANSMISSION TO THE LOWER ANIMAL." J Exp Med **40**(6): 817-833.

Harrison, D. A. (2012). "The JAK/STAT Pathway." Cold Spring Harbor Perspectives in Biology **4**(3): a011205.

Harrison, D. A., P. E. McCoon, R. Binari, M. Gilman and N. Perrimon (1998). "Drosophila unpaired encodes a secreted protein that activates the JAK signaling pathway." Genes Dev **12**(20): 3252-3263.

Hase, T., P. L. Summers, K. H. Eckels and W. B. Baze (1987). "An electron and immunoelectron microscopic study of dengue-2 virus infection of cultured mosquito cells: maturation events." Arch Virol **92**(3-4): 273-291.

Hase, T., P. L. Summers, K. H. Eckels and W. B. Baze (1987). "Maturation process of Japanese encephalitis virus in cultured mosquito cells in vitro and mouse brain cells in vivo." Arch Virol **96**(3-4): 135-151.

Hashiyama, K., S. Shigenobu and S. Kobayashi (2009). "Expression of genes involved in sumoylation in the Drosophila germline." Gene Expression Patterns **9**(1): 50-53.

Hay, R. T. (2005). "SUMO: A History of Modification." Molecular Cell **18**(1): 1-12.

Heaton, P. R., A. F. Deyrieux, X. L. Bian and V. G. Wilson (2011). "HPV E6 proteins target Ubc9, the SUMO conjugating enzyme." Virus Res **158**(1-2): 199-208.

Hecker, C. M., M. Rabiller, K. Haglund, P. Bayer and I. Dikic (2006). "Specification of SUMO1- and SUMO2-interacting motifs." J Biol Chem **281**(23): 16117-16127.

Heckman, K. L. and L. R. Pease (2007). "Gene splicing and mutagenesis by PCR-driven overlap extension." Nat Protoc **2**(4): 924-932.

Hertzog, J., A. G. Dias Junior, R. E. Rigby, C. L. Donald, A. Mayer, E. Sezgin, C. Song, B. Jin, P. Hublitz, C. Eggeling, A. Kohl and J. Rehwinkel (2018). "Infection with a

Brazilian isolate of Zika virus generates RIG-I stimulatory RNA and the viral NS5 protein blocks type I IFN induction and signaling." Eur J Immunol.

Hietakangas, V., J. Anckar, H. A. Blomster, M. Fujimoto, J. J. Palvimo, A. Nakai and L. Sistonen (2006). "PDSM, a motif for phosphorylation-dependent SUMO modification." Proc Natl Acad Sci U S A **103**(1): 45-50.

Hietakangas, V., J. Anckar, H. A. Blomster, M. Fujimoto, J. J. Palvimo, A. Nakai and L. Sistonen (2006). "PDSM, a motif for phosphorylation-dependent SUMO modification." Proceedings of the National Academy of Sciences **103**(1): 45-50.

Hilton, L., K. Moganeradj, G. Zhang, Y. H. Chen, R. E. Randall, J. W. McCauley and S. Goodbourn (2006). "The NPro product of bovine viral diarrhea virus inhibits DNA binding by interferon regulatory factor 3 and targets it for proteasomal degradation." J Virol **80**(23): 11723-11732.

Hochstrasser, M. (2001). "SP-RING for SUMO: New Functions Bloom for a Ubiquitin-like Protein." Cell **107**(1): 5-8.

Hochstrasser, M. (2009). "Origin and function of ubiquitin-like proteins." Nature **458**(7237): 422-429.

Hoenen, A., W. Liu, G. Kochs, A. A. Khromykh and J. M. Mackenzie (2007). "West Nile virus-induced cytoplasmic membrane structures provide partial protection against the interferon-induced antiviral MxA protein." Journal of General Virology **88**(11): 3013-3017.

Hoffman, G. R., N. J. Moerke, M. Hsia, C. E. Shamu and J. Blenis (2010). "A High-Throughput, Cell-Based Screening Method for siRNA and Small Molecule Inhibitors of mTORC1 Signaling Using the In Cell Western Technique." Assay and Drug Development Technologies **8**(2): 186-199.

Holden, P. and A. D. Hess (1959). "Cache Valley virus, a previously undescribed mosquito-borne agent." Science **130**(3383): 1187-1188.

Hölscher, C., F. Sonntag, K. Henrich, Q. Chen, J. Beneke, P. Matula, K. Rohr, L. Kaderali, N. Beil, H. Erfle, J. A. Kleinschmidt and M. Müller (2015). "The SUMOylation Pathway Restricts Gene Transduction by Adeno-Associated Viruses." PLOS Pathogens **11**(12): e1005281.

Hombría, J. C.-G., S. Brown, S. Häder and M. P. Zeidler (2005). "Characterisation of Upd2, a Drosophila JAK/STAT pathway ligand." Developmental Biology **288**(2): 420-433.

Hou, W., R. Cruz-Cosme, N. Armstrong, L. A. Obwolo, F. Wen, W. Hu, M. H. Luo and Q. Tang (2017). "Molecular cloning and characterization of the genes encoding the proteins of Zika virus." Gene **628**: 117-128.

Hou, X. S., M. B. Melnick and N. Perrimon (1996). "marelle Acts Downstream of the Drosophila HOP/JAK Kinase and Encodes a Protein Similar to the Mammalian STATs." Cell **84**(3): 411-419.

Hu, Q. and S. Chen (2013). "Cloning, genomic structure and expression analysis of ubc9 in the course of development in the half-smooth tongue sole (Cynoglossus semilaevis)." Comp Biochem Physiol B Biochem Mol Biol **165**(3): 181-188.

Huang, C. Y. H., S. Butrapet, K. J. Moss, T. Childers, S. M. Erb, A. E. Calvert, S. J. Silengo, R. M. Kinney, C. D. Blair and J. T. Roehrig (2010). "The dengue virus type 2 envelope protein fusion peptide is essential for membrane fusion." Virology **396**(2): 305-315.

Huang, H., G. Du, H. Chen, X. Liang, C. Li, N. Zhu, L. Xue, J. Ma and R. Jiao (2011). "Drosophila Smt3 negatively regulates JNK signaling through sequestering Hipk in the nucleus." Development **138**(12): 2477-2485.

Huang, T. T., S. M. Wuerzberger-Davis, Z.-H. Wu and S. Miyamoto (2003). "Sequential Modification of NEMO/IKKγ by SUMO-1 and Ubiquitin Mediates NF-κB Activation by Genotoxic Stress." Cell **115**(5): 565-576.

Huang, Y., S. Minaker, C. Roth, S. Huang, P. Hieter, V. Lipka, M. Wiermer and X. Li (2014). "An E4 ligase facilitates polyubiquitination of plant immune receptor resistance proteins in Arabidopsis." Plant Cell **26**(1): 485-496.

Hubalek, Z. (2008). "Mosquito-borne viruses in Europe." Parasitol Res **103 Suppl 1**: S29-43.

Hubalek, Z., I. Rudolf and N. Nowotny (2014). "Arboviruses pathogenic for domestic and wild animals." Adv Virus Res **89**: 201-275.

Hudson, A. M., L. N. Petrella, A. J. Tanaka and L. Cooley (2008). "Mononuclear muscle cells in Drosophila ovaries revealed by GFP protein traps." Dev Biol **314**(2): 329-340.

Hussain, M., S. Torres, E. Schnettler, A. Funk, A. Grundhoff, G. P. Pijlman, A. A. Khromykh and S. Asgari (2012). "West Nile virus encodes a microRNA-like small RNA in the 3′ untranslated region which up-regulates GATA4 mRNA and facilitates virus replication in mosquito cells." Nucleic Acids Research **40**(5): 2210-2223.

Igaki, T. (2009). "Correcting developmental errors by apoptosis: lessons from Drosophila JNK signaling." Apoptosis **14**(8): 1021-1028.

Iribarren, P. A., L. A. Di Marzio, M. A. Berazategui, J. G. De Gaudenzi and V. E. Alvarez (2018). "SUMO polymeric chains are involved in nuclear foci formation and chromatin organization in Trypanosoma brucei procyclic forms." PLoS One **13**(2): e0193528.

Jardin, C., A. H. Horn and H. Sticht (2015). "Binding properties of SUMO-interacting motifs (SIMs) in yeast." J Mol Model **21**(3): 50.

Jariyapan, N., W. Choochote, A. Jitpakdi, T. Harnnoi, P. Siriyasatein, M. C. Wilkinson, A. Junkum and P. A. Bates (2007). "Salivary gland proteins of the human malaria vector, Anopheles dirus B (Diptera: Culicidae)." Rev Inst Med Trop Sao Paulo **49**(1): 5-10.

Jiang, L., A. N. Saavedra, G. Way, J. Alanis, R. Kung, J. Li, W. Xiang and J. Liao (2014). "Specific substrate recognition and thioester intermediate determinations in ubiquitin and SUMO conjugation cascades revealed by a high-sensitive FRET assay." Mol Biosyst **10**(4): 778-786.

Jiménez-Lara, A. M., M. J. S. Heine and H. Gronemeyer (2002). "PIAS3 (protein inhibitor of activated STAT-3) modulates the transcriptional activation mediated by the nuclear receptor coactivator TIF2." FEBS Letters **526**(1-3): 142-146.

Jin, L., X. Guo, C. Shen, X. Hao, P. Sun, P. Li, T. Xu, C. Hu, O. Rose, H. Zhou, M. Yang, C.-F. Qin, J. Guo, H. Peng, M. Zhu, G. Cheng, X. Qi and R. Lai (2018). "Salivary factor LTRIN from Aedes aegypti facilitates the transmission of Zika virus by interfering with the lymphotoxin-β receptor." Nature Immunology **19**(4): 342-353.

Johnson, E. S. (2004). "Protein modification by SUMO." Annu Rev Biochem **73**: 355-382.

Johnson, E. S. and A. A. Gupta (2001). "An E3-like Factor that Promotes SUMO Conjugation to the Yeast Septins." Cell **106**(6): 735-744.

Johnson, K. M. and D. H. Martin (1974). "Venezuelan equine encephalitis." ADV.VET.SCI.COMP.MED. **vol.18**: 79-116.

Jongjitwimol, J., R. A. Baldock, S. J. Morley and F. Z. Watts (2016). "Sumoylation of eIF4A2 affects stress granule formation." Journal of Cell Science **129**(12): 2407-2415.

Joseph, J., S.-H. Tan, T. S. Karpova, J. G. McNally and M. Dasso (2002). "SUMO-1 targets RanGAP1 to kinetochores and mitotic spindles." The Journal of Cell Biology **156**(4): 595-602.

Junjhon, J., J. G. Pennington, T. J. Edwards, R. Perera, J. Lanman and R. J. Kuhn (2014). "Ultrastructural characterization and three-dimensional architecture of replication sites in dengue virus-infected mosquito cells." J Virol **88**(9): 4687-4697.

Kakumani, P. K., S. S. Ponia, R. K. S, V. Sood, M. Chinnappan, A. C. Banerjea, G. R. Medigeshi, P. Malhotra, S. K. Mukherjee and R. K. Bhatnagar (2013). "Role of RNA Interference (RNAi) in Dengue Virus Replication and Identification of NS4B as an RNAi Suppressor." Journal of Virology **87**(16): 8870-8883.

Kamitani, T., H. P. Nguyen, K. Kito, T. Fukuda-Kamitani and E. T. Yeh (1998). "Covalent modification of PML by the sentrin family of ubiquitin-like proteins." J Biol Chem **273**(6): 3117-3120.

Kamitani, T., H. P. Nguyen, K. Kito, T. Fukuda-Kamitani and E. T. H. Yeh (1998). "Covalent Modification of PML by the Sentrin Family of Ubiquitin-like Proteins." Journal of Biological Chemistry **273**(6): 3117-3120.

Kamitani, T., H. P. Nguyen and E. T. H. Yeh (1997). "Preferential Modification of Nuclear Proteins by a Novel Ubiquitin-like Molecule." Journal of Biological Chemistry **272**(22): 14001-14004.

Kaslow, R. A., L. R. Stanberry, J. W. LeDuc and SpringerLink (2014). Viral infections of humans : epidemiology and control. New York, Springer.

Kato, N., R. Dasgupta, C. T. Smartt and B. M. Christensen (2002). "Glucosamine:fructose-6-phosphate aminotransferase: gene characterization, chitin biosynthesis and peritrophic matrix formation in Aedes aegypti." Insect Mol Biol **11**(3): 207-216.

Kaukinen, P., V. Koistinen, O. Vapalahti, A. Vaheri and A. Plyusnin (2001). "Interaction between molecules of hantavirus nucleocapsid protein." J Gen Virol **82**(Pt 8): 1845-1853.

Kaur, K., H. Park, N. Pandey, Y. Azuma and R. N. De Guzman (2017). "Identification of a new small ubiquitin-like modifier (SUMO)-interacting motif in the E3 ligase PIASy." Journal of Biological Chemistry **292**(24): 10230-10238.

Kawai, T., S. Sato, K. J. Ishii, C. Coban, H. Hemmi, M. Yamamoto, K. Terai, M. Matsuda, J. Inoue, S. Uematsu, O. Takeuchi and S. Akira (2004). "Interferon-alpha induction through Toll-like receptors involves a direct interaction of IRF7 with MyD88 and TRAF6." Nat Immunol **5**(10): 1061-1068.

Kelley, L. A. and M. J. Sternberg (2009). "Protein structure prediction on the Web: a case study using the Phyre server." Nat Protoc **4**(3): 363-371.

Kerscher, O., R. Felberbaum and M. Hochstrasser (2006). "Modification of proteins by ubiquitin and ubiquitin-like proteins." Annu Rev Cell Dev Biol **22**: 159-180.

Kilpatrick, A. M. and S. E. Randolph (2012). "Drivers, dynamics, and control of emerging vector-borne zoonotic diseases." The Lancet **380**(9857): 1946-1955.

Knipe, D. M., P. M. Howley, D. Griffin, R. Lamb, M. Martin, B. Roizman and S. Straus (2007). "Fields virology, vol. 2." Philadelphia (EUA): Lippincott Williams & Wilkins: 1741-1790.

Kohl, A., R. F. Clayton, F. Weber, A. Bridgen, R. E. Randall and R. M. Elliott (2003). "Bunyamwera virus nonstructural protein NSs counteracts interferon regulatory factor 3-mediated induction of early cell death." J Virol **77**(14): 7999-8008.

Kokernot, R. H., K. C. Smithburn, B. De Meillon and H. E. Paterson (1958). "Isolation of Bunyamwera virus from a naturally infected human being and further isolations from Aedes (Banksinella) circumluteolus theo." Am J Trop Med Hyg **7**(6): 579-584.

Kotaja, N., U. Karvonen, O. A. Jänne and J. J. Palvimo (2002). "PIAS Proteins Modulate Transcription Factors by Functioning as SUMO-1 Ligases." Molecular and Cellular Biology **22**(14): 5222-5234.

Kotenko, S. V., G. Gallagher, V. V. Baurin, A. Lewis-Antes, M. Shen, N. K. Shah, J. A. Langer, F. Sheikh, H. Dickensheets and R. P. Donnelly (2003). "IFN-lambdas mediate antiviral protection through a distinct class II cytokine receptor complex." Nat Immunol **4**(1): 69-77.

Kraemer, M. U., M. E. Sinka, K. A. Duda, A. Mylne, F. M. Shearer, O. J. Brady, J. P. Messina, C. M. Barker, C. G. Moore, R. G. Carvalho, G. E. Coelho, W. Van Bortel, G. Hendrickx, F. Schaffner, G. R. Wint, I. R. Elyazar, H. J. Teng and S. I. Hay (2015). "The global compendium of Aedes aegypti and Ae. albopictus occurrence." Sci Data **2**: 150035.

Kubota, T., M. Matsuoka, T.-H. Chang, P. Tailor, T. Sasaki, M. Tashiro, A. Kato and K. Ozato (2008). "Virus Infection Triggers SUMOylation of IRF3 and IRF7, Leading to the Negative Regulation of Type I Interferon Gene Expression." Journal of Biological Chemistry **283**(37): 25660-25670.

Kujala, P., A. Ikaheimonen, N. Ehsani, H. Vihinen, P. Auvinen and L. Kaariainen (2001). "Biogenesis of the Semliki Forest virus RNA replication complex." J Virol **75**(8): 3873-3884.

Kuno, G., G.-J. J. Chang, K. R. Tsuchiya, N. Karabatsos and C. B. Cropp (1998). "Phylogeny of the Genus Flavivirus." Journal of Virology **72**(1): 73-83.

Landis, H., A. Simon-Jodicke, A. Kloti, C. Di Paolo, J. J. Schnorr, S. Schneider-Schaulies, H. P. Hefti and J. Pavlovic (1998). "Human MxA protein confers resistance to Semliki Forest virus and inhibits the amplification of a Semliki Forest virus-based replicon in the absence of viral structural proteins." J Virol **72**(2): 1516-1522.

Lappin, D. F., G. W. Nakitare, J. W. Palfreyman and R. M. Elliott (1994). "Localization of Bunyamwera bunyavirus G1 glycoprotein to the Golgi requires association with G2 but not with NSm." J Gen Virol **75 (Pt 12)**: 3441-3451.

Lednicky, J. A., S. K. White, C. J. Stephenson, K. Cherabuddi, J. C. Loeb, N. Moussatche, A. Lednicky and J. J. G. Morris (2018). "Keystone Virus Isolated From a Florida Teenager With Rash and Subjective Fever: Another Endemic Arbovirus in the Southeastern United States?" Clinical Infectious Diseases: ciy485-ciy485.

Lee, B. H., K. Yoshimatsu, A. Maeda, K. Ochiai, M. Morimatsu, K. Araki, M. Ogino, S. Morikawa and J. Arikawa (2003). "Association of the nucleocapsid protein of the Seoul and Hantaan hantaviruses with small ubiquitin-like modifier-1-related molecules." Virus Res **98**(1): 83-91.

Lee, Moon H., Angela M. Mabb, Grace B. Gill, Edward T. H. Yeh and S. Miyamoto (2011). "NF-κB Induction of the SUMO Protease SENP2: A Negative Feedback Loop to Attenuate Cell Survival Response to Genotoxic Stress." Molecular Cell **43**(2): 180-191.

Lees, J. F., C. R. Pringle and R. M. Elliott (1986). "Nucleotide sequence of the Bunyamwera virus M RNA segment: conservation of structural features in the Bunyavirus glycoprotein gene product." Virology **148**(1): 1-14.

Lehembre, F., P. Badenhorst, S. Müller, A. Travers, F. Schweisguth and A. Dejean (2000). "Covalent Modification of the Transcriptional Repressor Tramtrack by the Ubiquitin-Related Protein Smt3 in Drosophila Flies." Molecular and Cellular Biology **20**(3): 1072-1082.

Lemaitre, B., E. Nicolas, L. Michaut, J.-M. Reichhart and J. A. Hoffmann (1996). "The Dorsoventral Regulatory Gene Cassette spätzle/Toll/cactus Controls the Potent Antifungal Response in Drosophila Adults." Cell **86**(6): 973-983.

Léonard , V. H. J., A. Kohl, T. J. Hart and R. M. Elliott (2006). "Interaction of Bunyamwera Orthobunyavirus NSs Protein with Mediator Protein MED8: a Mechanism for Inhibiting the Interferon Response." Journal of Virology **80**(19): 9667-9675.

Lequime, S. and L. Lambrechts (2014). "Vertical transmission of arboviruses in mosquitoes: a historical perspective." Infect Genet Evol **28**: 681-690.

Leung, J. Y., M. M. Ng and J. J. Chu (2011). "Replication of alphaviruses: a review on the entry process of alphaviruses into cells." Adv Virol **2011**: 249640.

Li, F. Q., H. Xiao, J. P. Tam and D. X. Liu (2005). "Sumoylation of the nucleocapsid protein of severe acute respiratory syndrome coronavirus." FEBS Lett **579**(11): 2387-2396.

Li, G. and C. M. Rice (1993). "The signal for translational readthrough of a UGA codon in Sindbis virus RNA involves a single cytidine residue immediately downstream of the termination codon." J Virol **67**(8): 5062-5067.

Li, S.-J. and M. Hochstrasser (1999). "A new protease required for cell-cycle progression in yeast." Nature **398**: 246.

Li, S. J. and M. Hochstrasser (2000). "The yeast ULP2 (SMT4) gene encodes a novel protease specific for the ubiquitin-like Smt3 protein." Mol Cell Biol **20**(7): 2367-2377.

Liang, Q., Z. Luo, J. Zeng, W. Chen, S. S. Foo, S. A. Lee, J. Ge, S. Wang, S. A. Goldman, B. V. Zlokovic, Z. Zhao and J. U. Jung (2016). "Zika Virus NS4A and NS4B Proteins Deregulate Akt-mTOR Signaling in Human Fetal Neural Stem Cells to Inhibit Neurogenesis and Induce Autophagy." Cell Stem Cell **19**(5): 663-671.

Liang, Y. C., C. C. Lee, Y. L. Yao, C. C. Lai, M. L. Schmitz and W. M. Yang (2016). "SUMO5, a Novel Poly-SUMO Isoform, Regulates PML Nuclear Bodies." Sci Rep **6**: 26509.

Lima, C. D. and D. Reverter (2008). "Structure of the human SENP7 catalytic domain and poly-SUMO deconjugation activities for SENP6 and SENP7." J Biol Chem **283**(46): 32045-32055.

Lin, C.-C., C.-M. Chou, Y.-L. Hsu, J.-C. Lien, Y.-M. Wang, S.-T. Chen, S.-C. Tsai, P.-W. Hsiao and C.-J. Huang (2004). "Characterization of Two Mosquito STATs, AaSTAT and CtSTAT: DIFFERENTIAL REGULATION OF TYROSINE PHOSPHORYLATION AND DNA

BINDING ACTIVITY BY LIPOPOLYSACCHARIDE TREATMENT AND BY JAPANESE ENCEPHALITIS VIRUS INFECTION." Journal of Biological Chemistry **279**(5): 3308-3317.

Liu, B., M. Gross, J. ten Hoeve and K. Shuai (2001). "A transcriptional corepressor of Stat1 with an essential LXXLL signature motif." Proceedings of the National Academy of Sciences **98**(6): 3203-3207.

Liu, B., J. Liao, X. Rao, S. A. Kushner, C. D. Chung, D. D. Chang and K. Shuai (1998). "Inhibition of Stat1-mediated gene activation by PIAS1." Proceedings of the National Academy of Sciences of the United States of America **95**(18): 10626-10631.

Liu, B., J. Liao, X. Rao, S. A. Kushner, C. D. Chung, D. D. Chang and K. Shuai (1998). "Inhibition of Stat1-mediated gene activation by PIAS1." Proc Natl Acad Sci U S A **95**(18): 10626-10631.

Liu, B., S. Mink, K. A. Wong, N. Stein, C. Getman, P. W. Dempsey, H. Wu and K. Shuai (2004). "PIAS1 selectively inhibits interferon-inducible genes and is important in innate immunity." Nature Immunology **5**: 891.

Liu, H., X.-q. Shao, B. Hu, J.-j. Zhao, L. Zhang, H.-l. Zhang, X. Bai, R.-x. Zhang, D.-y. Niu, Y.-g. Sun and X.-j. Yan (2014). "Isolation and complete nucleotide sequence of a Batai virus strain in Inner Mongolia, China." Virology Journal **11**: 138-138.

Liu, Q., C. Jin, X. Liao, Z. Shen, D. J. Chen and Y. Chen (1999). "The Binding Interface between an E2 (UBC9) and a Ubiquitin Homologue (UBL1)." Journal of Biological Chemistry **274**(24): 16979-16987.

Liu, R., R. C. McEachin and D. J. States (2003). "Computationally Identifying Novel NF-κB-Regulated Immune Genes in the Human Genome." Genome Research **13**(4): 654-661.

Liu, W., Y. Xie, J. Ma, X. Luo, P. Nie, Z. Zuo, U. Lahrmann, Q. Zhao, Y. Zheng, Y. Zhao, Y. Xue and J. Ren (2015). "IBS: an illustrator for the presentation and visualization of biological sequences." Bioinformatics **31**(20): 3359-3361.

Liu, W. J., H. B. Chen, X. J. Wang, H. Huang and A. A. Khromykh (2004). "Analysis of Adaptive Mutations in Kunjin Virus Replicon RNA Reveals a Novel Role for the Flavivirus Nonstructural Protein NS2A in Inhibition of Beta Interferon Promoter-Driven Transcription." Journal of Virology **78**(22): 12225-12235.

Lloyd, R. E. (2012). "How Do Viruses Interact with Stress-Associated RNA Granules?" PLoS Pathogens **8**(6): e1002741.

Lobigs, M., H. X. Zhao and H. Garoff (1990). "Function of Semliki Forest virus E3 peptide in virus assembly: replacement of E3 with an artificial signal peptide abolishes spike heterodimerization and surface expression of E1." J Virol **64**(9): 4346-4355.

Lois, L. M. and C. D. Lima (2005). "Structures of the SUMO E1 provide mechanistic insights into SUMO activation and E2 recruitment to E1." EMBO J **24**(3): 439-451.

Lowrey, A. J., W. Cramblet and G. L. Bentz (2017). "Viral manipulation of the cellular sumoylation machinery." Cell Communication and Signaling **15**(1): 27.

Lundstrom, J. O. (1999). "Mosquito-borne viruses in western Europe: a review." J Vector Ecol **24**(1): 1-39.

Lyst, M. J. and I. Stancheva (2007). "A role for SUMO modification in transcriptional repression and activation." Biochemical Society transactions **35**(Pt 6): 1389-1392.

Mabb, A. M., S. M. Wuerzberger-Davis and S. Miyamoto (2006). "PIASy mediates NEMO sumoylation and NF-κB activation in response to genotoxic stress." Nature Cell Biology **8**: 986.

Mackenzie, J. S., D. J. Gubler and L. R. Petersen (2004). "Emerging flaviviruses: the spread and resurgence of Japanese encephalitis, West Nile and dengue viruses." Nature Medicine **10**: S98.

Macpherson, I. and M. Stoker (1962). "Polyoma transformation of hamster cell clones--an investigation of genetic factors affecting cell competence." Virology **16**: 147-151.

Maeda, A., B. H. Lee, K. Yoshimatsu, M. Saijo, I. Kurane, J. Arikawa and S. Morikawa (2003). "The intracellular association of the nucleocapsid protein (NP) of hantaan virus (HTNV) with small ubiquitin-like modifier-1 (SUMO-1) conjugating enzyme 9 (Ubc9)." Virology **305**(2): 288-297.

Mancini, E. J., M. Clarke, B. E. Gowen, T. Rutten and S. D. Fuller (2000). "Cryo-electron microscopy reveals the functional organization of an enveloped virus, Semliki Forest virus." Mol Cell **5**(2): 255-266.

Manokaran, G., E. Finol, C. Wang, J. Gunaratne, J. Bahl, E. Z. Ong, H. C. Tan, O. M. Sessions, A. M. Ward, D. J. Gubler, E. Harris, M. A. Garcia-Blanco and E. E. Ooi (2015). "Dengue subgenomic RNA binds TRIM25 to inhibit interferon expression for epidemiological fitness." Science **350**(6257): 217-221.

Mansfield, K. L., N. Johnson, S. L. Cosby, T. Solomon and A. R. Fooks (2010). "Transcriptional upregulation of SOCS 1 and suppressors of cytokine signaling 3 mRNA in the absence of suppressors of cytokine signaling 2 mRNA after infection with West Nile virus or tick-borne encephalitis virus." Vector Borne Zoonotic Dis **10**(7): 649-653.

Markoff, L. (1989). "In vitro processing of dengue virus structural proteins: cleavage of the pre-membrane protein." Journal of Virology **63**(8): 3345-3352.

Martinez, J., A. Patkaniowska, H. Urlaub, R. Lührmann and T. Tuschl (2002). "Single-Stranded Antisense siRNAs Guide Target RNA Cleavage in RNAi." Cell **110**(5): 563-574.

Matic, I., J. Schimmel, I. A. Hendriks, M. A. van Santen, F. van de Rijke, H. van Dam, F. Gnad, M. Mann and A. C. Vertegaal (2010). "Site-specific identification of SUMO-2 targets in cells reveals an inverted SUMOylation motif and a hydrophobic cluster SUMOylation motif." Molecular cell **39**(4): 641-652.

Matic, I., J. Schimmel, I. A. Hendriks, M. A. van Santen, F. van de Rijke, H. van Dam, F. Gnad, M. Mann and A. C. Vertegaal (2010). "Site-specific identification of SUMO-2 targets in cells reveals an inverted SUMOylation motif and a hydrophobic cluster SUMOylation motif." Mol Cell **39**(4): 641-652.

Matic, I., M. van Hagen, J. Schimmel, B. Macek, S. C. Ogg, M. H. Tatham, R. T. Hay, A. I. Lamond, M. Mann and A. C. O. Vertegaal (2008). "In vivo identification of human small ubiquitin-like modifier polymerization sites by high accuracy mass spectrometry and an in vitro to in vivo strategy." Mol Cell Proteomics **7**(1): 132-144.

Matranga, C., Y. Tomari, C. Shin, D. P. Bartel and P. D. Zamore (2005). "Passenger-strand cleavage facilitates assembly of siRNA into Ago2-containing RNAi enzyme complexes." Cell **123**(4): 607-620.

Mattingly, P. F. (1967). "Aedes aegypti and other mosquitos in relation to the dengue syndrome." Bulletin of the World Health Organization **36**(4): 533-535.

Matunis, M. J., E. Coutavas and G. Blobel (1996). "A novel ubiquitin-like modification modulates the partitioning of the Ran-GTPase-activating protein RanGAP1 between the cytosol and the nuclear pore complex." J Cell Biol **135**(6 Pt 1): 1457-1470.

Matunis, M. J., J. Wu and G. Blobel (1998). "SUMO-1 modification and its role in targeting the Ran GTPase-activating protein, RanGAP1, to the nuclear pore complex." J Cell Biol **140**(3): 499-509.

Maul, G. G., A. M. Ishov and R. D. Everett (1996). "Nuclear Domain 10 as Preexisting Potential Replication Start Sites of Herpes Simplex Virus Type-1." Virology **217**(1): 67-75.

Mazzon, M., M. Jones, A. Davidson, B. Chain and M. Jacobs (2009). "Dengue virus NS5 inhibits interferon-alpha signaling by blocking signal transducer and activator of transcription 2 phosphorylation." J Infect Dis **200**(8): 1261-1270.

McFarlane, M., C. Arias-Goeta, E. Martin, Z. O'Hara, A. Lulla, L. Mousson, S. M. Rainey, S. Misbah, E. Schnettler, C. L. Donald, A. Merits, A. Kohl and A. B. Failloux (2014). "Characterization of Aedes aegypti innate-immune pathways that limit Chikungunya virus replication." PLoS Negl Trop Dis **8**(7): e2994.

McInerney, G. M., N. L. Kedersha, R. J. Kaufman, P. Anderson and P. Liljestrom (2005). "Importance of eIF2alpha phosphorylation and stress granule assembly in alphavirus translation regulation." Mol Biol Cell **16**(8): 3753-3763.

Melancon, P. and H. Garoff (1987). "Processing of the Semliki Forest virus structural polyprotein: role of the capsid protease." J Virol **61**(5): 1301-1309.

Mellor, P. S. (2000). "Replication of arboviruses in insect vectors." J Comp Pathol **123**(4): 231-247.

Merrill, J. C., T. A. Melhuish, M. H. Kagey, S.-H. Yang, A. D. Sharrocks and D. Wotton (2010). "A Role for Non-Covalent SUMO Interaction Motifs in Pc2/CBX4 E3 Activity." PLOS ONE **5**(1): e8794.

Mi, Z., J. Fu, Y. Xiong and H. Tang (2010). "SUMOylation of RIG-I positively regulates the type I interferon signaling." Protein & Cell **1**(3): 275-283.

Mi, Z., J. Fu, Y. Xiong and H. Tang (2010). "SUMOylation of RIG-I positively regulates the type I interferon signaling." Protein Cell **1**(3): 275-283.

Miller, S., S. Sparacio and R. Bartenschlager (2006). "Subcellular localization and membrane topology of the Dengue virus type 2 Non-structural protein 4B." J Biol Chem **281**(13): 8854-8863.

Minty, A., X. Dumont, M. Kaghad and D. Caput (2000). "Covalent modification of p73alpha by SUMO-1. Two-hybrid screening with p73 identifies novel SUMO-1-interacting proteins and a SUMO-1 interaction motif." J Biol Chem **275**(46): 36316-36323.

Miteva, M., K. Keusekotten, K. Hofmann, G. J. Praefcke and R. J. Dohmen (2010). "Sumoylation as a signal for polyubiquitylation and proteasomal degradation." Subcell Biochem **54**: 195-214.

Mohideen, F., A. D. Capili, P. M. Bilimoria, T. Yamada, A. Bonni and C. D. Lima (2009). "A molecular basis for phosphorylation-dependent SUMO conjugation by the E2 UBC9." Nature structural & molecular biology **16**(9): 945.

Moon, S. L., B. J. T. Dodd, D. E. Brackney, C. J. Wilusz, G. D. Ebel and J. Wilusz (2015). "Flavivirus sfRNA suppresses antiviral RNA interference in cultured cells and mosquitoes and directly interacts with the RNAi machinery." Virology **485**: 322-329.

Moro, M. L., C. Gagliotti, G. Silvi, R. Angelini, V. Sambri, G. Rezza, E. Massimiliani, A. Mattivi, E. Grilli, A. C. Finarelli, N. Spataro, A. M. Pierro, T. Seyler and P. Macini (2010). "Chikungunya Virus in North-Eastern Italy: A Seroprevalence Survey." The American Journal of Tropical Medicine and Hygiene **82**(3): 508-511.

Morrison, J., M. Laurent-Rolle, A. M. Maestre, R. Rajsbaum, G. Pisanelli, V. Simon, L. C. F. Mulder, A. Fernandez-Sesma and A. García-Sastre (2013). "Dengue Virus Co-opts UBR4 to Degrade STAT2 and Antagonize Type I Interferon Signaling." PLOS Pathogens **9**(3): e1003265.

Mossessova, E. and C. D. Lima (2000). "Ulp1-SUMO Crystal Structure and Genetic Analysis Reveal Conserved Interactions and a Regulatory Element Essential for Cell Growth in Yeast." Molecular Cell **5**(5): 865-876.

Mossman, K. L., H. A. Saffran and J. R. Smiley (2000). "Herpes Simplex Virus ICP0 Mutants Are Hypersensitive to Interferon." Journal of Virology **74**(4): 2052-2056.

Muaddi, H., M. Majumder, P. Peidis, A. I. Papadakis, M. Holcik, D. Scheuner, R. J. Kaufman, M. Hatzoglou and A. E. Koromilas (2010). "Phosphorylation of eIF2α at Serine 51 Is an Important Determinant of Cell Survival and Adaptation to Glucose Deficiency." Molecular Biology of the Cell **21**(18): 3220-3231.

Mullen, J. R. and S. J. Brill (2008). "Activation of the Slx5-Slx8 ubiquitin ligase by poly-small ubiquitin-like modifier conjugates." J Biol Chem **283**(29): 19912-19921.

Muller, S., C. Hoege, G. Pyrowolakis and S. Jentsch (2001). "SUMO, ubiquitin's mysterious cousin." Nat Rev Mol Cell Biol **2**(3): 202-210.

Muñoz-Jordán, J. L., G. G. Sánchez-Burgos, M. Laurent-Rolle and A. García-Sastre (2003). "Inhibition of interferon signaling by dengue virus." Proceedings of the National Academy of Sciences **100**(24): 14333-14338.

Mustafa, M. S., V. Rasotgi, S. Jain and V. Gupta (2015). "Discovery of fifth serotype of dengue virus (DENV-5): A new public health dilemma in dengue control." Medical Journal, Armed Forces India **71**(1): 67-70.

Mutebi, J. P., R. C. Rijnbrand, H. Wang, K. D. Ryman, E. Wang, L. D. Fulop, R. Titball and A. D. Barrett (2004). "Genetic relationships and evolution of genotypes of yellow fever virus and other members of the yellow fever virus group within the Flavivirus genus based on the 3' noncoding region." J Virol **78**(18): 9652-9665.

Mutso, M., S. Saul, K. Rausalu, O. Susova, E. Žusinaite, S. Mahalingam and A. Merits (2017). "Reverse genetic system, genetically stable reporter viruses and packaged subgenomic replicon based on a Brazilian Zika virus isolate." Journal of General Virology **98**(11): 2712-2724.

Myles, K. M., M. R. Wiley, E. M. Morazzani and Z. N. Adelman (2008). "Alphavirus-derived small RNAs modulate pathogenesis in disease vector mosquitoes." Proceedings of the National Academy of Sciences **105**(50): 19938-19943.

Nakagawa, K. and H. Yokosawa (2002). "PIAS3 induces SUMO-1 modification and transcriptional repression of IRF-1." FEBS Lett **530**(1-3): 204-208.

Namanja, A. T., Y. J. Li, Y. Su, S. Wong, J. Lu, L. T. Colson, C. Wu, S. S. Li and Y. Chen (2012). "Insights into high affinity small ubiquitin-like modifier (SUMO) recognition by SUMO-interacting motifs (SIMs) revealed by a combination of NMR and peptide array analysis." J Biol Chem **287**(5): 3231-3240.

Nashed, N. W., J. G. Olson and A. El-Tigani (1993). "Isolation of Batai Virus (Bunyaviridae:Bunyavirus) from the Blood of Suspected Malaria Patients in Sudan." The American Journal of Tropical Medicine and Hygiene **48**(5): 676-681.

Nayak, A. and S. Muller (2014). "SUMO-specific proteases/isopeptidases: SENPs and beyond." Genome Biol **15**(7): 422.

Newton, S. E., N. J. Short and L. Dalgarno (1981). "Bunyamwera Virus Replication in Cultured Aedes albopictus (Mosquito) Cells: Establishment of a Persistent Viral Infection." Journal of Virology **38**(3): 1015-1024.

NHS. (2016). "Japanese encephalitis." Retrieved 21/06/2018, from https://www.nhs.uk/conditions/japanese-encephalitis/.

Nicholson, A. (1921). "The Development of the Ovary and Ovarien Egg of a Mosquito, Anopheles Maculipennis." Meig. Ibid **65**.

Nicolas, E., J. M. Reichhart, J. A. Hoffmann and B. Lemaitre (1998). "In Vivo Regulation of the IκB Homologuecactus during the Immune Response ofDrosophila." Journal of Biological Chemistry **273**(17): 10463-10469.

Nie, M., Y. Xie, J. A. Loo and A. J. Courey (2009). "Genetic and proteomic evidence for roles of Drosophila SUMO in cell cycle control, Ras signaling, and early pattern formation." PLoS One **4**(6): e5905.

Nir, Y., R. Goldwasser, Y. Lasowski and J. Margalit (1968). "Isolation of West Nile virus strains from mosquitoes in Israel." Am J Epidemiol **87**(2): 496-501.

Notredame, C., D. G. Higgins and J. Heringa (2000). "T-Coffee: A novel method for fast and accurate multiple sequence alignment." J Mol Biol **302**(1): 205-217.

Obijeski, J. F., D. H. Bishop, F. A. Murphy and E. L. Palmer (1976). "Structural proteins of La Crosse virus." Journal of Virology **19**(3): 985-997.

Oehler, E., L. Watrin, P. Larre, I. Leparc-Goffart, S. Lastere, F. Valour, L. Baudouin, H. Mallet, D. Musso and F. Ghawche (2014). "Zika virus infection complicated by Guillain-Barre syndrome--case report, French Polynesia, December 2013." Euro Surveill **19**(9).

Okuda, K., A. de Souza Caroci, P. E. Ribolla, A. G. de Bianchi and A. T. Bijovsky (2002). "Functional morphology of adult female Culex quinquefasciatus midgut during blood digestion." Tissue Cell **34**(3): 210-219.

Olsen, S. K., A. D. Capili, X. Lu, D. S. Tan and C. D. Lima (2010). "Active site remodelling accompanies thioester bond formation in the SUMO E1." Nature **463**(7283): 906-912.

Olson, K. E. and C. D. Blair (2015). "Arbovirus-mosquito Interactions: RNAi Pathway." Current opinion in virology **15**: 119-126.

Onomoto, K., M. Jogi, J.-S. Yoo, R. Narita, S. Morimoto, A. Takemura, S. Sambhara, A. Kawaguchi, S. Osari, K. Nagata, T. Matsumiya, H. Namiki, M. Yoneyama and T. Fujita (2012). "Critical Role of an Antiviral Stress Granule Containing RIG-I and PKR in Viral Detection and Innate Immunity." PLOS ONE **7**(8): e43031.

Överby, A. K., R. F. Pettersson and E. P. A. Neve (2007). "The Glycoprotein Cytoplasmic Tail of Uukuniemi Virus (Bunyaviridae) Interacts with Ribonucleoproteins and Is Critical for Genome Packaging." Journal of Virology **81**(7): 3198-3205.

Överby, A. K., V. L. Popov, M. Niedrig and F. Weber (2010). "Tick-Borne Encephalitis Virus Delays Interferon Induction and Hides Its Double-Stranded RNA in Intracellular Membrane Vesicles." Journal of Virology **84**(17): 8470-8483.

Panas, M. D., M. Varjak, A. Lulla, K. Er Eng, A. Merits, G. B. Karlsson Hedestam and G. M. McInerney (2012). "Sequestration of G3BP coupled with efficient translation

inhibits stress granules in Semliki Forest virus infection." Molecular Biology of the Cell **23**(24): 4701-4712.

Paradkar, P. N., J.-B. Duchemin, R. Voysey and P. J. Walker (2014). "Dicer-2-Dependent Activation of Culex Vago Occurs via the TRAF-Rel2 Signaling Pathway." PLOS Neglected Tropical Diseases **8**(4): e2823.

Paradkar, P. N., L. Trinidad, R. Voysey, J.-B. Duchemin and P. J. Walker (2012). "Secreted Vago restricts West Nile virus infection in Culex mosquito cells by activating the Jak-STAT pathway." Proceedings of the National Academy of Sciences **109**(46): 18915-18920.

Paradkar, P. N., L. Trinidad, R. Voysey, J. B. Duchemin and P. J. Walker (2012). "Secreted Vago restricts West Nile virus infection in Culex mosquito cells by activating the Jak-STAT pathway." Proc Natl Acad Sci U S A **109**(46): 18915-18920.

Paredes, A., S. Weaver, S. Watowich and W. Chiu (2005). "Structural biology of old world and new world alphaviruses." Arch Virol Suppl(19): 179-185.

Parikh, G. R., J. D. Oliver and L. C. Bartholomay (2009). "A haemocyte tropism for an arbovirus." J Gen Virol **90**(Pt 2): 292-296.

Pearce, M. J., J. Mintseris, J. Ferreyra, S. P. Gygi and K. H. Darwin (2008). "Ubiquitin-Like Protein Involved in the Proteasome Pathway of Mycobacterium tuberculosis." Science (New York, N.Y.) **322**(5904): 1104-1107.

Peleg, J. (1968). "Growth of arboviruses in monolayers from subcultured mosquito embryo cells." Virology **35**(4): 617-619.

Peleg, J. (1968). "Growth of arboviruses in primary tissue culture of Aedes aegypti embryos." Am J Trop Med Hyg **17**(2): 219-223.

Peranen, J., M. Rikkonen, P. Liljestrom and L. Kaariainen (1990). "Nuclear localization of Semliki Forest virus-specific nonstructural protein nsP2." J Virol **64**(5): 1888-1896.

Perez-Cidoncha, M., M. J. Killip, J. C. Oliveros, V. J. Asensio, Y. Fernandez, J. A. Bengoechea, R. E. Randall and J. Ortin (2014). "An unbiased genetic screen reveals the polygenic nature of the influenza virus anti-interferon response." J Virol **88**(9): 4632-4646.

Perrone, J. B. and A. Spielman (1988). "Time and site of assembly of the peritrophic membrane of the mosquito Aedes aegypti." Cell Tissue Res **252**(2): 473-478.

Pettersen, E. F., T. D. Goddard, C. C. Huang, G. S. Couch, D. M. Greenblatt, E. C. Meng and T. E. Ferrin (2004). "UCSF Chimera--a visualization system for exploratory research and analysis." J Comput Chem **25**(13): 1605-1612.

Pfander, B., G. L. Moldovan, M. Sacher, C. Hoege and S. Jentsch (2005). "SUMO-modified PCNA recruits Srs2 to prevent recombination during S phase." Nature **436**(7049): 428-433.

Pham, J. W., J. L. Pellino, Y. S. Lee, R. W. Carthew and E. J. Sontheimer (2004). "A Dicer-2-dependent 80s complex cleaves targeted mRNAs during RNAi in Drosophila." Cell **117**(1): 83-94.

Phattanawiboon, B., N. Jariyapan, S. Roytrakul, A. Paemanee, S. Sor-suwan, N. Intakhan, W. Chanmol, P. Siriyasatien, A. Saeung and W. Choochote (2014). "Morphological and protein analyses of adult female salivary glands of Anopheles barbirostris species A1 (Diptera: Culicidae)." Trop Biomed **31**(4): 813-827.

Piccini, L. E., V. Castilla and E. B. Damonte (2015). "Dengue-3 Virus Entry into Vero Cells: Role of Clathrin-Mediated Endocytosis in the Outcome of Infection." PLOS ONE **10**(10): e0140824.

Pichler, A., A. Gast, J. S. Seeler, A. Dejean and F. Melchior (2002). "The nucleoporin RanBP2 has SUMO1 E3 ligase activity." Cell **108**(1): 109-120.

Pickart, C. M. (2001). "Mechanisms underlying ubiquitination." Annu Rev Biochem **70**: 503-533.

Pickart, C. M. and M. J. Eddins (2004). "Ubiquitin: structures, functions, mechanisms." Biochim Biophys Acta **1695**(1-3): 55-72.

Pingen, M., S. R. Bryden, E. Pondeville, E. Schnettler, A. Kohl, A. Merits, J. K. Fazakerley, G. J. Graham and C. S. McKimmie (2016). "Host Inflammatory Response to

Mosquito Bites Enhances the Severity of Arbovirus Infection." Immunity **44**(6): 1455-1469.

Pompon, J., M. Manuel, G. K. Ng, B. Wong, C. Shan, G. Manokaran, R. Soto-Acosta, S. S. Bradrick, E. E. Ooi, D. Missé, P.-Y. Shi and M. A. Garcia-Blanco (2017). "Dengue subgenomic flaviviral RNA disrupts immunity in mosquito salivary glands to increase virus transmission." PLOS Pathogens **13**(7): e1006535.

Powers, A. M., A. C. Brault, Y. Shirako, E. G. Strauss, W. Kang, J. H. Strauss and S. C. Weaver (2001). "Evolutionary relationships and systematics of the alphaviruses." J Virol **75**(21): 10118-10131.

Powers, A. M. and C. H. Logue (2007). "Changing patterns of chikungunya virus: re-emergence of a zoonotic arbovirus." Journal of General Virology **88**(9): 2363-2377.

Prudden, J., S. Pebernard, G. Raffa, D. A. Slavin, J. J. Perry, J. A. Tainer, C. H. McGowan and M. N. Boddy (2007). "SUMO-targeted ubiquitin ligases in genome stability." EMBO J **26**(18): 4089-4101.

Ramirez, J. L. and G. Dimopoulos (2010). "The Toll immune signaling pathway control conserved anti-dengue defenses across diverse Ae. aegypti strains and against multiple dengue virus serotypes." Developmental & Comparative Immunology **34**(6): 625-629.

Ramirez, J. L., J. Souza-Neto, R. Torres Cosme, J. Rovira, A. Ortiz, J. M. Pascale and G. Dimopoulos (2012). "Reciprocal Tripartite Interactions between the Aedes aegypti Midgut Microbiota, Innate Immune System and Dengue Virus Influences Vector Competence." PLOS Neglected Tropical Diseases **6**(3): e1561.

Rand, T. A., S. Petersen, F. Du and X. Wang (2005). "Argonaute2 cleaves the anti-guide strand of siRNA during RISC activation." Cell **123**(4): 621-629.

Raquin, V., M. Wannagat, K. Zouache, C. Legras-Lachuer, C. V. Moro and P. Mavingui (2012). "Detection of dengue group viruses by fluorescence in situ hybridization." Parasit Vectors **5**: 243.

Rasmussen, S. A., D. J. Jamieson, M. A. Honein and L. R. Petersen (2016). "Zika Virus and Birth Defects--Reviewing the Evidence for Causality." N Engl J Med **374**(20): 1981-1987.

Rechsteiner, M. (1988). Ubiquitin, Plenum.

Reindle, A., I. Belichenko, G. R. Bylebyl, X. L. Chen, N. Gandhi and E. S. Johnson (2006). "Multiple domains in Siz SUMO ligases contribute to substrate selectivity." Journal of Cell Science **119**(22): 4749-4757.

Reineke, L. C., N. Kedersha, M. A. Langereis, F. J. M. van Kuppeveld and R. E. Lloyd (2015). "Stress Granules Regulate Double-Stranded RNA-Dependent Protein Kinase Activation through a Complex Containing G3BP1 and Caprin1." mBio **6**(2).

Reineke, L. C. and R. E. Lloyd (2015). "The Stress Granule Protein G3BP1 Recruits Protein Kinase R To Promote Multiple Innate Immune Antiviral Responses." Journal of Virology **89**(5): 2575-2589.

Ren, J., L. Wen, X. Gao, C. Jin, Y. Xue and X. Yao (2009). "DOG 1.0: illustrator of protein domain structures." Cell Res **19**(2): 271-273.

Riedel, B. and D. T. Brown (1979). "Novel antiviral activity found in the media of Sindbis virus-persistently infected mosquito (Aedes albopictus) cell cultures." Journal of Virology **29**(1): 51-60.

Rivas, F., L. A. Diaz, V. M. Cardenas, E. Daza, L. Bruzon, A. Alcala, O. De la Hoz, F. M. Caceres, G. Aristizabal, J. W. Martinez, D. Revelo, F. De la Hoz, J. Boshell, T. Camacho, L. Calderon, V. A. Olano, L. I. Villarreal, D. Roselli, G. Alvarez, G. Ludwig and T. Tsai (1997). "Epidemic Venezuelan equine encephalitis in La Guajira, Colombia, 1995." J Infect Dis **175**(4): 828-832.

Rodriguez, M. S., C. Dargemont and R. T. Hay (2001). "SUMO-1 conjugation in vivo requires both a consensus modification motif and nuclear targeting." J Biol Chem **276**(16): 12654-12659.

Rogers, R. S., C. M. Horvath and M. J. Matunis (2003). "SUMO Modification of STAT1 and Its Role in PIAS-mediated Inhibition of Gene Activation." Journal of Biological Chemistry **278**(32): 30091-30097.

Ronau, J. A., J. F. Beckmann and M. Hochstrasser (2016). "Substrate specificity of the ubiquitin and Ubl proteases." Cell Research **26**(4): 441-456.

Rosen, L. (1988). "Further observations on the mechanism of vertical transmission of flaviviruses by Aedes mosquitoes." Am J Trop Med Hyg **39**(1): 123-126.

Rotin, D. and S. Kumar (2009). "Physiological functions of the HECT family of ubiquitin ligases." Nat Rev Mol Cell Biol **10**(6): 398-409.

Royle, J., C. L. Donald, A. Merits, A. Kohl and M. Varjak (2017). "Differential effects of lipid biosynthesis inhibitors on Zika and Semliki Forest viruses." Vet J **230**: 62-64.

Rytinki, M. M., S. Kaikkonen, P. Pehkonen, T. Jääskeläinen and J. J. Palvimo (2009). "PIAS proteins: pleiotropic interactors associated with SUMO." Cellular and Molecular Life Sciences **66**(18): 3029.

Sachdev, S., L. Bruhn, H. Sieber, A. Pichler, F. Melchior and R. Grosschedl (2001). "PIASy, a nuclear matrix-associated SUMO E3 ligase, represses LEF1 activity by sequestration into nuclear bodies." Genes Dev **15**(23): 3088-3103.

Saitoh, H. and J. Hinchey (2000). "Functional heterogeneity of small ubiquitin-related protein modifiers SUMO-1 versus SUMO-2/3." J Biol Chem **275**(9): 6252-6258.

Salazar, M. I., J. H. Richardson, I. Sanchez-Vargas, K. E. Olson and B. J. Beaty (2007). "Dengue virus type 2: replication and tropisms in orally infected Aedes aegypti mosquitoes." BMC Microbiol **7**: 9.

Samuel, G. H., M. R. Wiley, A. Badawi, Z. N. Adelman and K. M. Myles (2016). "Yellow fever virus capsid protein is a potent suppressor of RNA silencing that binds double-stranded RNA." Proceedings of the National Academy of Sciences **113**(48): 13863-13868.

Sanders, H. R., B. D. Foy, A. M. Evans, L. S. Ross, B. J. Beaty, K. E. Olson and S. S. Gill (2005). "Sindbis virus induces transport processes and alters expression of innate immunity pathway genes in the midgut of the disease vector, Aedes aegypti." Insect Biochemistry and Molecular Biology **35**(11): 1293-1307.

Sanz, M. A., V. Madan, L. Carrasco and J. L. Nieva (2003). "Interfacial domains in Sindbis virus 6K protein. Detection and functional characterization." J Biol Chem **278**(3): 2051-2057.

Scheffner, M., U. Nuber and J. M. Huibregtse (1995). "Protein ubiquitination involving an E1-E2-E3 enzyme ubiquitin thioester cascade." Nature **373**(6509): 81-83.

Schmaljohn, A. L. and D. McClain (1996). Alphaviruses (Togaviridae) and Flaviviruses (Flaviviridae). Medical Microbiology. S. Baron. Galveston (TX).

Schmaljohn, Connie S., and Stuart T. Nichol. "49." *Fields Virology*, by Bernard N. Fields et al., Lippincott Williams & Wilkins, 2013, pp. 1741–1789

Schnettler, E., C. L. Donald, S. Human, M. Watson, R. W. Siu, M. McFarlane, J. K. Fazakerley, A. Kohl and R. Fragkoudis (2013). "Knockdown of piRNA pathway proteins results in enhanced Semliki Forest virus production in mosquito cells." J Gen Virol **94**(Pt 7): 1680-1689.

Schnettler, E., M. G. Sterken, J. Y. Leung, S. W. Metz, C. Geertsema, R. W. Goldbach, J. M. Vlak, A. Kohl, A. A. Khromykh and G. P. Pijlman (2012). "Noncoding Flavivirus RNA Displays RNA Interference Suppressor Activity in Insect and Mammalian Cells." Journal of Virology **86**(24): 13486-13500.

Scholle, F., Y. A. Girard, Q. Zhao, S. Higgs and P. W. Mason (2004). "trans-Packaged West Nile virus-like particles: infectious properties in vitro and in infected mosquito vectors." J Virol **78**(21): 11605-11614.

Schuessler, A., A. Funk, H. M. Lazear, D. A. Cooper, S. Torres, S. Daffis, B. K. Jha, Y. Kumagai, O. Takeuchi, P. Hertzog, R. Silverman, S. Akira, D. J. Barton, M. S. Diamond and A. A. Khromykh (2012). "West Nile virus noncoding subgenomic RNA contributes to viral evasion of the type I interferon-mediated antiviral response." J Virol **86**(10): 5708-5718.

Schwarz, S. E., K. Matuschewski, D. Liakopoulos, M. Scheffner and S. Jentsch (1998). "The ubiquitin-like proteins SMT3 and SUMO-1 are conjugated by the

UBC9 E2 enzyme." Proceedings of the National Academy of Sciences of the United States of America **95**(2): 560-564.

Seeler, J.-S. and A. Dejean (2017). "SUMO and the robustness of cancer." Nature Reviews Cancer **17**: 184.

Semenza, J. C. and B. Menne (2009). "Climate change and infectious diseases in Europe." Lancet Infect Dis **9**(6): 365-375.

Severson, W., L. Partin, C. S. Schmaljohn and C. B. Jonsson (1999). "Characterization of the Hantaan Nucleocapsid Protein-Ribonucleic Acid Interaction." Journal of Biological Chemistry **274**(47): 33732-33739.

Shen, T. H., H.-K. Lin, P. P. Scaglioni, T. M. Yung and P. P. Pandolfi (2006). "The Mechanisms of PML-Nuclear Body Formation." Molecular Cell **24**(3): 331-339.

Shi, X., D. F. Lappin and R. M. Elliott (2004). "Mapping the Golgi Targeting and Retention Signal of Bunyamwera Virus Glycoproteins." Journal of Virology **78**(19): 10793-10802.

Shirako, Y. and J. H. Strauss (1994). "Regulation of Sindbis virus RNA replication: uncleaved P123 and nsP4 function in minus-strand RNA synthesis, whereas cleaved products from P123 are required for efficient plus-strand RNA synthesis." J Virol **68**(3): 1874-1885.

Shrinet, J., S. Jain, J. Jain, R. K. Bhatnagar and S. Sunil (2014). "Next Generation Sequencing Reveals Regulation of Distinct Aedes microRNAs during Chikungunya Virus Development." PLOS Neglected Tropical Diseases **8**(1): e2616.

Shrivastava, S., D. Tiraki, A. Diwan, S. K. Lalwani, M. Modak, A. C. Mishra and V. A. Arankalle (2018). "Co-circulation of all the four dengue virus serotypes and detection of a novel clade of DENV-4 (genotype I) virus in Pune, India during 2016 season." PLoS ONE **13**(2): e0192672.

Shuai, K., G. Stark, I. Kerr and J. Darnell (1993). "A single phosphotyrosine residue of Stat91 required for gene activation by interferon-gamma." Science **261**(5129): 1744-1746.

Silvennoinen, O., J. N. Ihle, J. Schlessinger and D. E. Levy (1993). "Interferon-induced nuclear signalling by Jak protein tyrosine kinases." Nature **366**: 583.

Sim, S. and G. Dimopoulos (2010). "Dengue Virus Inhibits Immune Responses in Aedes aegypti Cells." PLOS ONE **5**(5): e10678.

Sim, S., N. Jupatanakul and G. Dimopoulos (2014). "Mosquito Immunity against Arboviruses." Viruses **6**(11): 4479.

Simon, L. V. and B. Kruse (2018). Encephalitis, Japanese. StatPearls. Treasure Island (FL), StatPearls Publishing

StatPearls Publishing LLC.

Singh, K. R. and K. M. Pavri (1966). "Isolation of Chittoor virus from mosquitoes and demonstration of serological conversions in sera of domestic animals at Manjri, Poona, India." Indian J Med Res **54**(3): 220-224.

Singh, U. B., A. Maitra, S. Broor, A. Rai, S. T. Pasha and P. Seth (1999). "Partial Nucleotide Sequencing and Molecular Evolution of Epidemic Causing Dengue 2 Strains." The Journal of Infectious Diseases **180**(4): 959-965.

Sirisena, P., A. Kumar and S. Sunil (2018). "Evaluation of Aedes aegypti (Diptera: Culicidae) Life Table Attributes Upon Chikungunya Virus Replication Reveals Impact on Egg-Laying Pathways." J Med Entomol.

Siu, R. W. C., R. Fragkoudis, P. Simmonds, C. L. Donald, M. E. Chase-Topping, G. Barry, G. Attarzadeh-Yazdi, J. Rodriguez-Andres, A. A. Nash, A. Merits, J. K. Fazakerley and A. Kohl (2011). "Antiviral RNA Interference Responses Induced by Semliki Forest Virus Infection of Mosquito Cells: Characterization, Origin, and Frequency-Dependent Functions of Virus-Derived Small Interfering RNAs." Journal of Virology **85**(6): 2907-2917.

Sklan, E. H., K. Staschke, T. M. Oakes, M. Elazar, M. Winters, B. Aroeti, T. Danieli and J. S. Glenn (2007). "A Rab-GAP TBC domain protein binds hepatitis C virus NS5A and mediates viral replication." J Virol **81**(20): 11096-11105.

Sluss, H. K., Z. Han, T. Barrett, R. J. Davis and Y. T. Ip (1996). "A JNK signal transduction pathway that mediates morphogenesis and an immune response in Drosophila." Genes & Development **10**(21): 2745-2758.

Smith, D. R., A. P. Adams, J. L. Kenney, E. Wang and S. C. Weaver (2008). "Venezuelan equine encephalitis virus in the mosquito vector Aedes taeniorhynchus: infection initiated by a small number of susceptible epithelial cells and a population bottleneck." Virology **372**(1): 176-186.

Smith, H. H., H. A. Penna and A. Paoliello (1938). "Yellow Fever Vaccination with Cultured Virus (17D) without Immune Serum1." The American Journal of Tropical Medicine and Hygiene **s1-18**(5): 437-468.

Smith, M. C., E. T. Goddard, M. Perusina Lanfranca and D. J. Davido (2013). "hTERT Extends the Life of Human Fibroblasts without Compromising Type I Interferon Signaling." PLoS ONE **8**(3): e58233.

Smith, T. J., W. E. Brandt, J. L. Swanson, J. M. McCown and E. L. Buescher (1970). "Physical and biological properties of dengue-2 virus and associated antigens." J Virol **5**(4): 524-532.

Smithburn, K. C., A. J. Haddow and A. F. Mahaffy (1946). "A neurotropic virus isolated from Aedes mosquitoes caught in the Semliki forest." Am J Trop Med Hyg **26**: 189-208.

Snodgrass, R. (1935). "Principles of insect morphology." New York and London: McGraw-Hill Book Company. 667p.

Soderlund, H., L. Kaariainen and C. H. von Bonsdorff (1975). "Properties of Semliki Forest virus nucleocapsid." Med Biol **53**(5): 412-417.

Sodja, A., H. Fujioka, F. J. A. Lemos, M. Donnelly-Doman and M. Jacobs-Lorena (2007). "Induction of actin gene expression in the mosquito midgut by blood ingestion correlates with striking changes of cell shape." Journal of insect physiology **53**(8): 833-839.

Soldan, S. S., M. L. Plassmeyer, M. K. Matukonis and F. Gonzalez-Scarano (2005). "La Crosse virus nonstructural protein NSs counteracts the effects of short interfering RNA." J Virol **79**(1): 234-244.

Solomon, T. and M. Mallewa (2001). "Dengue and Other Emerging Flaviviruses." Journal of Infection **42**(2): 104-115.

Soumahoro, M. K., P. Y. Boelle, B. A. Gauzere, K. Atsou, C. Pelat, B. Lambert, G. La Ruche, M. Gastellu-Etchegorry, P. Renault, M. Sarazin, Y. Yazdanpanah, A. Flahault, D. Malvy and T. Hanslik (2011). "The Chikungunya epidemic on La Reunion Island in 2005-2006: a cost-of-illness study." PLoS Negl Trop Dis **5**(6): e1197.

Souphron, J., M. B. Waddell, A. Paydar, Z. Tokgöz-Gromley, M. F. Roussel and B. A. Schulman (2008). "Structural Dissection of a Gating Mechanism Preventing Misactivation of Ubiquitin by NEDD8's E1." Biochemistry **47**(34): 8961-8969.

Sourisseau, M., C. Schilte, N. Casartelli, C. Trouillet, F. Guivel-Benhassine, D. Rudnicka, N. Sol-Foulon, K. Le Roux, M. C. Prevost, H. Fsihi, M. P. Frenkiel, F. Blanchet, P. V. Afonso, P. E. Ceccaldi, S. Ozden, A. Gessain, I. Schuffenecker, B. Verhasselt, A. Zamborlini, A. Saib, F. A. Rey, F. Arenzana-Seisdedos, P. Despres, A. Michault, M. L. Albert and O. Schwartz (2007). "Characterization of reemerging chikungunya virus." PLoS Pathog **3**(6): e89.

Southam, C. M. and A. E. Moore (1951). "West Nile, Ilheus, and Bunyamwera virus infections in man." Am J Trop Med Hyg **31**(6): 724-741.

Souza-Neto, J. A., S. Sim and G. Dimopoulos (2009). "An evolutionary conserved function of the JAK-STAT pathway in anti-dengue defense." Proc Natl Acad Sci U S A **106**(42): 17841-17846.

Stadler, K., S. L. Allison, J. Schalich and F. X. Heinz (1997). "Proteolytic activation of tick-borne encephalitis virus by furin." Journal of Virology **71**(11): 8475-8481.

Stehmeier, P. and S. Muller (2009). "Phospho-regulated SUMO interaction modules connect the SUMO system to CK2 signaling." Mol Cell **33**(3): 400-409.

Stöven, S., I. Ando, L. Kadalayil, Y. Engström and D. Hultmark (2000). "Activation of the Drosophila NF-κB factor Relish by rapid endoproteolytic cleavage." EMBO reports **1**(4): 347-352.

Strauss, J. H. and E. G. Strauss (2008). CHAPTER 2 - The Structure of Viruses. Viruses and Human Disease (Second Edition). London, Academic Press**:** 35-62.

Styczynski, A. R., J. M. A. S. Malta, E. R. Krow-Lucal, J. Percio, M. E. Nóbrega, A. Vargas, T. M. Lanzieri, P. L. Leite, J. E. Staples, M. X. Fischer, A. M. Powers, G.-J. J. Chang, P. L. Burns, E. M. Borland, J. P. Ledermann, E. C. Mossel, L. B. Schonberger, E. B. Belay, J. L. Salinas, R. D. Badaro, J. J. Sejvar and G. E. Coelho (2017). "Increased rates of Guillain-Barré syndrome associated with Zika virus outbreak in the Salvador metropolitan area, Brazil." PLoS Neglected Tropical Diseases **11**(8): e0005869.

Su, C. I., C. H. Tseng, C. Y. Yu and M. M. Lai (2016). "SUMO Modification Stabilizes Dengue Virus Nonstructural Protein 5 To Support Virus Replication." J Virol **90**(9): 4308-4319.

Sucharit, S., K. Surathin and S. R. Shrestha (1989). "Vectors of Japanese encephalitis virus (JEV): species complexes of the vectors." Southeast Asian J Trop Med Public Health **20**(4): 611-621.

Suhrbier, A., M. C. Jaffar-Bandjee and P. Gasque (2012). "Arthritogenic alphaviruses--an overview." Nat Rev Rheumatol **8**(7): 420-429.

Suzuki, T., A. Ichiyama, H. Saitoh, T. Kawakami, M. Omata, C. H. Chung, M. Kimura, N. Shimbara and K. Tanaka (1999). "A New 30-kDa Ubiquitin-related SUMO-1 Hydrolase from Bovine Brain." Journal of Biological Chemistry **274**(44): 31131-31134.

Szemiel, A. M. (2011). Replication of Bunyamwera virus in mosquito cells. PhD, University of St Andrews.

Szemiel, A. M., A.-B. Failloux and R. M. Elliott (2012). "Role of Bunyamwera Orthobunyavirus NSs Protein in Infection of Mosquito Cells." PLOS Neglected Tropical Diseases **6**(9): e1823.

Takahashi, Y., A. Toh-e and Y. Kikuchi (2001). "A novel factor required for the SUMO1/Smt3 conjugation of yeast septins." Gene **275**(2): 223-231.

Takeuchi, O. and S. Akira (2010). "Pattern Recognition Receptors and Inflammation." Cell **140**(6): 805-820.

Talamillo, A., L. Herboso, L. Pirone, C. Pérez, M. González, J. Sánchez, U. Mayor, F. Lopitz-Otsoa, M. S. Rodriguez, J. D. Sutherland and R. Barrio (2013). "Scavenger Receptors Mediate the Role of SUMO and Ftz-f1 in Drosophila Steroidogenesis." PLoS Genetics **9**(4): e1003473.

Talmon, Y., B. V. Prasad, J. P. Clerx, G. J. Wang, W. Chiu and M. J. Hewlett (1987). "Electron microscopy of vitrified-hydrated La Crosse virus." Journal of Virology **61**(7): 2319-2321.

Tamberg, N., V. Lulla, R. Fragkoudis, A. Lulla, J. K. Fazakerley and A. Merits (2007). "Insertion of EGFP into the replicase gene of Semliki Forest virus results in a novel, genetically stable marker virus." J Gen Virol **88**(Pt 4): 1225-1230.

Tan, J. A., S. H. Hall, K. G. Hamil, G. Grossman, P. Petrusz and F. S. French (2002). "Protein inhibitors of activated STAT resemble scaffold attachment factors and function as interacting nuclear receptor coregulators." J Biol Chem **277**(19): 16993-17001.

Tatham, M. H., Y. Chen and R. T. Hay (2003). "Role of Two Residues Proximal to the Active Site of Ubc9 in Substrate Recognition by the Ubc9·SUMO-1 Thiolester Complex." Biochemistry **42**(11): 3168-3179.

Tatham, M. H., M. C. Geoffroy, L. Shen, A. Plechanovova, N. Hattersley, E. G. Jaffray, J. J. Palvimo and R. T. Hay (2008). "RNF4 is a poly-SUMO-specific E3 ubiquitin ligase required for arsenic-induced PML degradation." Nat Cell Biol **10**(5): 538-546.

Tatham, M. H., E. Jaffray, O. A. Vaughan, J. M. Desterro, C. H. Botting, J. H. Naismith and R. T. Hay (2001). "Polymeric chains of SUMO-2 and SUMO-3 are conjugated to protein substrates by SAE1/SAE2 and Ubc9." J Biol Chem **276**(38): 35368-35374.

Tatham, M. H., S. Kim, B. Yu, E. Jaffray, J. Song, J. Zheng, M. S. Rodriguez, R. T. Hay and Y. Chen (2003). "Role of an N-terminal site of Ubc9 in SUMO-1, -2, and -3 binding and conjugation." Biochemistry **42**(33): 9959-9969.

Tchankouo-Nguetcheu, S., E. Bourguet, P. Lenormand, J. C. Rousselle, A. Namane and V. Choumet (2012). "Infection by chikungunya virus modulates the expression of several proteins in Aedes aegypti salivary glands." Parasit Vectors **5**: 264.

Thomas, D., G. Blakqori, V. Wagner, M. Banholzer, N. Kessler, R. M. Elliott, O. Haller and F. Weber (2004). "Inhibition of RNA polymerase II phosphorylation by a viral interferon antagonist." J Biol Chem **279**(30): 31471-31477.

Toivanen, A. (2008). "Alphaviruses: an emerging cause of arthritis?" Curr Opin Rheumatol **20**(4): 486-490.

Tong, H., G. Hateboer, A. Perrakis, R. Bernards and T. K. Sixma (1997). "Crystal Structure of Murine/Human Ubc9 Provides Insight into the Variability of the Ubiquitin-conjugating System." Journal of Biological Chemistry **272**(34): 21381-21387.

Toribio, R., I. Diaz-Lopez, J. Boskovic and I. Ventoso (2016). "An RNA trapping mechanism in Alphavirus mRNA promotes ribosome stalling and translation initiation." Nucleic Acids Res **44**(9): 4368-4380.

Treffers, E. E., A. Tas, F. E. Scholte, M. N. Van, M. T. Heemskerk, A. H. de Ru, E. J. Snijder, M. J. van Hemert and P. A. van Veelen (2015). "Temporal SILAC-based quantitative proteomics identifies host factors involved in chikungunya virus replication." Proteomics **15**(13): 2267-2280.

Troupin, A., B. Londono-Renteria, M. J. Conway, E. Cloherty, S. Jameson, S. Higgs, D. L. Vanlandingham, E. Fikrig and T. M. Colpitts (2016). "A novel mosquito ubiquitin targets viral envelope protein for degradation and reduces virion production during dengue virus infection." Biochimica et Biophysica Acta (BBA) - General Subjects **1860**(9): 1898-1909.

Truong, K., T. Lee and Y. Chen (2012). "SUMO modification of the E1 Cys domain inhibits its enzymatic activity." Journal of Biological Chemistry.

Truong, K., T. D. Lee and Y. Chen (2012). "Small Ubiquitin-like Modifier (SUMO) Modification of E1 Cys Domain Inhibits E1 Cys Domain Enzymatic Activity." Journal of Biological Chemistry **287**(19): 15154-15163.

Truong, K., T. D. Lee, B. Li and Y. Chen (2012). "Sumoylation of SAE2 C Terminus Regulates SAE Nuclear Localization." The Journal of Biological Chemistry **287**(51): 42611-42619.

Truong, K., T. D. Lee, B. Li and Y. Chen (2012). "Sumoylation of SAE2 C Terminus Regulates SAE Nuclear Localization." Journal of Biological Chemistry **287**(51): 42611-42619.

Tsetsarkin, K. A., D. L. Vanlandingham, C. E. McGee and S. Higgs (2007). "A Single Mutation in Chikungunya Virus Affects Vector Specificity and Epidemic Potential." PLoS Pathogens **3**(12): e201.

Tuittila, M. T., M. G. Santagati, M. Roytta, J. A. Maatta and A. E. Hinkkanen (2000). "Replicase complex genes of Semliki Forest virus confer lethal neurovirulence." J Virol **74**(10): 4579-4589.

Uhlen, M., L. Fagerberg, B. M. Hallstrom, C. Lindskog, P. Oksvold, A. Mardinoglu, A. Sivertsson, C. Kampf, E. Sjostedt, A. Asplund, I. Olsson, K. Edlund, E. Lundberg, S. Navani, C. A. Szigyarto, J. Odeberg, D. Djureinovic, J. O. Takanen, S. Hober, T. Alm, P. H. Edqvist, H. Berling, H. Tegel, J. Mulder, J. Rockberg, P. Nilsson, J. M. Schwenk, M. Hamsten, K. von Feilitzen, M. Forsberg, L. Persson, F. Johansson, M. Zwahlen, G. von Heijne, J. Nielsen and F. Ponten (2015). "Proteomics. Tissue-based map of the human proteome." Science **347**(6220): 1260419.

Uhlen, M., P. Oksvold, L. Fagerberg, E. Lundberg, K. Jonasson, M. Forsberg, M. Zwahlen, C. Kampf, K. Wester, S. Hober, H. Wernerus, L. Bjorling and F. Ponten (2010). "Towards a knowledge-based Human Protein Atlas." Nat Biotechnol **28**(12): 1248-1250.

Ulrich, H. D. (2008). "The Fast-Growing Business of SUMO Chains." Molecular Cell **32**(3): 301-305.

Ulu-Kilic, A. and M. Doganay (2014). "An overview: Tularemia and travel medicine." Travel Medicine and Infectious Disease **12**(6, Part A): 609-616.

Uniprot P55854 (2014). Small Ubiquitin Related Modifier-3. UniProtKB Knowledgebase.

Uniprot P61956 (2014). Small Ubiquitin Related Modifier-2. UniProt KB Knowledgebase.

Uniprot P63165 (2014). Small Ubiquitin Related Modifier-1. UniProtKB Knowledgebase.

Uniprot Q6EEV6 (2014). Small Ubiquitin Related Modifier-4. UniProtKB Knowledgebase.

Urena, E., L. Pirone, S. Chafino, C. Perez, J. D. Sutherland, V. Lang, M. S. Rodriguez, F. Lopitz-Otsoa, F. J. Blanco, R. Barrio and D. Martin (2016). "Evolution of SUMO Function and Chain Formation in Insects." Mol Biol Evol **33**(2): 568-584.

Vagin, V. V., A. Sigova, C. Li, H. Seitz, V. Gvozdev and P. D. Zamore (2006). "A distinct small RNA pathway silences selfish genetic elements in the germline." Science **313**(5785): 320-324.

van Wijk, S. J. and H. T. Timmers (2010). "The family of ubiquitin-conjugating enzymes (E2s): deciding between life and death of proteins." FASEB J **24**(4): 981-993.

Vancini, R., R. Hernandez and D. Brown (2015). "Alphavirus entry into host cells." Prog Mol Biol Transl Sci **129**: 33-62.

Varjak, M., K. Maringer, M. Watson, V. B. Sreenu, A. C. Fredericks, E. Pondeville, C. L. Donald, J. Sterk, J. Kean, M. Vazeille, A. B. Failloux, A. Kohl and E. Schnettler (2017). "Aedes aegypti Piwi4 Is a Noncanonical PIWI Protein Involved in Antiviral Responses." mSphere **2**(3).

Varma, M. G. and M. Pudney (1969). "The growth and serial passage of cell lines from Aedes aegypti (L.) larvae in different media." J Med Entomol **6**(4): 432-439.

Ventoso, I., M. A. Sanz, S. Molina, J. J. Berlanga, L. Carrasco and M. Esteban (2006). "Translational resistance of late alphavirus mRNA to eIF2alpha phosphorylation: a strategy to overcome the antiviral effect of protein kinase PKR." Genes Dev **20**(1): 87-100.

Verbruggen, P., M. Ruf, G. Blakqori, A. K. Överby, M. Heidemann, D. Eick and F. Weber (2011). "Interferon Antagonist NSs of La Crosse Virus Triggers a DNA Damage Response-like Degradation of Transcribing RNA Polymerase II." Journal of Biological Chemistry **286**(5): 3681-3692.

Verger, A., J. Perdomo and M. Crossley (2003). "Modification with SUMO. A role in transcriptional regulation." EMBO Rep **4**(2): 137-142.

Vethantham, V. and J. L. Manley (2009). "In vitro sumoylation of recombinant proteins and subsequent purification for use in enzymatic assays." Cold Spring Harb Protoc **2009**(1): pdb.prot5121.

Vogel, P., W. M. Kell, D. L. Fritz, M. D. Parker and R. J. Schoepp (2005). "Early Events in the Pathogenesis of Eastern Equine Encephalitis Virus in Mice." The American Journal of Pathology **166**(1): 159-171.

Vogel, R. H., S. W. Provencher, C. H. von Bonsdorff, M. Adrian and J. Dubochet (1986). "Envelope structure of Semliki Forest virus reconstructed from cryo-electron micrographs." Nature **320**(6062): 533-535.

Voss, J. E., M. C. Vaney, S. Duquerroy, C. Vonrhein, C. Girard-Blanc, E. Crublet, A. Thompson, G. Bricogne and F. A. Rey (2010). "Glycoprotein organization of Chikungunya virus particles revealed by X-ray crystallography." Nature **468**(7324): 709-712.

Waddell, M. B. and R. M. Taylor (1948). "Studies on cyclic passage of yellow fever virus in South American mammals and mosquitoes; marsupials (Metachirus nudicaudatus and Marmosa) in combination with Aedes aegypti as vector." Am J Trop Med Hyg **28**(1): 87-100.

Walden, H., M. S. Podgorski, D. T. Huang, D. W. Miller, R. J. Howard, D. L. Minor, J. M. Holton and B. A. Schulman (2003). "The Structure of the APPBP1-UBA3-NEDD8-ATP Complex Reveals the Basis for Selective Ubiquitin-like Protein Activation by an E1." Molecular Cell **12**(6): 1427-1437.

Wang, L., H. Pan and D. L. Smith (2002). "Hydrogen exchange-mass spectrometry: optimization of digestion conditions." Mol Cell Proteomics **1**(2): 132-138.

Wang, Y. G. and M. Dasso (2009). "SUMOylation and deSUMOylation at a glance." Journal of Cell Science **122**(23): 4249-4252.

Wasik, U. and A. Filipek (2014). "Non-nuclear function of sumoylated proteins." Biochim Biophys Acta **1843**(12): 2878-2885.

Watling, D., D. Guschin, M. Müller, O. Silvennoinen, B. A. Witthuhn, F. W. Quelle, N. C. Rogers, C. Schindler, G. R. Stark, J. N. Ihle and I. M. Kerr (1993).

"Complementation by the protein tyrosine kinase JAK2 of a mutant cell line defective in the interferon-& gamma; signal transduction pathway." Nature **366**: 166.

Weber, F., E. F. Dunn, A. Bridgen and R. M. Elliott (2001). "The Bunyamwera virus nonstructural protein NSs inhibits viral RNA synthesis in a minireplicon system." Virology **281**(1): 67-74.

Weiss, B., H. Nitschko, I. Ghattas, R. Wright and S. Schlesinger (1989). "Evidence for specificity in the encapsidation of Sindbis virus RNAs." J Virol **63**(12): 5310-5318.

Wek, R. C., H.-Y. Jiang and T. G. Anthony (2006). "Coping with stress: eIF2 kinases and translational control." Biochemical Society Transactions **34**(1): 7-11.

Welsch, S., S. Miller, I. Romero-Brey, A. Merz, C. K. Bleck, P. Walther, S. D. Fuller, C. Antony, J. Krijnse-Locker and R. Bartenschlager (2009). "Composition and three-dimensional architecture of the dengue virus replication and assembly sites." Cell Host Microbe **5**(4): 365-375.

Wen, Z., H. Song and G.-l. Ming (2017). "How does Zika virus cause microcephaly?" Genes & Development **31**(9): 849-861.

Westaway, E. G., M. A. Brinton, S. Gaidamovich, M. C. Horzinek, A. Igarashi, L. Kaariainen, D. K. Lvov, J. S. Porterfield, P. K. Russell and D. W. Trent (1985). "Togaviridae." Intervirology **24**(3): 125-139.

White, J. and A. Helenius (1980). "pH-dependent fusion between the Semliki Forest virus membrane and liposomes." Proc Natl Acad Sci U S A **77**(6): 3273-3277.

Whitfield, A. E., B. W. Falk and D. Rotenberg (2015). "Insect vector-mediated transmission of plant viruses." Virology **479-480**: 278-289.

Whitfield, S. G., F. A. Murphy and W. D. Sudia (1973). "St. Louis encephalitis virus: an ultrastructural study of infection in a mosquito vector." Virology **56**(1): 70-87.

WHO (2009). Dengue: guidelines for diagnosis, treatment, prevention and control, World Health Organization.

WHO (2014) "A global brief on vector-borne diseases."

WHO. (2015). "Japanese Encephalitis." Retrieved 12/06/2018, from http://www.who.int/news-room/fact-sheets/detail/japanese-encephalitis.

WHO. (2018). "Dengue and severe dengue." Retrieved 12/06/2018, from http://www.who.int/news-room/fact-sheets/detail/dengue-and-severe-dengue.

Wilson, V. G. (2012). "Sumoylation at the host-pathogen interface." Biomolecules **2**(2): 203-227.

Wilson, V. G. (2017). SUMO regulation of cellular processes, Springer.

Wimmer, P. and S. Schreiner (2015). "Viral Mimicry to Usurp Ubiquitin and SUMO Host Pathways." Viruses **7**(9): 4854-4872.

World Health Organization. (2012). Global strategy for dengue prevention and control 2012-2020 (in IRIS). Geneva, World Health Organization.

Wu, C. Y., K. S. Jeng and M. M. Lai (2011). "The SUMOylation of matrix protein M1 modulates the assembly and morphogenesis of influenza A virus." J Virol **85**(13): 6618-6628.

Xi, Z., J. L. Ramirez and G. Dimopoulos (2008). "The Aedes aegypti toll pathway controls dengue virus infection." PLoS Pathog **4**(7): e1000098.

Xi, Z., J. L. Ramirez and G. Dimopoulos (2008). "The Aedes aegypti Toll Pathway Controls Dengue Virus Infection." PLOS Pathogens **4**(7): e1000098.

Xu, Y., A. Plechanovova, P. Simpson, J. Marchant, O. Leidecker, S. Kraatz, R. T. Hay and S. J. Matthews (2014). "Structural insight into SUMO chain recognition and manipulation by the ubiquitin ligase RNF4." Nat Commun **5**: 4217.

Yadav, P. D., A. B. Sudeep, A. C. Mishra and D. T. Mourya (2012). "Molecular characterization of Chittoor (Batai) virus isolates from India." Indian J Med Res **136**(5): 792-798.

Yaegashi, T., V. N. Vakharia, K. Page, Y. Sasaguri, R. Feighny and R. Padmanabhan (1986). "Partial sequence analysis of cloned dengue virus type 2 genome." Gene **46**(2): 257-267.

Yan, R., S. Small, C. Desplan, C. R. Dearolf and J. E. Darnell (1996). "Identification of a Stat Gene That Functions in Drosophila Development." Cell **84**(3): 421-430.

Yanase, T., T. Kato, M. Yamakawa, K. Takayoshi, K. Nakamura, T. Kokuba and T. Tsuda (2006). "Genetic characterization of Batai virus indicates a genomic reassortment between orthobunyaviruses in nature." Archives of Virology **151**(11): 2253-2260.

Yang, D. K., B. H. Kim, C. H. Kweon, J. H. Kwon, S. I. Lim and H. R. Han (2004). "Biophysical characterization of Japanese encephalitis virus (KV1899) isolated from pigs in Korea." J Vet Sci **5**(2): 125-130.

Yang, S.-H., A. Galanis, J. Witty and A. D. Sharrocks (2006). "An extended consensus motif enhances the specificity of substrate modification by SUMO." The EMBO Journal **25**(21): 5083-5093.

Yang, S. H., A. Galanis, J. Witty and A. D. Sharrocks (2006). "An extended consensus motif enhances the specificity of substrate modification by SUMO." The EMBO journal **25**(21): 5083-5093.

Yang, W. S., M. Campbell, H. J. Kung and P. C. Chang (2018). "In Vitro SUMOylation Assay to Study SUMO E3 Ligase Activity." J Vis Exp(131).

Yasumura and Kawakita (1963). "The research for the SV40 by means of tissue culture technique." Nippon Rinsho **21**(6): 1201-1219.

Yavuz, A. S. and O. U. Sezerman (2014). "Predicting sumoylation sites using support vector machines based on various sequence features, conformational flexibility and disorder." BMC Genomics **15**(Suppl 9): S18-S18.

Yildiz, M., S. Ghosh, J. A. Bell, W. Sherman and J. A. Hardy (2013). "Allosteric inhibition of the NS2B-NS3 protease from dengue virus." ACS Chem Biol **8**(12): 2744-2752.

Yoda, M., T. Kawamata, Z. Paroo, X. Ye, S. Iwasaki, Q. Liu and Y. Tomari (2010). "ATP-dependent human RISC assembly pathways." Nat Struct Mol Biol **17**(1): 17-23.

Zacks, M. A. and S. Paessler (2010). "Encephalitic alphaviruses." Veterinary Microbiology **140**(3): 281-286.

Zambon, R. A., M. Nandakumar, V. N. Vakharia and L. P. Wu (2005). "The Toll pathway is important for an antiviral response in Drosophila." Proceedings of the National Academy of Sciences of the United States of America **102**(20): 7257-7262.

Zhang, F. P., L. Mikkonen, J. Toppari, J. J. Palvimo, I. Thesleff and O. A. Janne (2008). "Sumo-1 function is dispensable in normal mouse development." Mol Cell Biol **28**(17): 5381-5390.

Zhang, W., P. R. Chipman, J. Corver, P. R. Johnson, Y. Zhang, S. Mukhopadhyay, T. S. Baker, J. H. Strauss, M. G. Rossmann and R. J. Kuhn (2003). "Visualization of membrane protein domains by cryo-electron microscopy of dengue virus." Nat Struct Biol **10**(11): 907-912.

Zhang, X., M. Fugere, R. Day and M. Kielian (2003). "Furin processing and proteolytic activation of Semliki Forest virus." J Virol **77**(5): 2981-2989.

Zhang, Y., W. Zhang, S. Ogata, D. Clements, J. H. Strauss, T. S. Baker, R. J. Kuhn and M. G. Rossmann (2004). "Conformational Changes of the Flavivirus E Glycoprotein." Structure (London, England : 1993) **12**(9): 1607-1618.

Zhu, J., L. Chen and A. S. Raikhel (2003). "Posttranscriptional control of the competence factor ßFTZ-F1 by juvenile hormone in the mosquito Aedes aegypti." Proceedings of the National Academy of Sciences **100**(23): 13338-13343.

Zou, Z., J. Souza-Neto, Z. Xi, V. Kokoza, S. W. Shin, G. Dimopoulos and A. Raikhel (2011). "Transcriptome analysis of Aedes aegypti transgenic mosquitoes with altered immunity." PLoS Pathog **7**(11): e1002394.

Appendix A: Amino acid sequence comparison between *Hs* and *Aa*SAE1/2, and *Hs* and *Aa*PIAS

*Aa*SAE1 and *Hs*SAE1

```
AaSAE1     1 MVEA--NGIELTEQEAELYDRQIRLWGLDSQKRLRAARILIAGVNGLGAEIAKNVILSGV
HsSAE1     1 MVEKEEAGGGISEEEAAQYDRQIRLWGLEAQKRLRASRVLLVGLKGLGAEIAKNLILAGV

AaSAE1    59 KAVTLLDDQVVKEADFCSQFLAPQDSLRTNRAEASLSRAQQLNPMVELKADTEELPKKTD
HsSAE1    61 KGLTMLDHEQVTPEDPGAQFLIRTGSVGRNRAEASLERAQNLNPMVDVKVDTEDIEKKPE

AaSAE1   119 DFFKGFDVVCVIGANTEQLLRIDGVCREAGIKFFAADLWGMFGFSFADLQEHNFAEDVVK
HsSAE1   121 SFFTQFDAVCLTCCSRDVIVKVDQICHKNSIKFFTGDVFGYHGYTFANLGEHEFVEEKTK

AaSAE1   179 HKIVSKPHEKTKTE----L---VTSTVKRTLSYPAYQVLLDFDYKAQSYARKLKRSGPAL
HsSAE1   181 VAKVSQGVEDGPDTKRAKLDSSETTMVKKKVVFCPVKEALEVDWSSEKAKAALKRTTSDY

AaSAE1   232 PLLRVLQKFRDDEKRDPLYSEREADLQKLLKIRDEV------AADLIPDNAFLHVFAQIS
HsSAE1   241 FLLQVLLKFRTDKGRDPSSDTYEEDSELLLQIRNDVLDSLGISPDLLPEDFVRYCFSEMA

AaSAE1   286 PAAAIVGGAVAHEIIKTVSQKEAPHHNVFLFDPESCCGFIESIGVDA
HsSAE1   301 PVCAVVGGILAQEIVKALSQRDPPHNNFFFFDGMKGNGIVECLGP-K
```

*Aa*SAE2 and *Hs*SAE2

```
AaSAE2     1 MAAQIVGVFEPELQEKISNSKILVVGAGGIGCEILKNLVLSGFQDIEIIDLDTIDVSNLN
HsSAE2     1 MA--LSRGLPRELAEAVAGGRVLVVGAGGIGCELLKNLVLTGFSHIDLIDLDTIDVSNLN

AaSAE2    61 RQFLFHKEHVGKSKANVARESALSFNPNVKIKAYHDSITTSNYGVNFFQQFNLVLNALDN
HsSAE2    59 RQFLFQKKHVGRSKAQVAKESVLQFYPKANIVAYHDSIMNPDYNVEFFRQFILVMNALDN

AaSAE2   121 RAARNHVNRLCLTADVPLIESGTAGYNGQVELIKRGLTQCYECTPKAAQKTFPGCTIRNT
HsSAE2   119 RAARNHVNRMCLAADVPLIESGTAGYLGQVTTIKKGVTECYECHPKPTQRTFPGCTIRNT

AaSAE2   181 PSEPIHCIVWAKHLFNQLFGESNEDEDVSPDTADPEAGAEAGES-ALAAEANEKGNVDRV
HsSAE2   179 PSEPIHCIVWAKYLFNQLFGEEDADQEVSPDRADPEAAWEPTEAEARARASNEDGDIKRI

AaSAE2   240 NTRTWAQQCGYDPEKIFNKLFYDDINYLLSMSNLWKSRTPPNPAKWDALEEDGEAAP---
HsSAE2   239 STKEWAKSTGYDPVKLFTKLFKDDIRYLLTMDKLWRKRKPPVPLDWAEVQSQGEETNASD

AaSAE2   297 --TD-T-VLRDQKVLSLTESAKVFGESITALKKDFEKLAEGDHLVWDKDDKHAMDFVAAC
HsSAE2   299 QQNEPQLGLKDQQVLDVKSYARLFSKSIETLRVHLAEKGDGAELIWDKDDPSAMDFVTSA

AaSAE2   353 ANIRAQIFNIPRKSRFEVKSMAGNIIPAIATTNAITAGVVVMHAFRVLKGELDKCKSVYM
HsSAE2   359 ANLRMHIFSMNMKSRFDIKSMAGNIIPAIATTNAVIAGLIVLEGLKILSGKIDQCRTIFL

AaSAE2   413 RLRPNARNQLFVPDRTLNPPNPKCYVCAAKPEVTLKVDTKNVTVKELRDDILIKALNMLN
HsSAE2   419 CALDPPNPNCYVCASKPEVTVRLNVHKVTVLTLQDKIVKEKFAMVANKQPNPRKKLLVP-

AaSAE2   473 PDVI-LDGKGTIVISSEEGETDCNNDKKLEDLQIVDGCILKVDDFVQNYELTVTVIHKDP
HsSAE2   478 PDVQIEDGKGTILISSEEGETEANNHKKLSEFGIRNGSRLQADDFLQDYTLLINILHSED

AaSAE2   532 GRDESSFDIVA-DPDSLKPKEDEDQKTDDVQPSTSGQNGNSKASTSNNGAVDDDDDMCIV
HsSAE2   538 LGKDVEFEVVGDAPEKVGPKQAEDA-A---KSITNGSDDGAQPS---TSTAQEQDDVLIV

AaSAE2   591 EEDAEKPSTSDAGAGPSSSGSEKRKIEDSEGPSTKKARVSNDDDDDDLIVIN
HsSAE2   591 DSDEEDS-SNNADVSEE-ERSRKRKLDEKENLSAKRSRIEQKEELDDVIALD
```

* catalytically active cysteine (Lois and Lima 2005)

*Aa*PAIS and *Hs*PIAS

```
AaPIAS      1 MRKTRQVAEFTELKDLVHQLRVSDLQQLLGENNISRSGRKSELIERVLILVRQNISV-LK
HsPIAS1     1 ------MADSAELKQMVMSLRVSELQVLLGYAGRNKHGRKHELLTKALHLLKAGCSPAVQ
HsPIAS2α    1 ------MADFEELRNMVSSFRVSELQVLLGFAGRNKSGRKHDLLMRALHLLKSGCSPAVQ
HsPIAS2β    1 ------MADFEELRNMVSSFRVSELQVLLGFAGRNKSGRKHDLLMRALHLLKSGCSPAVQ
HsPIAS3     1 ------MAELGELKHMVMSFRVSELQVLLGFAGRNKSGRKHELLAKALHLLKSSCAPSVQ
HsPIAS4     1 -----MAAELVEAKNMVMSFRVSDLQMLLGFVGRSKSGLKHELVTRALQLVQFDCSPELF

AaPIAS     60 YKVRDLHKKAQEETELLKQAAETPVITTQPIQPPPPVLPPEPPVISRVPQGMYQQQYANA
HsPIAS1    55 MKIKELYRRRFPQKIMTPADLS-----IPNVHSSP--MPAT----L-SPSTIPQLTYDGH
HsPIAS2α   55 IKIRELYRRRYPRTLEGLSDLSTIKSSVFSLDGGS--SPVEPDLAVAGIHSLPSTSVTPH
HsPIAS2β   55 IKIRELYRRRYPRTLEGLSDLSTIKSSVFSLDGGS--SPVEPDLAVAGIHSLPSTSVTPH
HsPIAS3    55 MKIKELYRRRFPRKTLGPSDLS-----LLSLPPGT--SPVG------SPGPLAPIP----
HsPIAS4    56 KKIKELYETRYAKKNSEPAPQP-----HRPLDPLT--MHSTYD----RAGAVPRTPLAGP

AaPIAS    120 VQNDNRGGQVHANGIVPIPYPEATPNPGYPIHPDVKLKKLAFFDVLATLLKPATLVPSNT
HsPIAS1   103 PASSPLLPVSLLGPKHELELPHLT-SALHPVHPDIKLQKLPFYDLLDELIKPTSLASD-N
HsPIAS2α  113 SPSSPVGSVLLQDTKPTFEMQQPS-PPIPPVHPDVQLKNLPFYDVLDVLIKPTSLVQS-S
HsPIAS2β  113 SPSSPVGSVLLQDTKPTFEMQQPS-PPIPPVHPDVQLKNLPFYDVLDVLIKPTSLVQS-S
HsPIAS3    98 --PTLLAPGTLLGPKREVDMH--P-PLPQPVHPDVTMKPLPFYEVYGELIRPTTLAST-S
HsPIAS4   105 NIDYPVLYGKYLNGLG-------R-LPAKTLKPEVRLVKLPFFNMLDELLKPTELVPQ-N

AaPIAS    180 TQRIQEGSFFFHLTPQQATDIATNRDIRNVNKIEHTIQVQLRFCLLETSCEQEDYFPPNI
HsPIAS1   161 SQRFRETCFAFALTPQQVQQISSSMDIS-GTKCDFTVQVQLRFCLSETSCPQEDHFPPNL
HsPIAS2α  171 IQRFQEKFFIFALTPQQVREICISRDFLPGGRRDYTVQVQLRLCLAETSCPQEDNYPNSL
HsPIAS2β  171 IQRFQEKFFIFALTPQQVREICISRDFLPGGRRDYTVQVQLRLCLAETSCPQEDNYPNSL
HsPIAS3   152 SQRFEEAHFTFALTPQQVQQILTSREVLPGAKCDYTIQVQLRFCLCETSCPQEDYFPPNL
HsPIAS4   156 NEKLQESPCIFALTPRQVELIRNSRELQPGVKA---VQVVLRICYSDTSCPQEDQYPPNI

AaPIAS    240 VVKVNNKLCPLPNPIPTNKPGVEPKRPPRPVNITPNVKLSPLVANHIAVSWCTEYNRGYA
HsPIAS1   220 CVKVNTKPCSLPGYLPPTKNGVEPKRPSRPINITSLVRLSTTVPNTIVVSWTAEIGRNYS
HsPIAS2α  231 CIKVNGKLFPLPGYAPPPKNGIEQKRPGRPLNITSLVRLSSAVPNQISISWASEIGKNYS
HsPIAS2β  231 CIKVNGKLFPLPGYAPPPKNGIEQKRPGRPLNITSLVRLSSAVPNQISISWASEIGKNYS
HsPIAS3   212 FVKVNGKLCPLPGYLPPTKNGAEPKRPSRPINITPLARLSATVPNTIVVNWSSEFGRNYS
HsPIAS4   213 AVKVNHSYCSVPGYYPSNKPGVEPKRPCRPINLTHLMYLSSAT-NRITVTWG-NYGKSYS

AaPIAS    300 AACYLVRKLTSSQLLQRMKTKGVKPADYTRALIKEKLNEDADCEIATTMLKVSLVCPLGK
HsPIAS1   280 MAVYLVKQLSSTVLLQRLRAKGIRNPDHSRALIKEKLTADPDSEIATTSLRVSLLCPLGK
HsPIAS2α  291 MSVYLVRQLTSAMLLQRLKMKGIRNPDHSRALIKEKLTADPDSEIATTSLRVSLMCPLGK
HsPIAS2β  291 MSVYLVRQLTSAMLLQRLKMKGIRNPDHSRALIKEKLTADPDSEIATTSLRVSLMCPLGK
HsPIAS3   272 LSVYLVRQLTAGTLLQKLRAKGIRNPDHSRALIKEKLTADPDSEVATTSLRVSLMCPLGK
HsPIAS4   271 VALYLVRQLTSSELLQRLKTIGVKHPELCKALVKEKLRLDPDSEIATTGVRVSLICPLVK
```

```
AaPIAS    360 MRMATPCRSSTCSHLQCFDASLYLQMNERKPTWNCPVCDKAAIYDNLVIDGYFQEVLASN
HsPIAS1   340 MRLTIPCRALTCSHLQCFDATLYIQMNEKKPTWVCPVCDKKAPYEHLIIDGLFMEIL---
HsPIAS2α  351 MRLTIPCRAVTCTHLQCFDAALYLQMNEKKPTWICPVCDKKAAYESLILDGLFMEIL---
HsPIAS2β  351 MRLTIPCRAVTCTHLQCFDAALYLQMNEKKPTWICPVCDKKAAYESLILDGLFMEIL---
HsPIAS3   332 MRLTVPCRALTCAHLQSFDAALYLQMNEKKPTWTCPVCDKKAPYESLIIDGLFMEIL---
HsPIAS4   331 MRLSVPCRAETCAHLQCFDAVFYLQMNEKKPTWMCPVCDKPAPYDQLIIDGLLSKIL---

AaPIAS    420 KLSSEDNEIQLHKDGSWSTHVKTNDSCTLDTPSKPVQKVEV--VSD-DIEIITTDPPKSS
HsPIAS1   397 KYCTDCDEIQFKEDGTWAPMRSKKEVQEVS--ASY-NGVDGCLSSTLEHQVASHHQSSNK
HsPIAS2α  408 NDCSDVDEIKFQEDGSWCPMRPKKEAMKVS--SQPCTKIES--SSVLSKPCSVTVASEAS
HsPIAS2β  408 NDCSDVDEIKFQEDGSWCPMRPKKEAMKVS--SQPCTKIES--SSVLSKPCSVTVASEAS
HsPIAS3   389 SSCSDCDEIQFMEDGSWCPMKPKKEASEVC--PPPGYGLDG----L-QYSPVQGGDPSEN
HsPIAS4   388 SECEDADEIEYLVDGSWCPIRAEKERS--C--SPQ-------------GAILVLGPSDAN

AaPIAS    477 INQASVISSSEPSSTTAPSSDTVDLTLSDSDDDLPL-KRKTVTRAAAGG--Q
HsPIAS1   454 N-------------KKVEVIDLTIDSSSDEEEEEPSAKRTCPSLSPTS-P-L
HsPIAS2α  464 K-------------KKVDVIDLTIESSSDEEEDPPA-KRKCIFMSETQS--S
HsPIAS2β  464 K-------------KKVDVIDLTIESSSDEEEDPPA-KRKCIFMSETQS--S
HsPIAS3   442 K-------------KKVEVIDLTIESSSDEEDLPPT-KKHCSVTSAAIPALP
HsPIAS4   431 G-----------------LLPAPSVNGSGALGSTGG-GGPVGSMENGK---P
```

Appendix B: Purification of *Aa*SAE1/2

Initially, a Ni^{2+} affinity purification was used on *Aa*SAE1/2, with a 6xHis tag cloned in frame with either *Aa*SAE1 or *Aa*SAE2. During purification the heterodimer appeared to dissociate, and consequently there was a bias towards the protein which possesses the 6xHis tag. Optimisation studies revealed that this is due to the imidazole concentration, used for elution which induced heterodimer dissociation. Further analysis of the modelled structure of *Aa*SAE1/2 revealed non-conserved histidine residues at the interface of *Aa*SAE1 and *Aa*SAE2, which are likely the cause of the dissociation. We hypothesise that the imidazole competitively binds to the histamine residues at the interface of *Aa*SAE1 and *Aa*SAE2, leading to heterodimer dissociation. Consequently, the *Aa*SAE1/2 heterodimer was cloned into a Strep.II tag vector, interestingly, when the Strep.II tag was cloned onto the N-terminal of *Aa*SAE1, the heterodimer was inactive (data not shown). However, when the Strep.II tag was cloned onto the N-terminal of *Aa*SAE2, a functional heterodimer was produced that was utilised for the rest of the biochemical studies.

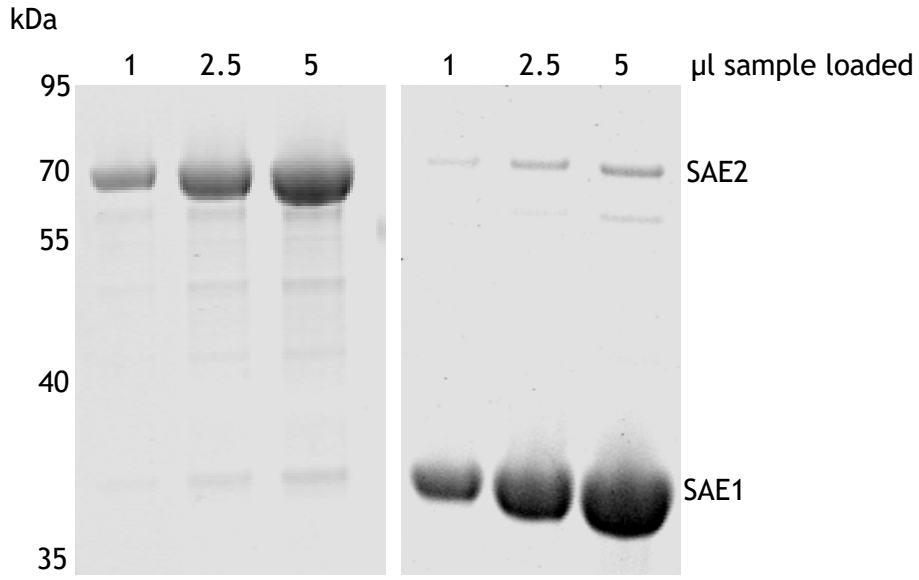

Purification of 6x His *Aa*SAE1/2 through Nickel affinity chromatography

Coomassie stained SDS-PAGE gel of purified *Aa*SAE1/2, containing a 6xHis tag on the N-terminal of either the SAE2 protein (left), or the SAE1 protein (right). Regardless of which protein was tagged, the heterodimer dissociated during purification.

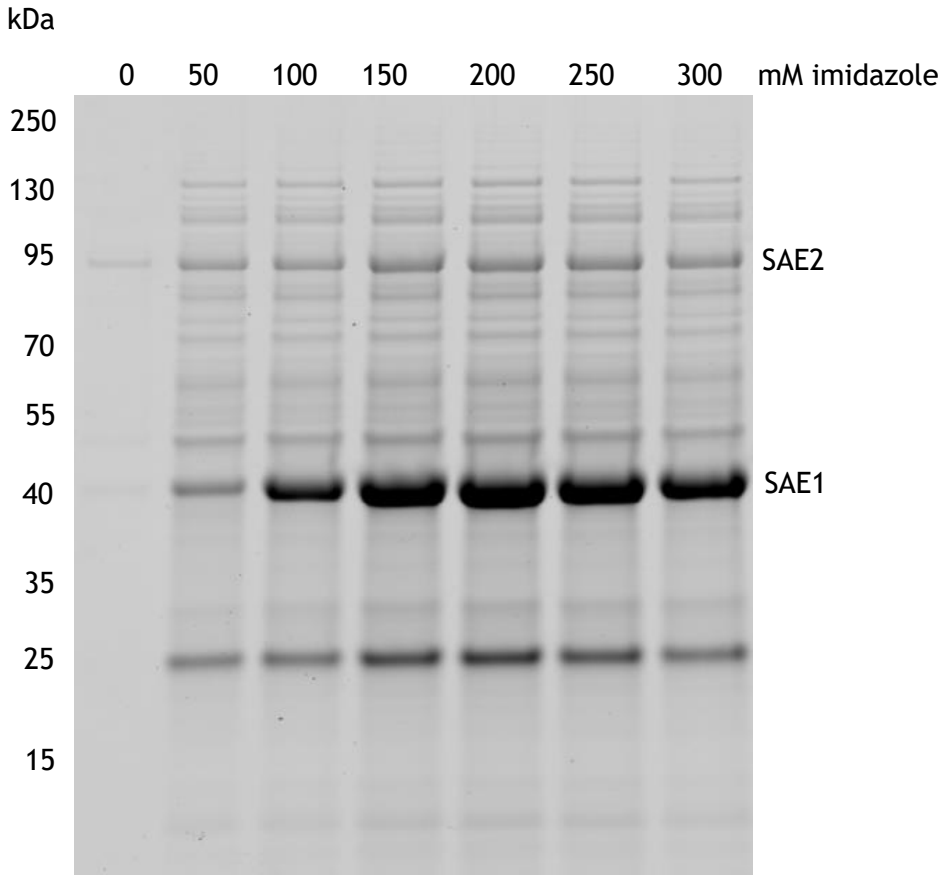

Imidazole titration performed during purification of 6xHis-*Aa*SAE1/*Aa*SAE2

Coomassie stained SDS-PAGE gel of 6xHis-*Aa*SAE1/*Aa*SAE2 samples grown and purified using increasing concentrations of imidazole in the elution buffer. As the concentration of imidazole increased, the ratio of 6xHis-*Aa*SAE1 to *Aa*SAE2 became more skewed in favour of 6xHis-*Aa*SAE1.

A

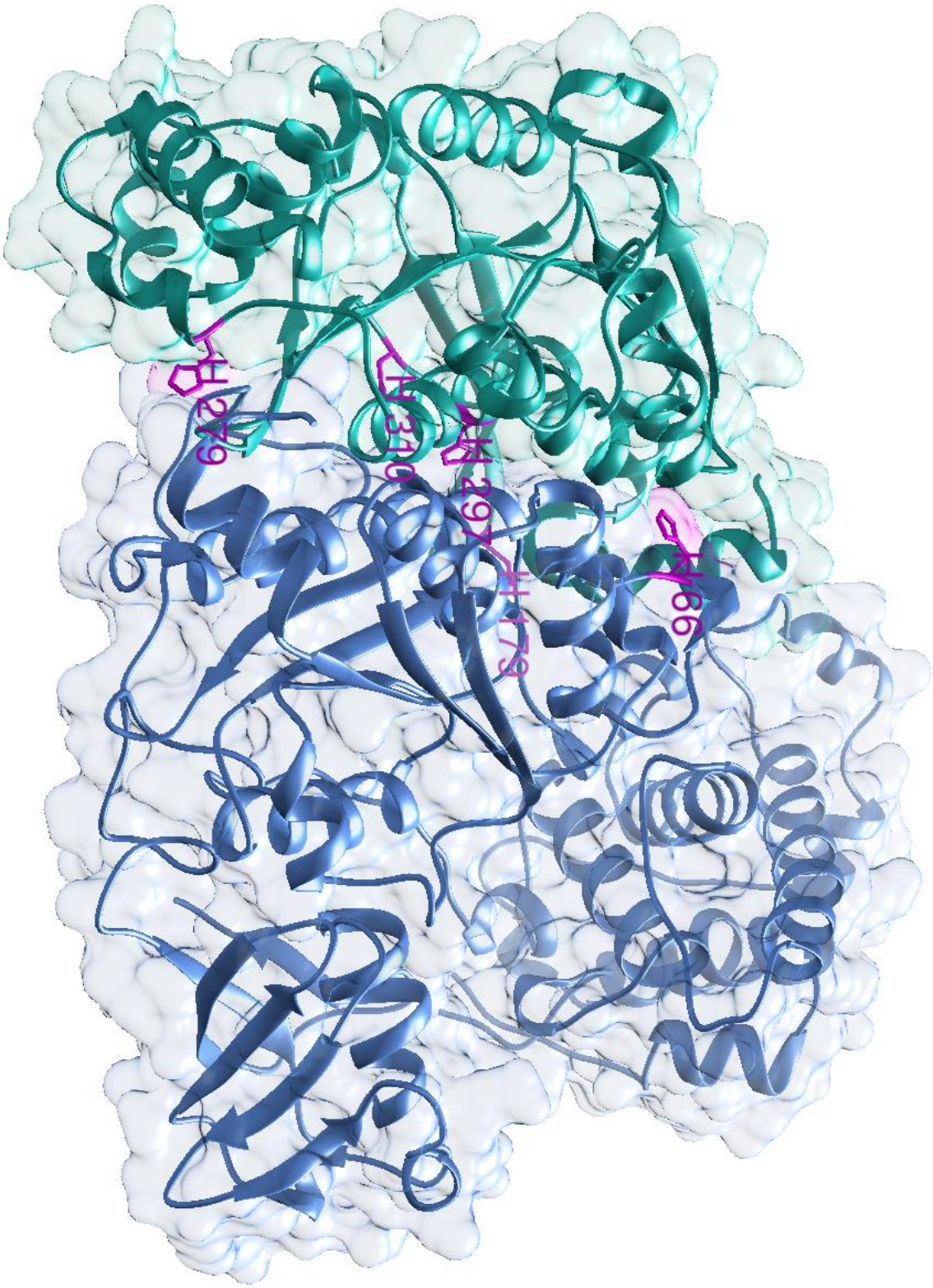

B

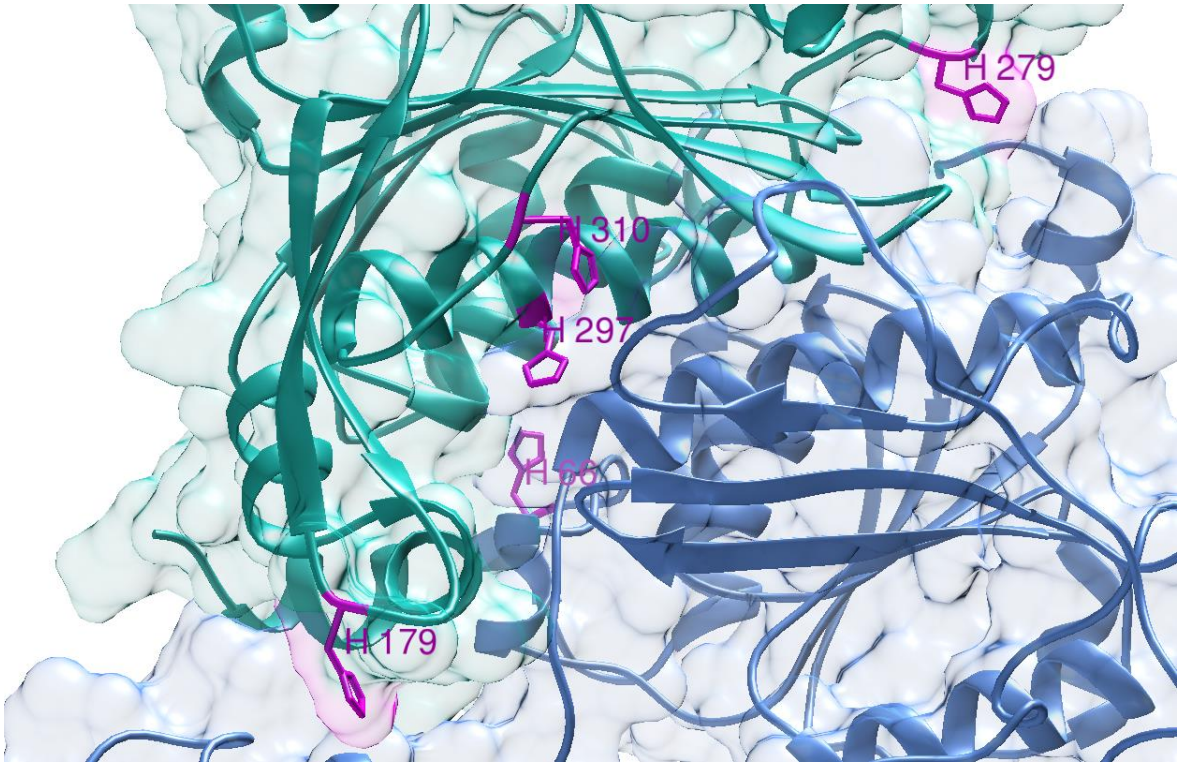

Histidine residues at the *Aa*SAE1/2 interface

(**A**) The predicted structure of *Aa*SAE1/2 was modelled and histidine residues (pink, labelled) located around the *Aa*SAE1 (light sea green), *Aa*SAE2 (cornflower blue) interface were identified. (**B**) 180˚ rotation on the Y-axis focusing on the interface of *Aa*SAE1 and *Aa*SAE2.

Appendix C: Purified *Aa*Ubc9 C93S, the SUMO chimaera, and the SUMO chimaera K11R

In order to characterise biochemical properties of proteins in the *Aa*SUMOylation pathway, catalytically inactive, and chimaeric proteins were produced. A catalytically inactive *Aa*Ubc9 (Ubc9 C93S) was produced and cloned as described (**Section 2.2.1.10; Section 2.2.9.3**), and purified through the 6xHis tag (**Section 2.2.2.2**). A chimaeric SUMO protein and a chimaeric SUMO containing a K11R mutation were also synthesised, cloned as described and purified through 6xHis tag (**Section 2.2.9.2; Section 2.2.2.2**).

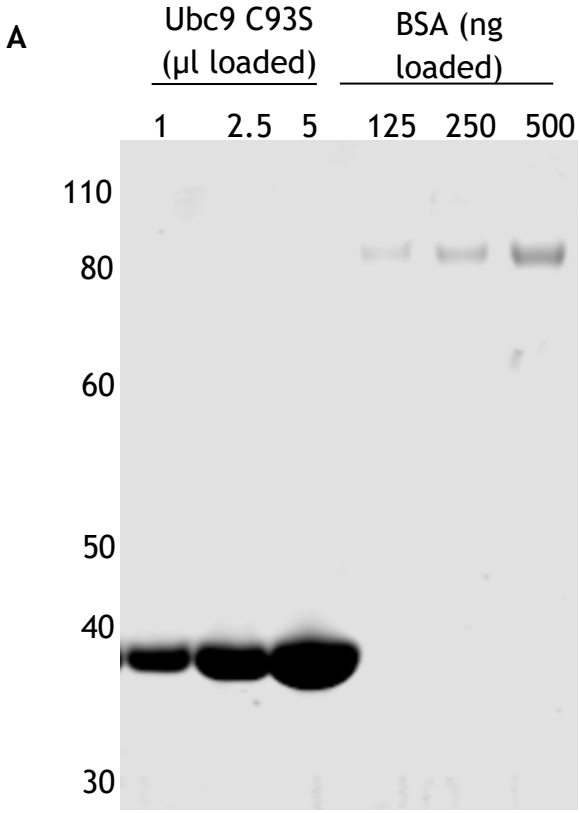

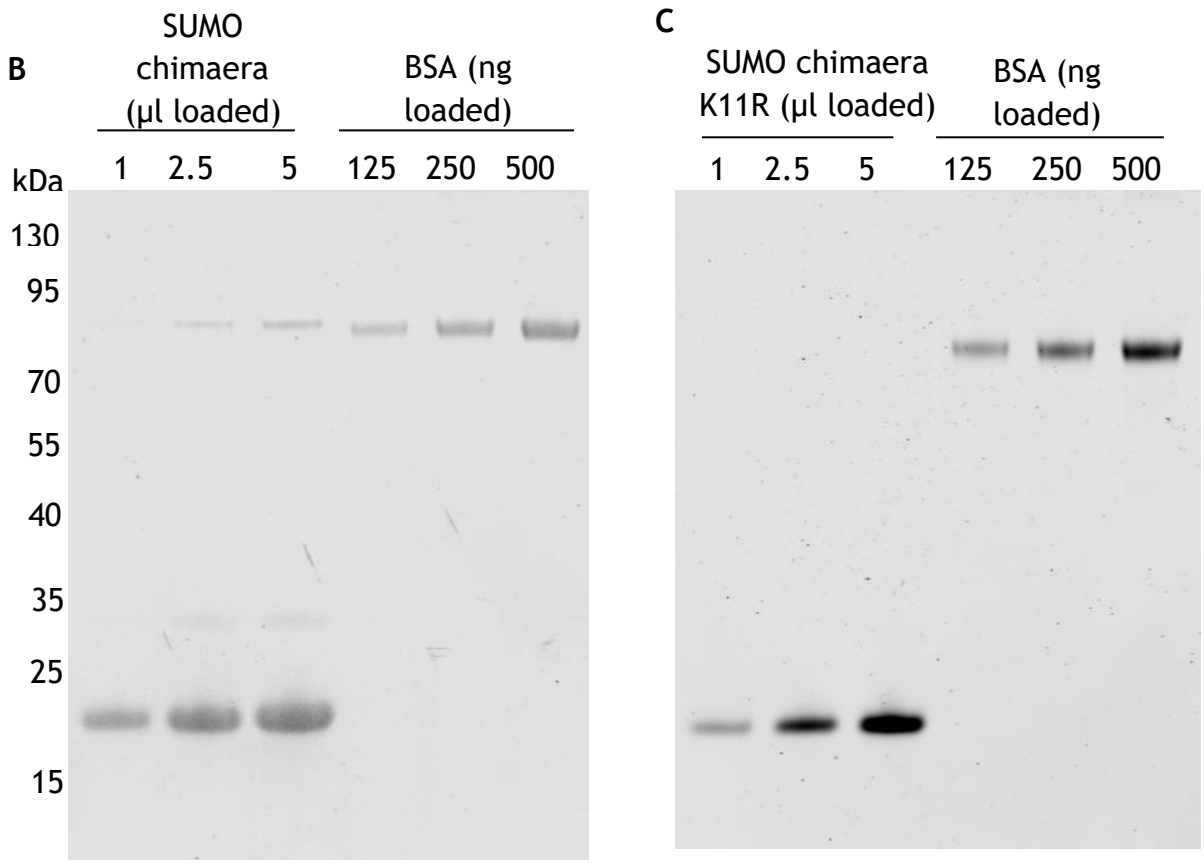

Purification of chimaeric proteins, and proteins containing point mutations

Coomassie stained SDS-PAGE gel of 6xHis purified (**A**) Ubc9 C93S, (**B**) SUMO chimaera, and (**C**) SUMO chimaera K11R. BSA standards included to determine concentration. Molecular weight markers indicated.

Appendix D: No primary antibody controls of SUMO expression in *Ae. aegypti* tissues

Confocal microscopy of tissues stained with no primary antibody

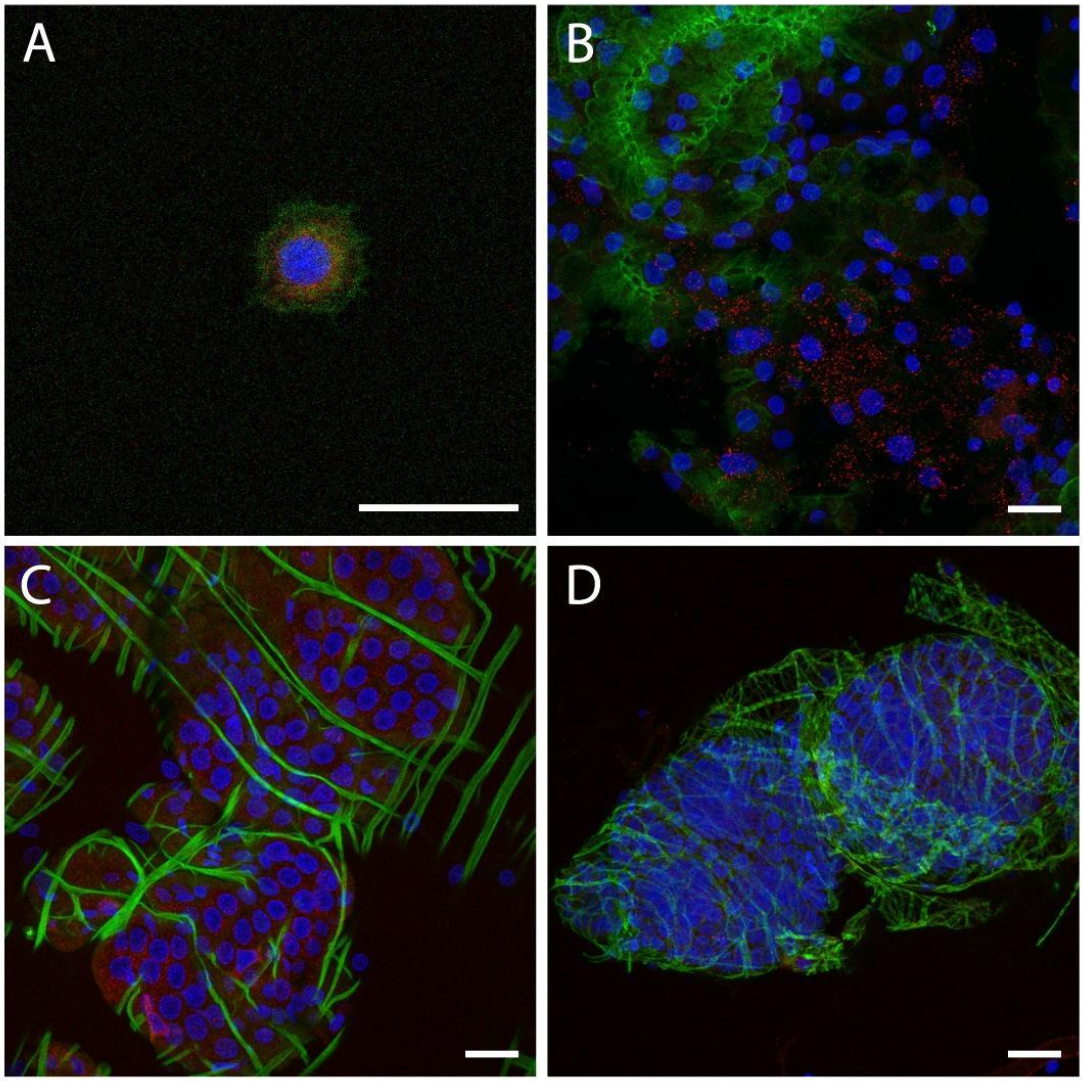

Non blood-fed adult female *Ae. aegypti* had cells and organs dissected. Confocal microscopy was conducted without primary (αSUMO2/3) antibody, tissues were stained with DAPI (nuclei, blue), and Phalloidin 488 (F-actin, green), secondary antibody Alexa Fluor 568 goat anti-mouse IgG was diluted 1:1000 (red). Experiment was conducted on haemocytes (A), salivary glands (B), midgut (C), and ovaries (D). Images were acquired on a Zeiss LSM 880 confocal microscope with 40x or 63x oil-immersion lens using the same settings as the samples incubated with a primary antibody. Scale bar represents 20 μm.

Appendix E: Melt curve analysis of q-PCR primers

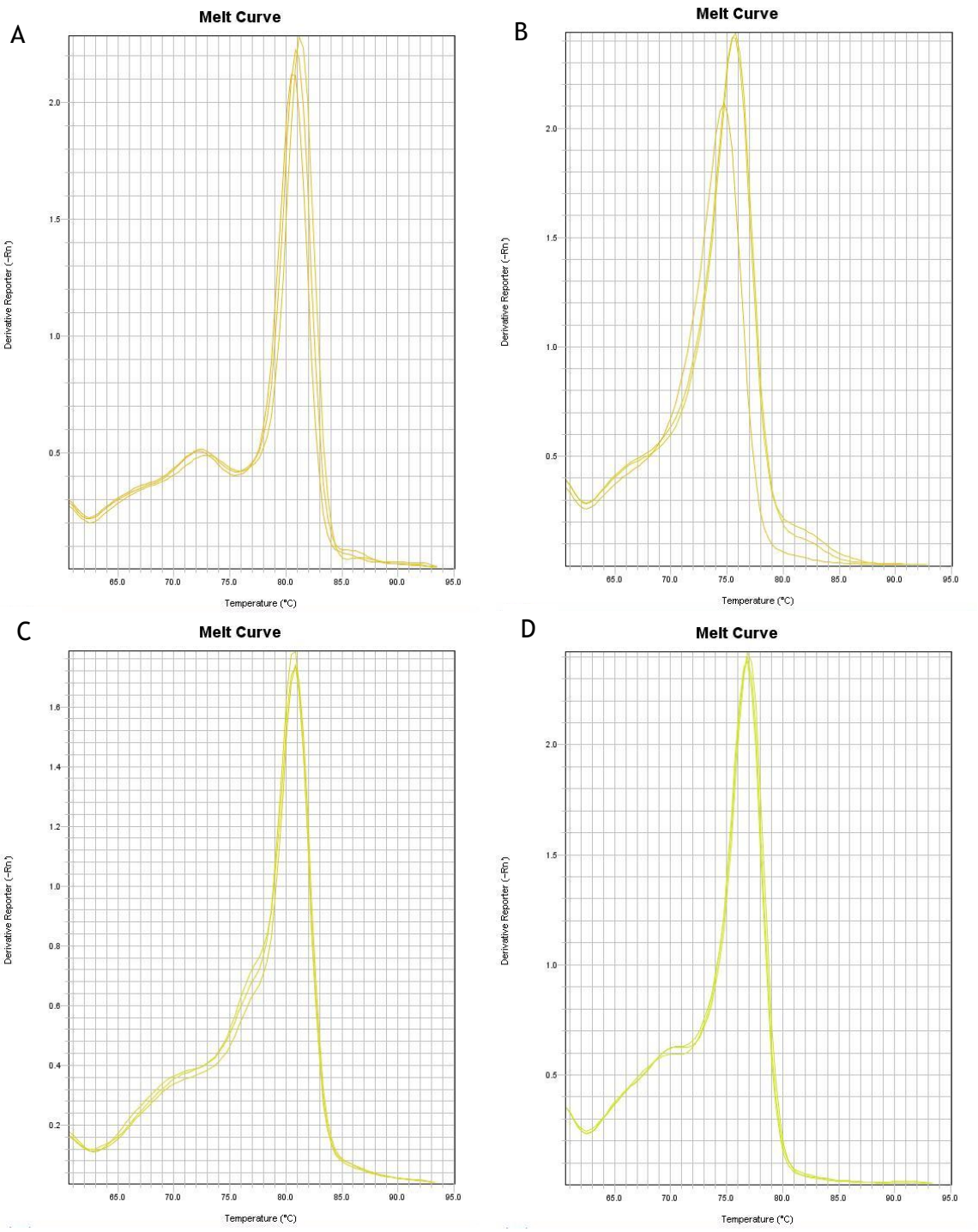

RNA was harvested from either mosquito AF5 cells or *Ae. aegypti* organs, cDNA was synthesised and q-PCR analysis was conducted. Subsequent melt curves were conducted to ensure no primer dimers were interfering with analysis. (**A**) melt curves following q-PCR of primers targeting the ribosomal S7, (**B**) melt curves following q-PCR of primers targeting SUMO, (**C**) melt curves following q-PCR of primers targeting Ubc9, and (**D**) melt curves following q-PCR of primers targeting PIAS.

“Have no fear of perfection – you’ll never reach it”

– Salvador Dali